

# **Efficient Synthesis of Rigid, Functional Macrocycles *via* Reversible Reactions**

Zur Erlangung des akademischen Grades

DOKTOR DER NATURWISSENSCHAFTEN

(Dr. rer. nat.)

der KIT-Fakultät für Chemie und Biowissenschaften

des Karlsruher Instituts für Technologie (KIT)

genehmigte

DISSERTATION

von

M.Sc. Gregor Markus Klein

aus

Karlsruhe

Dekan: Prof. Dr. Reinhard Fischer

Referent: Prof. Dr. Michael A. R. Meier

Korreferent: Prof. Dr. Patrick Théato

Tag der mündlichen Prüfung: 18.10.2018



*“In the moment of action remember the value of silence and order.”*

*Phormio of Athens*



Die vorliegende Arbeit wurde von Mai 2015 bis September 2018 unter Anleitung von Prof. Dr. Michael A. R. Meier am Institut für Organische Chemie (IOC) des Karlsruher Instituts für Technologie (KIT) in Kooperation mit Prof. Dr. Christopher Barner-Kowollik am Institut für Technische Chemie und Polymerchemie (ITCP) und am Materials Science and Engineering Science and Engineering Faculty, Chemistry, Physics, Mechanical Engineering, Nanotechnology and Molecular Science an der Queensland University of Technology (QUT) durchgeführt.

Hiermit versichere ich, dass ich die Arbeit selbstständig angefertigt, nur die angegebenen Quellen und Hilfsmittel benutzt und mich keiner unzulässigen Hilfe Dritter bedient habe. Insbesondere habe ich wörtlich oder sinngemäß aus anderen Werken übernommene Inhalte als solche kenntlich gemacht. Die Satzung des Karlsruher Instituts für Technologie (KIT) zur Sicherung wissenschaftlicher Praxis habe ich beachtet. Des Weiteren erkläre ich, dass ich mich derzeit in keinem laufenden Promotionsverfahren befinde, und auch keine vorausgegangenen Promotionsversuche unternommen habe.

---

Ort, Datum

---

Unterschrift



## Danksagung

Zunächst möchte ich mich ganz herzlich bei meinen beiden betreuenden Professoren, Prof. Michael Meier und Prof. Christopher Barner-Kowollik, bedanken. Zum einen für die Chance, in ihren Arbeitsgruppen diese Promotion durchführen zu können, zum anderen für die exzellente Betreuung. Außerdem danke ich ihnen dafür, dass sie mir die Möglichkeit und finanzielle Unterstützung gegeben haben, im Rahmen meiner Promotion einen Auslandsaufenthalt absolvieren zu können. Hierbei gilt besonderer Dank Pinar Sancar, die mir bei der Organisation des Aufenthaltes sehr geholfen hat und immer mit Rat zur Verfügung stand.

Bei Prof. Patrick Theato bedanke ich mich dafür, dass er als Korreferent eingesprungen ist.

Benjamin Bitterer, Pia Löser und Audrey Llevot möchte ich für die Vorarbeiten danken und besonders Audrey möchte ich für die Unterstützung bei wissenschaftlichen Problemen danken. Bei Dr. Julian Helfferich möchte ich mich für die Simulation der Makrozyklen bedanken.

Des Weiteren möchte ich mich bei beiden Arbeitsgruppen (inklusive der Alumni) am KIT sowie der Arbeitsgruppe an der QUT für die angenehme Arbeitsatmosphäre und Unterstützung bedanken.

Außerdem möchte ich mich bei Thomas Sattelberger, Caroline Albrech, und The Anh Nguyen für ihre Mithilfe im Labor und ihren Beitrag zur Synthese einiger der beschriebenen Moleküle bedanken. Bei Rebecca Seim bedanke ich mich für die freundschaftliche Arbeitsatmosphäre und die Organisation im Labor und Arbeitskreis.

Für die Messung von IR, Massenspektrometrie und NMR-Spektroskopie danke ich der Analytikabteilung des IOC. Dem SEC-ESI-Team, Waldemar Konrad, Andrea Lauer, Janin Offenloch und Charlotte Petite danke ich für die Messungen an der SEC-ESI. Dabei möchte ich mich bei Waldemar Konrad für die Unterstützung mit der Puriflash besonders bedanken; ebenso bei Florian Feist für die Unterstützung während meiner Zeit an der QUT.

Dr. Dafni Moatsou, Dr. Audrey Llevot, Simon Veith, Dr. Patrick Dannecker, Katharina Wetzels, Julian Windbiel, Philip Scholten und Kevin Waibel haben diese Arbeit Korrektur gelesen und damit einen wichtigen Beitrag zum Entstehen geleistet.





# Table of Contents

<b>Abstract</b> .....	<b>1</b>
<b>Kurzdarstellung</b> .....	<b>3</b>
<b>I. Introduction</b> .....	<b>5</b>
<b>II. Background Information</b> .....	<b>7</b>
II.1. Dynamic Covalent Chemistry .....	7
• II.1.1. Preface .....	7
• II.1.2. Requirements .....	9
• II.1.3. Reaction Types.....	10
• II.1.4. Alkyne Metathesis .....	13
• II.1.5. Olefin metathesis.....	17
• II.1.6. Imine Condensation.....	23
II.2. Shape-persistent Macrocycles .....	28
• II.2.1. Kinetic Approach .....	31
• II.2.2. Thermodynamic Approach .....	38
II.3. 2D Polymers.....	70
• II.3.1. Graphene as the Prototype of 2D Polymers .....	71
• II.3.2. Synthetic Approaches to 2D Polymers.....	75
<b>III. Motivation and Aim of the Thesis</b> .....	<b>96</b>
<b>IV. Results and Discussion</b> .....	<b>99</b>
IV.1. Simulations .....	99
• IV.1.1. Method .....	99
• IV.1.2. Results .....	99
IV.2. Olefin Metathesis .....	102
• IV.2.1. Previous Studies & Motivation .....	102
• IV.2.2. Monomer Synthesis .....	103
• IV.2.3. Macrocyclization.....	113
IV.3. Imine Condensation .....	122
• IV.3.1. Previous Studies .....	122
• IV.3.2. Monomer Synthesis .....	126
• IV.3.3. Synthesis of Macrocycles .....	133
• IV.3.4. Purification of Macrocycle .....	155
• IV.3.5. Network Formation.....	157
<b>V. Conclusion &amp; Outlook</b> .....	<b>162</b>

<b>VI. Experimental Part</b> .....	<b>164</b>
VI.1 Analytics and Equipment.....	164
• VI.1.1 Nuclear Magnetic Resonance (NMR) Spectroscopy .....	164
• VI.1.2 Mass Spectrometry (MS) .....	164
• VI.1.3 Size exclusion chromatography (SEC) .....	165
• VI.1.4 Size Exclusion Chromatography- Electrospray Ionization (SEC-ESI) .....	165
• VI.1.5 Solvents and Reagents .....	166
• VI.1.6 High-Pressure Laboratory Reactor .....	167
• VI.1.7 Microwave Reactor .....	167
• VI.1.8. Thin-layer chromatography .....	168
• VI.1.9. Flash Chromatography.....	168
VI.2. Reaction Procedures .....	169
• VI.2.1. Reaction Procedures for the Olefin Metathesis Approach.....	169
• VI.2.2. Reaction Procedures for the Imine Condensation Approach .....	171
<b>VII. Appendix</b> .....	<b>179</b>
VII.1. List of Abbreviations.....	179
VII.2. List of References .....	182

# Abstract

Rigid macrocycles display potential for many applications, due to their exclusive structure leading to unique properties. Nevertheless, the rigid structure often impedes solubility making solubilizing groups necessary to keep the cycles in solution. These solubilizing groups are usually integrated at the outer rim of a cycle or in the inner for large cavities. Simulations suggest that solubilizing groups find sufficient space inside the smaller cavities by arranging themselves pointing alternately up and down out of the cycle. Therefore, the outer margin would be available for other functional groups and the cycle would still be soluble.

Due to their planarity, rigid macrocycles are suitable building blocks for 2D polymers. At the current state, 2D polymers are obtained either by a surface/interface approach or by modular synthesis in solution. The application of rigid macrocycles as monomers combines both approaches. On one hand, the growing 2D species should stay in solution due to the solubilizing groups; on the other hand, the planarity of the rigid macrocycles forces a two-dimensional structure.

The aim of the current thesis was to synthesize macrocycles with different solubilizing groups of sizes at the inner rim to confirm simulation results experimentally. The further aim was the integration of functional groups at the outer rim and to investigate their reactivity for further reactions.

Within this thesis, suitable monomers were successfully synthesized with alkyl groups of various lengths as solubilizing groups, as well as different functional groups directly on the backbone, such as bromine and vinyl, which make the macrocycles accessible for further reactions. These monomers were evaluated for the synthesis of rigid macrocycles by cyclooligomerization *via* olefin metathesis or imine condensation, allowing a thermodynamic control over the reaction due to their reversibility.

While the olefin approach did not work as expected, a series of rigid macrocycles with different solubilizing groups at the inner and functional groups at the outer rim were synthesized by imine condensation. According to a recent literature search, these functional six-membered macrocycles consisting of monomers with amines respectively

aldehydes in *meta*-position have not been reported before. The resulting macrocycles or rather the mixtures of linear and cyclic oligomers were analyzed by SEC, SEC-ESI mass spectrometry and NMR spectroscopy. Furthermore, the isolation of the macrocycles was attempted.

Contrary to the expectations, based on the simulations, the cyclization was impeded significantly by larger solubilizing groups. Besides, the macrocycles exhibit a low solubility, preventing the application as monomers for 2D polymers. Even after reduction of the imine macrocycles to the corresponding amines – hence, the breakup of the fully-conjugated, rigid system – they show low solubility in common solvents.

# Kurzdarstellung

Rigide Makrozyklen zeigen aufgrund ihrer einzigartigen Struktur und den daraus resultierenden besonderen Eigenschaften Potential für viele Anwendungen. Allerdings erschwert die rigide Struktur die Löslichkeit, weshalb der Einbau löslichkeitsvermittelnder Gruppen nötig ist. Diese werden meist am äußeren Rand eines Ringes angebracht; bei einer großen Kavität können diese auch im Innern angebracht werden. Simulationen zeigen, dass löslichkeitsvermittelnde Gruppen auch im Innern kleiner Kavitäten genug Platz hätten, da sie sich so anordnen können, dass sie alternierend nach oben und unten zeigen. Damit stünde der äußere Rand der Zyklen für den Einbau funktioneller Gruppen zur Verfügung und der Zyklus wäre trotzdem löslich.

Aufgrund ihrer Planarität sind rigide Makrozyklen geeignete Bausteine für 2D-Polymere. Momentan werden 2D Polymere entweder mittels Oberflächen/Grenzflächen oder aufwendigen, modularen Synthesen in Lösung hergestellt. Die Anwendung von rigiden Makrozyklen als Monomere könnte beide Ansätze miteinander verbinden. Einerseits sollte durch die löslichkeitsvermittelnden Gruppen die wachsende 2D-Spezies in Lösung verbleiben, andererseits erzwingt die Planarität der rigiden Makrozyklen eine zwei-dimensionale Struktur.

Ziel dieser Arbeit war die Synthese von Makrozyklen mit löslichkeitsvermittelnden Gruppen verschiedener Größe im Innern, um die Simulationen experimentell zu belegen. Weiteres Ziel war der Einbau funktioneller Gruppen am äußeren Rand um zu zeigen, dass Folgereaktionen der Makrozyklen möglich sind.

Im Rahmen dieser Arbeit wurden zunächst Monomere mit verschiedenen langen Alkylketten als löslichkeitsvermittelnden Gruppen synthetisiert, sowie mit unterschiedlichen funktionellen Gruppen, wie Brom und Vinyl, welche die Makrozyklen zugänglich für Weiterreaktionen machen sollen. Aus diesen Monomeren wurde versucht, durch Cyclooligomerisation mittels Olefinmetathese bzw. Imin-Kondensation rigide Makrozyklen herzustellen, was eine thermodynamische Kontrolle der Reaktion aufgrund ihrer Reversibilität ermöglicht.

Während der Olefin-Metathese-Ansatz nicht so funktionierte wie erwartet, konnte mittels Imin-Kondensation eine Reihe rigider Makrozyklen mit verschiedenen Löslichkeitsvermittelnden Gruppen im Innern und verschiedenen funktionellen Gruppen am äußeren Rand synthetisiert werden. Eine kürzlich erfolgte Literaturrecherche ergab, dass diese funktionalen, sechsgliedrigen Makrozyklen, welche aus Monomeren mit Aminen bzw. Aldehyde in *meta*-Position bestehen, bisher nicht veröffentlicht wurden. Die erhaltenen Makrozyklen bzw. Gemische aus linearen und zyklischen Oligomeren wurden mittels SEC, SEC-ESI Massenspektrometrie und NMR-Spektroskopie untersucht. Weiterhin wurde versucht die Makrozyklen zu isolieren.

Entgegen der Erwartungen begründet durch die Simulation wurde die Zyklisierung durch größere Löslichkeitsvermittelnde Gruppen deutlich erschwert. Außerdem zeigten die Makrozyklen eine niedrige Löslichkeit, was den Einsatz als Monomere für 2D Polymere nicht möglich macht. Selbst nach Reduktion der Iminmakrozyklen zu den entsprechenden Aminen, also die Auflösung des durchkonjugierten, rigiden Systems, zeigten sie eine geringe Löslichkeit in gängigen Lösungsmitteln.

# I. Introduction

In rigid macrocycles, ring-members are connected such that flexibility is limited and the obtained structure is endowed with properties such as planarity,<sup>[1]</sup> defined cavity and position of functional groups<sup>[2]</sup> and in some cases a fully-conjugated system.<sup>[3]</sup> This special architecture gives rise to unique properties, making rigid macrocycles useful tools for various applications: the defined cavity and presence of functional groups enable host-guest interactions, making macrocycles applicable for sensor materials<sup>[4]</sup> and artificial enzymes.<sup>[1]</sup> Furthermore, rigid macrocycles form assemblies of high order depending on the moieties present, for instance in 2D supramolecular structures by hydrogen bonds<sup>[5]</sup> as a result of their planarity. In combination with their fixed structure, rigid macrocycles are applicable building blocks for larger structures<sup>[3,6,7]</sup> forcing a planar geometry, and have potential as monomers for 2D polymers. Due to their assembly behavior and presence of a characteristic cavity, macrocycles are also adequate candidates for three-dimensional and porous structures, thus making them suitable for catalysis<sup>[8]</sup> and artificial transmembrane transporters.<sup>[9]</sup> The fully-conjugated system gives rise to unique electric, magnetic and optical properties making such macrocycles applicable for organic electronics.<sup>[3]</sup>

The special structure is both a blessing and curse. On one hand, the rigid structure enables all these previously mentioned properties and applications; on the other hand, it is the reason why rigid macrocycles exhibit low solubility in common solvents compared to their linear or non-conjugated counterparts. To increase the solubility, solubilizing groups such as long alkyl chains have to be incorporated into the building blocks.<sup>[1]</sup> These moieties are usually integrated at the outer rim of the macrocycles, or at the inside if the cavity is large enough.<sup>[3]</sup>

Rigid macrocycles can be synthesized *via* kinetic or thermodynamic control. Thermodynamic control, more precisely reactions of dynamic covalent chemistry (DCvC), exhibit some outstanding advantages. In a kinetic approach, the macrocycles are usually built up by modular synthesis leading to a decreased yield. In contrast, by thermodynamic control a cyclooligomerization is more efficient, which means that a monomer grows to a linear oligomer, which finally undergoes a cyclization. DCvC enables control over a broad spectrum of macrocycles in various sizes and shapes as

well as different reaction pathways to connect the building blocks to one cycle,<sup>[10]</sup> for example *via* alkyne metathesis shown among others by Vollhardt *et al.*,<sup>[11]</sup> Moore *et al.*,<sup>[12]</sup> Fürstner *et al.*<sup>[13]</sup> and Zhang *et al.*<sup>[14]</sup>. Furthermore Moore *et al.*<sup>[15]</sup> illustrated the reordering effect of DCvC, which exhibits one of the benefits of a thermodynamic control compared to kinetic control. Zhang *et al.*<sup>[16]</sup> reported on a method for the synthesis of rigid macrocycles by olefin metathesis, which is also applied in this thesis. By imine condensation Nabeshima *et al.*<sup>[17]</sup> and MacLachlan *et al.*<sup>[18]</sup> obtained rigid macrocycles containing “salen” and “salphen” units, which exhibit a strong complexation behavior. Later, Zhang *et al.* showed that the orthogonal application of different reactions, like olefin metathesis and imine condensation in one-pot, is possible to access rigid macrocycles connected with various functional groups.<sup>[19]</sup>

Smart monomer design allows for dictating the geometry by setting the angle, and thus macrocyclization can be favored compared to the formation of linear oligomers. Methods to target a particular macrocycle within a spectrum of cyclic compounds have been established, for instance the complexation with a template ion (“template effect”).<sup>[20]</sup> In order to prevent the reaction’s equilibrium from being changed, a subsequent reaction that deactivates either the catalyst or the active functional groups allows its “freezing”.<sup>[21]</sup>



## II. Background Information

### II.1. Dynamic Covalent Chemistry

#### II.1.1. Preface

If a starting material A can react to form either a thermodynamically favored product B or the kinetically favored product C, the composition of the resulting product mixture depends on whether the reaction is reversible or irreversible under the given reaction conditions. If the reaction is irreversible, mainly product C will be formed since the corresponding transition state of A to C ( $\Delta G_{C^\ddagger}$ ) is more stable compared to B ( $\Delta G_{B^\ddagger}$ ) (*Figure 1*). Once C is formed, C reacting back to the starting material is impossible, due to the irreversible character of the reaction, and C is the main product (kinetical control).<sup>[22]</sup>

If the reaction is reversible on the other hand, product C is still more likely to be formed at the beginning; however, due to its reversible character, C reacts back to A and then forms B. Product B is energetically favored to C (thermodynamically more stable product;  $\Delta G_B > \Delta G_C$ ). Furthermore, C is more likely to react back to A than B is. The overall reaction equilibrium is shifted towards B. The reversible character of the reaction ensures that B is the main product and the reaction is thermodynamically controlled.<sup>[22]</sup> In practice, by preventing intermediates from getting removed from the reaction mixture, e.g., by precipitation due to low solubility, kinetic gaps are avoided and the reversible character of the reaction is guaranteed.<sup>[10]</sup>

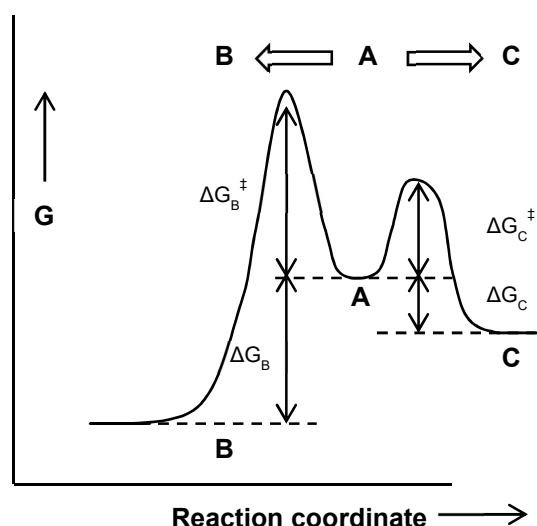
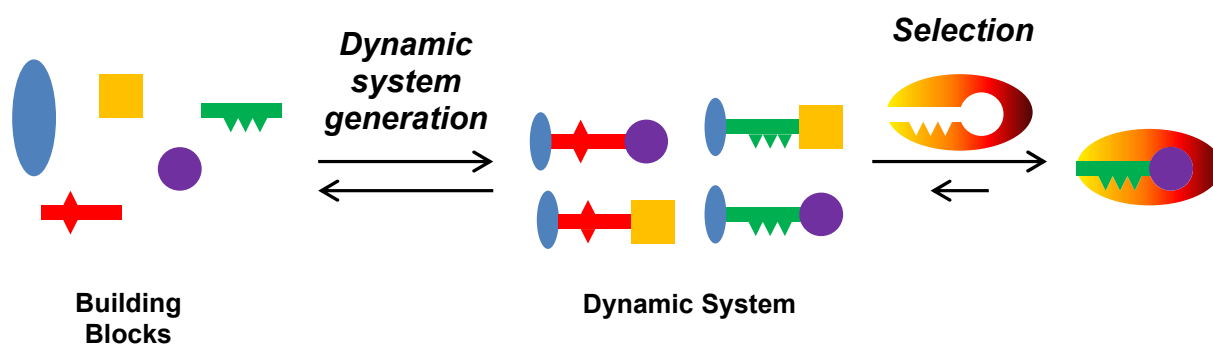


**Figure 1:** Energy diagram of a reaction of starting material A to product B and C. The ultimate product formation depends on the reversible or rather irreversible character of the reaction leading either to thermodynamic ( $A \rightarrow B$ ) or kinetic ( $A \rightarrow C$ ) control.<sup>[22]</sup>

In the kinetic approach, the stabilization of the transition state is targeted in order to obtain the desired product, while thermodynamic control aims to stabilize the product.<sup>[22]</sup> Alternatively, the equilibrium can be shifted towards the desired product by application of an external stimulus, for example following the principle of Le Châtelier through removal of the desired product or its related product (such as small molecules like water or methanol)<sup>[22]</sup> or adding a selector, e.g., a ligand or receptor.<sup>[10]</sup> Emil Fischer's lock-and-key metaphor explains this concept (*Scheme 1*): Under thermodynamic control, a mixture of different products is obtained (different keys); however, triggered by an external stimulus (a lock), a "re-equilibration"<sup>[10]</sup> takes place and only the desired product (the fitting key) is generated. In a kinetic approach, generated side-products need to be removed by purification; in contrast, thermodynamic control allows an "error correction" due to the reversible character; hence, higher yields and more practical experimental procedures are possible.



**Scheme 1:** The Emil Fischer's lock-and-key metaphor as an illustration of selection by external stimuli in a reaction under thermodynamic control.<sup>[10]</sup>

There is a broad spectrum of different reversible reactions to combine different molecules into one product under thermodynamic control. These reactions are summarized in dynamic combinatorial chemistry (DCC) concerning all kinds of bond formations, both covalent and non-covalent.

The formation of covalent bonds is particularly relevant to dynamic covalent chemistry (DCvC),<sup>[23]</sup> which has become an important tool in many applications such as complex molecular architecture, ligand screening, dynamic catalysis and catalytic screening, adaptive and responsive materials, sensing and pattern recognition, as well as functional systems.<sup>[10,23]</sup>

Synthesizing large molecules often requires many steps with the risk of unfavored side reactions that lead to decreased yield or structural defects. DCvC are considered self-sorting systems, which are defined by their ability for “spontaneous reorganization of a disordered multicomponent system into a set of subsystems of fewer components with greater order”.<sup>[24]</sup> This “error correction” or “proofreading”<sup>[25]</sup> leads to the minimization of undesired products.

## II.1.2. Requirements

Not every reversible reaction is by default a useful synthetic tool, but if certain criteria are met such as speed, orthogonality and the ability to be quenched, then the reaction can be a rather powerful one.

The equilibrium should be reached within a reasonable time frame of at most a week.<sup>[21]</sup> In order to accelerate the process, catalysts can be used;<sup>[22]</sup> however, the degradation of the catalyst can lead to a “false” product mixture before the actual equilibrium is reached.<sup>[10]</sup> A broad variety of different catalyst types is given, ranging from “simple” acidic or basic solutions to complex systems such as enzymes or metathesis catalysts, both homogeneous and heterogeneous.

The synthesis of complex macromolecules usually requires several steps applying different reactions, building blocks and templates. Therefore, mild reaction conditions and a tolerance towards various functionalities<sup>[21]</sup> as well as to oxygen and moisture<sup>[10]</sup> are necessary.

To prevent a shift of equilibrium during the isolation or storage of the desired product, the reaction has to be able to be quenched to “freeze” the equilibrium.<sup>[20]</sup> Quenching can occur by control of temperature or pH value, removing the catalyst or transforming the reactive species into unreactive species.<sup>[21]</sup>

### **II.1.3. Reaction Types**

The combination of molecules can either occur by exchange reactions, which means that the same kind of bond is broken and re-formed, or by generating a new type of covalent bond. In *Table 1*, an overview of selected reversible reactions is given.

In the following subchapters (*II.1.4. Alkyne Metathesis to II.1.6. Imine Condensation*), different reversible reactions and their role in supramolecular chemistry are presented, as well as their importance in shape-persistent macrocycles explained (*II.2. Shape-persistent Macrocycles*).

[10,21]

Table 1: Overview of several dynamic covalent chemistry (DCvC) reactions. [10,21]

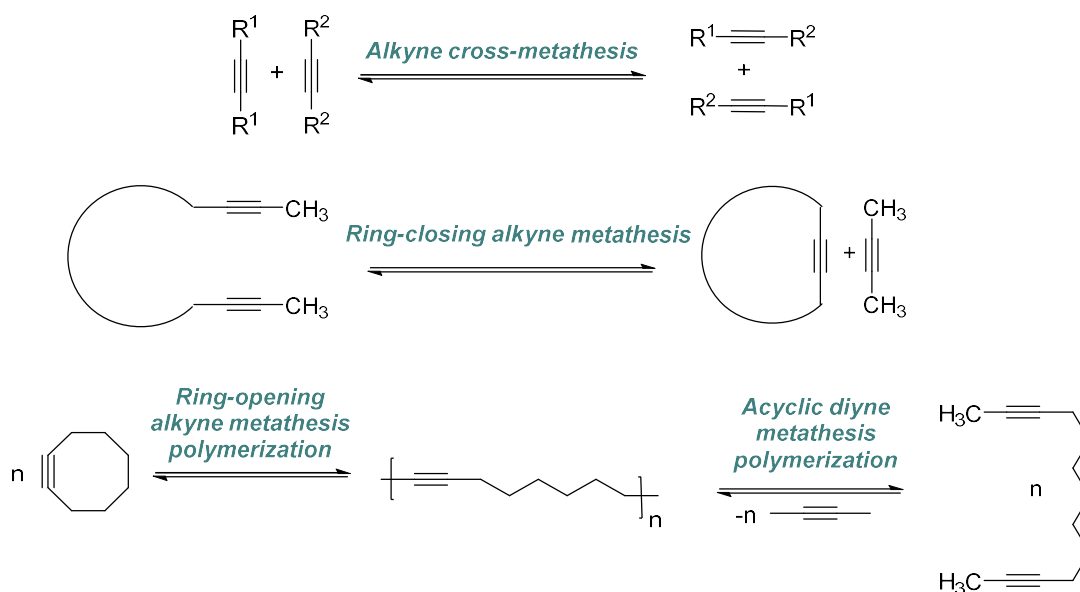
Reaction Name	Reaction Scheme	Species
<b>Dynamic C-C bond</b> <b>Aldol reaction</b> <sup>[26,27]</sup>		new bonds
<b>Diels-Alder reaction</b> <sup>[28]</sup>		new bonds
<b>Phenol/aldehyde condensation</b> <sup>[29]</sup>		new bonds
<b>Friedel-Crafts reaction</b> <sup>[30]</sup>		new bonds
<b>Stecker reaction</b> <sup>[31]</sup>		new bonds
<b>Nitroaldol reaction</b> <sup>[26]</sup>		new bonds
<b>Cyanohydrin formation</b> <sup>[31]</sup>		new bonds
<b>Knoevenagel reaction</b> <sup>[32]</sup>		new bonds
<b>Olefin metathesis</b> <sup>[33]</sup>		exchange reactions
<b>Alkyne metathesis</b> <sup>[16]</sup>		exchange reactions
<b>Carbene coupling</b> <sup>[34]</sup>		new bonds
<b>Dynamic C-N bond</b> <b>C=N bond formation/exchange</b> <sup>[24]</sup>	$R^1\text{-CHO} + R^2\text{-NH}_2 \rightleftharpoons R^1\text{-N}=\text{R}^2 + \text{H}_2\text{O}$ $R^1\text{-N}=\text{R}^2 + R^3\text{-NH}_2 \rightleftharpoons R^1\text{-N}=\text{R}^3 + R^2\text{-NH}_2$ $R^1\text{-N}=\text{R}^2 + R^4\text{-N}=\text{R}^5 \rightleftharpoons R^1\text{-N}=\text{R}^5 + R^4\text{-N}=\text{R}^2$ $R^1\text{-N}=\text{N}(\text{H})\text{R}^2 + R^3\text{-N}=\text{N}(\text{H})\text{R}^4 \rightleftharpoons R^1\text{-N}=\text{N}(\text{H})\text{R}^4 + R^3\text{-N}=\text{N}(\text{H})\text{R}^2$ $R^1\text{-N}=\text{N}(\text{O})\text{R}^2 + R^3\text{-N}=\text{N}(\text{O})\text{R}^4 \rightleftharpoons R^1\text{-N}=\text{N}(\text{O})\text{R}^4 + R^3\text{-N}=\text{N}(\text{O})\text{R}^2$ $\text{Ar-N}=\text{N}(\text{H})\text{R}^1 + R^2\text{-NH}_2 \rightleftharpoons \text{Ar-N}=\text{N}(\text{H})\text{R}^2 + R^1\text{-NH}_2$ $R^1\text{-N}=\text{N}(\text{H})\text{R}^2 \rightleftharpoons R^1\text{-N}=\text{N}(\text{H})\text{R}^2$	exchange reactions
<b>Aminal formation</b> <sup>[35]</sup>		new bonds

<b>Amide formation/exchange</b> <sup>[36]</sup>	$R^1\text{-COOH} + R^2\text{NH}_2 \rightleftharpoons R^1\text{-C(=O)NH-R}^2 + \text{H}_2\text{O}$ $R^1\text{-C(=O)NH-R}^2 + R^3\text{NH}_2 \rightleftharpoons R^1\text{-C(=O)NH-R}^3 + R^2\text{NH}_2$ $R^1\text{-C(=O)NH-R}^2 + R^3\text{-C(=O)NH-R}^4 \rightleftharpoons R^1\text{-C(=O)NH-R}^4 + R^3\text{-C(=O)NH-R}^2$	exchange reactions
<b>Dynamic C-O bond Ester formation/exchange</b> <sup>[23]</sup>	$R^1\text{-COOH} + R^2\text{OH} \rightleftharpoons R^1\text{-COOR}^2 + \text{H}_2\text{O}$ $R^1\text{-COOR}^2 + R^3\text{OH} \rightleftharpoons R^1\text{-COOR}^3 + R^2\text{OH}$ $R^1\text{-COOR}^2 + R^3\text{-COOR}^4 \rightleftharpoons R^1\text{-COOR}^4 + R^3\text{-COOR}^2$ $R^1\text{-CHO} + R^2\text{OH} \rightleftharpoons R^1\text{-CH(OR}^2) + \text{H}_2\text{O}$ $R^1\text{-CHO} + 2 R^2\text{OH} \rightleftharpoons R^1\text{-CH(OR}^2)_2 + 2 \text{H}_2\text{O}$	exchange reactions
<b>Acetal formation exchange</b> <sup>[37]</sup>	$R^1\text{-C(OR}^2)_2 + R^1\text{-C(OR}^3)_2 \rightleftharpoons R^1\text{-C(OR}^2)_2 + R^1\text{-C(OR}^3)_2$	exchange reactions
<b>Nicholas ether exchange</b> <sup>[38]</sup>		exchange reactions
<b>Hemiaminal ether exchange</b> <sup>[39]</sup>		exchange reactions
<b>Alkoxyamine exchange</b> <sup>[40]</sup>		exchange reactions
<b>Dynamic C-S bond Hemithioacetal exchange</b> <sup>[41]</sup>	$R^1\text{-CHO} + R^2\text{-SH} \rightleftharpoons R^1\text{-CH(OH)SR}^2$	exchange reactions
<b>Thioacetal exchange</b> <sup>[23]</sup>	$R^1\text{-C(SR}^2)_2 + R^3\text{-C(SR}^4)_2 \rightleftharpoons R^1\text{-C(SR}^2)_2 + R^3\text{-C(SR}^4)_2$	exchange reactions
<b>Thioester exchange</b> <sup>[42]</sup>	$R^1\text{-C(=S)SR}^2 + R^3\text{-SH} \rightleftharpoons R^1\text{-C(=S)SR}^3 + R^2\text{-SH}$	exchange reactions
<b>Thia-Michel reaction</b> <sup>[43]</sup>		exchange reactions
<b>Dynamic B-O bond Boronic acid condensation</b> <sup>[44]</sup>	$R\text{-B(OH)}_2 \rightleftharpoons R\text{-B(O)}_2\text{R} + \text{H}_2\text{O}$	new bonds
<b>Dynamic S-S bond Disulfide exchange</b> <sup>[45]</sup>	$R^1\text{-S-S-R}^2 + R^3\text{-S-S-R}^4 \rightleftharpoons R^1\text{-S-S-R}^4 + R^3\text{-S-S-R}^2$	exchange reactions
<b>Dynamic Se-Se bond Diselenide exchange</b> <sup>[46]</sup>	$R^1\text{SeSeR}^2 + R^3\text{SeSeR}^4 \rightleftharpoons R^1\text{SeSeR}^4 + R^3\text{SeSeR}^2$	exchange reactions

## II.1.4. Alkyne Metathesis

### II.1.4.1. Preface

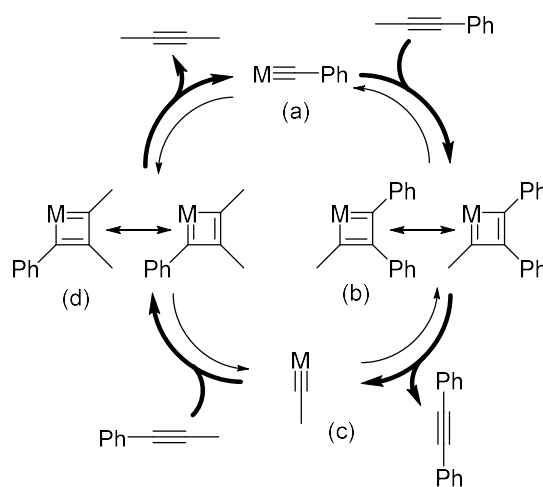
Alkyne or acetylene metathesis concerns the metal-catalyzed rearrangement of the substituents of a triple bond.<sup>[47]</sup> Several variations of alkyne metathesis exist (*Scheme 2*), such as alkyne cross-metathesis in which the substituents are exchanged. By ring-closing alkyne metathesis, cycles can be obtained. By a smart monomer design with methylene substituents as end groups, but-2-yne is formed, which can be removed under reduced pressure; hence, the equilibrium is shifted towards the formation of a cycle with an integrated triple bond. This method is also employable to linear molecules by acyclic diyne metathesis polymerization. Similarly to the cyclic counterpart, a linear molecule with a triple bond along the chain is obtained. These polyynes are also accessible by ring-opening alkyne metathesis polymerization, in which the driving force is the relief of the ring stress of the monomer.



**Scheme 2:** General reaction of alkyne cross-metathesis, ring-closing alkyne metathesis, as well as ring-opening alkyne metathesis polymerization & acyclic diyne metathesis polymerization.<sup>[47]</sup>

In 1975, Katz *et al.* suggested a mechanism for alkyne metathesis (*Scheme 3*) similar to one that Chauvin had proposed for the olefin metathesis process, which is further explained in chapter *II.1.5. Olefin metathesis*. According to this mechanism, alkyne metathesis is formally a metal-catalyzed [2+2] cycloaddition and subsequent cycloreversion.<sup>[48]</sup> As the catalyst, a metal carbyne (a) is used initiating the catalytic

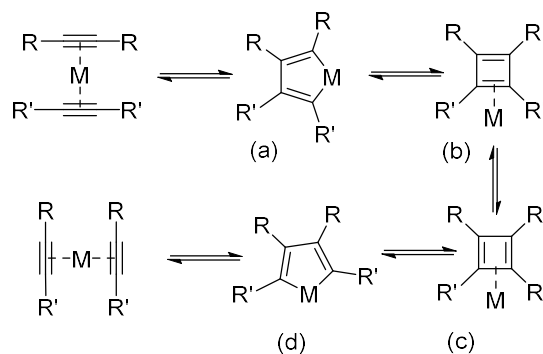
cycle by [2+2] cycloaddition with an alkyne forming a metallacyclobutadiene (b). After rearrangement, the alkyne metathesis product is released and a new metal carbyne species (c) is formed, which again can form a metallacyclobutadiene (d) with an alkyne. In the last step, butyne is generated and the catalytic cycle is closed.<sup>[48]</sup> Alkyne metathesis is a reversible reaction. Therefore, it is necessary to apply a driving force shifting the equilibrium to the desired product. As a gas, butyne can be removed in a practical way by applying a vacuum or a constant stream of inert gas thus pushing the equilibrium towards the products.



**Scheme 3:** Chauvin-like mechanism of alkyne metathesis proposed by Katz *et al.*<sup>[48]</sup>

Mori *et al.* suggested another mechanism (Scheme 4) in which the catalyst metal is coupled oxidatively<sup>[49]</sup> to two alkynes in a [2+2+2] cycloaddition<sup>[50]</sup> forming a metallacyclopentadiene (a). By reductive elimination, cyclobutadiene (b) is formed to which the metal is coordinated. Similar to the metallacyclobutadiene mechanism, an isomerization takes place (c). However, before releasing the metathesis products, again a metallacyclobutadiene is formed in an oxidative addition. By cycloreversion, the metathesis products are released.<sup>[49]</sup>



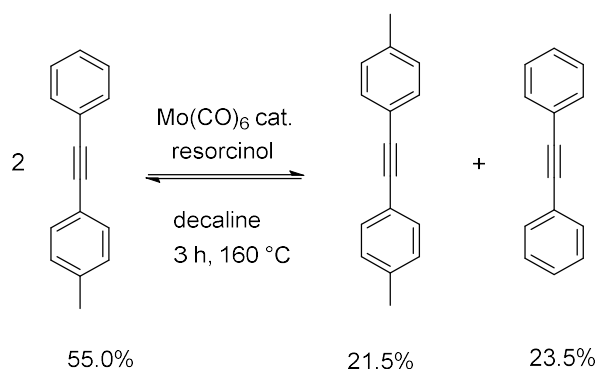


**Scheme 4:** Alkyne mechanism proposed by Mori *et al.*<sup>[49]</sup>

However, Schrock *et al.* confirmed the proposed intermediates spectroscopically; hence, delivered the experimental data suggesting the metallacyclobutadiene mechanism to be more likely.<sup>[48]</sup> The resolving of the reaction mechanism has enabled a more straightforward development of further catalytic systems.

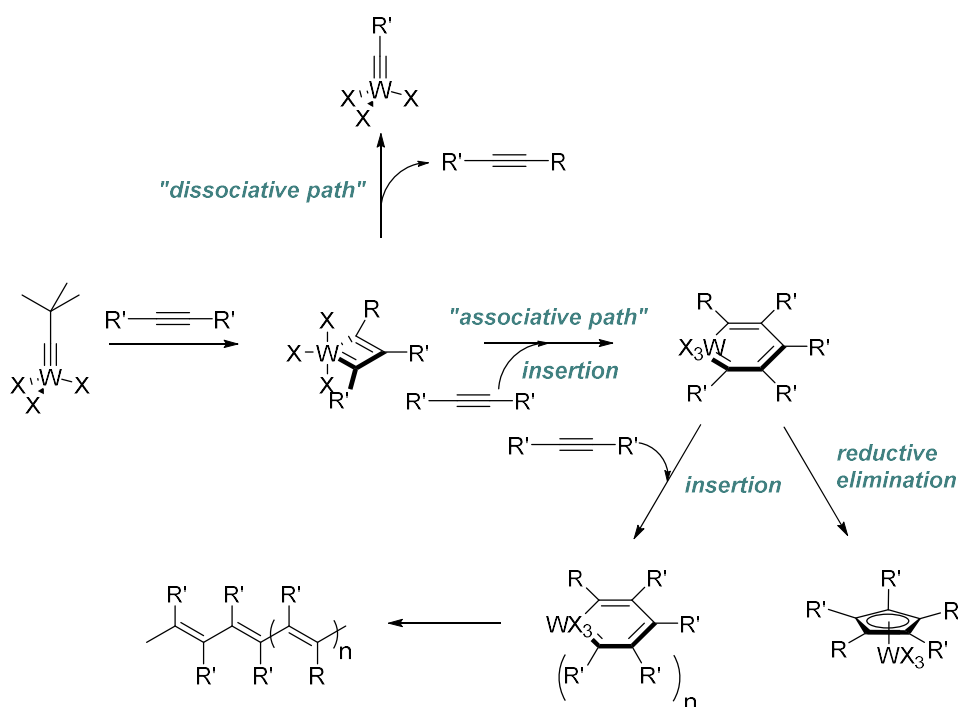
#### II.1.4.2. Alkyne Metathesis Catalysts

When alkyne metathesis was discovered by Penella *et al.* in 1968, the heterogeneous catalyst  $\text{WO}_3$  on silica was applied at high temperatures between 200 and 450 °C, which is impractical for most functional groups.<sup>[48]</sup> Later, Mortreux developed a homogenous catalyst working at lower temperatures of approx. 160 °C. Furthermore,  $\text{Mo}(\text{CO})_6$  is air stable and partly soluble in non-polar solvents. In the presence of resorcinol, a molybdenum alkylidyne is generated *in situ* (Scheme 5).<sup>[51]</sup> The “Mortreux system” has been the first commercially available and practical catalyst for alkyne metathesis, although the applied temperature is still rather high for many functional groups.<sup>[51]</sup>



**Scheme 5:** Alkyne metathesis catalyzed by Morteux system.<sup>[51]</sup>

Schrock *et al.* developed alkylidyne catalysts with the general structure of  $\text{X}_3\text{W}\equiv\text{CR}$ ,<sup>[48]</sup> which is a more efficient catalyst system working at milder conditions and being more selective even in the presence of an olefin.<sup>[51]</sup> The substituent R effects the stability of the catalyst and is cleaved in the first step, thereby affecting the rate of initiation.<sup>[48]</sup> The Schrock system can react with the alkynes in two possible pathways either *via* “dissociative” or “associative pathway” (Scheme 6).<sup>[48]</sup> Only the “dissociative” one leads to an alkyne metathesis. In the “associative pathway”, a reductive elimination takes place causing the degradation of the catalyst.



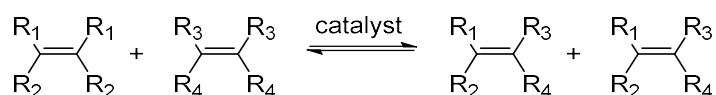
**Scheme 6:** Dissociative and associative pathway during the catalytic cycle of alkyne metathesis.<sup>[48]</sup>

The ionic ligands X (usually alkoxy, phenoxy, or siloxy groups)<sup>[52]</sup> determine which pathway is the favored one. Steric hindrance plays a major role to “shield the tungsten center”;<sup>[48]</sup> hence, while -Cl leads to the “associative path”, bulky ligands such as phenolates and -O<sup>t</sup>Bu show high catalytic activity. However, other bulky ligands such as -NR<sub>2</sub> or -SR lead to degradation as well, which is why the entire system is not yet fully understood and needs further clarification to find the optimal catalyst.<sup>[48]</sup> Another way to increase the stability of alkylidynes against oxygen is the use of a  $\sigma$ -nitrogen donor ligand which can be cleaved off by high temperatures (pyridine, for instance, dissociates at 80 °C). Due to the availability of more efficient and stable catalysts, alkyne metathesis has found its way into standard organic synthesis practices.<sup>[48]</sup> However, in comparison to olefin metathesis, alkyne metathesis plays a comparatively minor role.

## II.1.5. Olefin metathesis

### II.1.5.1. Preface

Olefin metathesis is the reversible, metal-catalyzed rearrangement of the substituents of a double bond (*Scheme 7*).<sup>[47]</sup>



**Scheme 7:** General reaction of olefin metathesis.<sup>[53]</sup>

Generally, the equilibrium can be shifted by a smart design of starting materials, leading to the formation of a volatile related product (e.g., ethylene) which can be practically removed by applying a vacuum or constant inert gas stream, shifting the equilibrium to the desired product. If the related product is removed, the reaction becomes pseudo-reversible, which means that a back reaction to the starting material is not possible anymore.

Similar to alkyne metathesis, several variations of olefin metathesis exist (*Scheme 8*).<sup>[53]</sup> An olefin species can undergo a metathesis reaction either with itself (self-metathesis) or with another olefin species (cross-metathesis). In latter case, the

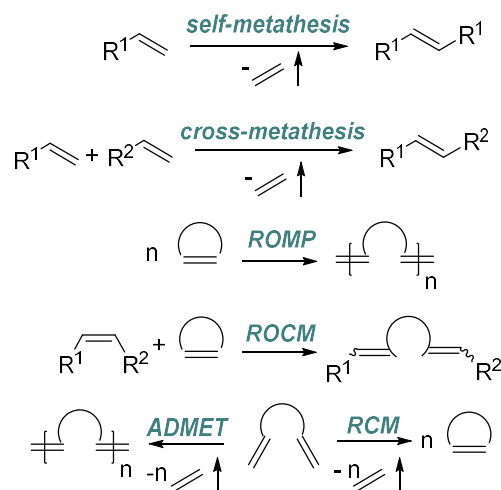
equilibrium can also be shifted by an excess of one of the starting materials. For instance, inner olefins can be cleaved to  $\alpha$ -olefins by a high excess of ethylene. This special form of olefin metathesis is called ethenolysis<sup>[54]</sup> and has become an important application in industry.<sup>[47]</sup>

Strained, unsaturated cyclic molecules can undergo ring-opening metathesis polymerization (ROMP).<sup>[54]</sup> The driving force is the release of the ring stress; hence, ROMP is a pseudo-reversible reaction due to the fact that back reaction towards a strained ring is unfavorable. ROMP was one of the first commercial applications of olefin metathesis, making it an important tool in organic chemistry. In the presence of a second olefin species, ring-opening cross-metathesis (ROCM) can occur, which means that in addition to the ring opening, an arrangement of substituents takes place.<sup>[54]</sup>

Nevertheless, olefin metathesis can be a tool to form cycles under diluted reaction conditions and if the resulting ring is not too strained.  $\alpha, \omega$ -Dienes can undergo such a ring-closing metathesis (RCM). The driving forces are the increasing entropy, since one reactant molecule forms two products, as well as the pseudo-reversibility due to the formation of internal double bonds. Olefin metathesis can be conducted with both terminal double bonds as well as internal ones.<sup>[47]</sup> However, internal double bonds are less reactive compared to terminal ones; this can be used to shift the equilibrium. In the case where the desired product is an unstrained cyclic compound, it is less likely to react back to the starting materials, and therefore the equilibrium is shifted towards the products.<sup>[16]</sup> The removal of related products can shift the equilibrium to the desired side and prevents a back reaction; however, rearrangement and error checking is still possible.<sup>[54]</sup> This means that a chain longer than the targeted cycle, can open and rearrange into the desired cyclic product, but a reaction back to the monomers is not possible. This correction of “overshooting” is explained in more detail in chapter //2.2. *Thermodynamic Approach.*

Instead of RCM, terminal diolefins can undergo acyclic diene metathesis polymerization (ADMET). To control this process, RCM are carried out at low concentrations.<sup>[52]</sup> ADMET allows the synthesis of unsaturated as well as functionalized polymers.<sup>[54]</sup> As a step-growth polymerization, the system can be described by Carother's equation, which means that a very high conversion (> 99%) is

necessary to achieve high molecular weights.<sup>[52]</sup> Therefore, it is necessary that the used catalyst remains active during the entire reaction to prevent a premature stop of the reaction.<sup>[52]</sup>

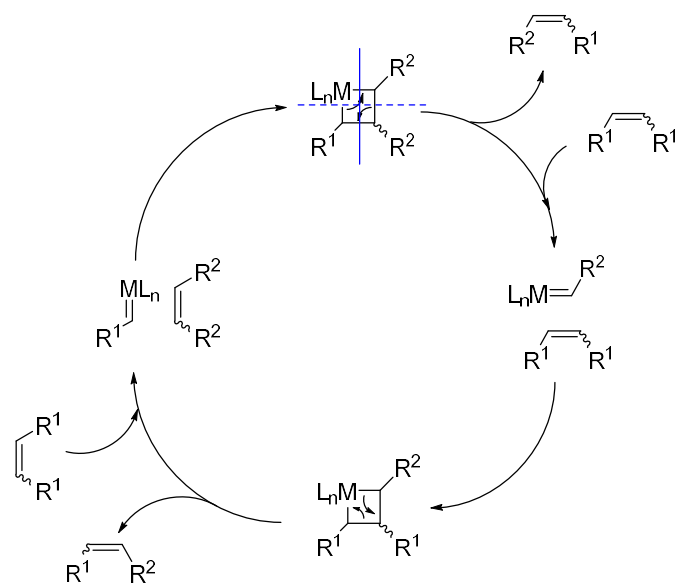


**Scheme 8:** General reaction of self-metathesis, cross-metathesis, ring-opening metathesis polymerization (ROMP), ring-opening cross-metathesis, acyclic diene metathesis (ADMET) polymerization, ring-closing metathesis (RCM).<sup>[53]</sup>

### II.1.5.2. Olefin Metathesis Mechanism & Catalysts

*This chapter was taken from the Master thesis “Efficient Access to Rigid Rings via Metathesis Reactions” written by Gregor Klein in 2015.<sup>[55]</sup>*

In 1971, Yves Chauvin postulated a mechanism for olefin metathesis (*Scheme 9*).<sup>[53]</sup> An olefin carrying the substituent  $R^1$  coordinates to the catalyst, a metal-alkylidene carrying a moiety  $R^2$ . In a [2+2] cycloaddition, a metallacyclobutane intermediate is formed. A subsequent ring-opening can occur in two ways. As a reversible reaction, the cycle can open along the continuous line, resulting in the starting materials. An opening along the dashed line results in the generation of the products: a new olefin species carrying different moieties ( $R^1$  and  $R^2$ ), as well as a metal-alkylidene. In a second step, a metallacyclobutane intermediate is formed and dissolved again, resulting in a new olefin species as well as recovery of the catalyst.<sup>[53]</sup>



**Scheme 9:** Chauvin mechanism of olefin metathesis.<sup>[53,56]</sup>

In 1980, Chauvin's postulation was confirmed by Schrock *et al.* by metathesis of *cis*-2-pentene catalyzed with  $[\text{Ta}(\text{=CH-}t\text{-Bu})\text{Cl}(\text{PMe}_3)(\text{O-}t\text{-Bu})_2]$ .<sup>[53]</sup> This catalyst was the first stable metal-alkylidene complex developed by Schrock *et al.*,<sup>[53]</sup> a property that was attributed to the alkoxide ligands. A series of molybdenum- and tungsten-alkylidene complexes of the general formula  $[\text{M}(\text{=CHCMe}_2\text{Ph})(\text{=N-Ar})(\text{OR}_2)]$  with bulky R groups (*Figure 2*) were reported by Schrock *et al.*, which are the most active catalysts for metathesis. However, these catalysts suffer from high sensitivity towards air and moisture and a lack of tolerance towards functional groups in general.<sup>[53]</sup>

Grubbs developed a new catalytic system with ruthenium as the metal center and phosphine as the ligands. It was proposed that a 14-electron ruthenium intermediate would be created by dissociation of one phosphine ligand, and that it would be able to react with an olefin.<sup>[53]</sup> In contrast to Schrock's catalyst, Grubbs' catalyst shows a high tolerance towards functional groups (except amines, nitriles and basic milieus) and stability against air. The Grubbs' 1<sup>st</sup> generation catalyst has become an important commercially available catalyst.<sup>[53]</sup>

In order to improve the stability of the 14-electron complex, one phosphine ligand has been replaced by an Arduengos cyclic bis-amino carbene ligand. This ligand is an excellent  $\sigma$ -donor without being a  $\pi$ -acceptor. Furthermore, the so-called Grubbs' 2<sup>nd</sup> generation catalyst is more stable against heat and nowadays the most used catalyst

for cross-metathesis reactions (Figure 2).<sup>[53]</sup> A third generation of catalyst was developed by replacing the phosphine with a pyridine ligand, which leads to a strong increase of the initiation rate.<sup>[57]</sup> Therefore, the Grubbs' 3<sup>rd</sup> generation catalyst is the appropriate choice for ROMP reactions at ambient conditions, providing polymers with low dispersity  $\bar{D}$ .<sup>[57]</sup> Hoveyda *et al.* modified the Grubbs' 2<sup>nd</sup> generation catalyst by replacing the phosphor ligand with a chelating oxygen, providing a phosphine free catalyst which is "extremely robust"<sup>[58]</sup> compared to the Grubbs' 2<sup>nd</sup> generation catalyst.<sup>[58]</sup> The olefin metathesis with Grubbs' 1<sup>st</sup> and 2<sup>nd</sup> generation catalyst can be quenched by addition of a large excess of ethyl vinyl ether, which undergoes a metathesis forming a stable Fischer carbene, which means that the catalyst is deactivated and a further reaction is prevented.<sup>[59]</sup>

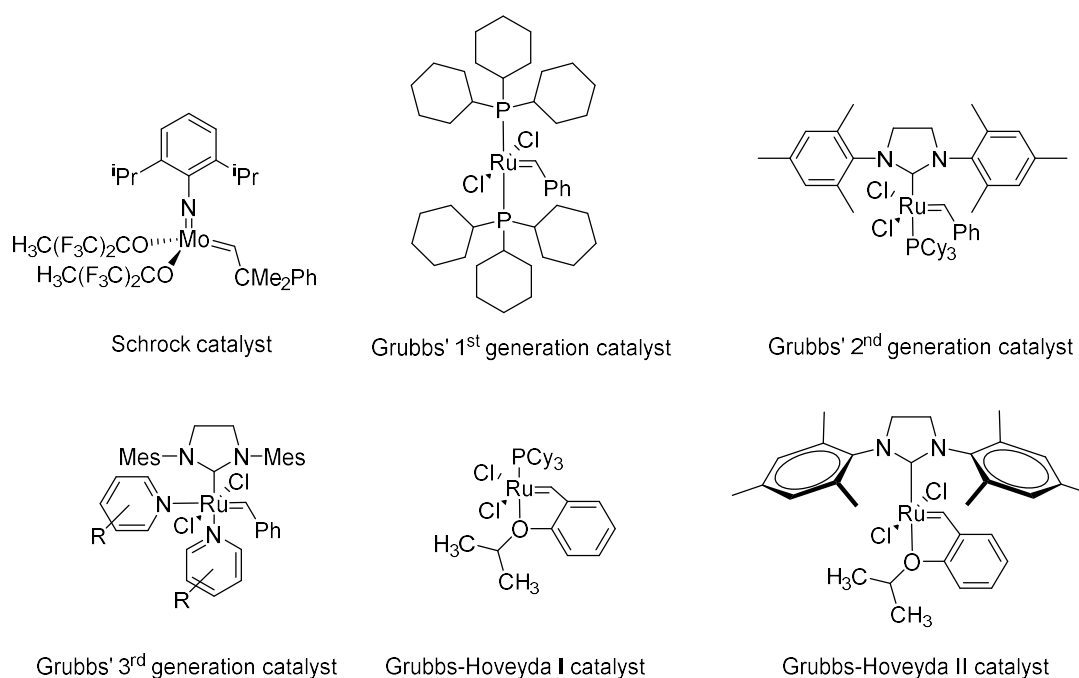


**Figure 2:** Summary of olefin metathesis catalyst; Schrock catalyst, Grubbs' 1<sup>st</sup>, 2<sup>nd</sup> and 3<sup>rd</sup> generation catalyst, as well as Grubbs-Hoveyda I and II catalyst.<sup>[47,53,57,58]</sup>

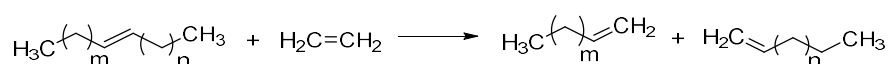
### II.1.5.3. Industrial Application

*This chapter was taken from the Master thesis "Efficient Access to Rigid Rings via Metathesis Reactions" written by Gregor Klein in 2015.<sup>[55]</sup>*

The relevance of olefin metathesis was acknowledged by awarding the Nobel Prize to Chauvin, Grubbs and Schrock in 2005.<sup>[60]</sup> Furthermore, its importance has become

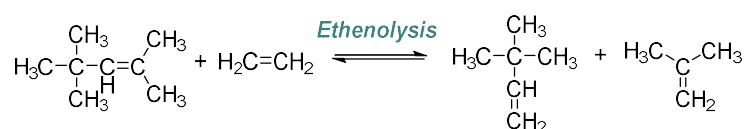
apparent in many applications in industry.<sup>[61]</sup> There, usually heterogeneous catalysts, like metal halogenides (e.g., MoCl<sub>5</sub>, WCl<sub>6</sub>, RuCl<sub>3</sub>/HCl) or metal oxides (e.g., Re<sub>2</sub>O<sub>7</sub>, WO<sub>3</sub>) on Al<sub>2</sub>O<sub>3</sub> or SiO<sub>2</sub>, are used.<sup>[47]</sup> In petro chemistry, the ratio of ethylene and propylene can be regulated by olefin metathesis in order to efficiently satisfy the market demand.<sup>[61]</sup>

In 1977, Shell developed the SHOP (Shell Higher Olefins Process), in which ethylene is oligomerized by a Ni-phosphine complex to obtain long-chained olefins with an even number of carbon atoms (C<sub>10</sub>-C<sub>18</sub>) used in the detergent industry. Undesired long-chained olefins can be cleaved using olefin metathesis with ethylene (*Scheme 10*); hence, desired chain lengths from C<sub>11</sub> to C<sub>14</sub> can be obtained.<sup>[61]</sup>



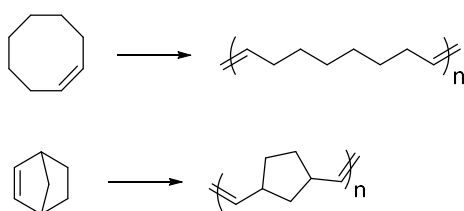
**Scheme 10:** Ethenolysis of long-chains olefins.<sup>[61]</sup>

A further application of ethenolysis is demonstrated by the production of neohexene from diisobuten and ethylene (*Scheme 11*), which is used in the perfume industry.<sup>[61]</sup>



**Scheme 11:** Production of neohexene process.<sup>[47]</sup>

Furthermore, industrial polymers can be synthesized by olefin metathesis. Starting from cyclooctene, polyoctenamers can be obtained by ROMP, whereas polynorbornenes are produced from norbornene (*Scheme 12*). Both polymers can be used as rubber material.



**Scheme 12:** Olefin metathesis for the production of industrial polymers.<sup>[61]</sup>

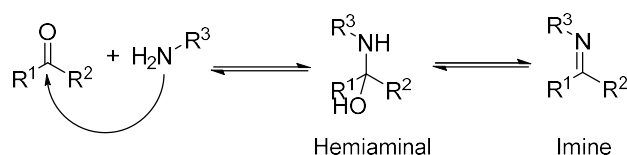


## II.1.6. Imine Condensation

### II.1.6.1. Preface

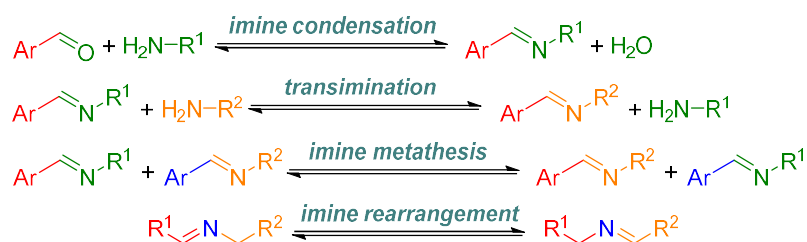
Imine reactions are a dynamic exchange of C-N bonds similar to hydrazones and oximes and represent some of the most used reversible reactions.<sup>[21]</sup>

The imine is formed by nucleophilic attack of an amine at the carbonyl carbon of an aldehyde or ketone *via* hemiaminal as an intermediate.<sup>[10]</sup> The reaction is completed by the elimination of water giving the imine, also called “Schiff’s base” (after the man to report them first, Hugo Schiff in 1864), with the general formula  $R^1R^2C=NR^3$  and is the nitrogen analog of aldehydes and ketones (*Scheme 13*).<sup>[62]</sup>



**Scheme 13:** General reaction equation of imine condensation.<sup>[62]</sup>

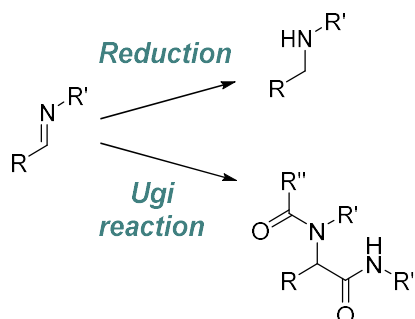
There are four types of imine reactions (*Scheme 14*). The reaction of an aldehyde or ketone with an amine as described before is called “imine condensation”, its back reaction “hydrolysis”, which occurs under acidic conditions. A reaction with another amine can lead to an “exchange”<sup>[24]</sup> of the substituents, also called “transimination”.<sup>[10]</sup> The composition of the product is influenced by the basicity of the amine. The more basic the amine, the more stable the corresponding imine is. Hence, the structure of the amine, including the presence of resonance stabilization as well as electron pushing or withdrawing groups, has a crucial impact on the equilibrium composition.<sup>[10]</sup> Furthermore, Lewis acids, such as Sc(OTf)<sub>3</sub>, catalyze the exchange efficiently.<sup>[63]</sup> Imines with different moieties can also exchange their substituents, a process which is called “imine metathesis”.<sup>[24]</sup> A fourth reaction is “imine rearrangement”, in which the double bond between nitrogen neighboring carbons is exchanged.<sup>[10]</sup>



**Scheme 14:** General equations of four different imine reactions.<sup>[10,24]</sup> [10]

Due to their reversible character, it is possible to shift the equilibrium of the reactions in, by, for instance, excess and removal of relative products, concentration, pH, and temperature, as well as steric and electronic effects.<sup>[24]</sup>

By quenching, the equilibrium can be “frozen” (Scheme 15). A typical quenching reaction is the reduction of the imines to the corresponding amines (reductive amination), e.g., with NaBH<sub>4</sub>, as well as the transformation into an amide by Ugi reaction with an isocyanide and an acid.<sup>[10]</sup> A back reaction is not possible anymore and the mixture can be handled and characterized without changing its composition.<sup>[20]</sup>



**Scheme 15:** Quenching of an imine by reduction and by Ugi reaction.<sup>[10]</sup>

### II.1.6.3. Application

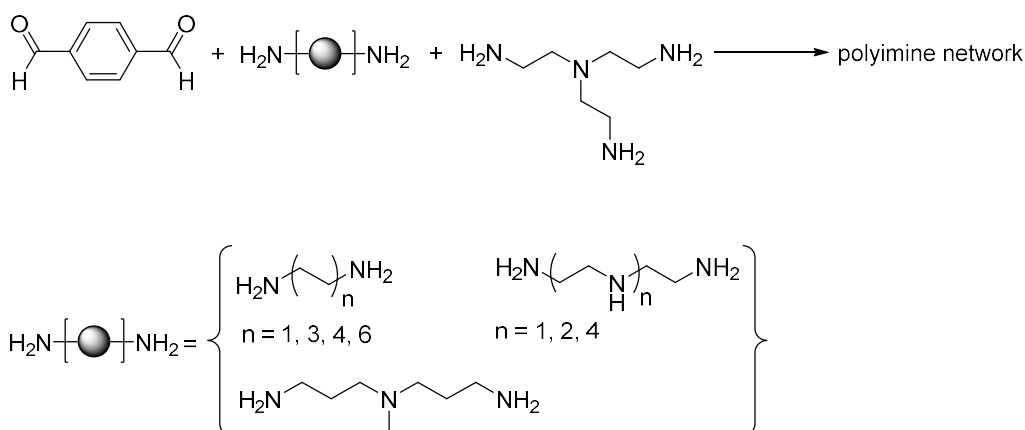
Imines are challenging to isolate due to their sensitivity towards hydrolysis; however, imines play an important role in many mechanisms, for example as intermediates in Strecker synthesis and Ugi reaction.<sup>[62]</sup> By removing the water, which is the condensation product, the imines can be isolated. Before practical characterization methods were established, imines had been used for the characterization of aldehydes and ketones. Hydrazine derivatives such as hydroxylamine, 2,4-dinitrophenylhydrazine and semicarbazide react with aldehydes and ketones to highly

crystalline imines with sharp melting points. By comparing the experimental melting points with the ones from existing libraries, aldehydes and ketones could be identified by this method.<sup>[62]</sup>

On the one hand, their sensitivity towards hydrolysis prevents imines from being used as isolated substances at large, industrial scale<sup>[62]</sup>; on the other hand, the reversibility can be seen as an advantage in the context of applications in responsive materials. Dynamic covalent bonds can be applied as cross-linkers between polymer chains. The resulting polymer networks can be broken by an external stimulus (pH, moisture, temperature);<sup>[25]</sup> hence, thermal and mechanical properties of the material drastically change. By regenerating the dynamic covalent bonds, the network is reobtained, which gives the material properties such as the ability for self-healing, reshaping, recycling and welding.<sup>[64]</sup>

Imine condensation is a suitable reaction for such a material, as it is also covalent and dynamic. As a stimulus, water or heat can be applied to initiate the back reaction. Furthermore, the reaction is relatively fast, can proceed without any catalyst and shows tolerance to a wide spectrum of other functional groups. The starting materials are widely used; hence, they are either commercially available or established experimental protocols exist for their preparation.<sup>[64]</sup>

Zhang *et al.* synthesized different polyimine networks varying the hydrophilicity of the amine monomer (*Scheme 16*). Longer carbon chains lead to an increased tensile strength and higher elastic modulus, which results in more elasticity on one hand; on the other hand, the glass transition temperature is decreased. For self-healing, moisture was applied as an external stimulus. The sensitivity towards the stimulus was tuned by hydrophilicity. Hydrophilic networks healed at room temperature already, while hydrophobic ones required higher temperatures.<sup>[64]</sup>

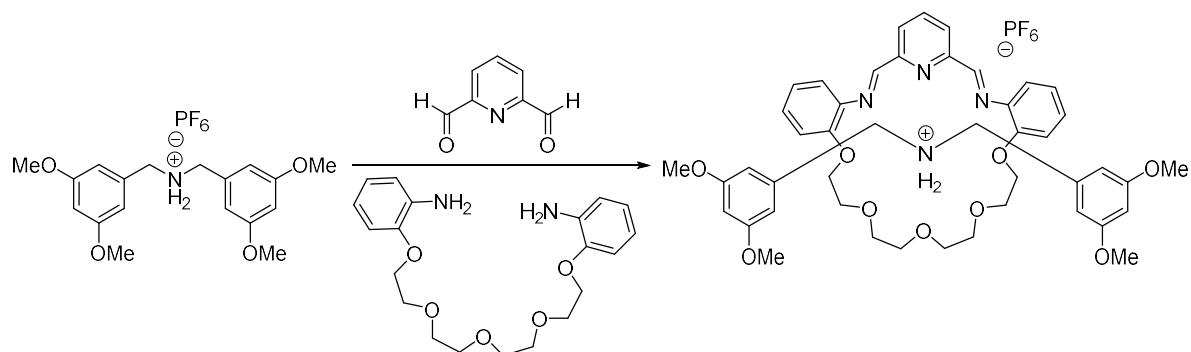


**Scheme 16:** Synthesis of self-healing polyimine networks.<sup>[64]</sup>

Furthermore, as part of DCvC, imines play an important role in the synthesis of catenanes, rotaxanes and knots, so called mechanically interlocked molecules (MIMs),<sup>[65]</sup> the relevance of which is indicated by the Nobel prize for Fraser Stoddart, Jean-Pierre Sauvage and Ben Feringa for their research on “molecular shuttles, switches, and machines”<sup>[65]</sup> in 2016. An efficient procedure to form catenanes is the “clipping” method. In this method, three components are necessary, which come to a close range, e.g., by forming a complex. Subsequently, two of these components react with each other to form a macrocycle in which the third one is trapped. With this strategy, it is possible to mechanically interlock<sup>[66]</sup> two rings in each other to form catenanes, or to catch a ring “around [a] dumbbell”<sup>[67]</sup> to form rotaxanes. The catching is a statistic process; hence, there always will be components which react without getting caught in each other when forming the free macrocycles. In a kinetic approach, this would significantly reduce the yield; however, by thermodynamic control, the bonds can open again, giving another chance to form the desired compound, which can, once the equilibrium is formed, be transformed into kinetically trapped, stable products.<sup>[67]</sup>

In 2001, Stoddart *et al.* synthesized a [2]rotaxane by imine condensation by the clipping method.<sup>[66]</sup> 2,6-Pyridinedicarboxaldehyde and tetraethylene glycol *bis*(2-aminophenyl)ether were the two components, which formed the cyclic compound, a [24]crown-8-like macrocycle, by imine condensation (Scheme 17). These two components formed a complex with a dialkylammonium, which was the center of a dumbbell molecule. Bulky substituents at both ends enabled the mechanical interlocking in the final molecule. The equilibrium was reached within four minutes and

was frozen by transforming the imines into the corresponding amines. The desired rotaxane was obtained in 70% yield after purification by column chromatography. Characterization by FAB mass spectrometry confirmed the stoichiometry of the predicted compound and by  $^1\text{H-NMR}$  spectroscopy and X-ray crystal structure, the interlocking was revealed. [66]



**Scheme 17:** Synthesis of a [2]rotaxane by imine condensation. [66]

## II.2. Shape-persistent Macrocycles

Rigid macrocycles are often referred to as shape-persistent macrocycles. Generally, shape-persistent macrocycles are cyclic compounds with a rigid structure in contrast to flexible cycles, like cycloalkanes or crown ethers. A more precise definition is that shape-persistent macrocycles have a diameter  $d$  which is equal to the contour length of their molecular backbone  $l$  divided by  $\pi$  (Equation 1).<sup>[2]</sup>

$$d = \frac{l}{\pi}$$

**Equation 1:** Equation to define shape-persistent macrocycles.<sup>[2]</sup>

Apart from the rigid structure of the cycle that influences the properties and supramolecular structure, the substituents, which have a defined position due to the rigid character of the molecule, also affect the overall properties. These characteristics define the “shape-persistent” and “cyclic” aspect. According to this definition, benzene would be a shape-persistent macrocycle; hence, a more precise definition is necessary to explain the “macro” qualifier which is defined by Höger as “an inside cavity in the size range from slightly less than 1 nm up to several nanometers”.<sup>[10]</sup>

Due to the large  $\pi$ -system, shape-persistent macrocycles show strong  $\pi$ - $\pi$  stacking and the space on the inside causes the cycles to form porous structures. The substituents have a large effect on the assembly behavior. Orthogonal polar substituents pointing out of the cycle plane tend to result in the formation of a tubular superstructure in the solid state (Figure 3, A). When the polar substituents point out of the cycle, but lie within the cycle plane, the cycles tend to form 2D networks in the solid state and then assemble into stacks to form pores (Figure 3, B).<sup>[1]</sup> Zhang *et al.* synthesized a macrocycle carrying hydroxy-groups on the outer rim which self-assembled into a porous two-dimensional network connected through hydrogen bonds with channels of about 9 Å (Figure 4).<sup>[5]</sup> If polar substituents point into the ring, the cycles can act as host-molecules and take up guest-molecules (Figure 3, C).<sup>[2]</sup> The behavior of non-polar moieties depends on their length: alkyl chains up to nine carbons tend to point laterally out of the cycle. Accordingly, the macrocycles assemble face to face. Once the number of carbons grows larger, the alkyl chains point up or down and

form an own layer. This leads to the formation of an alternating aryl-alkyl packing (Figure 5).<sup>[68]</sup>

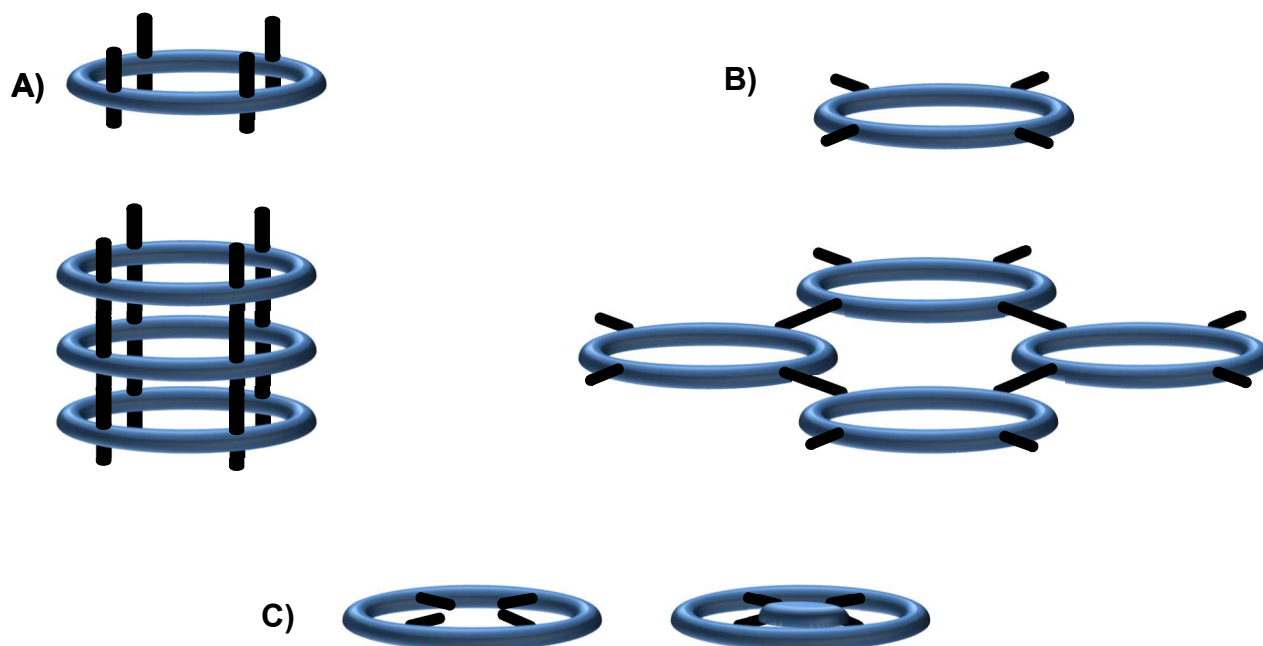


**Figure 3:** Illustrative depiction of macrocycles (blue) indicating the influence of side groups (black) on the superstructure upon the self-assembly in tubes (A) and stacked layers (B). Polar side groups, which point into the ring, can act as host-molecules (C).<sup>[2]</sup>

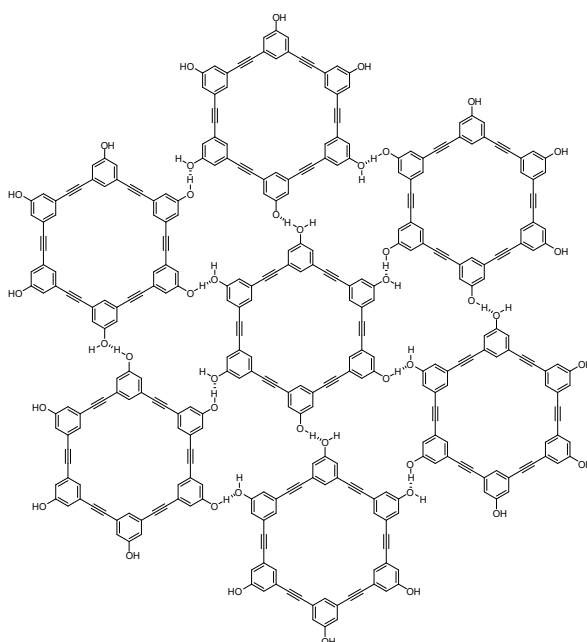


**Figure 4:** Schematic representation of the formation of a two-dimensional network by shape-persistent macrocycles via hydrogen bonds amongst the hydroxyl groups present on the outer rim of the macrocycles.<sup>[5]</sup>

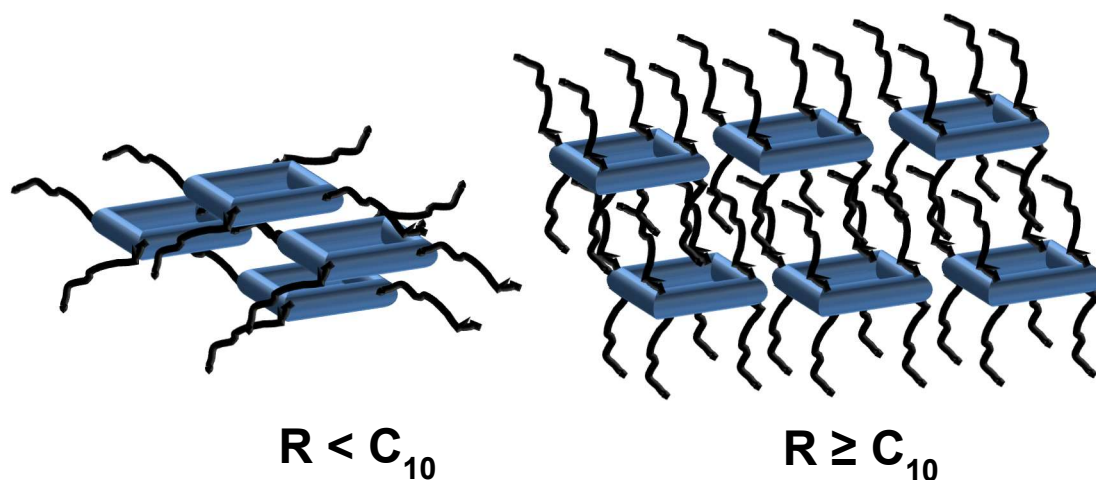


**Figure 5:** Illustrative depiction of arrangement of shape-persistent macrocycles depending on the length of their non-polar substituent:  $\pi$ -like stacks for side groups less than 10 carbons atoms (left) and intercalated porous structures for side groups with 10 carbons atoms or more (right).<sup>[68]</sup>

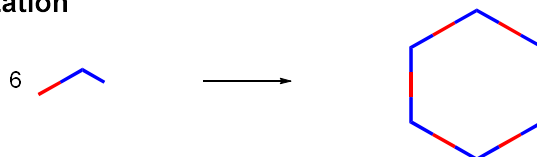
There are four major strategies to synthesize macrocycles for both the kinetic and the thermodynamic approach; however, under thermodynamic control cyclooligomerization is usually the method of choice (*Scheme 18*):

- a) Cyclooligomerization
- b) Intramolecular ring-closure of  $\alpha,\omega$ -difunctionalized oligomers
- c) Intermolecular coupling between two or more fragments
- d) Template cyclization of two or more fragments

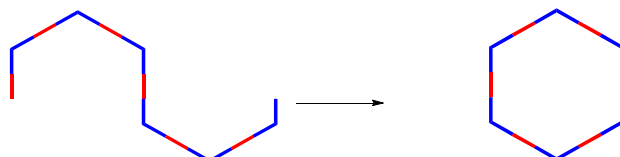
All of these approaches exhibit both advantages and challenges, which are further explained in chapter *II.2.1. Kinetic Approach*. Subsequently, in chapter *II.2.2. Thermodynamic Approach* it is explained why cyclooligomerization is the common method for thermodynamic control.



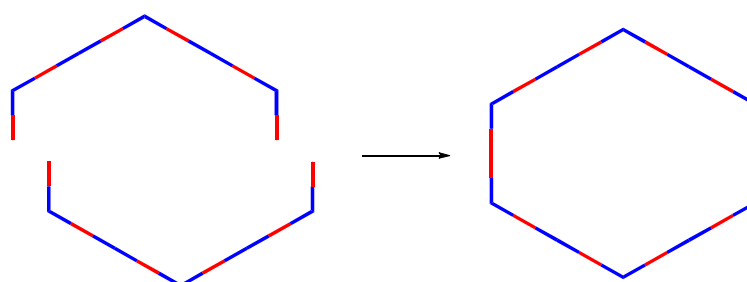
a) Cyclooligomerization



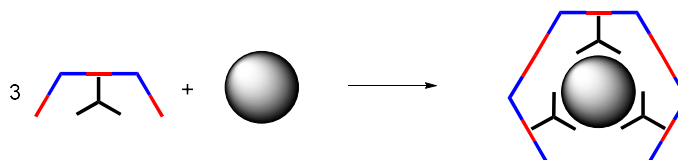
b) Intramolecular ring closure of  $\alpha,\omega$ -difunctionalized oligomers



c) Intermolecular coupling between two or more fragments



d) Template cyclization of two or more fragments



**Scheme 18:** Schematic display of methods of kinetic approach. <sup>[69]</sup>

## II.2.1. Kinetic Approach

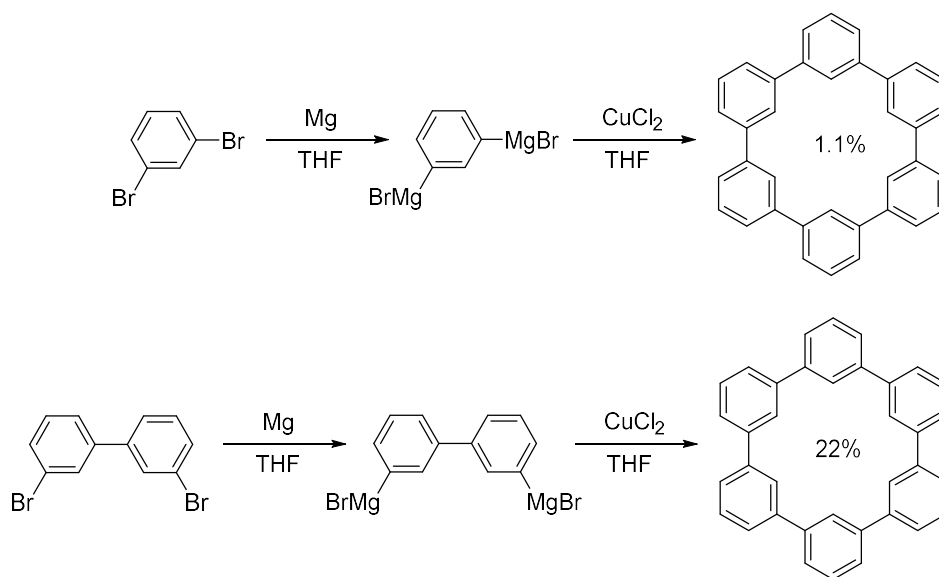
### II.2.1.1. Cyclooligomerization *via* the Kinetic Approach

In cyclooligomerization, monomers are linked together covalently, usually through a Grignard reaction or coupling reactions (Sonogashira, Negishi or Glaser). Due to their rigidity, arylenes do not show high flexibility, which facilitates a cyclization, thus are often the base of such rigid macrocycles. Furthermore, they are interesting monomers for conjugated systems and carbon rich materials.

On the one hand, cyclooligomerization is practical, because complex synthesis of building blocks is not necessary; on the other hand, it can be difficult to force a cyclization and prevent the formation of linear oligomers. In the kinetic approach, once

a bond is formed, it cannot be broken due to the irreversible character of the reaction. Therefore, such a synthesis strategy bears the risk of “overshooting”,<sup>[69]</sup> which means that a linear oligomer continues to grow in a linear way instead of reacting intramolecularly to form a cycle. In this way, the yield of the obtained macrocycle is reduced.<sup>[69]</sup>

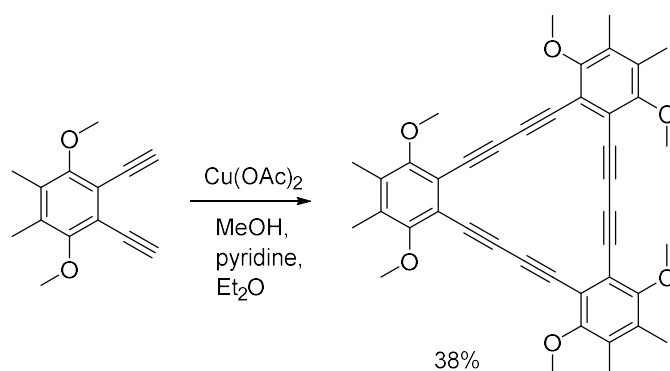
Despite these challenges, Staab and Binning reported the formation of a six-membered rigid macrocycle by a Grignard reaction in 1966 (*Scheme 19*).<sup>[70]</sup> The biphenylic di-Grignard monomers were linked together by a copper-catalyzed Grignard reaction and formed a mixture of linear and cyclic compounds. Hexa-*m*-phenylene was obtained in 22% yield next to traces of larger cyclic compounds, such as octa-*m*-phenylene (1.8%) and deca-*m*-phenylene 0.1%, as well as linear oligomers up to a length of five monomer units (deciphenyl).<sup>[70]</sup> On the contrary, the use of a monophenyl monomer led to only 1.1% yield of six-membered macrocycle. This shows how a smart choice of monomer with a pre-shaped structure design benefits a cyclization.<sup>[70]</sup>



**Scheme 19:** Schematic representation of the synthesis of a six-membered macrocycle by cyclooligomerization via a Grignard reaction with a phenyl monomer (top) and a biphenyl monomer (bottom).<sup>[70]</sup>

In 2004, Komatsu and co-workers synthesized a trimeric macrocycle *via* cyclooligomerization in one step in 38% yield in a copper-mediated oxidative coupling (*Scheme 20*), which is an alternative to the Grignard reaction to form carbon-carbon

bonds and do not require a Grignard reagent.<sup>[71]</sup> However, the yield drops significantly when larger cycles are aimed for due to “overshooting” and the low solubility of the growing oligomers, as it was illustrated by Staab and Neunhoeffer. Targeting a 30-membered phenyleneethynylene macrocycle by cyclooligomerization *via* Stephens-Castro coupling of the copper salt of *m*-iodophenylacetylene yielded only 4.6% of the desired compound.<sup>[72]</sup>



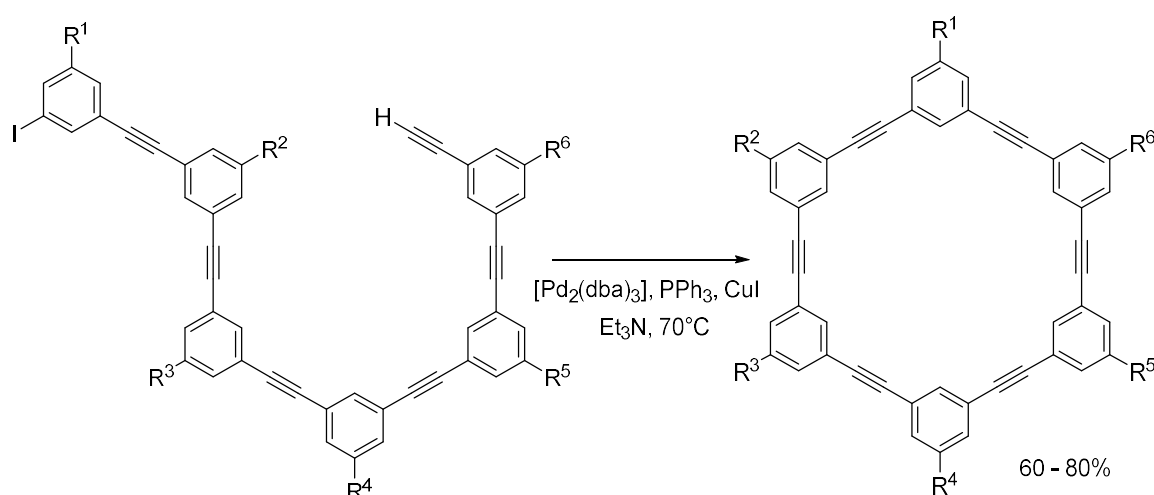
**Scheme 20:** Synthesis of a trimeric macrocycle by cyclooligomerization by copper-mediated oxidative coupling.<sup>[71]</sup>

### II.2.1.2. Modular Synthesis

Contrary to the cyclooligomerization, in method b, c and d (*Scheme 18*), namely intramolecular ring-closure of  $\alpha,\omega$ -difunctionalized oligomers, intermolecular coupling between two or more fragments and template cyclization of two or more fragments, the cycles are built up modularly; hence, the modules have to be synthesized beforehand. This often requires a multi-step procedure including protection, deprotection and purification (e.g., by column chromatography) steps. Although the yield of the individual reactions can be rather high,<sup>[10]</sup> the high number of reactions necessary means a rather impractical synthetic strategy with low overall yield.<sup>[73]</sup> Furthermore, method b (*Scheme 18*), namely intramolecular ring-closure of  $\alpha,\omega$ -difunctionalized oligomers, has to be carried out at high dilutions ( $< 1 \text{ mM}$ ) to favor an intramolecular ring-closure before an intermolecular oligomerization reaction, increasing the required reaction time.<sup>[69]</sup> In method c and a (*Scheme 18*), namely cyclooligomerization and intermolecular coupling between two or more fragments, high dilution cannot be applied because two building blocks need to meet and react with each other. After forming a linear oligomer intermolecularly, the subsequent ring-closure is

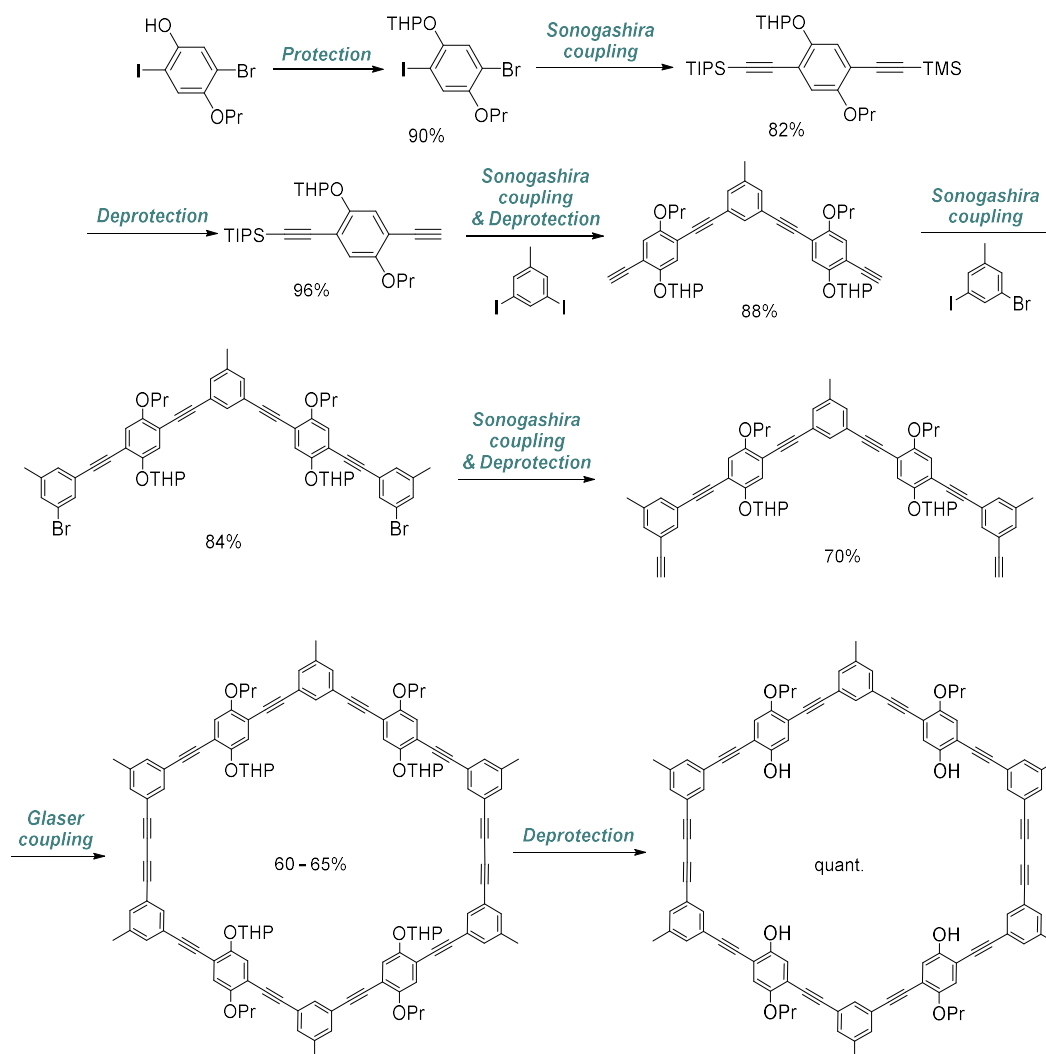
intramolecular. As possible side reactions, an intermolecular reaction with another building block can occur, decreasing the yield. As a possible solution, the application of a template can prevent the generation of those side products; however, at the cost of an extra step required: the template has to be removed after cyclization.

Moore *et al.* reported the synthesis of a phenyleneethynylene macrocycle in yields between 60 – 80% by intramolecular Sonogashira coupling of an  $\alpha,\omega$ -asymmetric six-membered oligomer (Scheme 21).<sup>[74]</sup> Compared to yields of the cyclooligomerization method, this result is herein considered a big step forward. However, the used precursors have to be synthesized in multi-step reactions decreasing the overall yield (an exact yield for the synthesis of the sequence is not given).<sup>[74]</sup>



**Scheme 21:** Schematic representation of the intramolecular ring closure of  $\alpha,\omega$ -asymmetrical six-membered oligomer by Sonogashira coupling.<sup>[74]</sup>

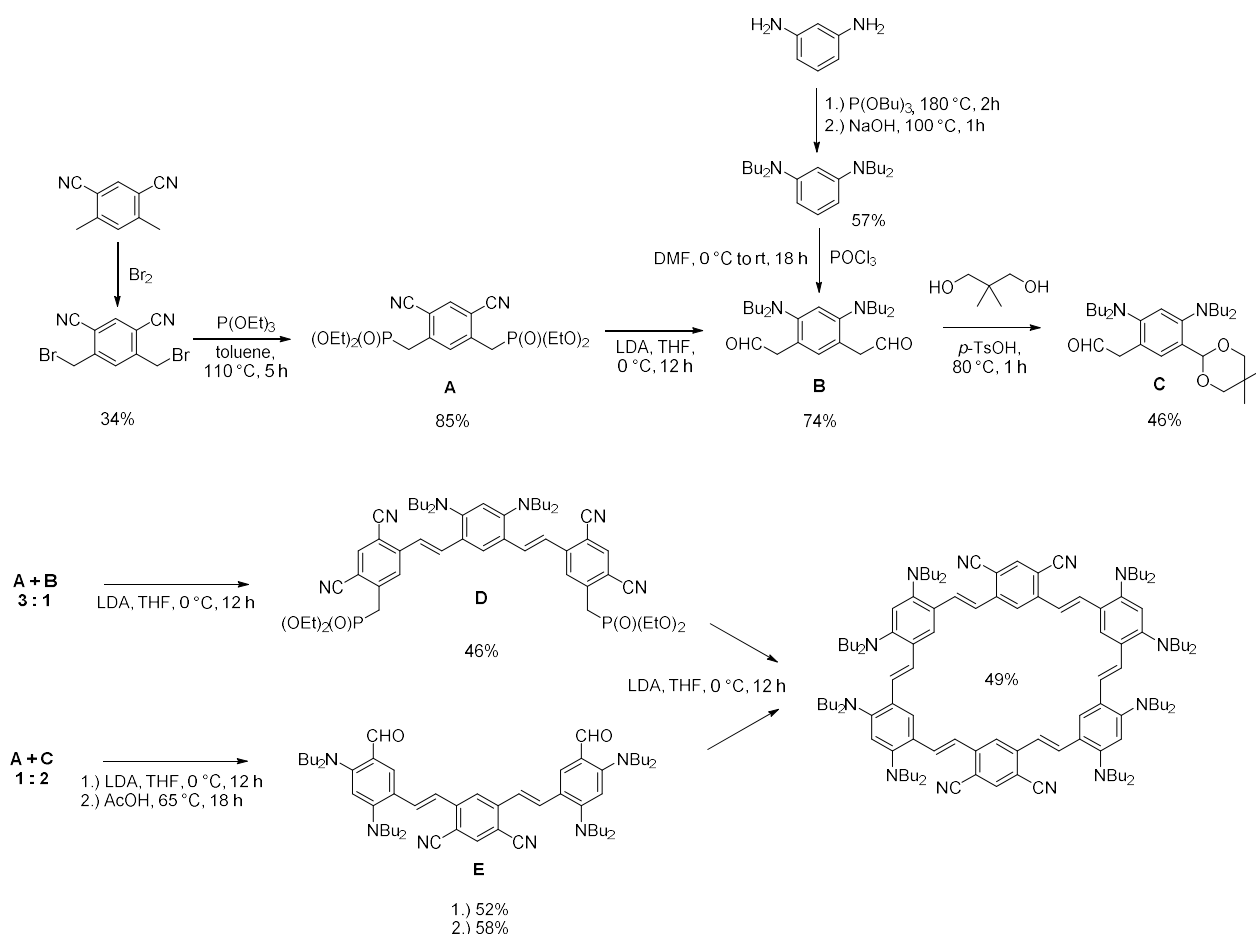
Analogous to the intramolecular coupling, the intermolecular coupling of two “half-rings” *via* Glaser coupling (Scheme 22) to form a cycle has been reported in a moderate yield of 60-65%; however, not only the cycle was formed but a broad mixture of many high molecular substances.<sup>[75]</sup> After isolation by recrystallization, the yield dropped to 40-45%.<sup>[76]</sup> Furthermore, the bisacetylene precursor was obtained in 37% overall yield in a multi-step synthesis including several protection, cross-coupling and deprotection steps.<sup>[75]</sup>



**Scheme 22:** Schematic representation of the synthetic pathway followed for the preparation of large macrocycles by the intermolecular reaction of two “half-rings” coupling.<sup>[75]</sup>

This approach is not limited to the synthesis of ethynyl-linked macrocycles. Cho *et al.* obtained a six-membered olefine macrocycle by modular synthesis.<sup>[77]</sup> The building blocks were synthesized in a multi-step process (*Scheme 23*): first, 1,3-dicyano-4,6-dimethylbenzene underwent bromination and subsequent phosphorylation to obtain the first precursor building block A with an overall yield of 29%. The alkylation of *m*-phenylenediamine with P(OBu)<sub>3</sub> and subsequent formylation provided the building block precursor B in an overall yield of 42%. B was used for the further reaction to C, which was obtained by the mono-protection with neopentyl glycol at a yield of 46%. Afterwards, A and B as well as A and C proceed were used to prepare building blocks

D (46% yield) and E (30% yield), respectively, by a Horner-Wadsworth-Emmons reaction, with E requiring an extra deprotection step. Finally, both building blocks were linked together by a Horner-Wadsworth-Emmons reaction, which allowed the stereoselective formation of the *E*-double bond in 49% yield. When every step is taken into account, the overall yield is relatively low (0.4%), a testament to the inefficiency of the kinetic approach.

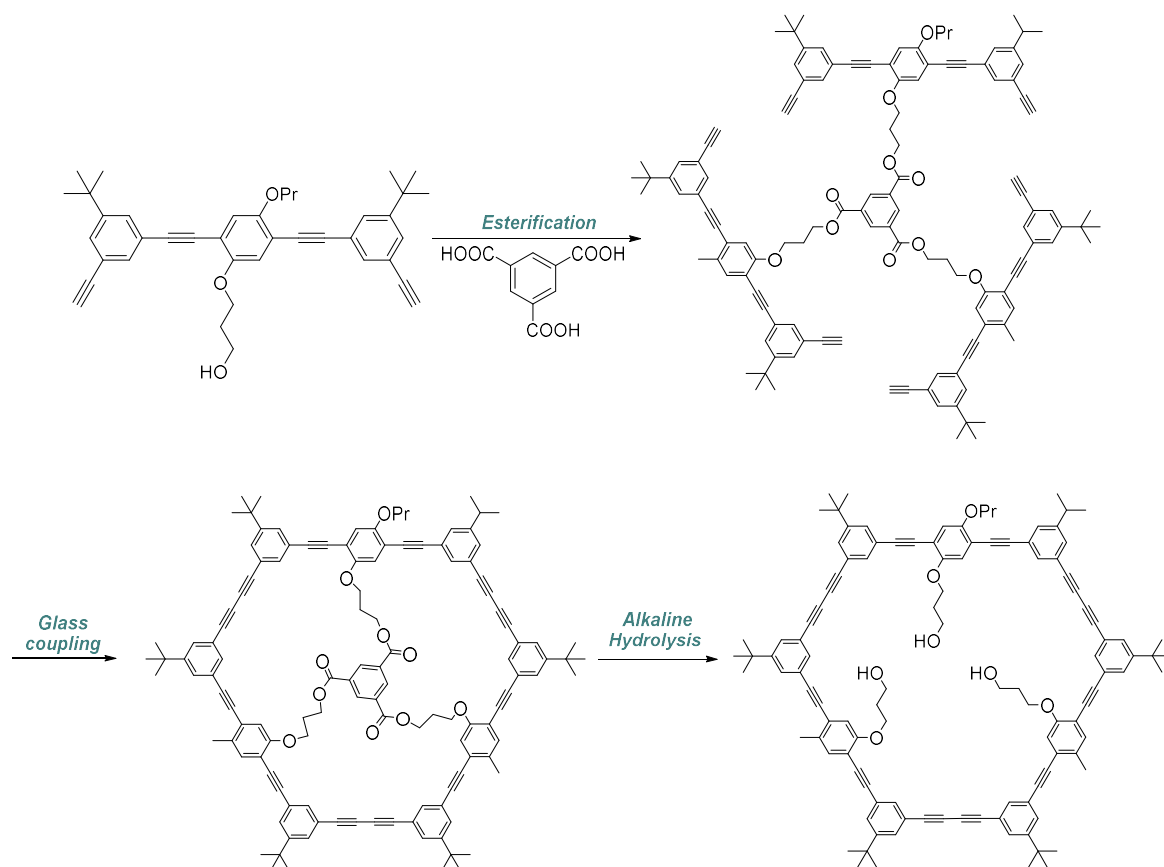


**Scheme 23:** Schematic representation of the multi-step synthesis of a six-membered olefin macrocycle.<sup>[77]</sup>

### II.2.1.3. Template Cyclization

Applying the same synthesis strategy as Moore in *Scheme 22* using subsequent cross-coupling, protection and deprotection steps,<sup>[75]</sup> Höger *et al.* synthesized a cyclic trimer using “thirds of a ring”<sup>[76]</sup> as building blocks. However, in the crude product mixture, only 20-25% of the desired cycles were present according to SEC.<sup>[76]</sup> This indicates, that depending on the sizes and the shapes of the desired macrocycles, the method

of intermolecular coupling between two or more fragments is limited.<sup>[76]</sup> The use of a template can help overcome this limitation (*Scheme 24*). Trimesic acid was used as a core molecule which was connected *via* flexible linker molecules, namely alkyl chains, to the rigid “third of a ring”-building blocks, forcing them into direct neighborhood and thereby making an intramolecular reaction more likely than an intermolecular one. As such, the desired macrocycle was obtained in 94% yield.<sup>[76]</sup>



**Scheme 24:** Schematic synthetic pathway of a trimeric cycle by application of a template.<sup>[76]</sup>

Although, the application of a template can help to increase the yield of the desired macrocycle, there is still a high practical effort to synthesize the precursors and to undergo the whole procedure of inserting and removing the template. Furthermore, the removal of the template itself can be a problem.<sup>[10,78]</sup>

Nevertheless, the kinetic approach has its advantages: a broad spectrum of different coupling reactions can be applied, allowing a broad range of functional groups to be incorporated. By the sequence-defined synthesis of the precursor, building blocks carrying different moieties and functional groups can be inserted at defined positions

in the resulting macrocycle. Furthermore, the use of *ortho*-, *meta*- and *para*-phenyleneethynylene fragments, makes the synthesis of cycles of different sizes and shapes possible.<sup>[69,79]</sup>

## II.2.2. Thermodynamic Approach

In contrast to the kinetic approach, the thermodynamic approach offers high yields and a broad variety of macrocyclic compounds synthesized by DCvC due to reversible nature of the reaction, which can overcome errors. Therefore, the impractical synthesis of building blocks is herein considered obsolete, being replaced by cyclooligomerization. Longer oligomers due to “overshooting” are no longer considered by-products, as they can re-arrange into smaller oligomers which in turn can result to the desired product.<sup>[69]</sup> Decisive for the resulting product is the free relative energy between the desired product and the possible linear and cyclic oligomers (*Figure 6*).

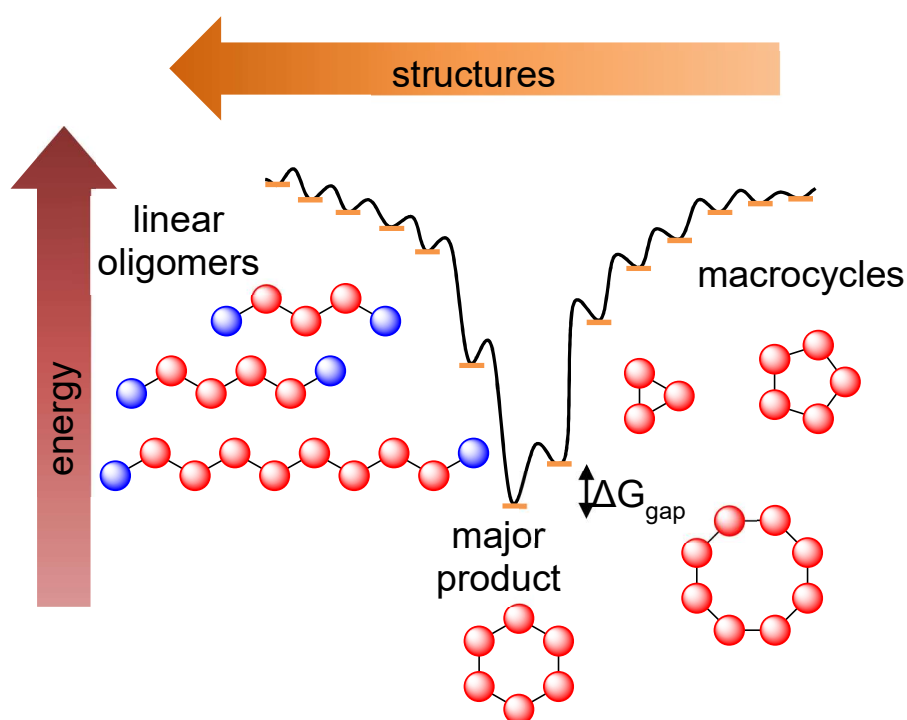


**Figure 6:** Energy landscape of the cyclooligomerization: The larger the energy gap ( $\Delta G_{\text{gap}}$ ) between the thermodynamically favored product and by-products, the easier the equilibrium is established.<sup>[69]</sup>

Entropy favors macrocycles consisting of the smallest possible number of monomers.<sup>[80]</sup> While one might wonder how larger cycles are thus obtainable, without

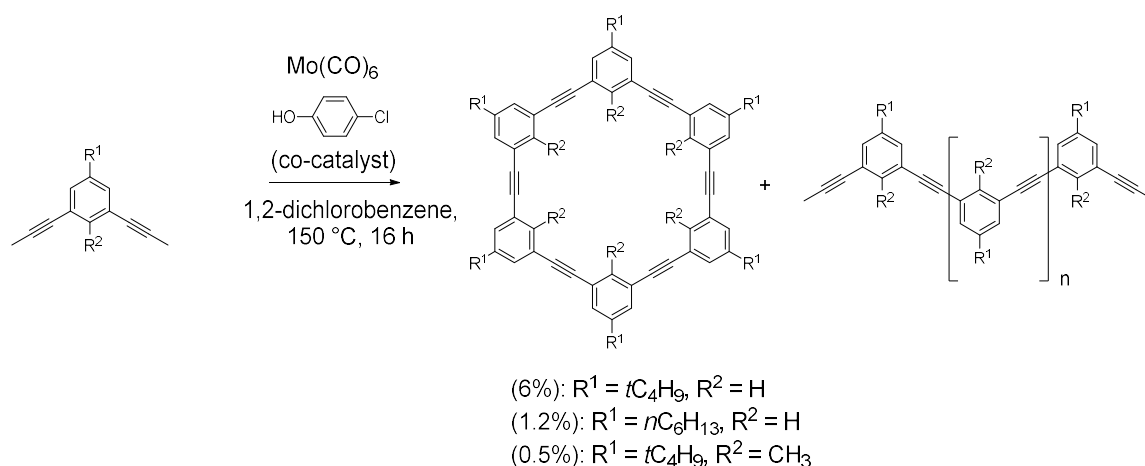


requiring the strenuous preparation of large building blocks, it is noted that the thermodynamic parameter is rather significant. Indeed, thermodynamic control enables to avoid this problem by using rigid monomers instead of flexible ones. Depending on the structure of the monomer, the smallest macrocycle may not be the most favored one as, due to the rigid structure, the angles for the smallest numbers of monomer units would cause an unfavorable cycle strain. These enthalpic parameters compensate for the entropy, giving kinetical control over the sizes of shape-persistent macrocycles in comparison with flexible ones.<sup>[69]</sup> By cyclooligomerization, it is possible to target one particular product within a broad range of macrocycles of different sizes and shapes through the smart design of monomers purporting angles similar to those of the desired macrocycles.<sup>[69]</sup> Furthermore, the selectivity towards one particular product can be increased by adjustment of certain reaction conditions (*e.g.*, solvent, temperature) or by templating.<sup>[20]</sup> Several reversible bonds have been successfully used in thermodynamic approach, such as disulfides<sup>[81]</sup>, imines<sup>[82]</sup>, olefins<sup>[16]</sup> and alkynes<sup>[83]</sup>.

### II.2.2.1. Shape-persistent Macrocycles *via* Alkyne Metathesis

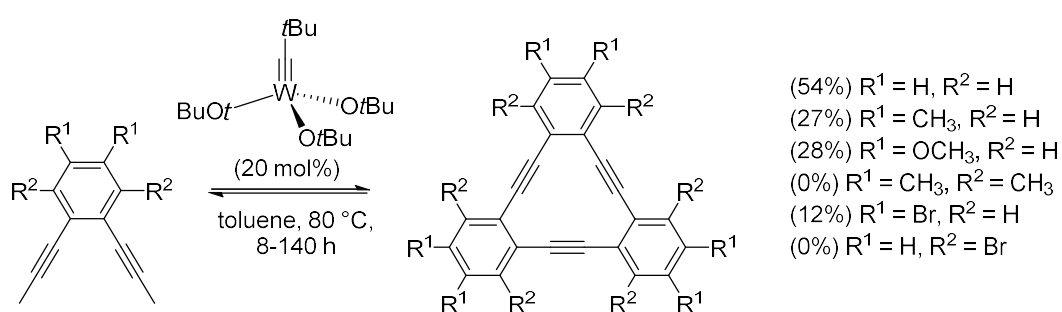
#### *a) Influence of the Catalytic System*

In 2000, Bunz *et al.* reported the synthesis of arylene-ethynylene macrocycles (AEMs), a shape-persistent type of macrocycle, *via* cyclooligomerization by alkyne metathesis for the first time (*Scheme 25*). The monomers carried alkyl moieties of different lengths and structures as well as two propynyl groups in *meta*-position, forcing an angle similar to the one in the resulting macrocycles. The alkyne metathesis was carried out using Mo(CO)<sub>6</sub> as the catalyst and 4-chlorophenol as a co-catalyst, creating the catalytic species *in situ* at 150 °C for 16 hours under an inert atmosphere to prevent degradation of the catalyst by oxygen or moisture. After completion of the reaction, a mixture of linear and cyclic oligomers was obtained, albeit the yield of the cyclic compounds was relatively low (depending on the substituents between 0.5-6%). The macrocycles were characterized by NMR spectroscopy and X-ray single-crystal diffraction analysis, proving the nearly planar structure of the macrocycles, which layered themselves in a crystal formed by van der Waals interactions.<sup>[84]</sup>



**Scheme 25:** Cyclooligomerization by alkyne metathesis resulting in linear oligomers and, in traces amounts, macrocycles.<sup>[84]</sup>

The yield of this approach was very low, even compared to the kinetic approach. A first step to improve the yield was the optimization of the catalytic system. Vollhardt *et al.* employed a Schrock catalyst with an alkyne monomer to efficiently prepare a three-membered macrocycle at yields between 12% and 54%. The propynyl functionalities were in vicinal positions, forcing an angle which led to the formation of 3-membered AEMs (Scheme 26). Monomers with moieties in *ortho*-position (R<sup>2</sup> other than H), however, yielded no macrocyclization, due to steric hindrance. By a constant nitrogen flow, the generated butyne was removed and the conversion increased.<sup>[11]</sup>

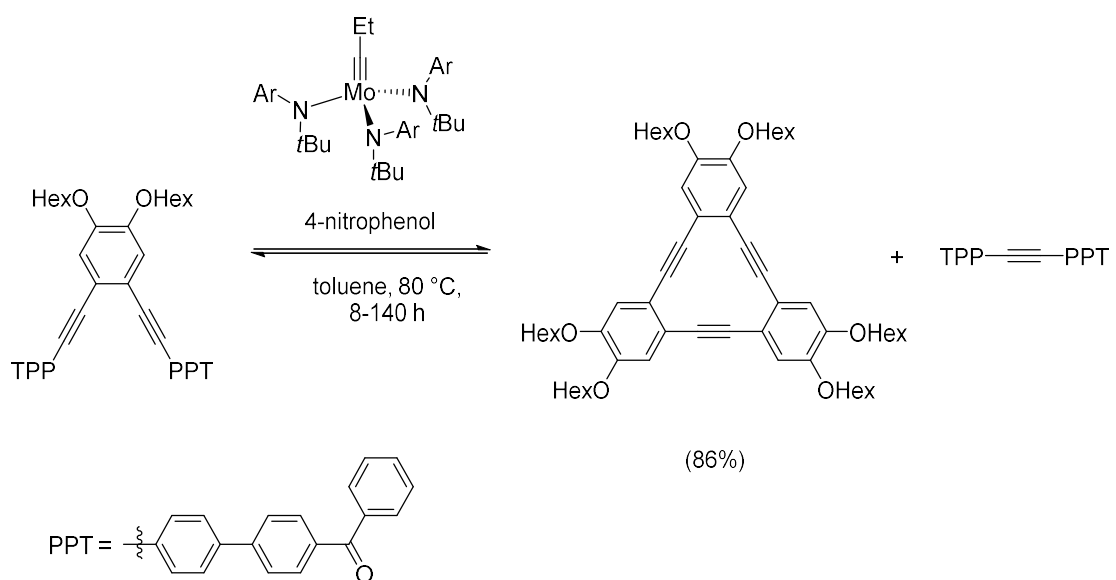


**Scheme 26:** Schematic representation of the synthesis of 3-membered AEMs butyne-driven by alkyne metathesis.<sup>[11]</sup>

Although no actual vacuum is applied, this strategy is known as “vacuum-driven” meaning that the monomers are designed in a way that gas is generated, which can

be removed either by vacuum or application of a transport gas, and hence the equilibrium is shifted towards the desired products.

A significant step was the development of a catalytic system by Moore *et al.* that was efficient at mild conditions (30 °C), within a short time frame (22 hours) and that provided high yields.<sup>[49]</sup> The synthesis of 3-membered macrocycles at a yield of 86% (Scheme 27) was thus reported.<sup>[12]</sup> The direct comparison with kinetic approaches providing yields of 2%<sup>[85]</sup> and 14%<sup>[86]</sup> for similar cycles indicates the superiority of macrocyclization by thermodynamic control.



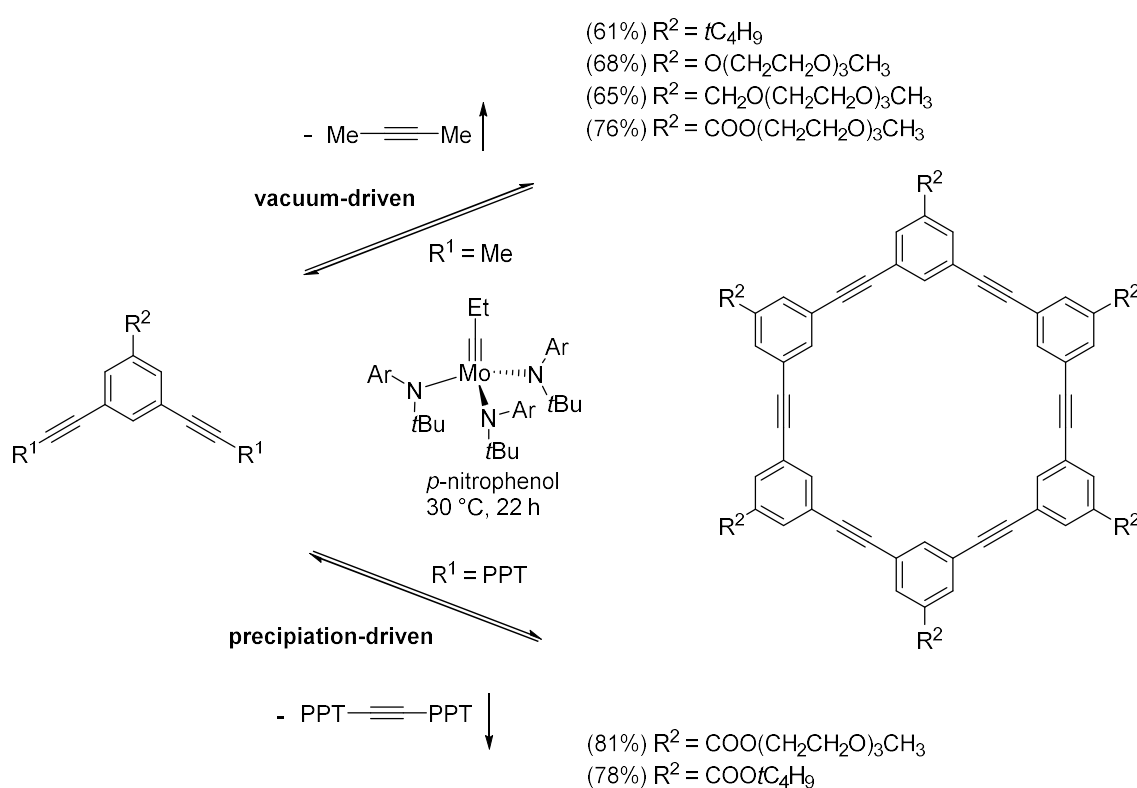
**Scheme 27:** Synthesis of 3-membered AEMs by precipitation-driven alkyne metathesis by Moore *et al.*<sup>[12]</sup>

The development of new catalytic systems, which have made alkyne metathesis an efficient tool, led also to higher yields of the synthesis of macrocycles by alkyne metathesis.

#### b) Removal Method

Besides the catalytic system, Moore *et al.* modified the “removal method”, *i.e.*, the fashion in which the reaction equilibrium is shifted towards the desired products through removal of a by-product. Careful monomer design allows the application of the principle of Le Châtelier by precipitation of the side-product.<sup>[12]</sup> Moore’s system was

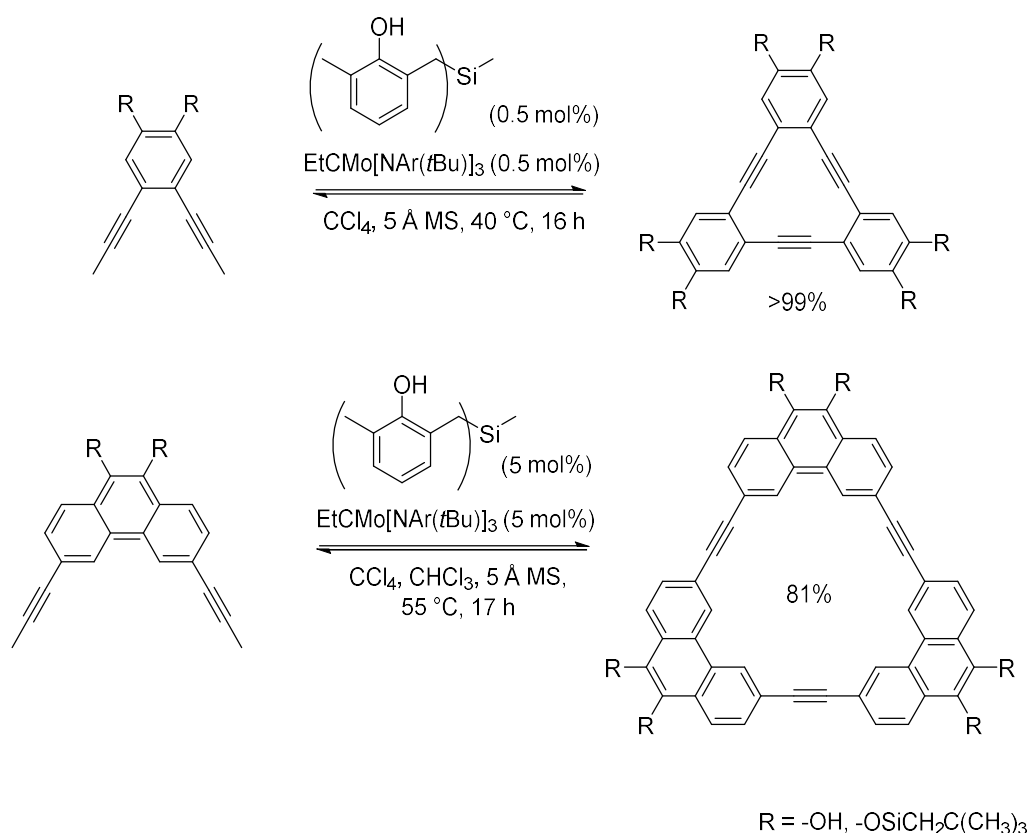
not only applicable for precipitation-driven and re-ordering systems, but for vacuum-driven systems as well. Furthermore, the monomer design forced the shape of the resulting cycle, allowing the formation of four-membered (*Scheme 30 top (84% yield) in chapter c) Influence of Moieties*) and six-membered macrocycles (*Scheme 28*).<sup>[83]</sup> Six-membered macrocycles similar to those reported by Bunz were also synthesized by Moore and co-workers, but in high yields instead of traces. Interestingly, multi-gram scale-up showed the limits of the vacuum-driven approach providing low yields (< 10%) compared to the precipitation-driven one (77%) for a reaction with same monomers ( $R^2 = \text{COO}(\text{CH}_2\text{CH}_2\text{O})_3\text{CH}_3$ ),<sup>[83]</sup> pointing to the need of an efficient evacuation system.



**Scheme 28:** Schematic representation of the synthesis of 6-membered macrocycles via alkyne metathesis either by vacuum-driven or by precipitation-driven method utilizing the catalytic system reported by Moore and co-workers.<sup>[83]</sup>

Indeed, Fürstner *et al.* reported the removal of butyne by 5Å molecular sieves as an efficient method to obtain a four-membered macrocycle, similar to the one previously synthesized by Moore, in similar yield (>80%).<sup>[13]</sup> The applicability of these new concepts was further optimized by Zhang and co-workers who reported the synthesis of the same four-membered macrocycle at even higher yields (>99%). Furthermore,

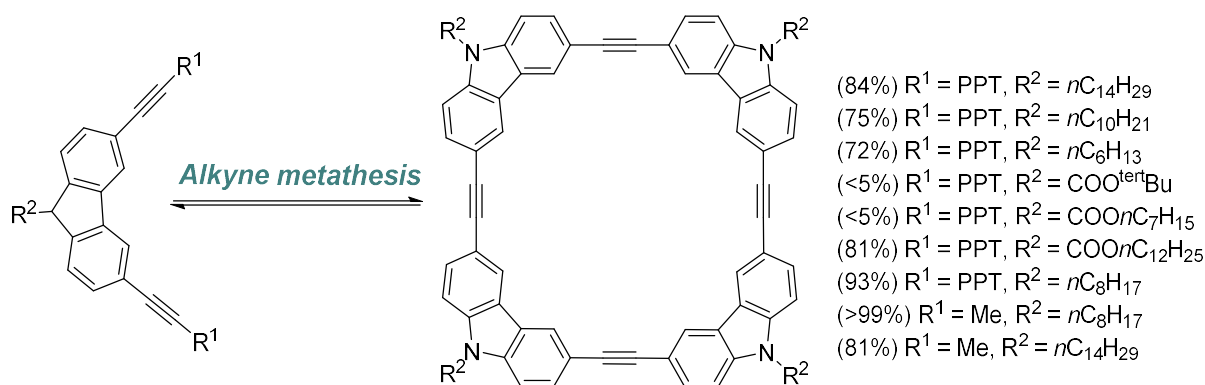
the concept was expanded to two other three-membered macrocycles in yields of >99% and 81% respectively (Scheme 29).<sup>[14]</sup>



**Scheme 29:** Schematic representation of the synthesis of 3-membered macrocycles in the presence of molecular sieves.<sup>[14]</sup>

### c) Influence of Moieties

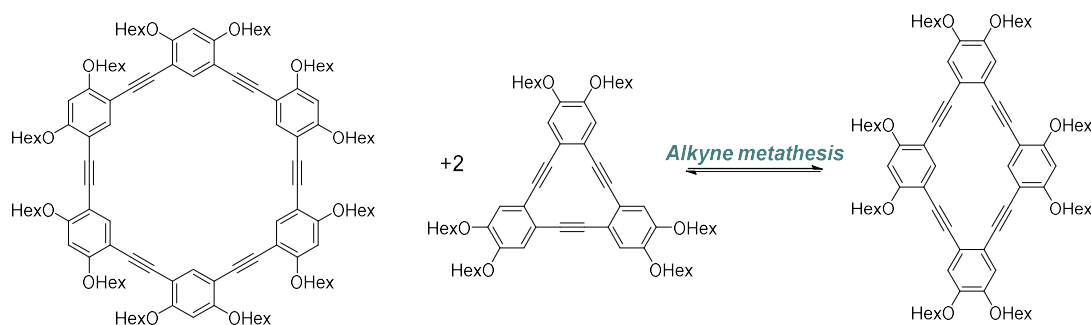
Moore *et al.* synthesized a series of four-membered macrocycles under thermodynamic control (Scheme 30), which gave significantly higher yields compared to synthesis under kinetic control (e.g., 14.3%, R<sup>2</sup> = C<sub>14</sub>H<sub>29</sub>).<sup>[10]</sup> Furthermore, the influence of moieties was investigated, as longer side groups led to higher yields compared to smaller moieties. An explanation could be that longer side groups increased the solubility of the growing linear oligomers, which was necessary to reach the adequate length to perform cyclization and prevent an early precipitation. Furthermore, the alkyl chains affected the macrocycles' stacking behavior: instead of an aryl-to-aryl packing, chains longer than nine carbons led to the formation of an alternate aryl-alkyl packing.<sup>[68]</sup>



**Scheme 30:** Synthesis of 4-membered macrocycles via alkyne metathesis with side groups of different lengths.<sup>[4,68,83,87]</sup>

#### d) Re-ordering

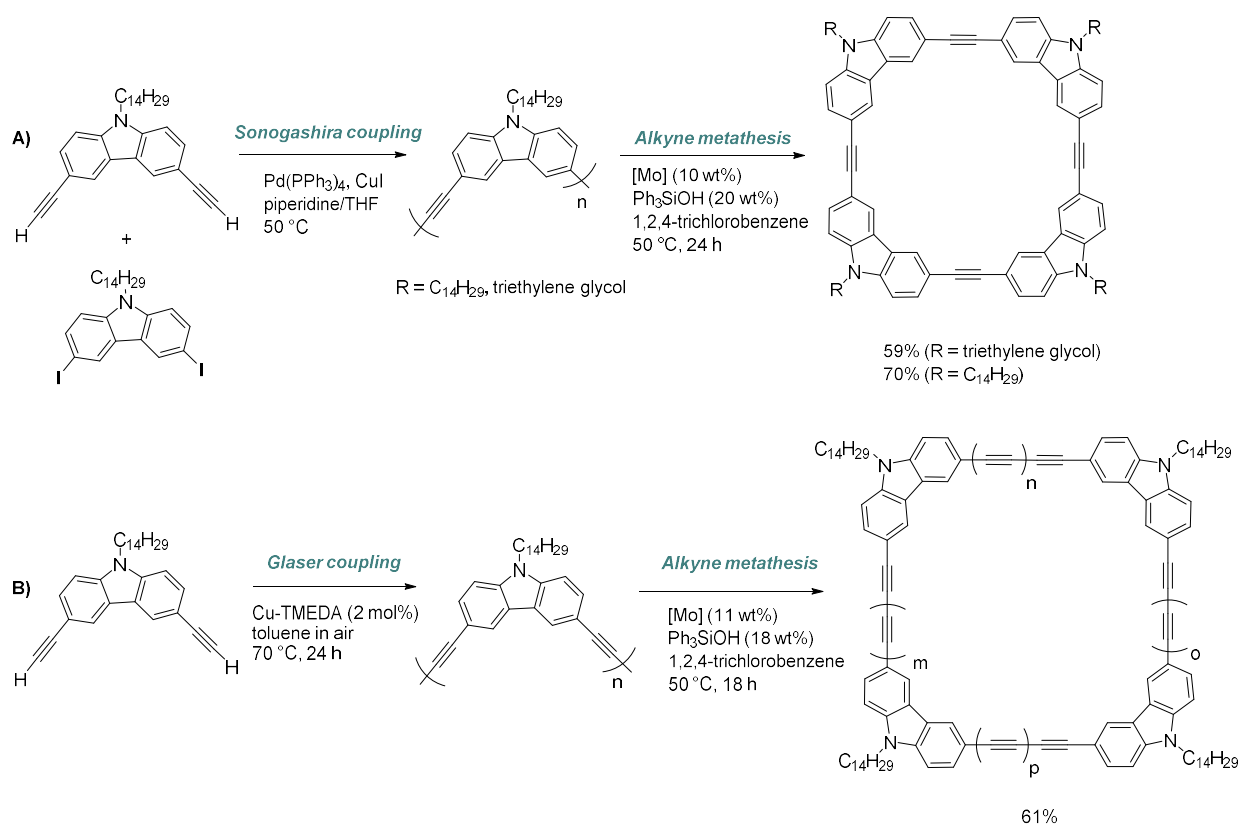
The ability of a thermodynamically controlled reaction for error correction or re-ordering was illustrated in an experiment by Moore *et al.* A six-membered and a three-membered macrocycle were shown to undergo rearrangement of their bonds in presence of an alkyne metathesis catalyst and form a four-membered macrocycle (*Scheme 31*).<sup>[12]</sup>



**Scheme 31:** Schematic representation of the re-ordering of three-membered and six-membered macrocycle by alkyne metathesis to form four-membered macrocycles.<sup>[12]</sup>

Moore *et al.* developed a further synthetic strategy comparing the possibilities of kinetic and thermodynamic approaches directly and illustrating the correcting effect of DCvC impressively. In a first reaction, carbazole derivatives carrying either two iodides or two ethynyl functionalities were polymerized *via* Sonogashira reaction (*Scheme 32, A*). Alternatively, the ethynyl carrying monomer was oligomerized in a Glaser coupling (*Scheme 32, B*).<sup>[15]</sup> In both cases, fully-conjugated stiff oligomers of different lengths

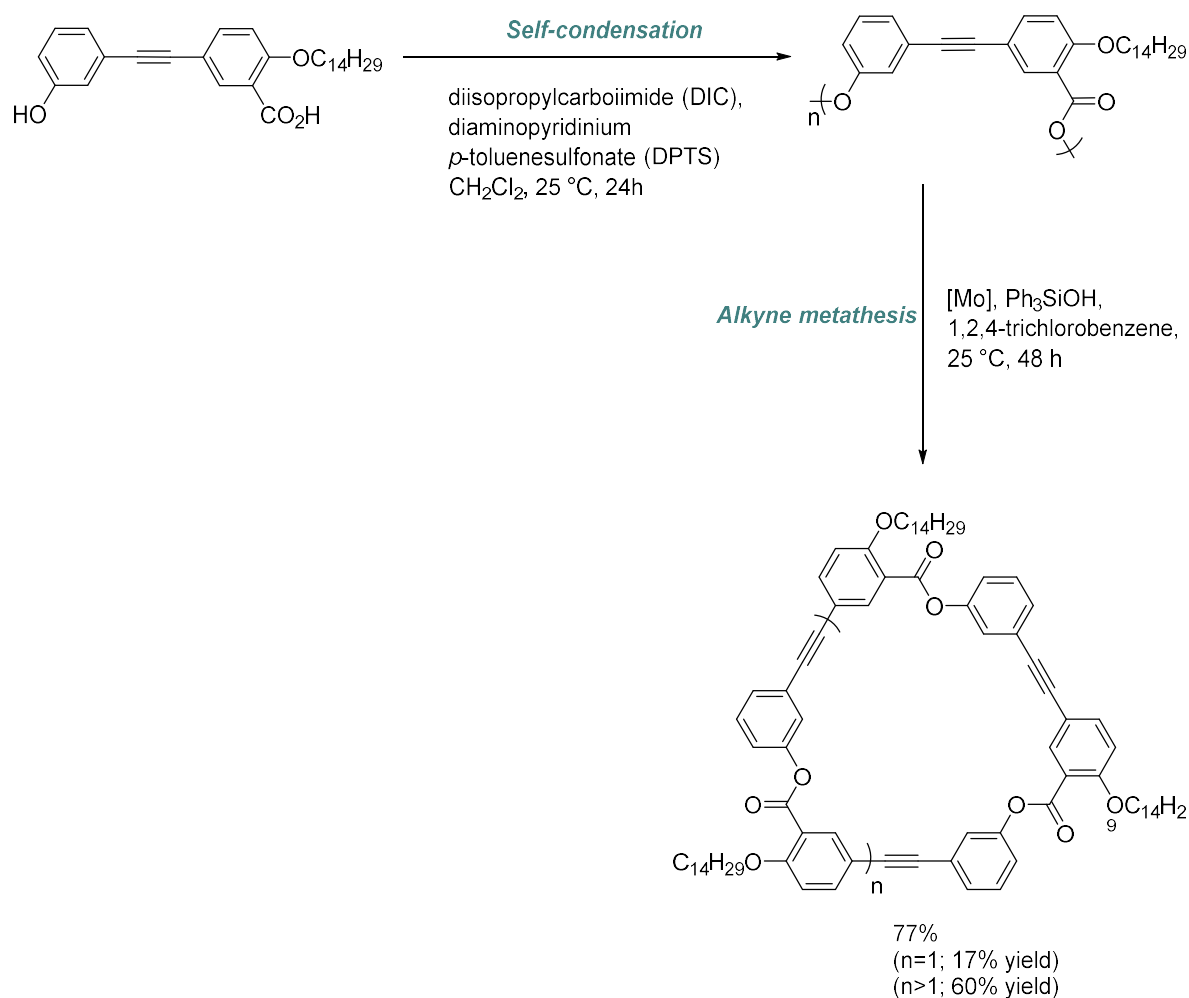
were formed. In the product mixture, some cyclic compounds were present; however, isolating them would require a challenging procedure risking potentially rather low yields. To optimize the selectivity, the oligomers were used in a subsequent alkyne metathesis, resulting in a re-arrangement of the bonds between the monomer units and thus the formation of a 4-membered macrocycle in yields between 59% and 70% for the oligomers made *via* Sonogashira coupling and 61% for the ones made by Glaser coupling. The AEMs were shown to form supramolecular nanostructures by self-assembly, making them suitable materials for one-dimensional nanofibrils, extended tubular channels, discotic liquid crystals and monolayers. The  $\pi$ -conjugated system was not only responsible for the stacking but also for semi-conductivity in the stacking direction.<sup>[15]</sup>



**Scheme 32:** Schematic representation of the oligomerization by Sonogashira coupling (A) and Glaser coupling (B) and subsequent re-arrangement of the generated linear oligomers by alkyne metathesis to form four-membered macrocycles.<sup>[15]</sup>

Moore and co-workers expanded the rearrangement concept by using directional oligomers (Scheme 33). First, linear, fully-conjugated polyesters were synthesized by

self-condensation of phenol- and carboxylic acid-functionalized tolane monomers. Similar to their previous approach, the oligomer mixture underwent an alkyne metathesis leading to a rearrangement of the bonds and the formation of a mixture of cyclic compounds at a total yield of 77%; however, this mixture consisted of a 3-membered cycle ( $n=1$ ; 17% yield) and other, insoluble cyclic species ( $n>1$ ; 60% yield).<sup>[88]</sup>

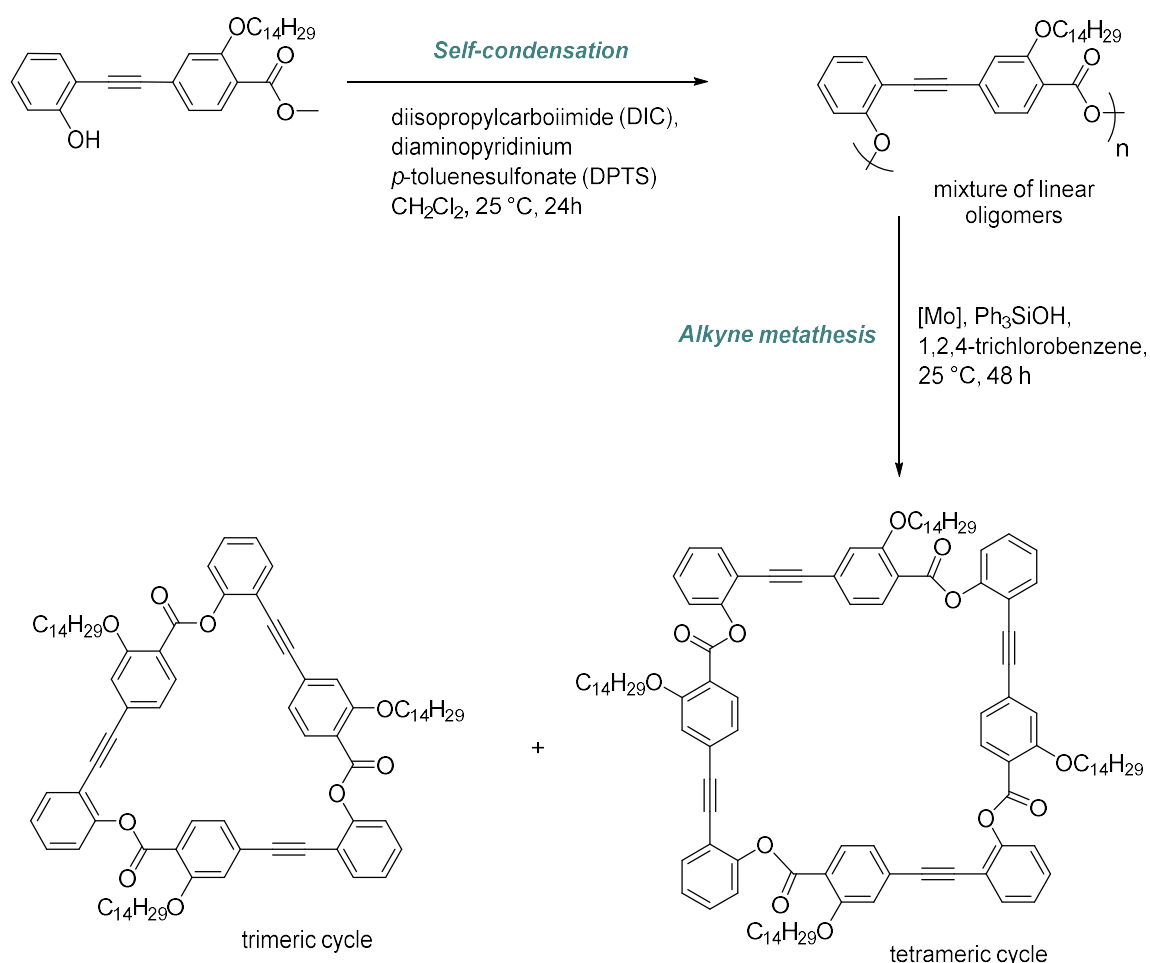


**Scheme 33:** Schematic representation of the synthetic pathways to obtain a mixture of cyclic oligomers via re-arrangement by alkyne metathesis.<sup>[88]</sup>

To compare the structural effect of the monomers, the same protocol was followed with an isomeric monomer with different positions of the hydroxyl and acid groups (*Scheme 34*). The oligomer mixture underwent a depolymerization *via* alkyne metathesis giving a mixture of two cyclic compounds, which could be separated (yield of the trimeric cycle: 35%, yield of tetrameric cycle: 19%).<sup>[88]</sup> This illustrates that smart monomer



design, forcing a useful bond angle, has a big impact on the resulting product composition.



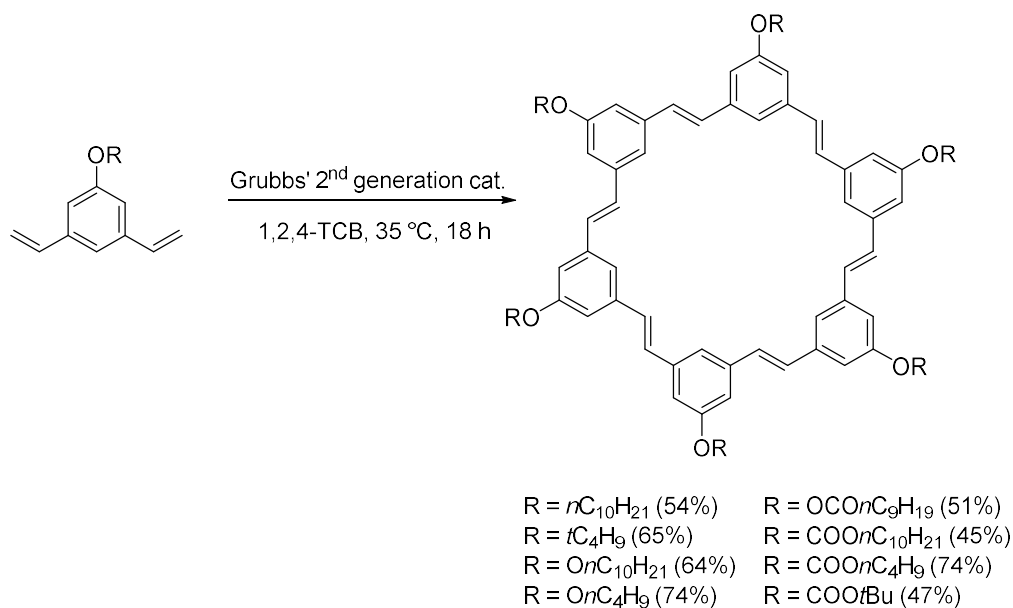
**Scheme 34:** Schematic representation of the synthetic pathway followed to obtain a mixture of trimeric and tetrameric cycles via re-arrangement by alkyne metathesis.<sup>[88]</sup>

Arguably, alkyne metathesis has become a powerful tool for the preparation of rigid macrocycles. Various aspects need to be taken into account to increase the efficiency of the method, namely the catalyst, the by-product removal, the presence of functional groups, but perhaps the most important is the design of the monomers. Indeed, the latter was shown to drastically influence the efficiency of the macrocycle synthesis, but also the molecular characteristics of the products altogether.<sup>[80]</sup>

### II.2.2.2. Shape-persistent Macrocycles via Olefin Metathesis

In 2007, Zhang *et al.* discussed shape-persistent macrocycles by olefin metathesis and described the challenges.<sup>[80]</sup> In contrast to the linearity of ethynyl groups, which leads to stiff macrocycles, double bonds are more flexible.<sup>[80]</sup> During cyclooligomerization, no control over the configuration (*E/Z*) is given; hence, a mixture of macrocycles of different sizes and shapes is formed, which reduces the selectivity towards one favored cycle. Internal double bonds are less active towards the olefin metathesis-catalyst in contrast to the terminal ones. As such, the reaction is considered not to be entirely reversible,<sup>[89]</sup> and therefore, exhibits the disadvantages of kinetic control, which further decreases the yield of the desired macrocycle.<sup>[80]</sup>

Zhang and co-workers showed that olefin metathesis exhibits the benefits of DCvC and is a suitable tool for the synthesis of shape-persistent macrocycles: they obtained arylenevinylene macrocycles (AVMs) *via* cyclooligomerization by olefin metathesis, more precisely by acyclic diene metathesis macrocyclization (ADMAC).<sup>[16]</sup> The resulting macrocycles exhibited properties similar to those of AEMs, as discussed in the previous chapter, such as planarity, shape-persistency and the ability to form ordered structures. The problem of *E/Z* isomerization control was overcome by smart monomer design and the shape of the targeted macrocycle. In a six-membered ring, for example, *trans* isomers are sterically favored compared to *cis* ones. A linear six-membered oligomer chain is unlikely to complete the ring-closure if one monomer link is *cis*. Once isomerization to *trans* occurs, the macrocyclization can take place.<sup>[19]</sup> Although the cycle formed by the fewest monomers was expected to be the thermodynamically favored one, the formation of macrocycles of various angles, geometries and sizes were expected to be formed as well.<sup>[16]</sup> The olefin metathesis catalyzed by second generation Grubbs' catalyst was performed at 35 °C in a nitrogen atmosphere and with 1,2,4-trichlorobenzene as solvent (*Scheme 35*). Utilizing *meta*-divinyl-substituted arylene monomers with diverse alkoxy chains, the correspondent six-membered macrocycles were obtained, which are the thermodynamically favored products. Some high molecular weight polymers and large cycles were formed as well, according to SEC; however, the six-membered macrocycles were isolated by column chromatography in yields between 45% and 74%.<sup>[16]</sup>

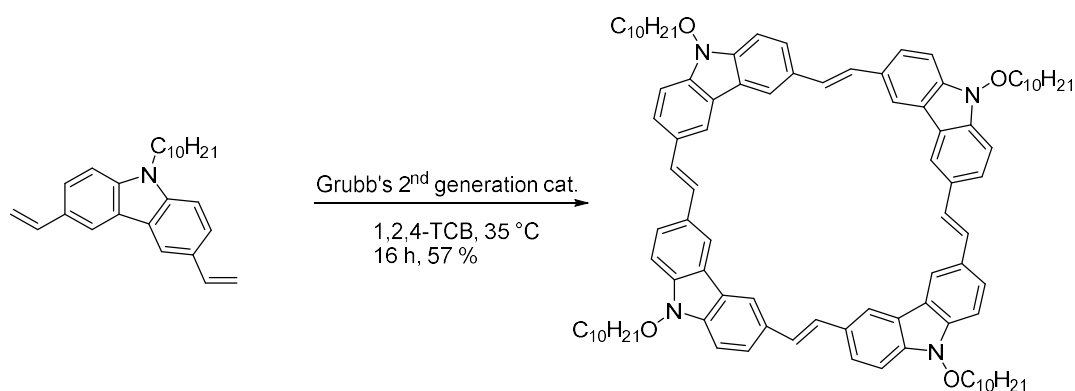


**Scheme 35:** Cyclization of divinyl arylene monomers via olefin metathesis resulting in six-membered macrocycles.<sup>[16]</sup>

The resulting rings assembled in nanofibrils, which were observed by scanning electron microscopy (SEM). Compared to AEM, AVMs form stronger aggregates. The assembly behavior is usually described by the polar/ $\pi$ -model, which suggests that electron withdrawing groups reduce the electron density of the  $\pi$ -system, leading to a decrease in electric repulsion and thus allowing  $\pi$ - $\pi$  stacking of the macrocycles.<sup>[90]</sup> Variation of the substituents of AEMs underpins this assumption: AEMs with electron-withdrawing groups showed a tendency to form aggregates, while AEMs with electron-donating groups did not. However, a variation of the moieties by Zhang *et al.* indicated that even AVMs with electron-donating groups form strong aggregates; hence, it was proposed that there was another driving force involved.<sup>[90]</sup> An explanation for this phenomenon can be found in the direct through-space interaction model.<sup>[90,91]</sup> By aggregation, AVMs undergo a gain of enthalpy quantitatively comparable to that of AEMs. However, AVMs are more flexible compared to AEMs; hence, they experience entropy loss, which contrasts the observation that AVMs have a higher tendency than AEMs to form aggregates. To minimize the entropy loss, AVMs arrange in a deformed,<sup>[90]</sup> “saddle-like conformation”<sup>[16,90]</sup> to adopt the “optimal stacked conformation”<sup>[90]</sup>. This conformation allows an interaction between electronegative atoms, *e.g.*, the oxygen atoms of the substituents and the hydrogens of the neighboring

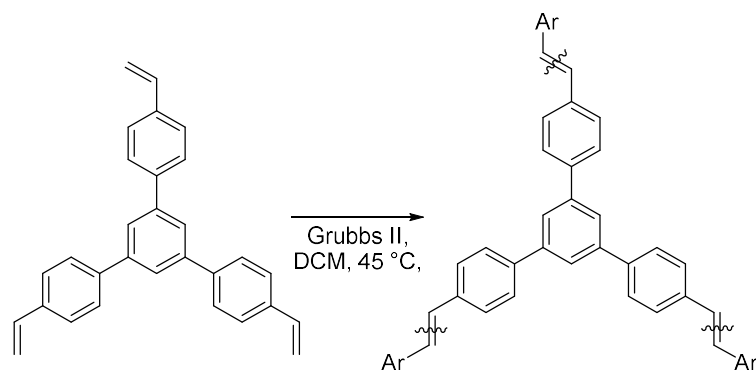
$\pi$ -system<sup>[91]</sup> and explains the strong tendency to form aggregates. DFT simulations support this assumption.<sup>[90,91]</sup>

So far, the olefin metathesis approach developed by Zhang *et al.* was only shown for *meta*-divinyl monomers as well as for carbazole monomers (Scheme 36), which formed a four-membered macrocycle at a yield comparable to that of the six-membered ones. Furthermore, a simple washing step yielded the pure product.



**Scheme 36:** Cyclization of divinyl-substituted carbazole monomer via olefin metathesis.<sup>[16]</sup>

Olefin metathesis can also be used to synthesize larger structures, such as networks. Dichtel *et al.* applied a phenylene vinylene monomer in an ADMET-polymerization catalyzed by the Grubbs 2<sup>nd</sup> generation catalyst and obtained a random three-dimensional network (Scheme 37).<sup>[92]</sup> The unordered structure was confirmed by X-ray diffraction. The decrease in signal for the vinyl group was determined by FT-IR. The resulting network showed fluorescence, which was quenched by trace amounts of 1,3,5-trinitroperhydro-1,3,5-triazine (RDX), an explosive which is 1000 times less volatile than 1,3,5-trinitrotoluene (TNT) and therefore difficult to detect. Dichtel *et al.* showed that the resulting network can be used as a detector for RDX.<sup>[92]</sup>

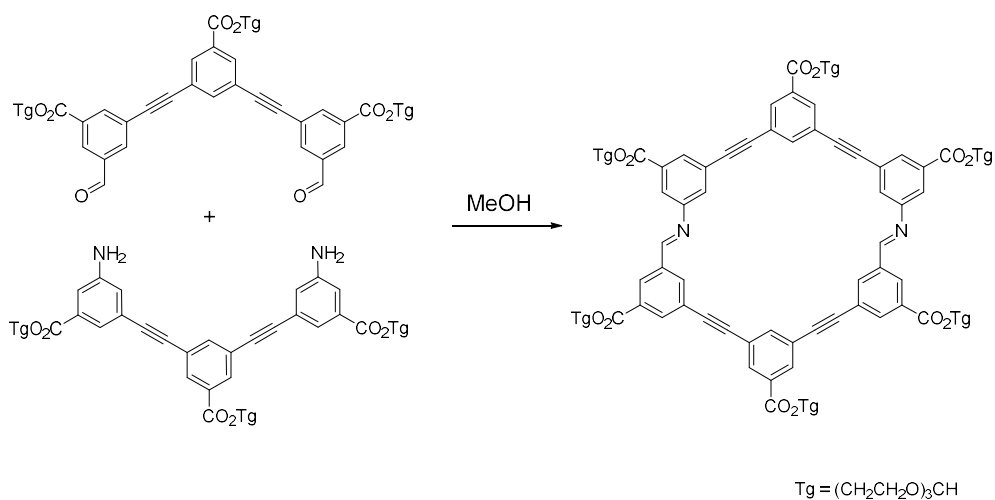


**Scheme 37:** ADMET-polymerization of a phenylene vinylene monomer to a random three-dimensional network.<sup>[92]</sup>

### II.2.2.3. Shape-persistent Macrocycles *via* Imine Condensation

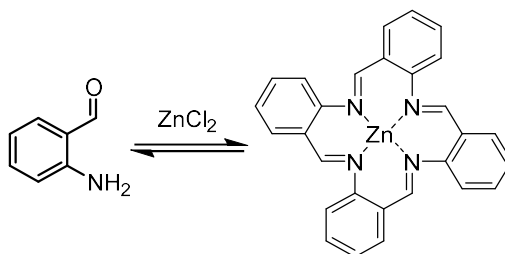
Shape-persistent macrocycles have also been synthesized by the combination of building blocks *via* imine condensation in high yields due to thermodynamic control. In contrast to the previous metathesis reactions, imine condensation can be carried out without the presence of a catalyst.

Moore and co-workers synthesized a macrocycle by intermolecular coupling between two aryl-ethynylene fragments (*Scheme 38*). While in  $\text{CDCl}_3$  and toluene only low conversions were obtained, the reaction in methanol gave, after purification by column chromatography, a yield of 95%. The yields of the imine condensation of the two fragments were very high, particularly compared to other kinetic approaches; nonetheless the synthesis of the fragments required six-steps (overall yield of 26%).<sup>[82]</sup>



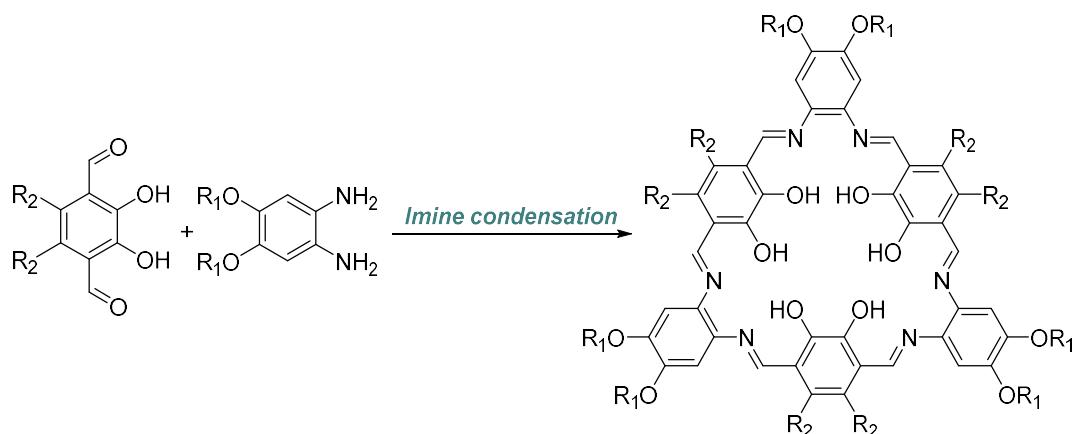
**Scheme 38:** Combination of two phenylene ethynylene fragments by imine condensation.<sup>[82]</sup>

Similar to the other approaches, imine condensations, also allows the formation of shape-persistent macrocycles by cyclooligomerization. Indeed, this concept was reported in the 1920s, when Seidel *et al.* discovered the formation of a four-membered cycle by reaction of 2-aminobenzaldehyde in presence of  $\text{ZnCl}_2$  (Scheme 39).<sup>[10]</sup>



**Scheme 39:** Self-macrocyclization of 2-aminobenzaldehyde in presence of  $\text{ZnCl}_2$ .<sup>[10]</sup>

More recently, Nabeshima and co-workers synthesized a six-membered macrocycle by imine condensation in acetonitrile at room temperatures over two weeks in a high yield of 91% (Scheme 40, 40a).<sup>[17]</sup> X-ray crystallography indicated that strong intramolecular hydrogen bonds between hydroxyl groups and the imines formed and the macrocycle acted as a host for one water molecule. Similar to the four-membered macrocycle by Seidel *et al.*, the cyclization was forced by complexation of a guest. The high yield was attributed to the low solubility of the produced macrocycle in the reaction solvent. Once the cycle was formed, it precipitated from the reaction mixture; hence, a back reaction is avoided.<sup>[17]</sup> Such a reaction combines the advantages of thermodynamic and kinetic approach: namely, the correction of undesired bonds while avoiding a back reaction of the desired product to the starting materials.

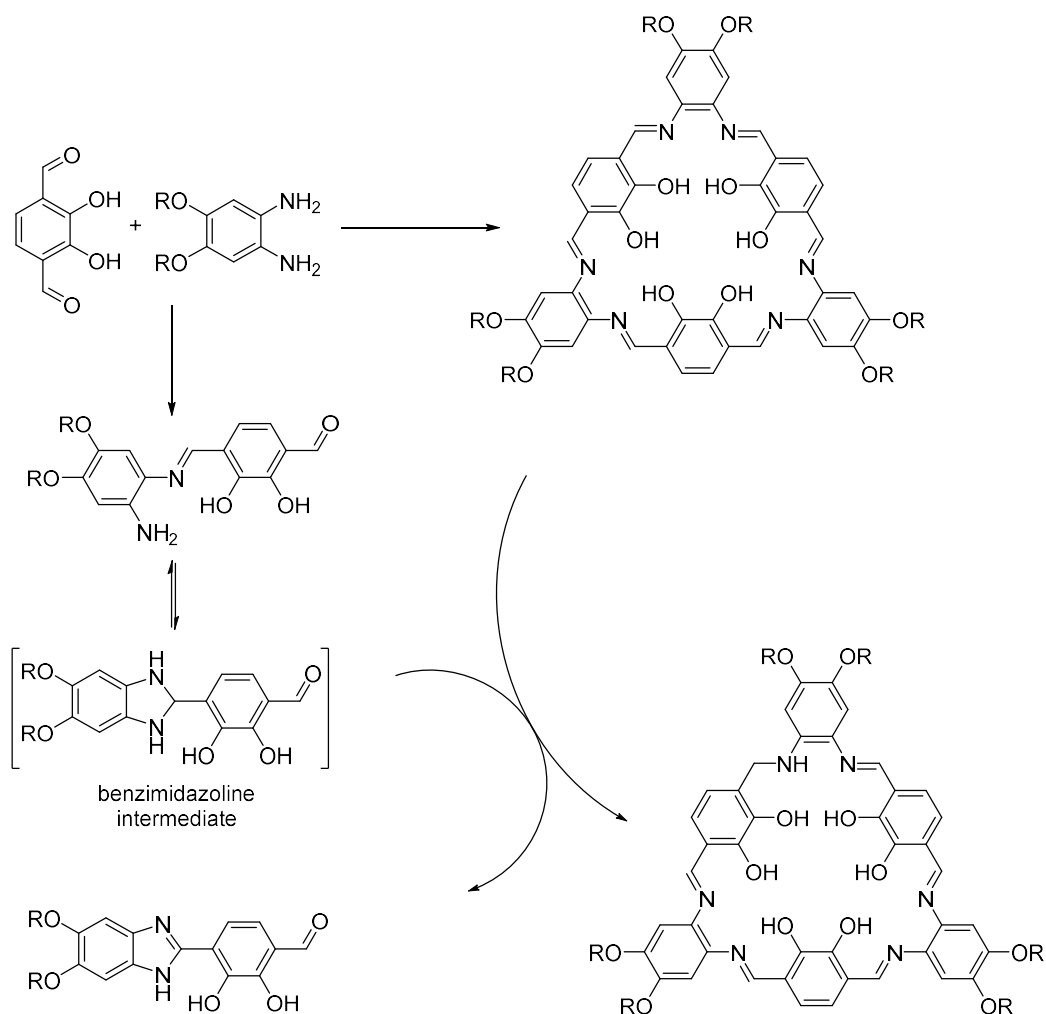


40a (91%): R <sub>1</sub> = H, R <sub>2</sub> = H	40g (70%): R <sub>1</sub> = C <sub>7</sub> H <sub>15</sub> , R <sub>2</sub> = H	40m (n/a): R <sub>1</sub> = CH <sub>3</sub> , R <sub>2</sub> = H
40b (77%): R <sub>1</sub> = C <sub>2</sub> H <sub>5</sub> , R <sub>2</sub> = H	40h (87%): R <sub>1</sub> = C <sub>8</sub> H <sub>17</sub> , R <sub>2</sub> = H	40n (87%): R <sub>1</sub> = C <sub>2</sub> H <sub>5</sub> , R <sub>2</sub> = CH <sub>3</sub>
40c (68%): R <sub>1</sub> = C <sub>3</sub> H <sub>7</sub> , R <sub>2</sub> = H	40i (59%): R <sub>1</sub> = C <sub>10</sub> H <sub>21</sub> , R <sub>2</sub> = H	40o (77%): R <sub>1</sub> = C <sub>5</sub> H <sub>11</sub> , R <sub>2</sub> = CH <sub>3</sub>
40d (79%): R <sub>1</sub> = C <sub>4</sub> H <sub>9</sub> , R <sub>2</sub> = H	40j (34%): R <sub>1</sub> = C <sub>12</sub> H <sub>25</sub> , R <sub>2</sub> = H	40p (24%): R <sub>1</sub> = H, R <sub>2</sub> = C <sub>4</sub> H <sub>9</sub>
40e (63%): R <sub>1</sub> = C <sub>5</sub> H <sub>11</sub> , R <sub>2</sub> = H	40k (36%): R <sub>1</sub> = C <sub>14</sub> H <sub>29</sub> , R <sub>2</sub> = H	40q (28%): R <sub>1</sub> = CH <sub>3</sub> , R <sub>2</sub> = C <sub>6</sub> H <sub>13</sub>
[93] 40f (75%): R <sub>1</sub> = C <sub>6</sub> H <sub>13</sub> , R <sub>2</sub> = H	40l (18%): R <sub>1</sub> = C <sub>16</sub> H <sub>33</sub> , R <sub>2</sub> = H	

**Scheme 40:** Synthesis of various six-membered macrocycles by imine condensation of a para-dialdehyde and an ortho-diamine.<sup>[17,18,94]</sup>

MacLachlan and co-workers conducted further investigations for this system and synthesized a library of macrocycles with alkyl chains of varied length (Scheme 40, b-q) as single products without observation of any imine oligomers or further imine cycles at yields between 18% and 79%.<sup>[18,94]</sup> Due to insolubility, the compound 40m (Scheme 40), carrying a methoxy group, could not be purified; hence, no yield was given. Instead of two weeks, MacLachlan and co-workers obtained these macrocycles in 1-3 hours for short chain moieties and in >12 hours for compounds with long alkyl chains. Intermediates indicating that linear short oligomers were formed first were successfully isolated. Furthermore, it was concluded that once an adequate chain length is reached, cyclization takes place. No longer linear oligomers nor larger cycles were observed apart from the targeted six-membered macrocycle, the formation of which was favored, and even in the presence of salicylaldehyde as “chain stopper”, it was found to be the major product.<sup>[18]</sup> The reaction towards the six-membered macrocycle was deemed tolerant to functional groups as despite the presence of hydroxyl and ether groups and thus possible side reactions, the targeted macrocycle was the major product. Side reactions were nonetheless observed, such as condensation of dialdehyde or diamine to benzimidazoline, thus affecting the overall yield. This product led to the reduction of

a single imine in the macrocycle to the corresponding amine promoted by the traces of acid present in the solvent (*Scheme 41*). Even more surprisingly multi-reductions were not observed.<sup>[18]</sup> Although the macrocycles appear to be planar, DFT calculations indicated a twisted structure due to the repulsion of the hydroxyl groups, and particularly due to the twist in the phenyl-imine bond.<sup>[18]</sup>

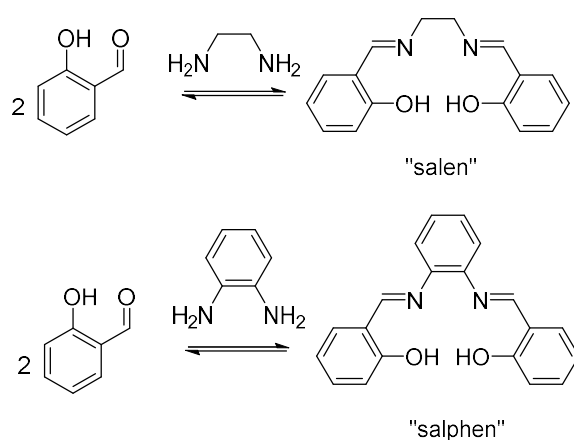


**Scheme 41:** Formation of benzimidazoline as side reaction and reduction of one imine bond of the macrocycles by benzimidazoline.<sup>[18]</sup>

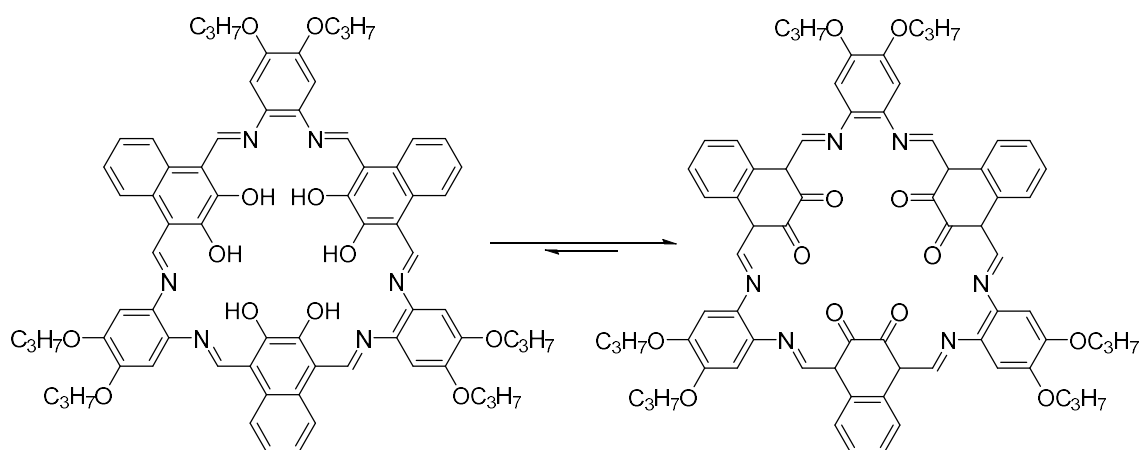
X-ray diffraction indicated the presence of hydrogen bonds as well as a water molecule in the cavity of the macrocycles. To investigate the main driving force of the reaction, macrocycles with long solubilizing groups were synthesized to prevent them from precipitating; however, the targeted macrocycles were consistently the main species, according to <sup>1</sup>H-NMR spectroscopy. This observation indicates that precipitation might be a minor driving force; while either the complexation of water and/or the formation of



hydrogen bonds play a bigger role. Screening of different solvent systems showed that none of them acted as a template for the cyclization.<sup>[18]</sup> Nevertheless, imine macrocycles show strong complexation behavior reminiscent of that of crown ethers,<sup>[10]</sup> which can be explained by two interesting units integrated into the macrocycle: *N,N'*-bis(salicylidene)phenylenediamine, also known as salphen, which is related to *N,N'*-bis(salicylidene)ethylenediamine, shortly salen (Scheme 42).<sup>[18,73]</sup> Tautomerization to the corresponding keto-enamines can take place, for example for naphthalene-based macrocycles;<sup>[10]</sup> however, macrocycles are mostly present as enol-imine tautomers (Scheme 43).<sup>[10]</sup>



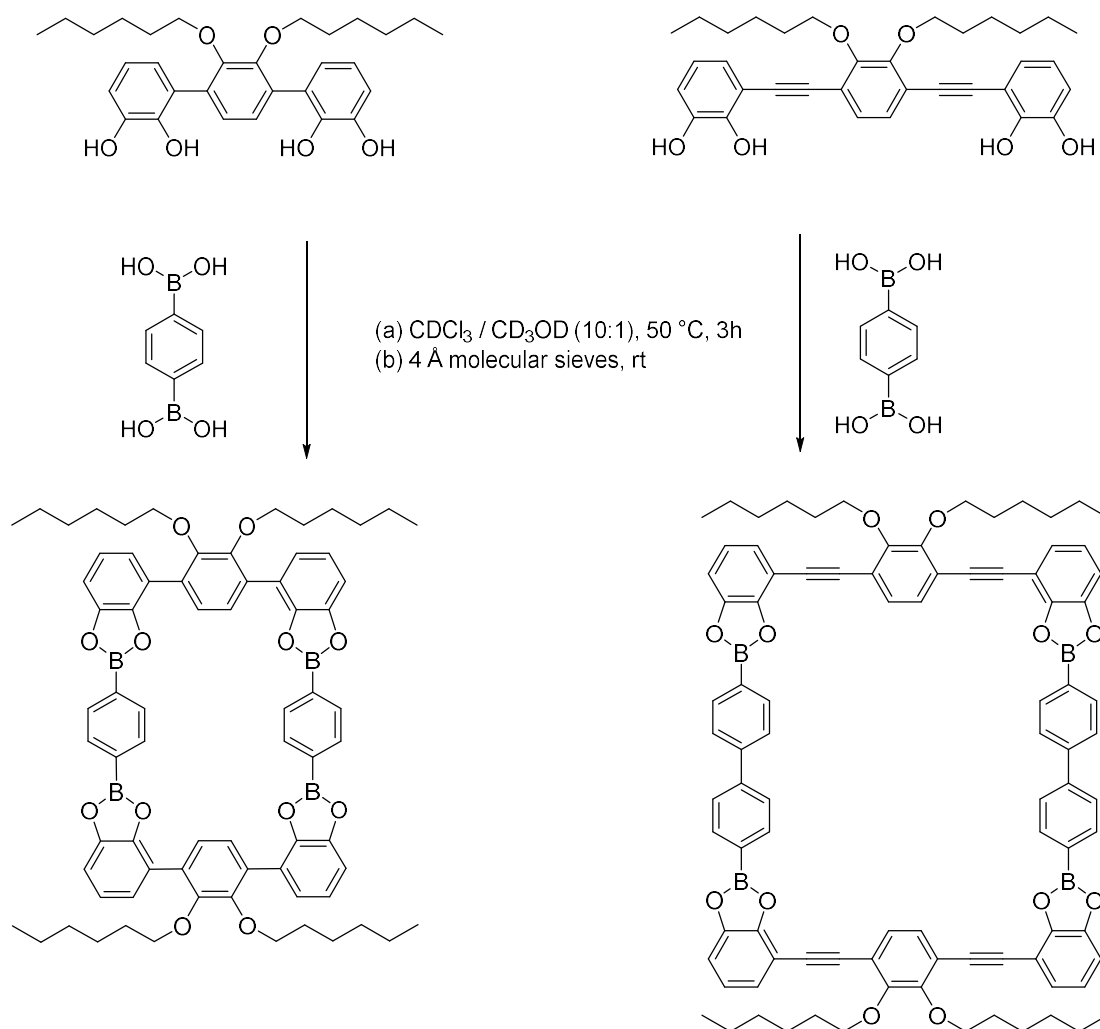
**Scheme 42:** Formation and general structure of "salen" and "salphen" by imine condensation.<sup>[18,73]</sup>



**Scheme 43:** Tautomerization of "salphen" consisting macrocycles.<sup>[10]</sup>

#### II.2.2.4. Shape-persistent Macrocycles *via* Boronate Ester Formation

Within the scope of DCvC, alternative reactions which can be used to form macrocycles, but which have not been used within the thesis or previous studies will be discussed, such as those involving the formation of boronate esters. Northrop and co-workers synthesized shape-persistent macrocycles by boronate ester formation (*Scheme 44*) in almost quantitative yield starting from rigid aromatic bis(catechol) derivatives as building blocks linked together through 1,4-benzene diboronic acid in the presence of molecular sieves.<sup>[95]</sup> Variation of the length of the bis(catechol) building block led to a change the size of fully-conjugated system and hence of the electronic properties.<sup>[95]</sup>

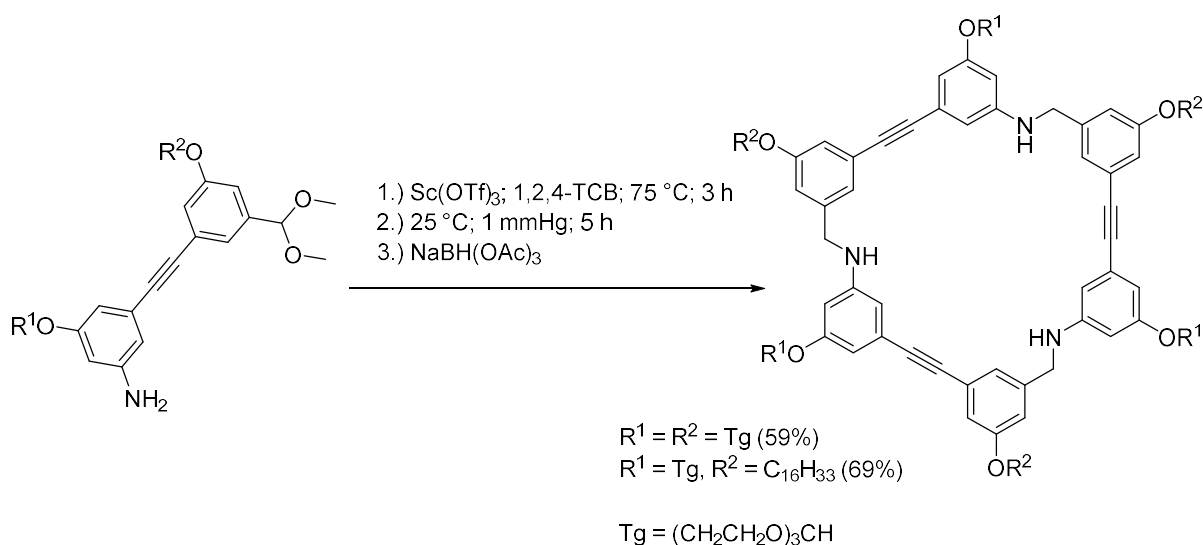


**Scheme 44:** Synthesis of shape-persistent macrocycles via boronate ester formation.<sup>[95]</sup>

#### II.2.2.4. Macrocycles *via* Orthogonal Dynamic Covalent Reactions

As presented in the previous chapters, rigid macrocycles can be synthesized by a broad range of reactions providing a certain functional group. The macrocycle can be linked together by an ethynyl moiety, which provides stiff macrocycles but suffers from the disadvantages of alkyne metathesis, such as the sensitivity towards oxygen and moisture. By olefin metathesis, macrocycles can be obtained linked together with vinyl groups, which provide a higher flexibility. By imine condensation, macrocycles with nitrogen and oxygen atoms in the inner cavity are formed, which show a high affinity to complex. Through the combination of these different reactions, shape-persistent macrocycles containing diverse functional groups are accessible.

In 2007, Moore and co-workers reported the preparation of such multi-functional and asymmetric macrocycles (Scheme 45).<sup>[96]</sup> In chapter II.2.2.3. *Shape-persistent Macrocycles via Imine Condensation* a similar approach was discussed. Arylene-containing building blocks were linked *via* imine condensation resulting in a macrocycle with triple bonds and secondary amine groups. This synthetic strategy can be considered an intermediate between regular DCvC reaction and orthogonal dynamic covalent chemistry (ODOC).<sup>[19]</sup> As the name indicates, monomers are designed and reactions chosen in such way that different functionalities react orthogonally to each other in a one-pot synthesis, in contrast to a modular approach requiring a multi-step synthesis of the building blocks, including the protection of the amine and aldehyde groups.<sup>[96]</sup>

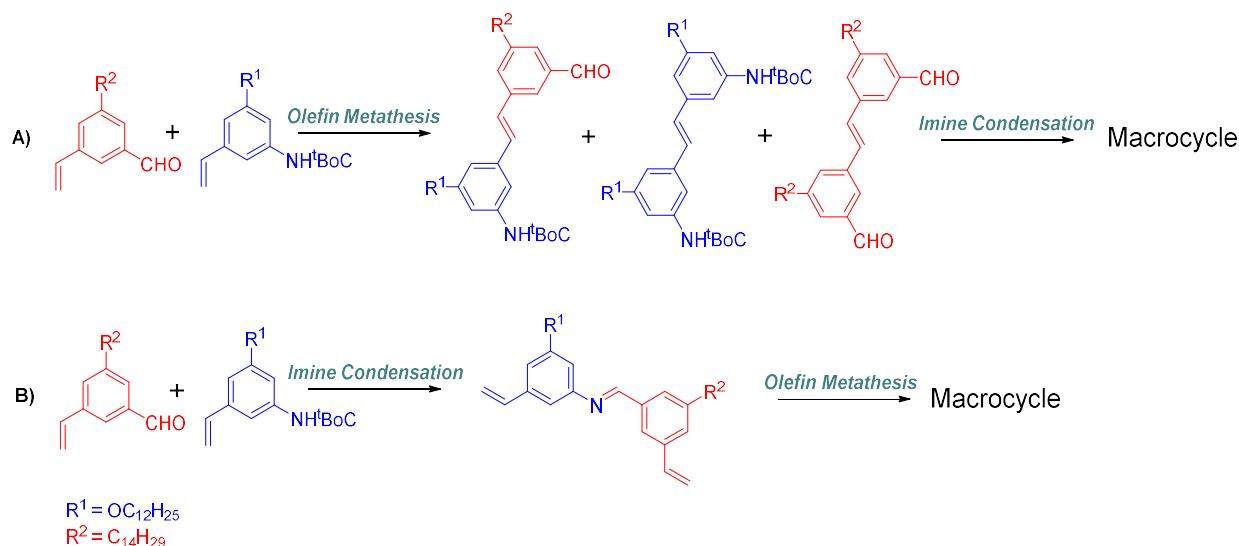


**Scheme 45:** Synthesis of multifunctional macrocycles by modular synthesis.<sup>[96]</sup>

Zhang and co-workers synthesized a range of macrocycles of different sizes, shapes and positions of functional groups by varying one of the monomers (*Scheme 46*). In all reactions, the same vinylaniline monomer was applied and the structure and functionality of the vinylaldehyde monomer was varied.<sup>[19]</sup> Thereby, it was shown possible to integrate two functions, double bonds and imines, in the macrocycles. Although this experiment was performed as one-pot synthesis, the two reactions were not carried out simultaneously. Indeed, when both reactions occurred at the same time, the selectivity decreased. Apart from the targeted macrocycle, substrates of high molecular weights were formed according to SEC.<sup>[19]</sup> By subsequent reactions, either “olefin-then-imine” (*Scheme 46, A*) or “imine-then-olefin” (*Scheme 46, B*), both reactions were carried out in one pot providing a relatively high selectivity. In a first step, dimers were formed. In the “olefin-then-imine” approach, three different reactions and thereby three different dimers were possible: either each monomer species reacted in a self-metathesis, or with the other monomer species in a cross-metathesis. Once the double bonds were consumed, these dimers formed the macrocycles in an imine condensation as a second step, which was orthogonal to the first one. Note that the “olefin-then-imine” strategy was not fully orthogonal, while the protection of the amine was necessary. Its deprotection occurred in one-pot before the imine condensation and the desired macrocycles were formed, however byproducts of high molecular weights were also observed by SEC. This observation was explained by the fact that the deprotection proceeds rather slowly and was not completed within the observed time frame, resulting in a non-equimolar ratio of aldehyde and imine monomers. These byproducts were ascribed to linear oligomers, which could not perform the ring-closure due to the lack of imine monomers as reaction partners. Although a higher selectivity was achieved compared to a simultaneous reaction, this approach was less selective according to SEC, compared to the “imine-then-olefin” concept.<sup>[19]</sup>

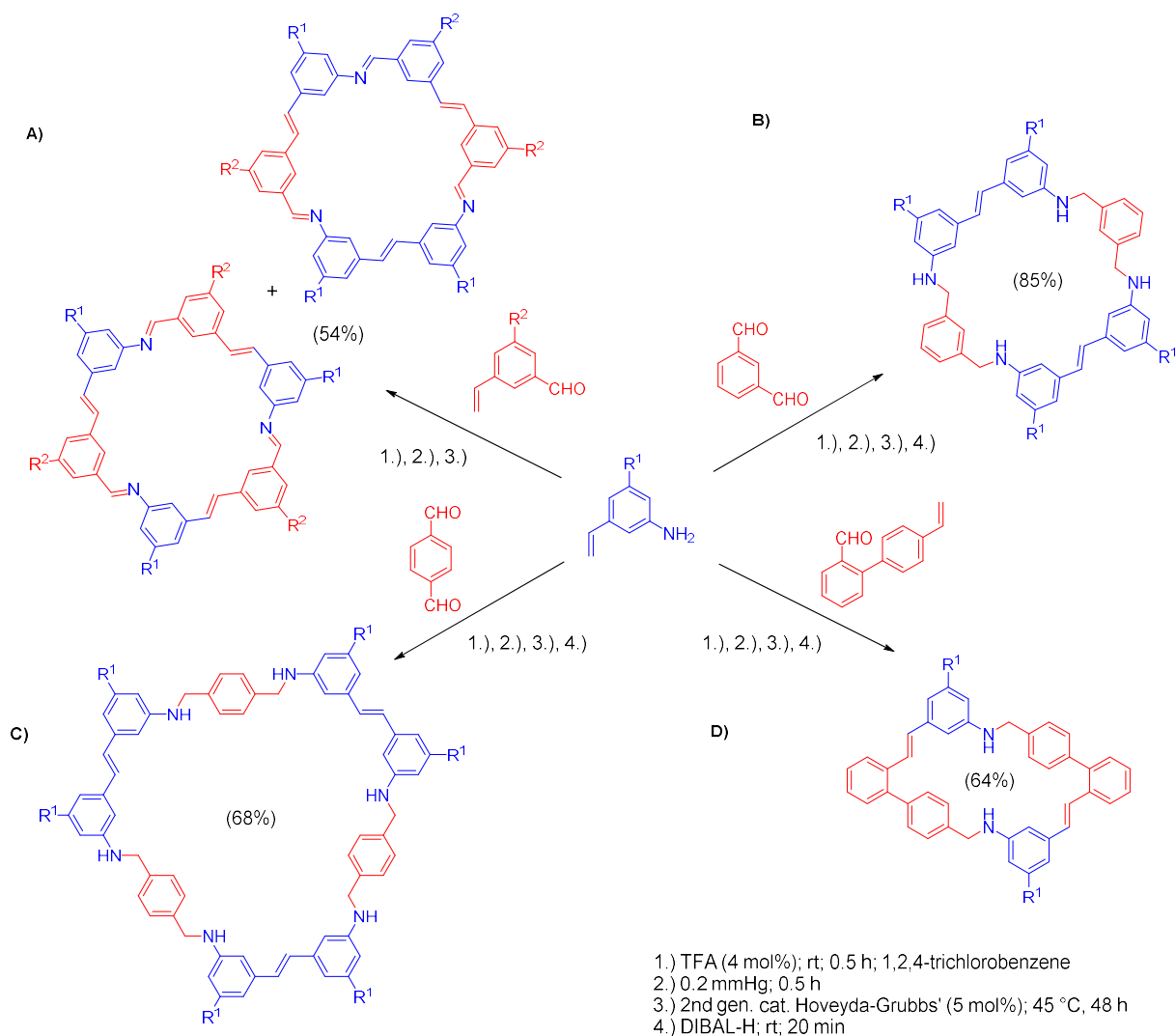
In the first step of “imine-then-olefin”, only one dimer was formed. The second step led to the formation of the same two isomeric macrocycles as in the “olefin-then-imine” approach. However, compared to this method, the “imine-then-olefin” concept showed the highest selectivity, although linear oligomers were still present. This was explained by a less efficient olefin metathesis due to the presence of TFA and the condensation product water degrading the catalyst. By application of vacuum to remove these

substances as well as the olefin metathesis by-product ethylene, the selectivity was shown to further increase. After purification by column chromatography, a mixture of isomeric macrocycles was achieved at 54% yield.<sup>[19]</sup>



**Scheme 46:** Synthesis of six-membered macrocycles via olefin-then-imine (A) and imine-then-olefin (B) strategy.<sup>[19]</sup>

Once the procedure was optimized, further macrocycles became accessible (Scheme 47). The imines were subsequently reduced to the corresponding secondary amines to freeze the equilibrium and the pure products were obtained *via* column chromatography. Applying a 1,3-dialdehyde (Scheme 47, B), the isomerization was shown to be avoided and only one six-membered macrocycle was formed at a yield of 85%. Changing the position of the aldehyde functions into *para*-position (Scheme 47, C) forces the formation of a 9-membered macrocycle at a yield of 68%. Furthermore, the usage of a vinyl-biphenyl-carbaldehyde monomer led to a distorted six-membered macrocycle at a yield of 64% (Scheme 47, D).

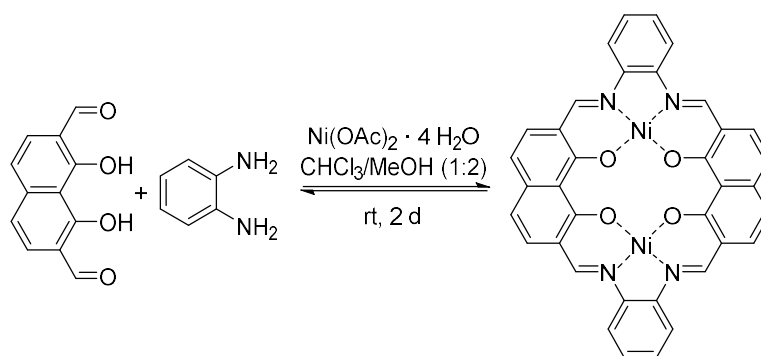


**Scheme 47:** Macrocycles synthesized by orthogonal dynamic covalent chemistry (ODOC) of olefin metathesis and imine condensation.<sup>[19]</sup>

### II.2.2.5. Template Effect

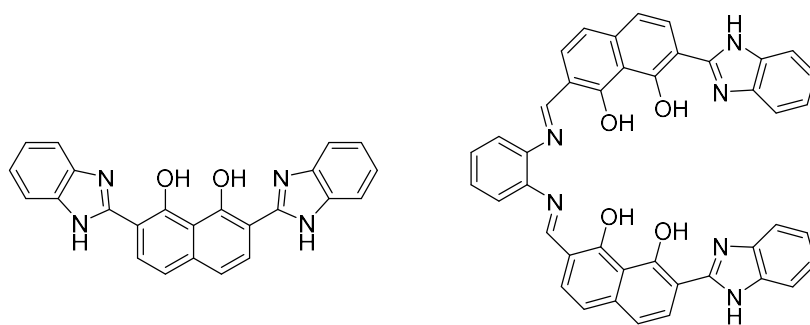
As previously mentioned, the research of Nabeshima and MacLachlan showed that hydrogen bonds and the presence of a water molecule can help induce cyclization.<sup>[17,18]</sup> As mentioned in Chapter II.2.2. *Thermodynamic Approach*, a template, e.g., a metal ion, can be introduced purposefully to selectively obtain one particular cyclic species within a broad range of cyclic products due to the template effect.

The influence of a metal ion on the cyclization behavior was shown by Nabeshima and co-workers.<sup>[97]</sup> As monomers, 1,8-naphthalendiol dialdehyde and a *ortho*-diamine were applied (Scheme 48).



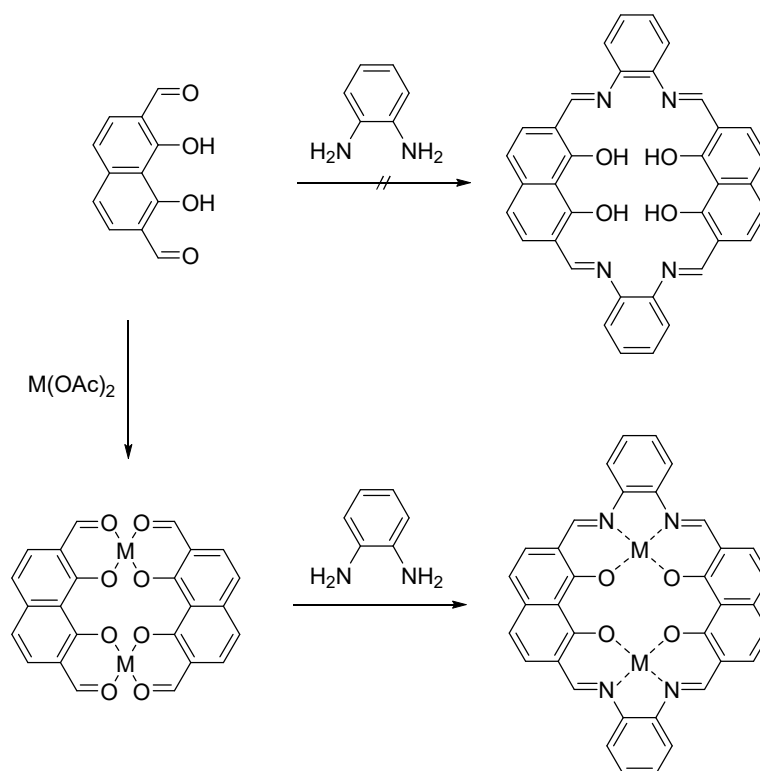
**Scheme 48:** Synthesis of a [2+2] macrocycle by imine condensation using metal ions as template.<sup>[97]</sup>

The composition of the resulting product mixture was analyzed by MALDI-TOF. If no metal ion template was added, only a small peak for the targeted [2+2] macrocycle was detected, as well as traces of a [3+3] macrocycle, while the main product was a benzimidazole derivative. It was found from the crystal structure of the resulting mixture that repulsion among the naphthalene impedes cyclization (*Scheme 49*).<sup>[97]</sup>



**Scheme 49:** Products of imine condensation of 1,8-naphthalenediol dialdehyde and an ortho-diamine without template metal ions. The naphthalene units of the condensation derivative repulse each other.<sup>[97]</sup>

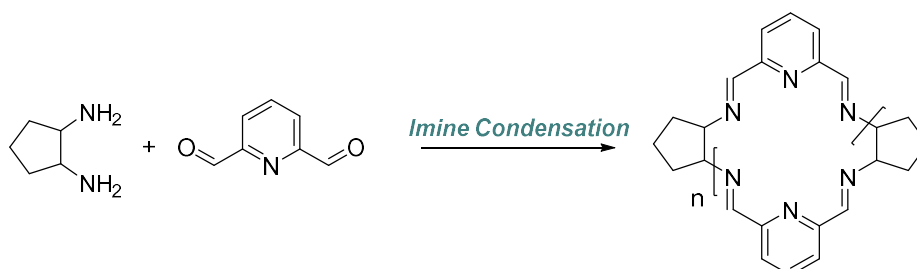
However, in the presence of metal ions, such as  $\text{Ni}^{2+}$ ,  $\text{Cu}^{2+}$ , and  $\text{Zn}^{2+}$ , the [2+2] macrocycle was generated in a yield of 82%. It was assumed that the naphthalene diol dialdehyde forms a complex with the metal ions first and forces a certain geometry whereby, after imine condensation, the nitrogen atoms of the diamine replace the aldehyde oxygen atoms as ligands (*Scheme 50*).



**Scheme 50:** Proposed mechanism by complexation for the formation of a [2+2] macrocycle by imine condensation.<sup>[97]</sup>

A template can not only influence whether a cyclization happens or not, it can also be a tool to control the size and shape of the cyclic species.

Lisowski and co-workers were able to synthesize a library of macrocycles of different sizes by only adjusting the reaction conditions.<sup>[20]</sup> As monomers, a diamine and a dialdehyde, namely 2,6-diformylpyridine and 1,2-diaminocyclopentane, respectively, were employed, thus introducing chirality in the resulting macrocycles (Scheme 51).



**Scheme 51:** Schematic of the reaction of 2,6-diformylpyridine and 1,2-diaminocyclopentane to macrocycles of various sizes.<sup>[20]</sup>



Initially, temperature and time were varied: when the reaction was carried out in methanol, a [2+2] macrocycle ( $n = 1$ ) was obtained in high selectivity (97%) (Figure 7). Due to the low solubility of this compound in the solvent, the macrocycle precipitated, thus shifting the reaction equilibrium towards the desired product. In acetonitrile, the [2+2] macrocycle was found to be more soluble, leading to the formation of traces of bigger macrocycles ( $n = 2$  & 3). The more unpolar the solvent system (elutropic series) was, the greater the concentration of larger macrocycles that was observed. In a benzene/methanol system, the [3+3] macrocycle ( $n = 2$ ) was found to be the dominant product (80%). The different affinity to various solvents allowed the separation of the particular products by fractionated recrystallization, or by preparative SEC after reduction to the corresponding secondary amine.

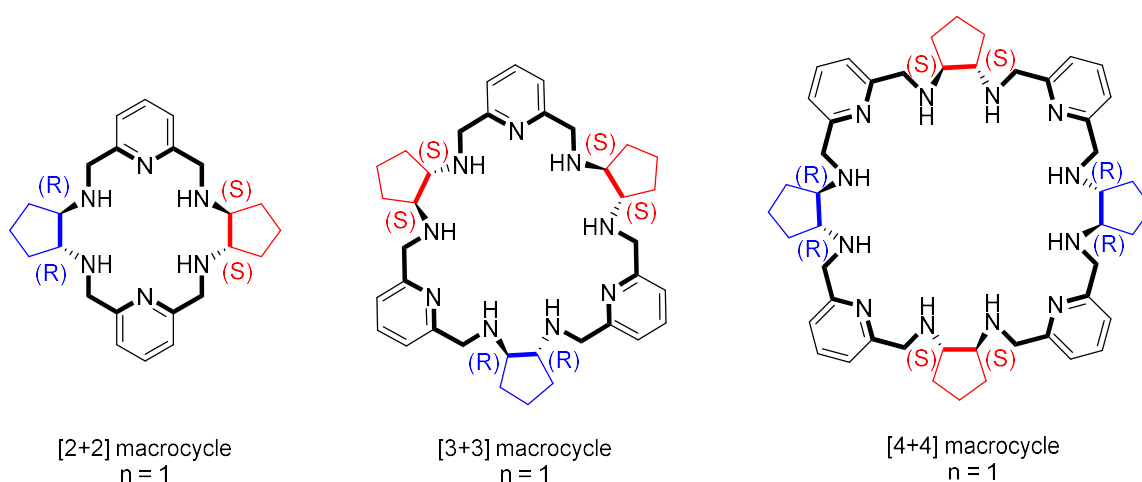


**Figure 7:** Macrocycles of different sizes from the reaction of 2,6-diformylpyridine with 1,2-diaminocyclopentane and reduction to the corresponding secondary amines.<sup>[20]</sup>

Furthermore, the solubility of the macrocycles and thus their precipitation properties was shown to be further influenced by addition of template salts.

By addition of Cd(II) chloride, a complex between macrocycles and the cation was formed, which increased the selectivity towards the [3+3] macrocycle up to 90%. According to DFT calculations, the metal ions complex to the three nitrogens (one of pyridine and two of the adjacent amines) of the growing species and form a “loop”<sup>[20]</sup>, which forces cyclization. The ionic radius of the metal ion was shown to determine the cavity size, hence the size of the macrocycle. Furthermore, the complexation was found to reduce the solubility of the macrocycles. The insolubility of the Cd<sup>2+</sup> complex increased the selectivity; although, the low solubility impedes the subsequent reduction

to the corresponding amine in order to freeze the equilibrium. Upon demetallation, the macrocycle was shown to lose its planarity, rigidity and was shown to gain flexibility, thus increasing its solubility and facilitating full characterization.

Applying  $\text{La}^{2+}$ , the [2+2] macrocycle was selectively obtained. Comparing the ionic radius of  $\text{Cd}^{2+}$  (103 pm) and  $\text{La}^{3+}$  (122 pm), it was observed that the size of the ion correlated inversely with the size of the cavity and that larger ions led to smaller macrocycles. However, in the [3+3] macrocycle, two cadmium ions were complexed instead of only one ion<sup>[98]</sup>, which was the case for the lanthanum-[2+2] macrocycle complex.<sup>[99]</sup>

The solubility of the macrocycles can not only be controlled by the solvent but also by complexation of a template salt, which further allows a control over the size of the generated macrocycles.

### II.2.2.6. Application of Shape-Persistent Macrocycles

#### a) Application in Biology

Rigid macrocycles play a major role in biology, e.g., as porphyrins. The simplest porphyrin is porphine, a rigid macrocycle consisting of four pyrrole units, which are linked together by methine groups and form an aromatic system of 18 delocalized  $\pi$  electrons (*Figure 8*). Due to the ability of nitrogen for metal complexes, porphyrins can act as ligands for metal cations. In hemoglobin, for example, which is responsible for oxygen transport in blood, the essential structure, the heme group complexing  $\text{Fe}^{2+}$  is a porphyrin. In chlorophyll, porphyrins are the essential structure as well, complexing  $\text{Mg}^{2+}$ .<sup>[62]</sup>

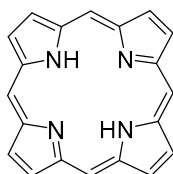


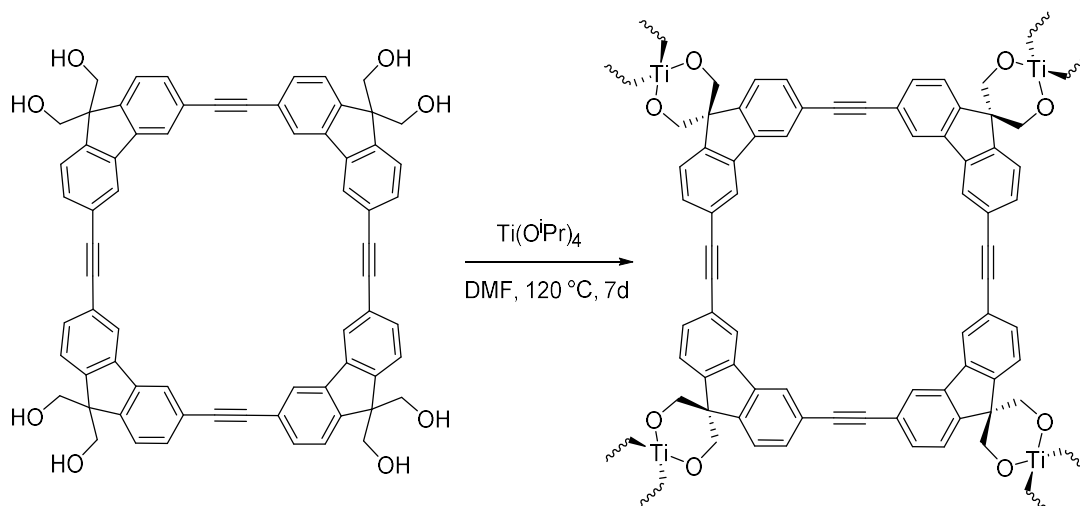
**Figure 8:** Structure of porphine, the simplest porphyrin.<sup>[62]</sup>

## b) Artificial Enzyme & Catalysis

Shape-persistent macrocycles are being discussed as possible artificial enzymes.<sup>[1]</sup> Sanders *et al.* published a butadiyne-linked porphyrin trimer consisting of three porphyrin derivatives complexed with Zn. This structure was shown to catalyze an intermolecular Diels-Alder reaction, giving selectively to the *exo*-product. In the diene and dienophile, nitrogen was incorporated, which complexed to Zn. Due to the rigid structure of the host macrocycles, the complexed reactants were forced into close proximity. Kinetic studies indicated that the reaction proceeded 6000 times faster in presence of the catalyst.<sup>[100]</sup> The same porphyrin trimer was also able to catalyze an acyl-transfer reaction.<sup>[101]</sup>

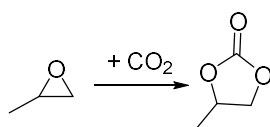
Höger *et al.* synthesized an AEM on which a flexible linker with functional groups was integrated, which could initiate atom transfer radical polymerization (ATRP).<sup>[102]</sup> By this grafting-from approach, polymer chains could be grown on the macrocycle. These macromolecular brushes were shown to be able to change their “structural transition from a cylindrical to a globular brush conformation”<sup>[102]</sup> by an external stimulus such as solvent, temperature or light. Although this was not demonstrated, such a macrocycle which catalyzes a reaction, as shown previously, surrounded by molecular branches providing the stimuli-responsive solubility is conceivable. By changing the conformation of the polymer, the accessibility to the macrocycle cavity by substrates can be switched.

Shape-persistent macrocycles have been reported for inorganic catalytic systems, illustrated by Zhang and co-workers.<sup>[8]</sup> To a four-membered arylene ethynyle macrocycle, which has a structure to the one presented in c) *Influence of Moieties* (consider that the nitrogen is replaced by a carbon), hydroxyl groups were integrated. These reacted with Ti(O*i*Pr)<sub>4</sub> to form titanium alkoxide and thus a porous coordination polymer (PCP) in DMF at 120 °C in 7 days in yield of 98% (*Scheme 52*). The integration of Ti was shown by FT-IR, magic angle spinning solid-state <sup>13</sup>C-NMR spectroscopy, elemental analysis, TGA, SEM, and powder XRD analyses.<sup>[8]</sup>



**Scheme 52:** Synthesis of a Ti-PCP.<sup>[8]</sup>

In presence of Bu<sub>4</sub>NBr (TBAB), as co-catalyst (1 mol% loading), Ti-PCP (0.9 wt% loading) was shown to catalyze the cycloaddition of CO<sub>2</sub> and epoxides to form carbonates (Scheme 53).<sup>[8]</sup>

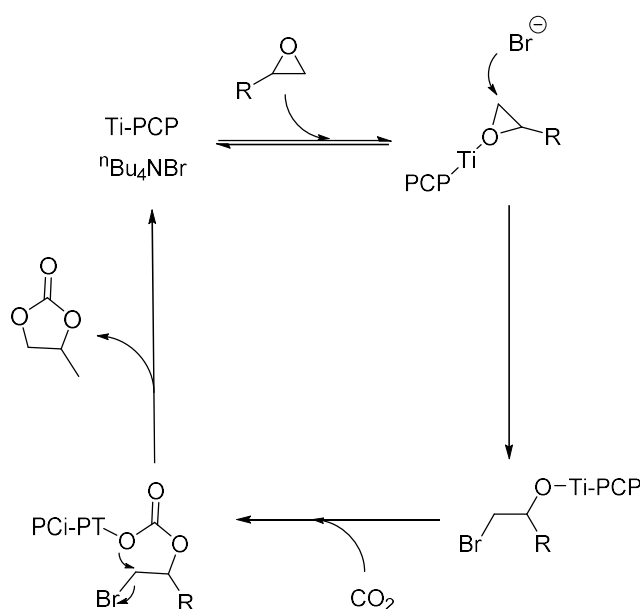


**Scheme 53:** Synthesis of carbonates by cycloaddition.<sup>[8]</sup>

A broad spectrum of different homogeneous and heterogeneous catalytic systems, such as metal oxides, microporous polymers, and organic networks, has been investigated in order to find a more sustainable alternative to synthesize carbonates.<sup>[8]</sup> Carbonates are suitable monomers for polycarbonates,<sup>[103]</sup> which show a potential for biomedical application due to their biodegradability and bio-compatibility<sup>[103]</sup> compared to similar polymers and therefore can be considered “green” materials. However, carbonates are conventionally synthesized using phosgene, which is highly toxic and corrosive.<sup>[8]</sup> Cycloaddition could be a sustainable alternative; however, usually high pressure and temperature are required, increasing the costs. Owing to the large surface area and high density of accessible active sites, the Ti-PCP system enabled the use of a relatively low pressures of only 1 bar CO<sub>2</sub> compared to other systems, which require up to 60 bar to obtain similar results, and with yields greater than >99%, although the

reaction time was relatively long (24 hours) and the temperature relatively high (100 °C). As a heterogeneous catalyst, Ti-PCP was shown to be easily recovered by filtration and did not show any decrease of catalytic efficiency within the observed catalytic runs.<sup>[8]</sup> It is noted that although Ti-PCP delivered good results for this sustainable reaction, the synthesis of the catalytic system cannot be considered “green”.

It is assumed that the epoxides were activated by coordination to the titanium, which facilitates a nucleophilic attack and ring opening by the bromide ion of the co-catalyst (Scheme 54). Subsequently, carbon dioxide was inserted and a ring-closure led to the desired carbonate product as well as recovery of the catalyst.<sup>[8]</sup>



**Scheme 54:** Proposed mechanism of cycloaddition of carbon dioxide to epoxides catalyzed by Ti-PCP and TBAB.<sup>[8]</sup>

### c) Sensor Materials

The host-guest interactions of macrocycles and relevant substrates can not only catalyze reactions, but also lead to a change of the macrocycles' properties, such as its fluorescence. The four-membered macrocycles presented in II.2.2.1. *Shape-persistent Macrocycles via Alkyne Metathesis Scheme 30* were used for the detection of the explosive compounds 2,4-dinitrotoluene (DNT) and 2,4,6-trinitrotoluene (TNT).<sup>[4]</sup> The intensity of the inherent fluorescence of the macrocycles was shown to increase

by long alkyl chains at the outer rim acting as electron donating groups. The macrocycles were dissolved in THF and spin-coated on glass as carrier material. In presence of the explosives' vapor, the fluorescence of the macrocycle was shown to be quenched. Subsequent treatment with hydrazine vapor removed the explosives from the detector, thus allowing recycling. The procedure was repeated five times without reducing the activity of the detector material.<sup>[4]</sup>

#### d) Mechanically Interlocked Molecules (MIMs)

The synthesis of rotaxanes and other MIMs is not limited to flexible cycles. Höger and co-workers showed the synthesis of phenylene-ethynylene-butadiynylene rotaxanes (Figure 9).<sup>[7]</sup> These particular shape-persistent macrocycles were obtained by template-assisted synthesis: the template for the middle cycle was introduced by an ester bond, which can be easily cleaved. To the template, stiff ethynyl linkers were added by cross-coupling to which the stopper macrocycles were coupled afterwards. Finally, the template of the middle cycle was removed without interfering with other bonds of the structure. In this way, the middle cycle could move along the stiff link but was mechanically locked. Due to long alkyl chains, the resulting [2]rotaxanes were soluble and could be characterized by NMR spectroscopy, MALDI-TOF and SEC.<sup>[7]</sup>

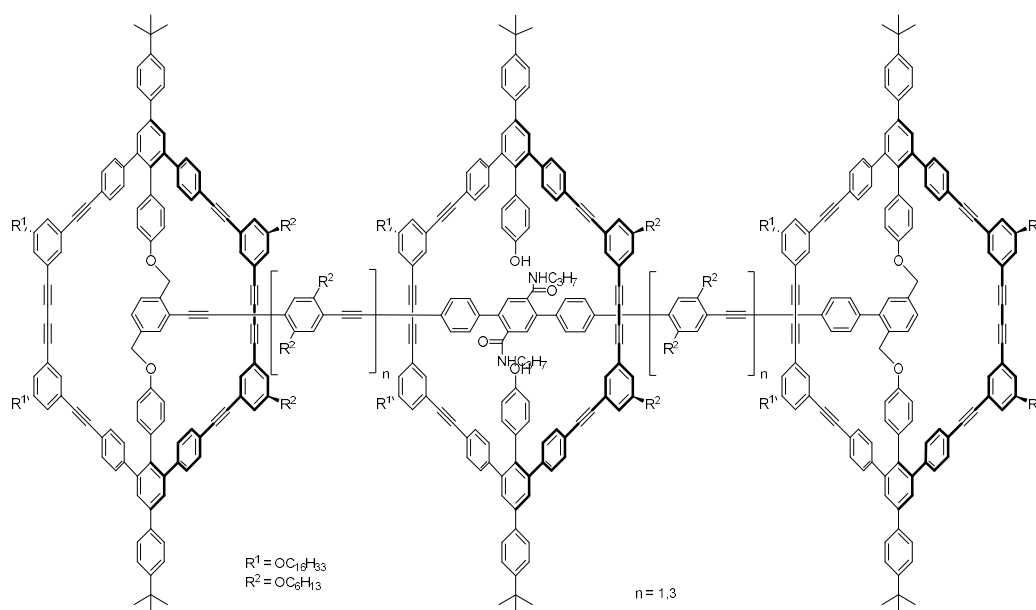


**Figure 9:** Phenylene-ethynylene-butadiynylene [2]rotaxanes.<sup>[7]</sup>

Two main approaches have been presented for the synthesis of macrocycles. While the kinetic approach requires a high synthetic effort, the thermodynamic approach is more straightforward in direct comparison due to the reversible character of the reactions. Different chemistries can be applied to obtain a broad spectrum of various macrocycles. Size and shape can be controlled by the applied reaction conditions and especially by the design of the applied monomers. Applications were presented, which illustrate not only the versatility of shape-persistent macrocycles for many different applications, but also show that they can be applied as building blocks for a large structure, forcing a certain geometry due to their rigid structure.

## II.3. 2D Polymers

*This chapter was taken partly from the Master thesis “Efficient Access to Rigid Rings via Metathesis Reactions” written by Gregor Klein in 2015.<sup>[55]</sup>*

Another important class of materials are 2D polymers. The synthesis of these materials exhibits two major challenges: forcing a planar structure and an efficient synthesis procedure with an atomic precision over large distances. Shape-persistent macrocycles with functional groups on the outer rim could not only act as monomers enabling a planarization, but the integration of solubilizing groups on the macrocycle could also increase the solubility of the resulting materials. DCvC provides a library of reactions allowing for error-correction and high selectivity towards a desired structure.

For two-dimensional polymers, no uniform definition exists yet.<sup>[104]</sup> Dichtel defines “a 2D polymer [...as] a covalently linked network of monomers with periodic bonds in two orthogonal directions”.<sup>[105]</sup> 2D polymers can exist as layered crystals, multilayer or monolayer films on surfaces or free-standing sheets.<sup>[106]</sup> On the other hand, according to Schlüter, 2D polymers are one monomer unit thick sheet-like polymers, in which the monomer units are periodically connected in two dimensions.<sup>[104,105]</sup> In this definition, the planarity of the structure is emphasized, as well as the separability, which means that 2D polymers should exist in individual entities.<sup>[107]</sup>

In spite of differences in definition, all interpretations have some criteria in common, which are

- the existence of a repeating unit (as in 1D polymers)
- which are connected by covalent bonds
- and form a one atom thick,
- two-dimensional periodic structure.

The position and arrangement of the covalent bonds form the structure of a 2D polymer. Hence, for their synthesis, atomic precision over a large area is required, which makes the synthesis a challenging task.<sup>[108]</sup> Due to their defined structure, 2D polymers should have a specific pore volume and position of functional groups, which can be further functionalized. Macromolecules with such properties have large



potential for gas separation, water desalination,<sup>[109]</sup> electrostatic sensing, catalysis, or in their application in membranes, filters and optoelectronic devices, among other applications.<sup>[108]</sup> As the definition of 2D polymers is still not set certain, some reports suggest that the synthesis of true 2D polymers has not been achieved, while others refer to certain existing structures of 2D polymers.<sup>[104,108]</sup> An already existing class of materials, which fits the requirements that define 2D polymers are the so-called covalent organic frameworks (COFs).<sup>[108]</sup> Depending on the monomer structure, the resulting COFs can be two- or three-dimensional. However, 2D COFs do not exist as free standing sheets but are obtained during synthesis as layered crystals. COFs can be compared to graphite and a COF layer as graphene; hence, only a COF layer can be regarded as a 2D polymer. Separation into individual sheets, e.g., by exfoliation, is challenging<sup>[110]</sup> but necessary for full characterization. Furthermore, full analysis of the characteristics of COFs, especially their optoelectronic properties, is challenging as COFs are typically powders which are difficult to attach to surfaces, such as electrodes.

The existing synthetic approaches for 2D polymers will be discussed in subchapter *II.3.2. Synthetic Approaches to 2D Polymers*, whereas the following subchapter focuses on a natural representative of 2D polymers: graphene.

### **II.3.1. Graphene as the Prototype of 2D Polymers**

Graphite is an allotrope of carbon and forms one carbon-atom thick molecular sheets. One of these sheets, graphene, can be considered the thinnest covalent film that one can image.<sup>[107]</sup> Furthermore, since the carbon atoms are bonded covalently, a layer of graphene is just one large molecule.<sup>[104]</sup>

Graphene consists of benzannulated rings with non-localized bonds forming a honeycomb structure.<sup>[107]</sup> As a polymer, defect-free graphene can be formally divided into repeating units. The smallest repeating unit is the  $sp^2$ -hybridized carbon atom with three electrons in the three  $sp^2$ -orbitals and one in the p-orbital.<sup>[104]</sup> Another reasonable repeating unit is the shaded hexagon(benzene-1,2,3,4,5,6-hexayl unit) (*Figure 10*).

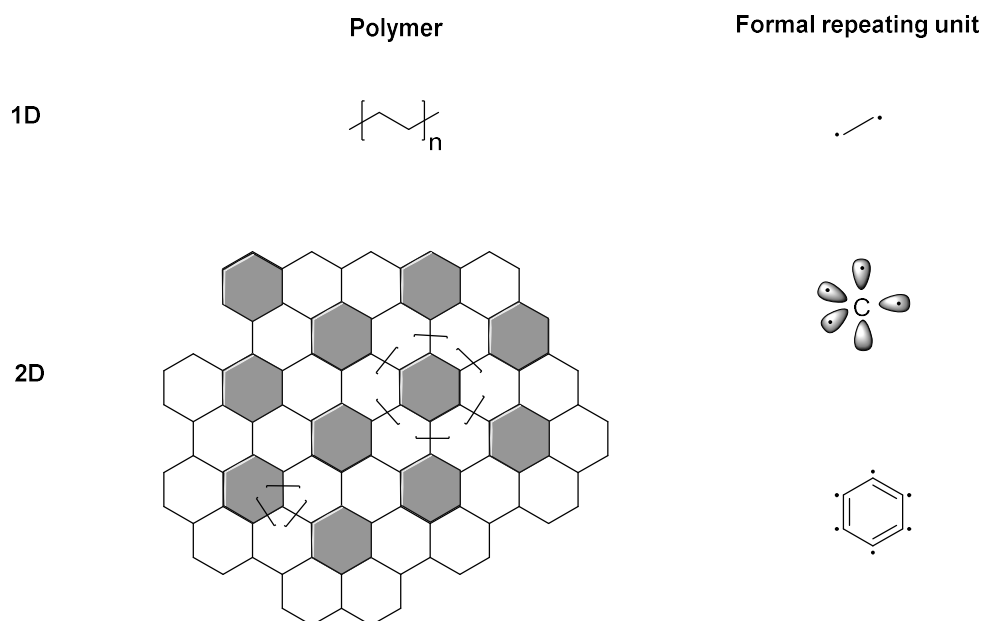


**Figure 10:** Formal division of graphene in repetitive fragments.<sup>[104]</sup>

Predicted to be thermodynamically unstable, it came as a surprise when Geim and Nososelov succeeded in isolating a single layer graphene crystal in 2004 by exfoliation of a graphene layer from graphite, which is in a metastable state.<sup>[107,111]</sup> According to theory, a perfect two-dimensional crystal cannot exist. Graphene does not contradict this theory due to the fact that a graphene sheet is not perfectly planar, but shows a crinkled structure in 3D space. Deformations protrude 1 nm from the plane, which was proven by transmission electron microscopy.<sup>[107,111]</sup>

Common methods to obtain graphene are epitaxial growth, pyrolytic decomposition techniques, or exfoliation.<sup>[108]</sup> In epitaxial growth, graphene can be obtained by thermal decomposition of a commercially available carbide silicon wafer. The silicon evaporates and the remaining carbon atoms form a single graphene layer.<sup>[112]</sup> Graphene can also be obtained by chemical vapor deposition (CVD) of carbon on a copper foil by heating a mixture of hydrogen and methane up to 1000 °C.<sup>[113]</sup> By exfoliation *via* the scotch tape procedure, a common adhesive film is used to isolate a layer of graphene from graphite.<sup>[111,114]</sup> Smaller graphene sheets, so-called “nanographenes” are structurally precise and can contain up to 200 carbon atoms, but require a complex multi-step synthesis which is explained in chapter II.3.2.1. *Solution Approach*.<sup>[115]</sup> These established preparation processes, however, are hindered by a poor reproducibility<sup>[114]</sup> or inefficiency in significantly larger systems.<sup>[108]</sup>

Graphene exhibits a wealth of interesting optical, mechanical and electronic properties promising for a variety of different applications.<sup>[108]</sup> For instance, due to higher mobility of electrons in graphene compared to silicon, graphene is being considered a material for semiconductors.<sup>[114,116]</sup> Graphene has a tensile strength of > 100 GPa and a tensile modulus of 1 TPa; hence, graphene is one of the strongest materials ever tested. Scientists and engineers are constantly developing new materials and systems that exploit these unique properties of graphene in order to access various applications, for example in aeronautics and “may permit such exotic structures as a space elevator”.<sup>[117]</sup>

Despite the seemingly unlimited applications due to the outstanding properties, graphene lacks of a preparation process to guarantee reproducibility and of a way to modify its surface covalently without losing the full-conjugated system. A 2D polymer with merely a graphene-like structure and additional functional groups could have properties similar to graphene and beyond that, which is one aspect to stimulate research for 2D polymers.

Hydrogenated derivatives of graphene are graphane (50% hydrogenation) and graphane (100%). Similar to graphene, these allotropes have interesting, unique properties resulting, such as a lower in-plane stiffness compared to graphene (approx. 30%).<sup>[118]</sup> Another two-dimensional allotrope of graphene is graphyne. While graphene is built on  $sp^2$ -hybridized carbons, graphyne additionally contains  $sp$ - hybridized carbons. The most commonly discussed graphyne is  $\gamma$ -graphyne (*Figure 11*).<sup>[118]</sup>

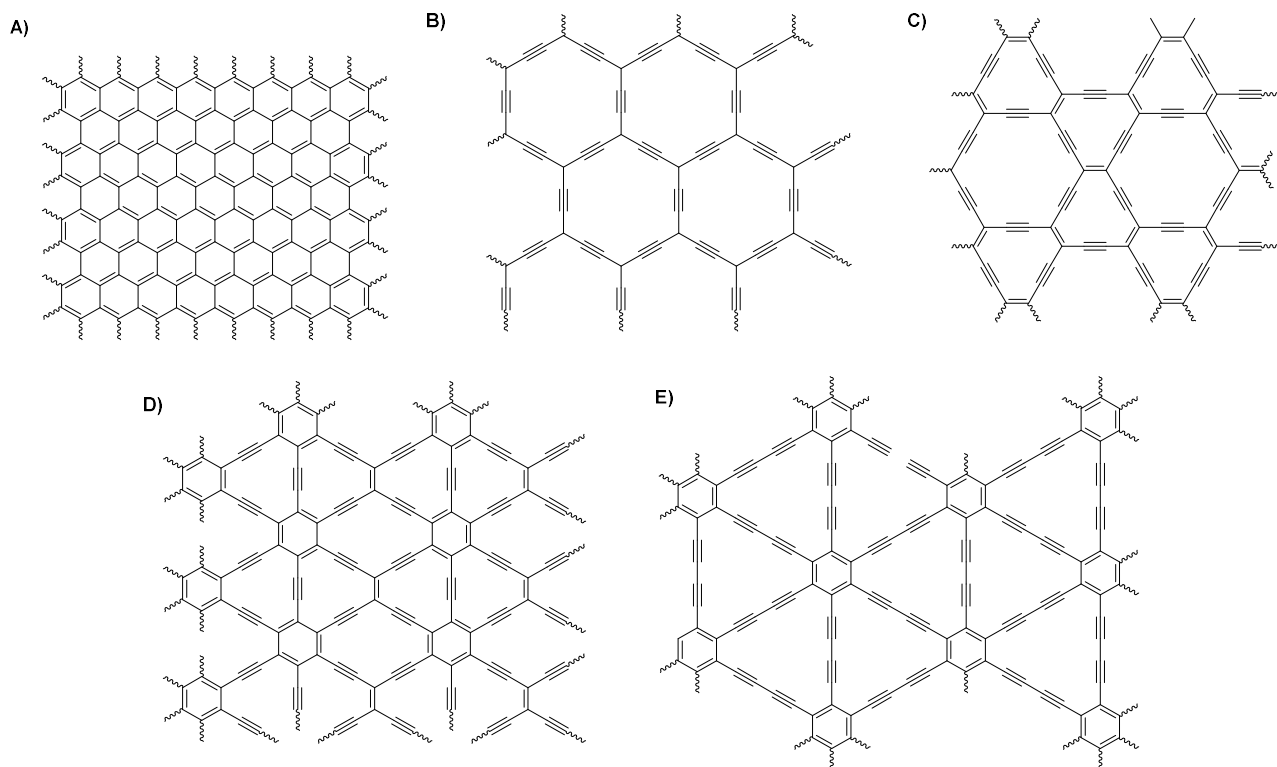
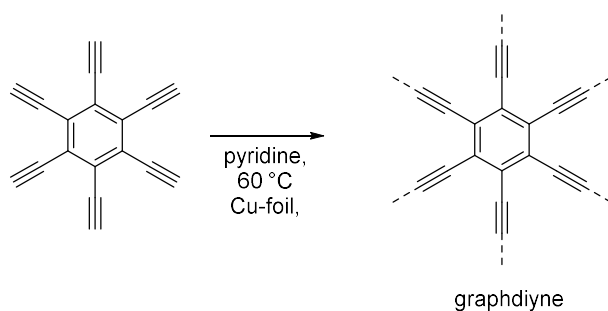


**Figure 11:** Structure of graphene (A),  $\alpha$ -graphyne (B),  $\beta$ -graphyne (C) and  $\gamma$ -graphyne (D) and graphdienes (E).<sup>[118]</sup>

Zhu and co-workers obtained graphdiyne by cross-coupling of hexaethynylbenzene in presence of pyridine and a Cu surface which acts both as a catalyst and a template (*Scheme 55*). Over the reaction time of two days, a black substance deposited on the Cu surface which was proven to be graphdiyne by EDX, XPS and XRD.<sup>[119]</sup> Furthermore, doping of graphdiyne in presence of melamine was reported.<sup>[120]</sup> Under the applied reaction conditions, melamine degraded to  $\text{NHCNH}_2^+$ , which reacted with graphdiyne and substituted a carbon atom with nitrogen. Those *sp*-N doped graphdiyne layers were used as metal-free catalyst.<sup>[120]</sup>



**Scheme 55:** Formation of graphdiyne by cross-coupling in presence of a Cu surface.<sup>[119]</sup>

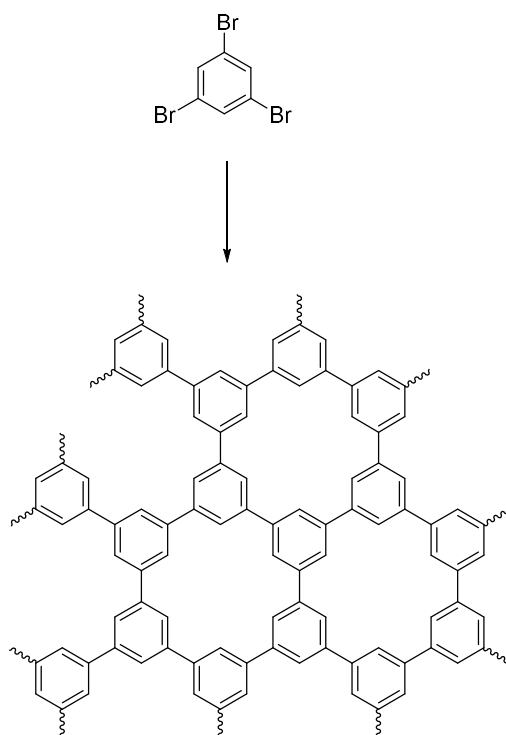
## II.3.2. Synthetic Approaches to 2D Polymers

Two main approaches to synthesize 2D polymers exist, which in turn are divided into different strategies. In the “solution” or “flask-type” approach, procedures from organic, supramolecular and polymer chemistry are chosen as synthetic pathways.<sup>[104]</sup> In the “template” or “surface approach”, a monomer interacts with a surface or interface, *e.g.*, a layered crystal, templating the formation of the 2D polymer.<sup>[108]</sup> Following the solution approach, larger batches can be synthesized than in the template approach in which the production of 2D polymers is only feasible at pmol- or nmol-scale. On the other hand, the solution approach requires smart monomer design, and even then, it is difficult to enable a planar structure due to the flexibility of the molecules in solution. In the template approach, the surface itself causes a planarization. Although the results of the template approach are perceived to be more promising at the current state, a lot of further research is necessary for a potential future (industrial) application. Currently, neither the solution nor the template approach has resulted in the big “breakthrough” to efficiently obtain 2D polymers.

### II.3.2.1. Solution Approach

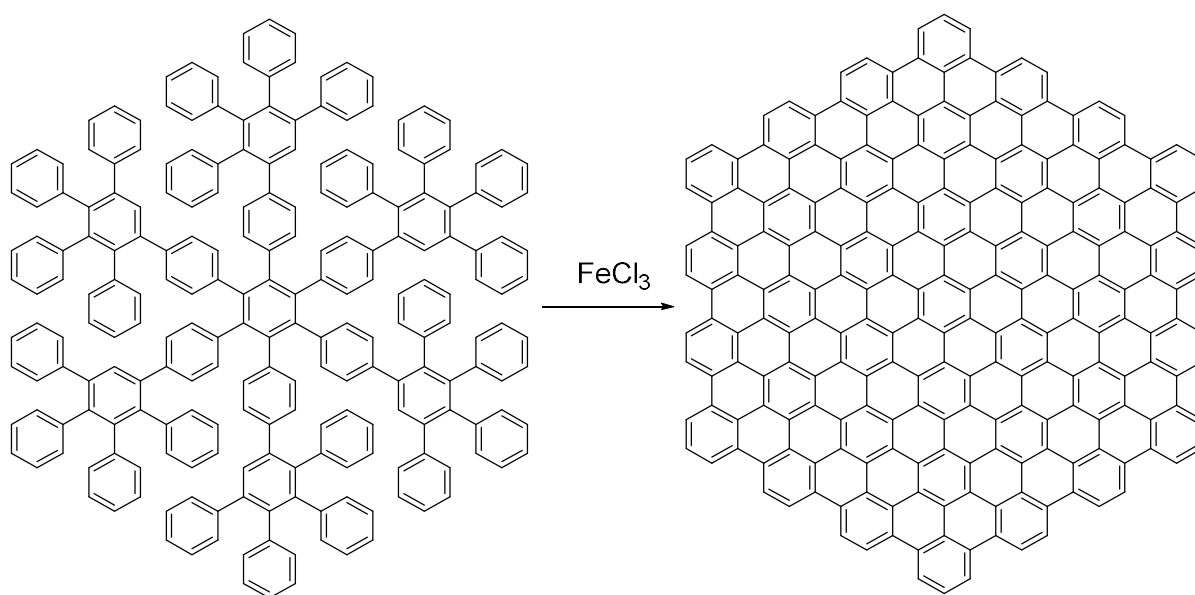
#### *a) The Organic Chemistry Approach*

The organic chemistry approach is based on linking small “dimensionless” organic molecules with covalent bonds. Various compounds have been proposed as monomers for 2D polymers. In order to form two-dimensional structures, the minimum requirements for the monomers are that they should at least be trifunctional and shape-persistent.<sup>[104]</sup> One of these hypothetical monomers is 1,3,5-tribromobenzene, for which the carbon-bromine bonds in the monomer are exchanged for carbon-carbon bonds in the polymer (*Scheme 56*).<sup>[104]</sup>



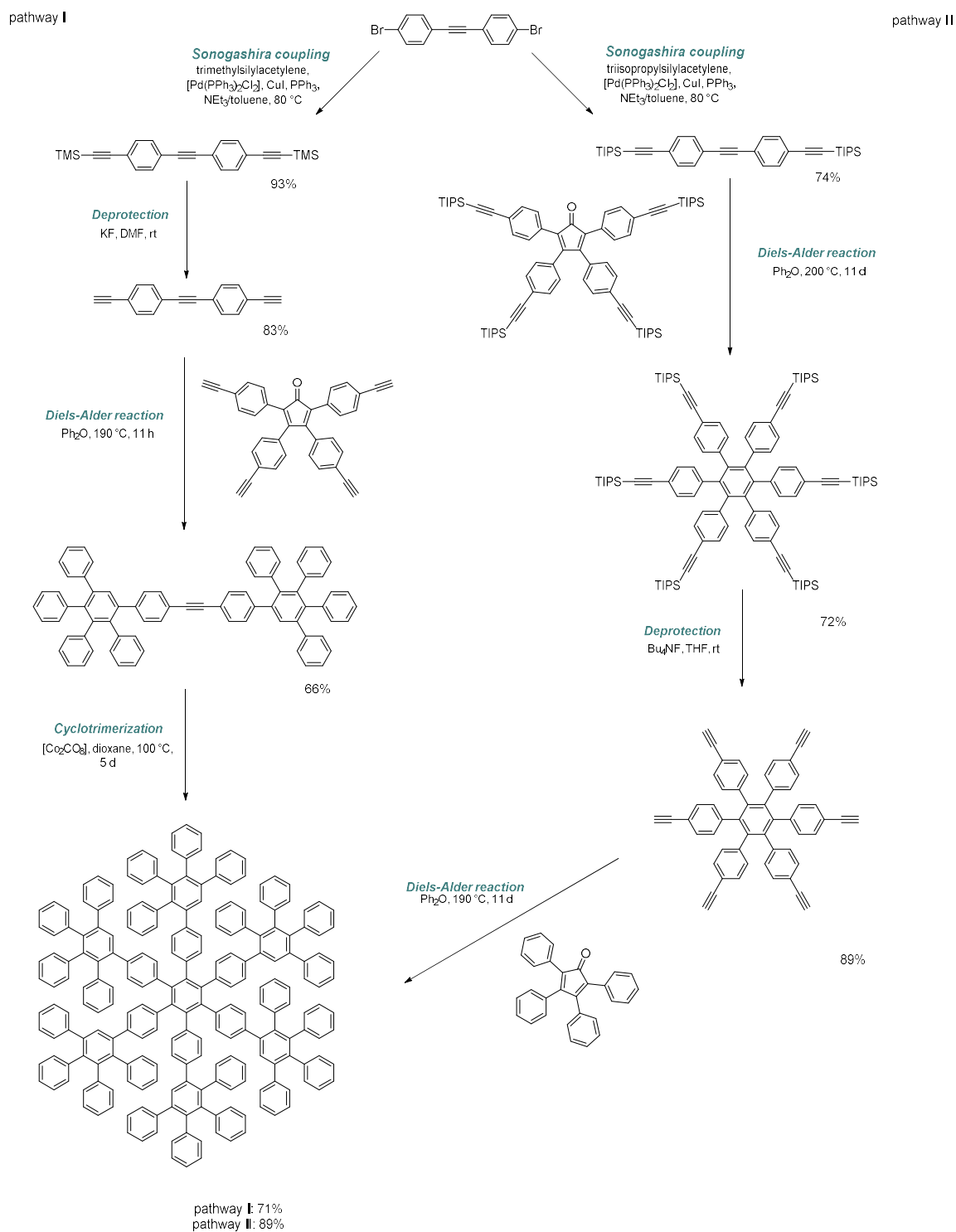
**Scheme 56:** Proposed formation of 2D polymers from 1,3,5-tribromobenzene.<sup>[104]</sup>

Not all proposed monomers remained a hypothetical idea. Müllen *et al.* succeeded in synthesizing the largest known “nanographene” consisting of 222 carbon atoms (Scheme 57).<sup>[115]</sup>



**Scheme 57:** Synthesis of a nanographene as described by Müllen *et al.*<sup>[115]</sup>

The synthesis of nano-graphene from precursors was achieved through two synthetic pathways both consisting of multiple steps of Sonogashira coupling, Diels-Alder reactions and cyclotrimerization reactions and differed in the sequence of the reactions (*Scheme 58*). Although the yield of the individual steps was relatively high between 66% and 93%, the sheer number of steps decreases the overall yields to 43% and 36%. This strenuous synthetic effort is herein perceived as a drawback of the organic chemistry approach. The formation of nano-graphene from a precursor with a “spherical”<sup>[115]</sup> structure and being soluble in common solvents, was witnessed by the precipitation of the nanographene, which was planar and insoluble. This transformation was accomplished by oxidative cyclodehydrogenation using copper(II) triflate/aluminium(III) chloride in carbon disulfide as the catalysis in a yield of 62% (*Scheme 57*).<sup>[115]</sup>

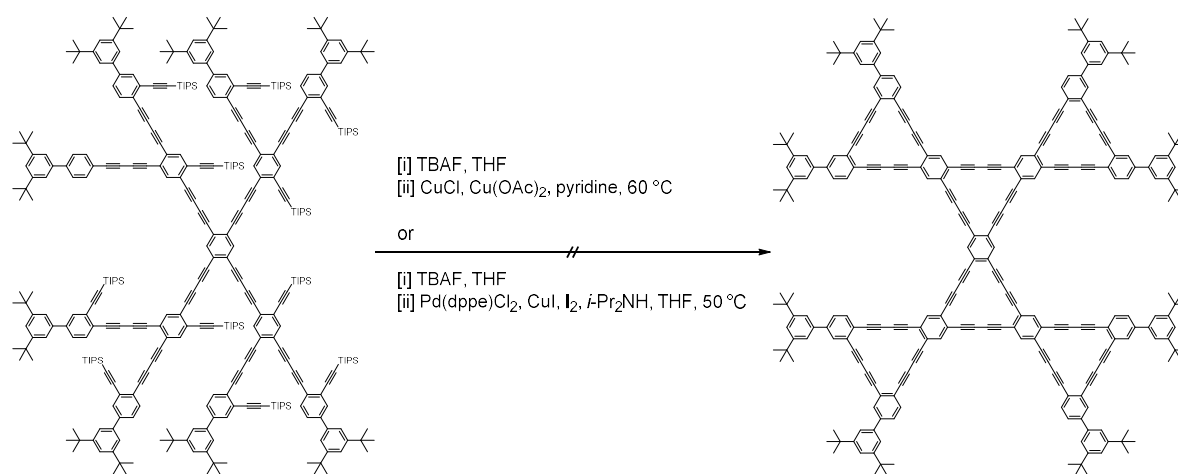


**Scheme 58:** Two synthetic pathways towards the precursor molecule for a nanographene by Müllen et al.<sup>[115]</sup>

The insolubility of such planar and rigid molecules is a big challenge for the synthesis of 2D polymers, impeding not only the characterization but also further reactions to enlarge the 2D structures.<sup>[109]</sup>



Apart from the lack of appropriate solvents, the large number of complex reaction steps necessary in 2D polymer synthesis approaches limits the size of the resulting 2D polymers. Marsden and Haley, for example, were able to synthesize a precursor molecule of the partial structure of a graphydine (a two-dimensional allotrope of graphene) (*Scheme 59, left side*). However, further transformation to the desired product (*Scheme 59, right side*) was unsuccessful due to many side reactions and “the number of simultaneous intramolecular homocouplings necessary for product formation”.<sup>[121]</sup>



**Scheme 59:** Unsuccessful homocoupling of a precursor molecule of a partial structure of graphydine.<sup>[121]</sup>

Others have found a way to synthesize well-defined two-dimensional networks by multi-step reactions. For example, Höger co-workers obtained a hexagonal rigid 2D molecule in a 17-step synthesis by transition metal-catalyzed cross-coupling reactions. The oligomer was synthesized using a modular approach consisting of one module as a “hub” and six other ones as “spokes” (*Figure 12*).<sup>[122]</sup> The “hub” was synthesized in a two-step synthesis with an overall yield of 60.1% (*Scheme 60*). After a multi-step synthesis, the “spokes” were obtained in an overall yield of 8.9%. The merging of the modules and the subsequent purification gave a yield of 27.1%, thus an overall yield of only 1.4%. The resulting product is 5.7 nm broad and thus is rather consider a dendrimer or star-shaped oligomer instead of a 2D polymer, owing to its small dimensions.<sup>[122]</sup>

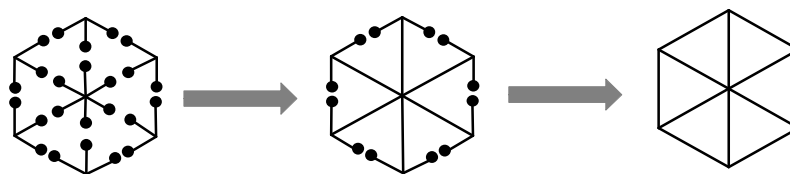
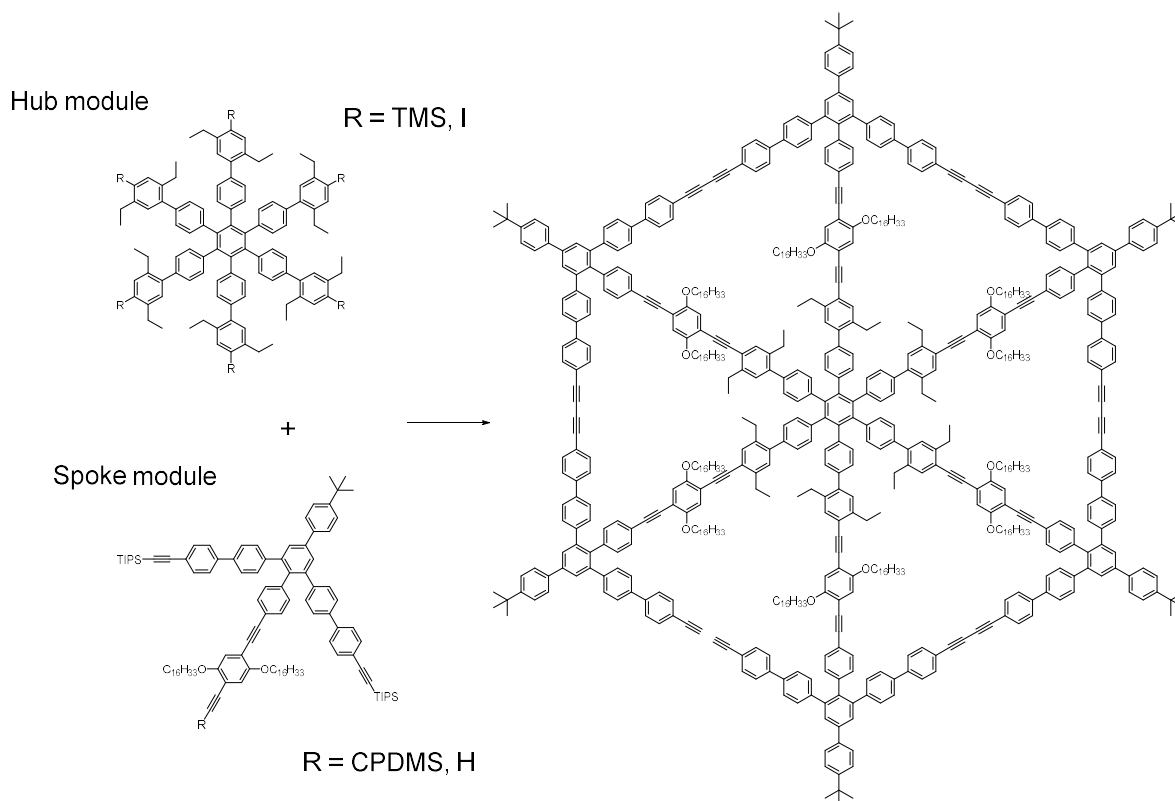


**Figure 12:** Modular synthesis of a dendrimer by Höger *et al.*<sup>[122]</sup>



**Scheme 60:** Creation of a 2D hexagonal network by module synthesis of hub and spoke modules.<sup>[122]</sup>

Subsequently, Höger *et al.* synthesized a “giant molecular spoked wheel” with a diameter of ca. 12 nm by modular synthesis, which is more than twice as big as the previous molecular wheel (Figure 13) and had a molecular weight of 25,260 Da. Despite its size and the fact that the wheel is one atom thick, it is considered a dendrimer-like structure. Impressively, the molecule was found to be soluble in common organic solvents due to the 96 units pointing up and down out of the plane of the wheel, thus counteracting the potential insolubility of the enormous aromatic system and its rigid structure. <sup>[6]</sup>

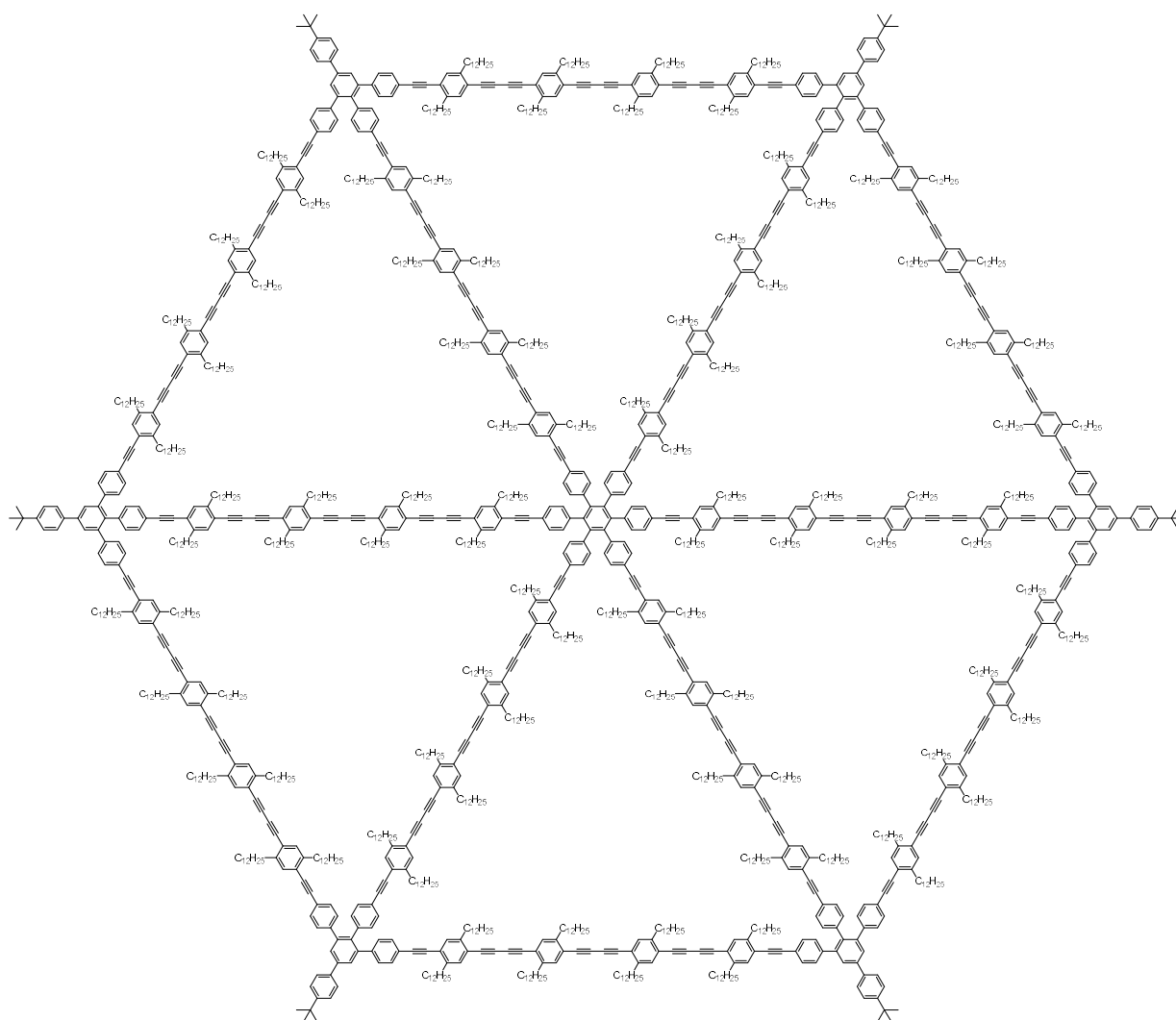


**Figure 13:** Structure of a "giant molecular wheel" by Höger & co-workers.<sup>[6]</sup>

### b) Multi-Strand Approach

In the organic chemistry approach, by starting from "dimensionless" molecules, many isotropic fragments are formed.<sup>[104]</sup> As an alternative, band-like molecules with an almost infinite length in at least one direction (*i.e.*, y-direction) can be used as monomers (*Figure 14*). These "one-dimensional" molecules can be expanded in a second dimension (*i.e.*, x-direction) to create a two-dimensional molecule with a larger area.<sup>[104]</sup>

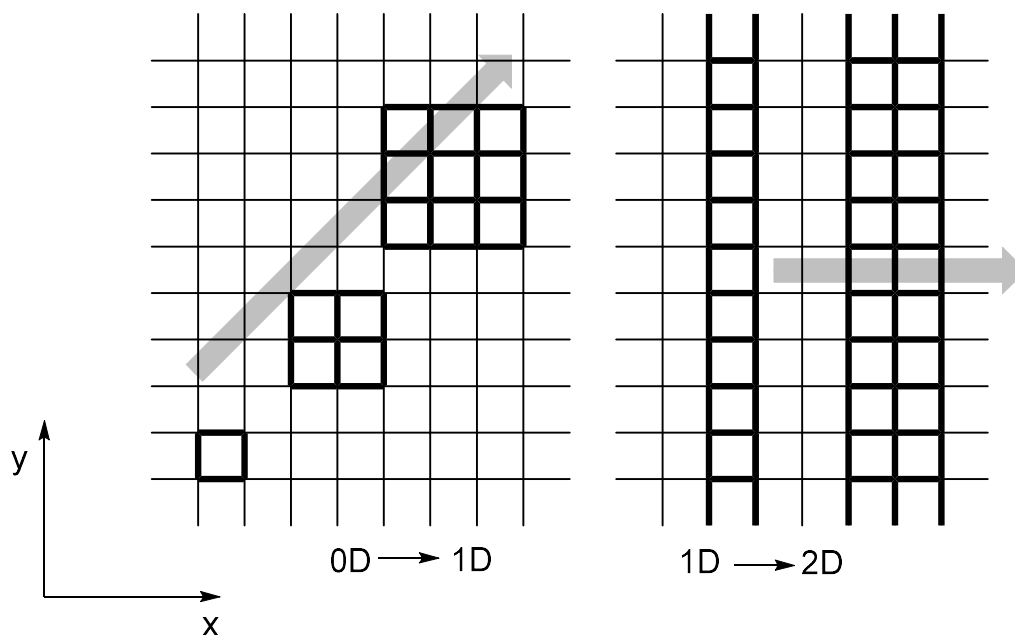
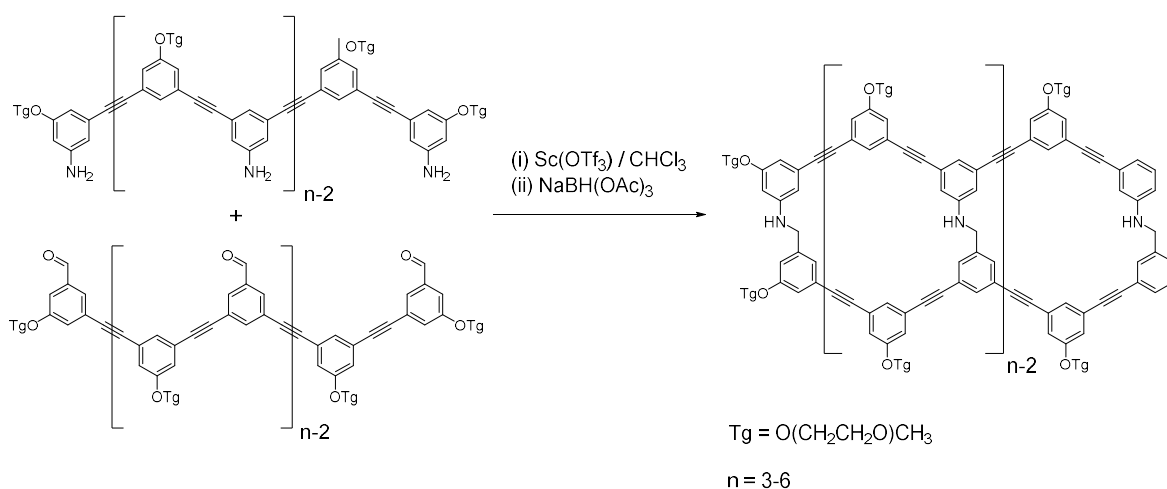


**Figure 14:** Schematic comparison between organic chemistry and multistranded approaches.<sup>[104]</sup>

Moore *et al.* connected long strands to obtain molecular ladders with a length of 6.2 nm.<sup>[123]</sup> Two chain-like molecules as “ladder spars” were synthesized in a laborious multi-step synthesis including several cross-coupling reactions, as well as protection and deprotection steps. The “ladder spars”, or chains, consisted of building blocks which were synthesized in 22 steps with yields between 58% and 97%. Each of these chains carried one type of functional groups, either aldehydes or amines, to prevent an intra-molecular coupling. Both parts were combined by imine condensation at a yield of 56% after purification by preparative SEC (*Scheme 61*). In order to freeze the equilibrium, the imines were reduced to the corresponding amines, which facilitated the analysis by MALDI mass spectrometry, SEC and <sup>1</sup>H-NMR spectroscopy.



**Scheme 61:** Synthesis of molecular ladders from oligomers.<sup>[123]</sup>

Broader ribbons, consisting of four strands, have been developed by Müllen co-workers (*Figure 15*). They were obtained by cyclodehydrogenation of polyphenylenes, which were processed in a multi-step synthesis. First, 1,4-diiodo-2,3,5,6-tetraphenylbenzene reacted in a Suzuki-Miyaura coupling with 4-bromophenylboronic acid. Afterwards, the resulting compound was converted to a boronic ester. By Suzuki-Miyaura coupling, oligomers were synthesized, which formed a quadruple-stranded compound by cyclodehydrogenation.<sup>[124]</sup> Although the yield of the individual steps was relatively high ranging between 93% and 65%, the overall yield was 37%. The ribbons were characterized by SEC and MALDI-TOF before and after cyclodehydrogenation. The success of the reaction was confirmed by the mass change, while the narrow molecular weight distribution did not undergo significant changes. UV spectroscopy showed a red shift of about 200 nm of the absorption maximum compared to the precursor molecule. Remarkably, despite of the size of 2.7 nm by *ca.* 9.2 nm and the large conjugated system, the quadruple-stranded ribbon was found to be soluble in common organic solvents such as DCM and THF due to the large number of pendant alkyl chains which prevented aggregation in solution.

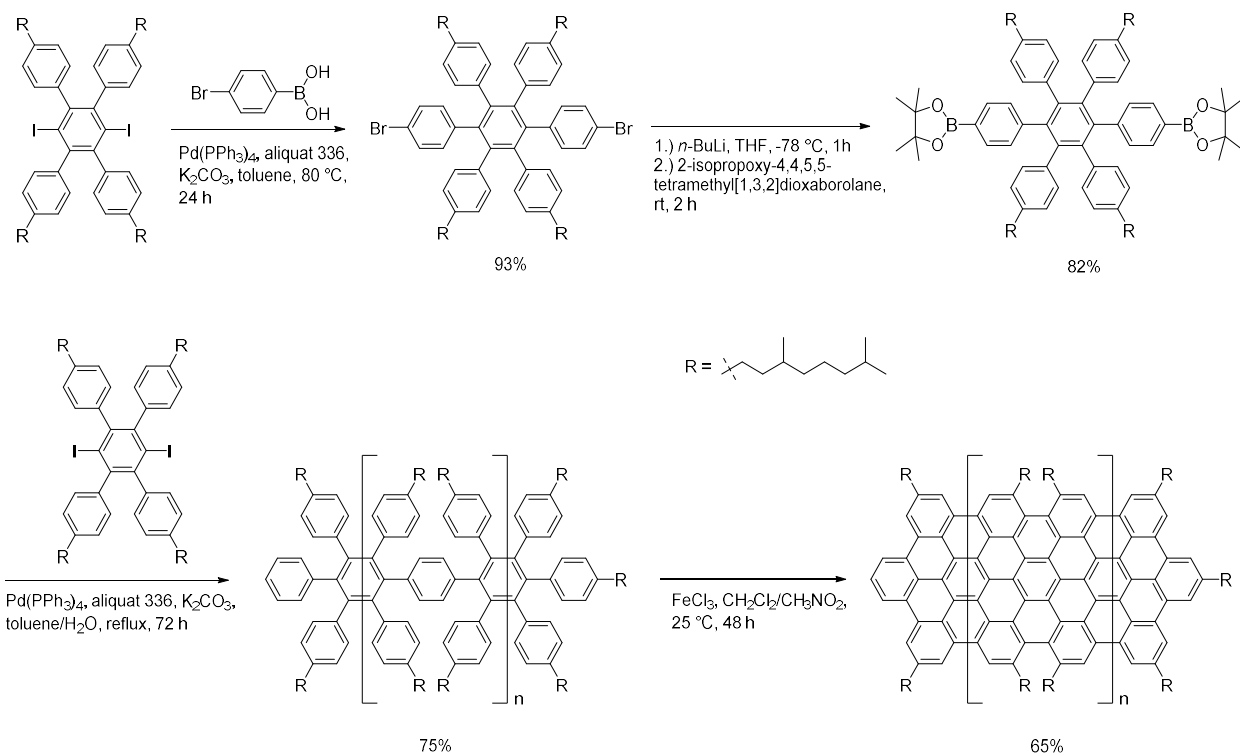
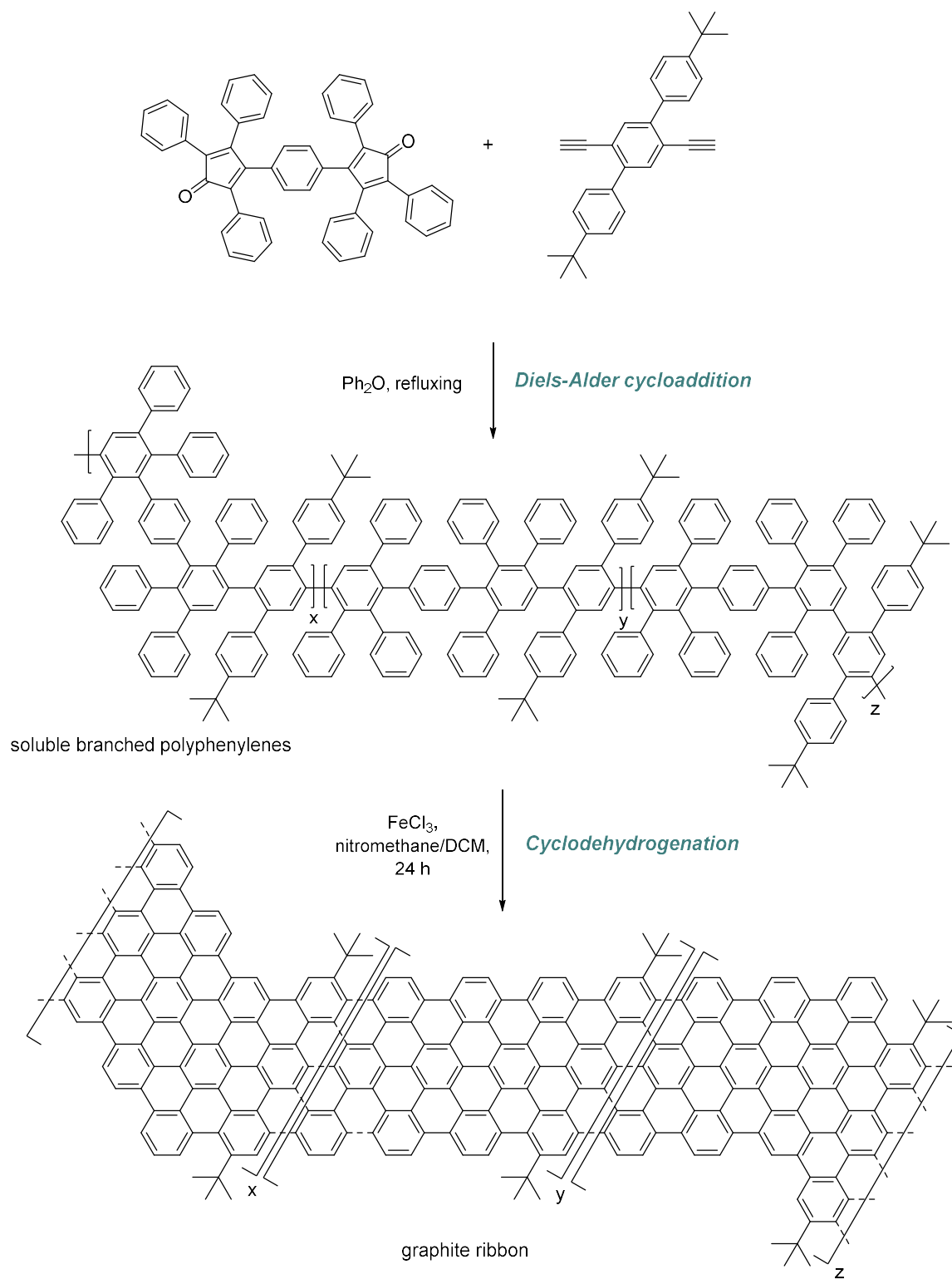


**Figure 15:** Synthesis of quadruple-stranded ribbon of different length in a multi-step synthesis.<sup>[124]</sup>

Subsequently, larger ribbons containing 200 condensed benzene rings, so-called graphene nanoribbons (GNRs), were created (Scheme 62).<sup>[125]</sup> The synthesis was achieved by Diels-Alder cycloaddition between a dibromoterphenylene and a diethynyldiphenylbenzene resulting in soluble branched polyphenylenes in 88% yields. After subsequent cyclodehydrogenation with  $\text{FeCl}_3$ , the resulting graphite ribbon was found to be insoluble, which impeded full characterization; however, solid-state UV/Vis-, Raman- and IR-spectroscopy confirmed the formation of a large conjugated framework. By TEM, it was observed clearly that the nanoribbon contained both ordered and disordered domains, which highlights that a perfect 2D polymer was not obtained.



**Scheme 62:** Synthetic pathway to obtain graphene nanoribbons.<sup>[125]</sup>

Although interesting structures were obtained *via* the multi-strand approach, it lacked in the ability to produce 2D polymers that meet all the criteria of the term. A main

disadvantage was that whilst an almost infinite extension in the y-direction was shown possible, extension in the x-direction was limited only to a few strands. A scale-up of the number of strands is to-date not reported, presumably due to the synthetic effort required being too strenuous as a result of the sheer number of reactions needed.<sup>[104]</sup>

Even rigid molecules exhibit a tendency of bending their backbone, which is not very energy-intensive but can lead over a large distance to intramolecular cross-linking and steric hindrance.<sup>[104]</sup> In order to overcome this issue, Shinkai *et al.* reported the formation of rigid polymer chains by conjugation along the backbone, so-called conjugated polymers (CPs), and to “clip” them together to obtain a pseudo-polyrotaxane (*Figure 16*).<sup>[126]</sup>

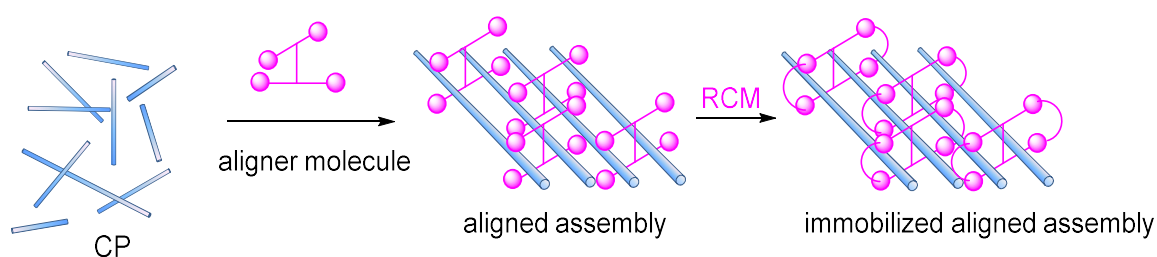


**Figure 16:** Schematic illustration of the mechanical fixation of a rigid, rod-like conjugated polymer (CP) by ring-closing metathesis and the formation of a pseudo-polyrotaxane.<sup>[126]</sup>

As a clip, aligner molecules were employed, such that they formed a complex with the CPs (*Figure 17*) and created a two-dimensional structure by self-assembly.

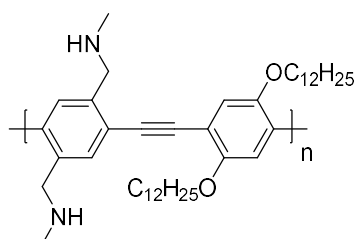


**Figure 17:** Structure of the conjugated polymer (CP) applied for the formation of a pseudo-polyrotaxane by Sinkai *et al.*<sup>[126]</sup>

In order to stabilize the assemblies of CPs permanently, template assisted ring-closing metathesis (RCM) of the aligner molecules was carried out to create poly-pseudo-



roaxanes, thus allowing the separation of the assemblies by SEC into different fractions.<sup>[25]</sup>

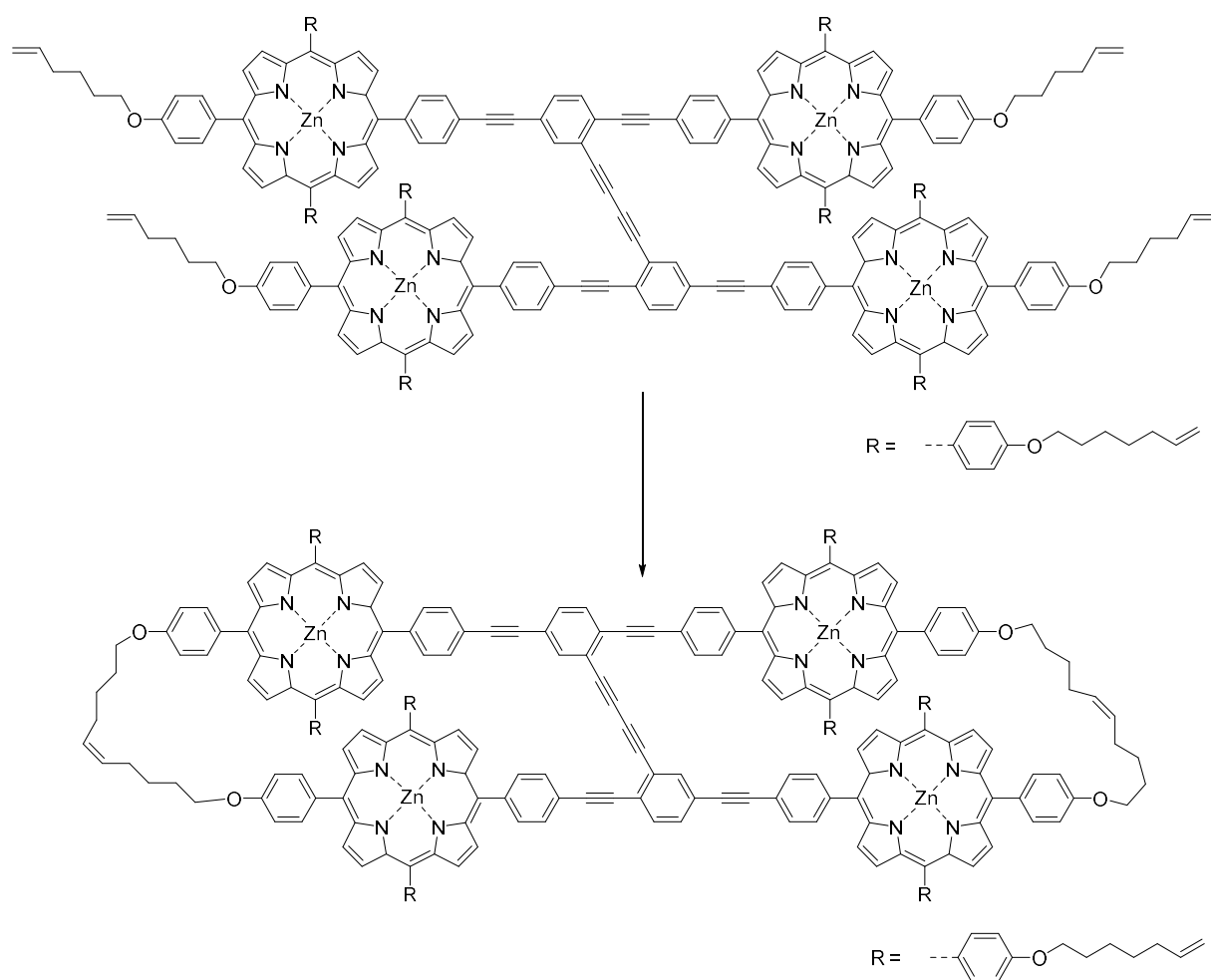


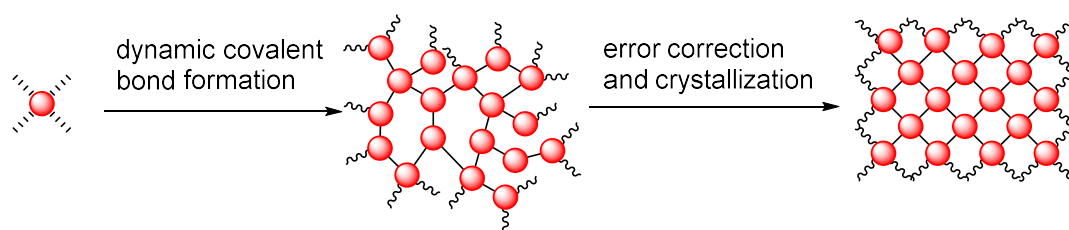
**Figure 18:** Structure of the aligner molecule, which formed the mechanical fixation by ring-closing metathesis (RCM) and led to the formation of a pseudo-polyrotaxane.<sup>[126]</sup>

A broad range of methods to synthesize 2D structures by the solution approach were reported; however, a high synthetic effort was necessary and the size of the generated structures rather small. A way to overcome the issue of insolubility of the 2D networks was the integration of solubilizing groups. Furthermore, rigid macrocycles were either formed during the synthesis and represented a unit within the 2D structure or could be applied in the 2D supramolecular polymerization as Sinkai and co-workers reported.

### II.3.2.2. Template Approach

In the template approach, the formation of a planar structure is templated by a surface or interface, which interacts with the monomers forcing a planarization.<sup>[108]</sup> The arrangement of the monomers on the template can be divided into two approaches: thermodynamic control and kinetic control. If the formation of covalent bonds and crystallization occur at the same time, it is thermodynamically controlled and any structural errors which occurred during bond formation can be corrected by re-ordering (*Figure 19*).<sup>[107,127]</sup> Kinetic control means that a non-covalent assembly takes place first, e.g., in lamellar or quasi-lamellar single crystals,<sup>[110]</sup> whilst rigid monomers can facilitate this crystallization. The supramolecular monomer assembly has the same general structure as the resulting polymer: after pre-organization, the covalent bonds are formed in a second step.<sup>[108]</sup> Reactions between two layers is minimized by separation of the monomers by solvent molecules, or free-volume.<sup>[110]</sup> During polymerization, the arrangement of the monomer arrangement should not be disturbed; therefore, the covalent bond formation should not involve mass transport or shrinkage or expansion of van der Waals distances.<sup>[110]</sup> If the polymerization proceeds without any significant cross-interactions with other layers, a 2D polymer is formed. However, the generated two-dimensional network can itself act as template; thus, further layers can be generated and a COF is formed. As mentioned in the introduction of chapter II.3. *2D Polymers*, 2D COFs meet the requirements of 2D polymers. 2D as well as 3D COFs are characterized by a large surface area, defined pore sizes and a long-range periodicity.<sup>[128]</sup> The properties can be tuned by an appropriate monomer design,<sup>[108]</sup> while defects can be minimized through reversible reactions. Common syntheses, e.g., by imine condensation or boron-ester formation, are practical and can be useful<sup>[110]</sup> for applications such as gas storage or separation and catalysis.<sup>[108]</sup> Using solvothermal conditions and a surface as template, mono- as well as multi-layers can be formed.

## Thermodynamic control



## Kinetic control

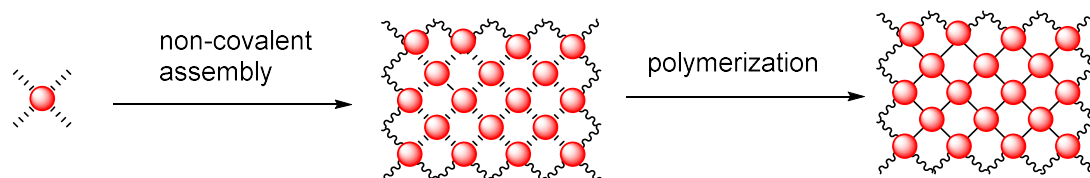
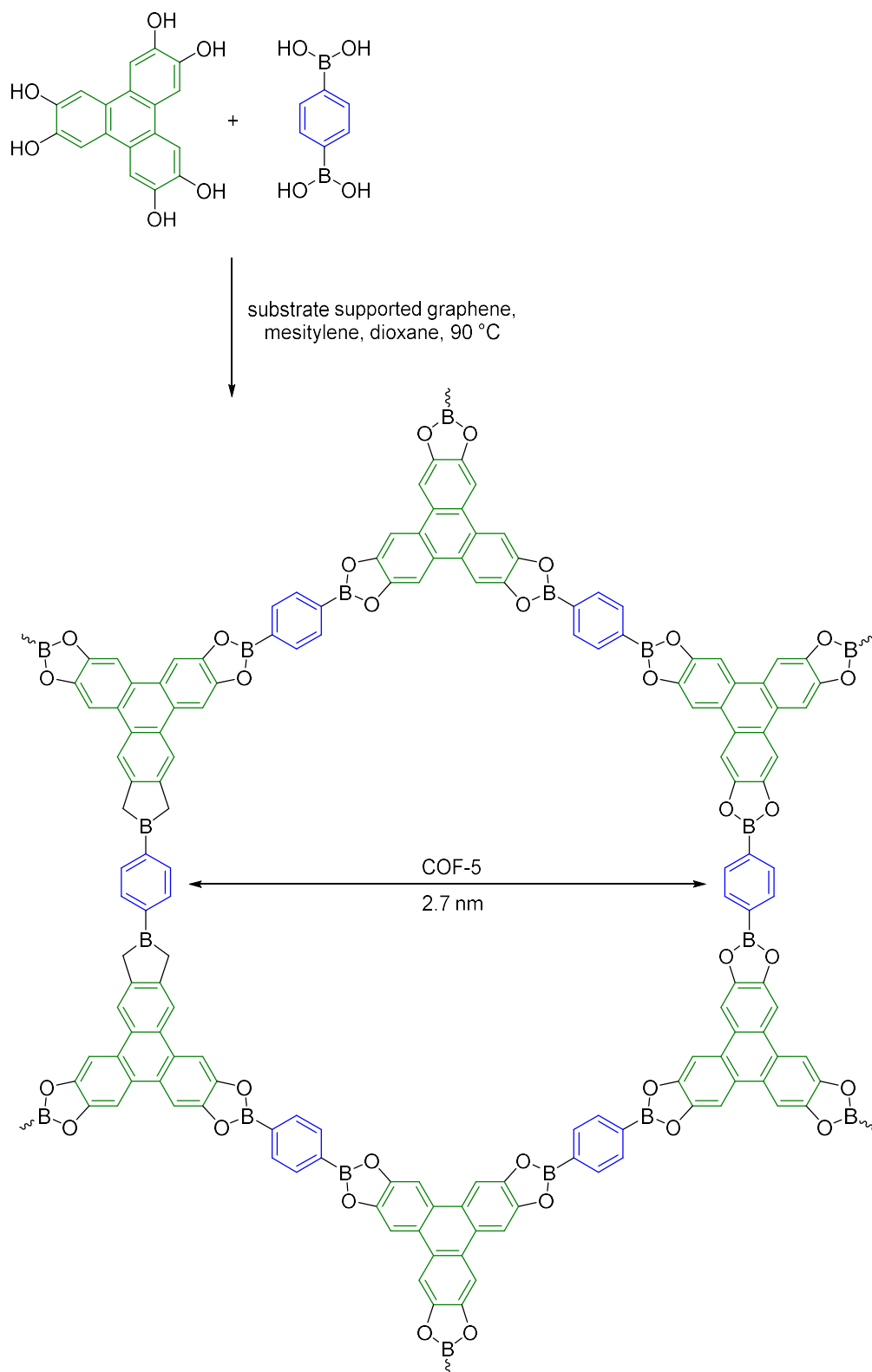


**Figure 19:** Schematic illustration of thermodynamic and kinetic control in the template approach.<sup>[108]</sup>

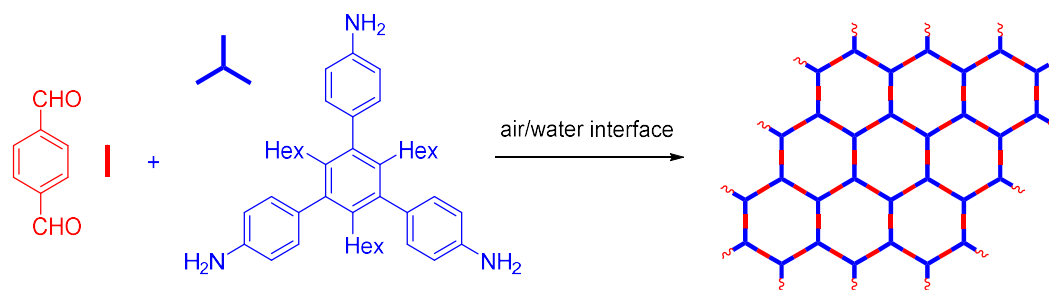
### a) Thermodynamic Control

Boronate ester formation is a common method to synthesize covalent organic frameworks (COFs). Dichtel *et al.* synthesized a two-dimensional COF using graphene supported on Cu as template. The template was added in a reaction flask together with the solvent (mesitylene and dioxane) and the monomers 1,4-phenylenebis(boronic acid) (PBBA) and 2,3,6,7,10,11-hexahydrotriphenylene (HHTP) (Scheme 63). Both an insoluble powder in the solution and a continuous film on the surface were formed by condensation of the monomers. X-ray scattering exhibited that the powder was randomly-ordered, while the film on the surface was highly ordered. The continuous multi-layered film was found to have a thickness of 25-400 nm.<sup>[129]</sup>



**Scheme 63:** Solvothermal condensation of HHTP and PBBA in presence of a substrate-supported graphene surface.<sup>[129]</sup>

Schlüter *et al.* synthesized mono-layered COFs, which can be considered 2D polymers, by imine condensation at an air/water interface (Langmuir-Blodgett method).<sup>[127]</sup> The building blocks were a bifunctional aldehyde and a trifunctional amine (*Scheme 64*). Apart from the polar amine groups pointing into the water phase, the trifunctional amine carried three hydrophobic n-hexyl groups which pointed out of the water phase. The building blocks oriented themselves in such a way that an ordered sheet structure was formed. Possible defects were self-corrected due to the reversible character of the imine reaction leading to the thermodynamically favored polymer product. The change of the interface was monitored by Brewster angle microscopy.<sup>[130]</sup> After polymerization, the resulting sheet was transferred onto a silicon wafer or a TEM grid, which allowed for the full structural analysis by optical microscopy, TEM, SEM and AFM. TEM images showed ruptures of the sheet which were hypothesized to have occurred during the drying and transfer process. A smooth monolayer of 0.7 nm thickness was observed by AFM. The chemical properties were analyzed by tip-enhanced Raman spectroscopy (TERS) showing the presence of imine bonds. However, characteristic monomer vibrations such as C=O and -NH<sub>2</sub> were only present in traces. The experimental data was supported by DFT simulations.<sup>[127]</sup>



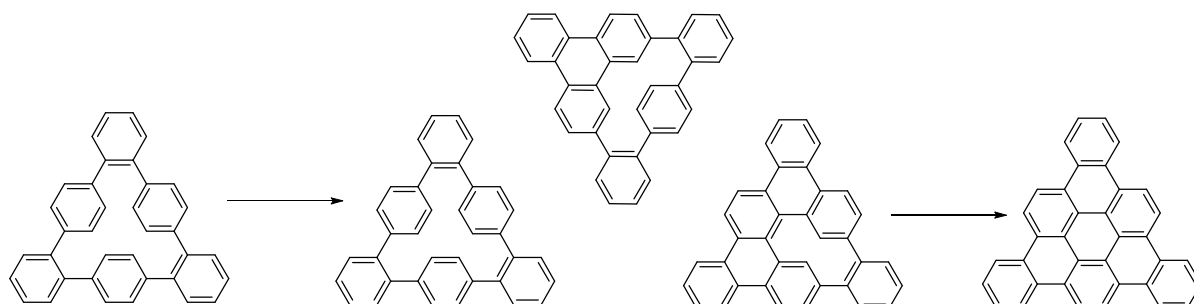
**Scheme 64:** Formation of a two-dimensional COF by imine condensation.<sup>[127]</sup>

These examples show that the formation of 2D structures can be successfully carried out *via* the *in situ* formation of macrocyclic units, which form the monomer component in the resulting network. Therefore, shape-persistent macrocycles are suitable building blocks for 2D structures.

#### *b) Kinetic Control*

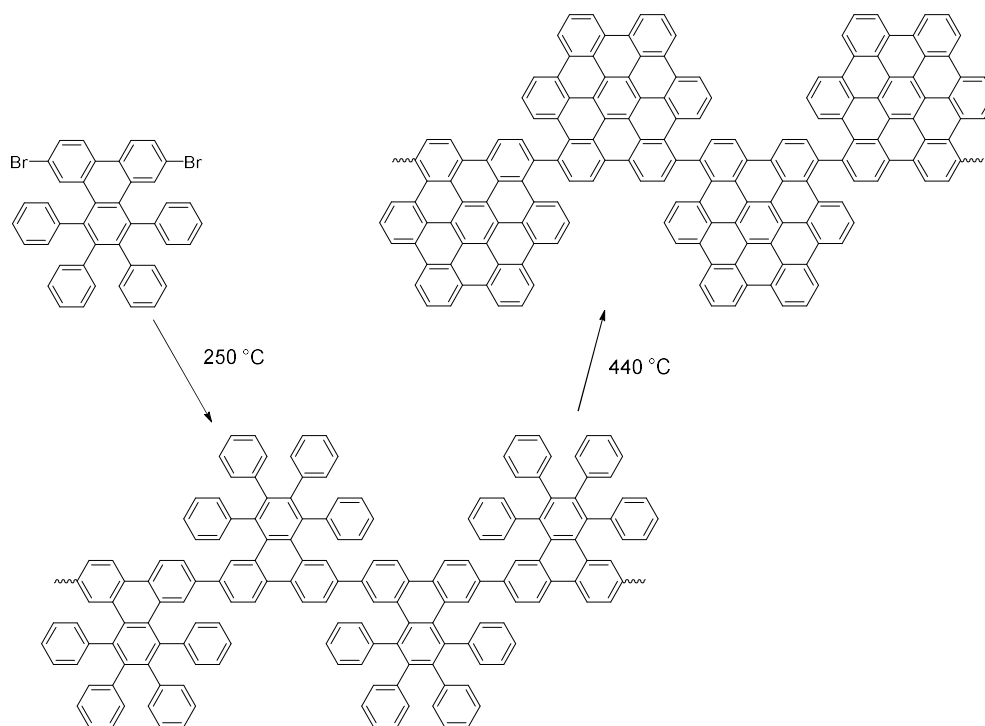
Müllen and co-workers synthesized nanographene by the template approach under kinetic control through the deposition of cyclohexa-*o-p-o-p-o-p*-phenylene on a Cu-

surface. The cross-linking was thermally initiated by a cyclodehydrogenation reaction (*Scheme 65*). With increasing temperature, the starting material formed a completely planar nanographene *via* different intermediates through a reaction that was catalyzed by the surface material through the weakening of the C-H bonds by van der Waals interactions.<sup>[131,132]</sup>



**Scheme 65:** Synthesis of nanographenes by thermally-initiated cyclodehydrogenation process of cyclohexa-o-p-o-p-o-p-phenylene.<sup>[131,132]</sup>

Larger structures, so-called graphene nanoribbons (GNRs), have been obtained in a similar fashion. 6,11-Dibromo-1,2,3,4-tetraphenyltriphenylene was deposited on a silver or gold surface and the bromine atoms were cleaved from the starting material at 250 °C (*Scheme 66*). The formed biradical species was stabilized by the surface material, and an aryl-aryl coupling reaction took place to form linear chains. At higher temperatures, intramolecular cyclodehydrogenation occurred and planar graphene nanoribbons were formed.<sup>[131]</sup>



**Scheme 66:** Reaction scheme for the formation of graphene nanoribbons.<sup>[131]</sup>

The appropriate choice of the precursor molecule allowed expansion in the second dimension with (defined) porosities, giving porous graphene. To test this hypothesis, a hexaiodohexaphenylene, instead of a bifunctional aromatic bromine monomer, was deposited onto a Ag surface (*Figure 20*) and by applying the same method as for GNRs, a porous graphene network was obtained.<sup>[131]</sup>

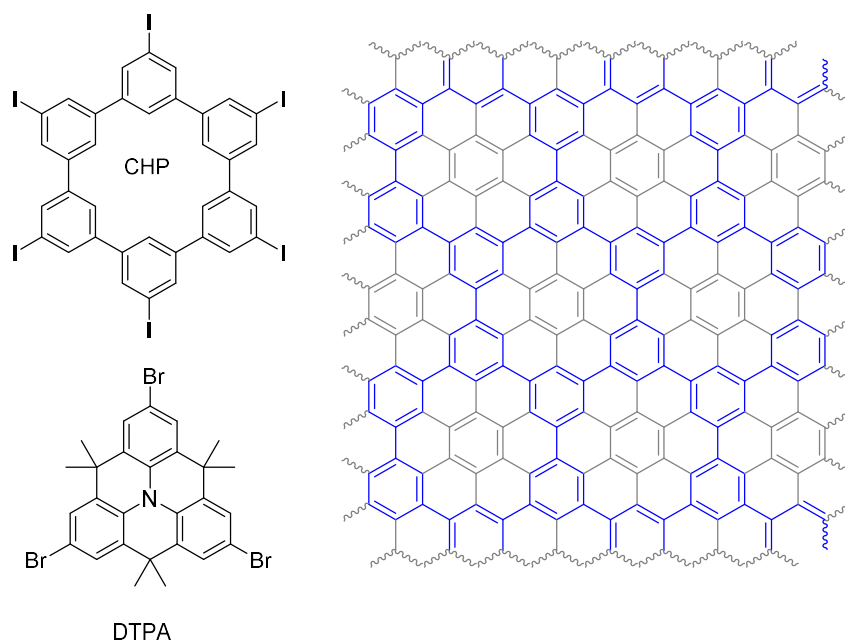
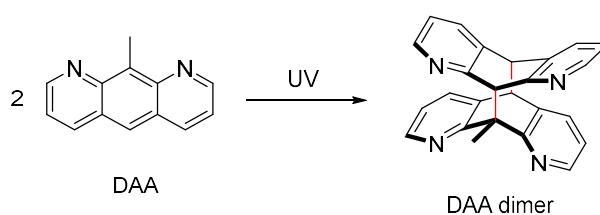


**Figure 20:** Monomers used for the synthesis of porous graphenes.<sup>[131]</sup>

Schlüter *et al.* have shown that monolayered sheets can also be formed at milder reaction conditions. With 1,8-diazaanthracene (DAA) as monomer at an air/water interface, photo-irradiation ( $\lambda = 365 \text{ nm}$ ) led to the formation of a 1.5 nm thick covalent monolayer, presumably formed by a [4+4] cycloaddition dimerization between the monomer units (*Scheme 67*). The resulting sheets were subsequently transferred onto a  $\text{SiO}_2$ -surface for microscopic analyses.<sup>[133]</sup>



**Scheme 67:** [4+4] cycloaddition dimerization of DAA.<sup>[133]</sup>

The previous examples exhibit the two major issues in the synthesis of 2D polymers: solubility and planarization. The solution approach shows that the integration of solubilizing groups can help keep large, two-dimensional structures in solution; however, forcing planarization can be difficult and usually means strenuous experimental processes. On one hand, the application of a template facilitates



planarization; nonetheless, the resulting sheets are insoluble and it can be difficult to remove the sheet from the template.

Soluble functional groups could combine both approaches. Rigid macrocycles could be connected to a 2D network *via* the functional groups. The rigid structure should template a planarization, while solubilizing groups help increase the solubility if not of the 2D polymer, at least of the 2D oligomers. This idea is discussed in detail in the next chapter III. Motivation and Aim of the Thesis.

### III. Motivation and Aim of the Thesis

Rigid macrocycles typically exhibit a low solubility in common solvents, which is why the integration of solubilizing groups is required to keep rigid macrocycles soluble and processible.<sup>[1]</sup> Usually, these solubilizing groups are positioned at the outer rim of a cycle or on the inside for large cavities.

Two six-membered macrocycles were simulated, one linked by vinyl groups, the other one by imine bonds, and the change of energy was observed for a variation of lengths of the intraannular solubilizing groups. The simulations suggested an almost planar, waved structure of the cycles, and that small moieties such as hydroxyl or methoxyl groups would point into the cycle, longer chains, such as propoxyl groups, arrange themselves and point alternately upwards or downwards out of the cycle. By positioning the solubilizing groups at the inside margin, the outside positions are available for the introduction of functional groups such as vinyl groups or halogens. Such functionalities should enable a post-modification, while the macrocycles would remain soluble in common solvents.

The aim of the current thesis was the synthesis of rigid macrocycles with functional groups at the outer rim and solubilizing groups at the inner rim to prove the simulations experimentally.

To achieve this goal, monomers suitable for macrocyclization by olefin metathesis and imine condensation should be synthesized. The synthesis of the monomers for the imine approach as well as the macrocyclization continues the previous studies performed by Audrey Llevot, Pia Löser and Benjamin Bitterer.<sup>[134,135]</sup> By integration into the monomers, the solubilizing and functional groups should end up in the resulting macrocycles. Furthermore, the monomers should be designed in a way that cyclization is favored. This is the reason why the functional groups, which can undergo a cyclization (vinyl group for the olefin metathesis and aldehyde respectively amine group for the imine condensation), are in *meta*-position to each other. In between, the solubilizing group (*R* in Figure 21) is integrated and in *para*-position of the latter, the functional group (*X* in Figure 21) for the post-modification. The functional groups should be orthogonal to the corresponding cyclization reaction. After monomer synthesis, the

reaction conditions for a cyclization should be optimized. For the olefin metathesis approach, reaction procedures similar to the one of Zhang *et al.* were followed. It should be proven that the cyclization can proceed independently of the sizes of the solubilizing groups. The resulting macrocycles, respectively the mixtures of linear and cyclic oligomers, should be analyzed by SEC, SEC-ESI mass spectrometry and NMR spectroscopy.

After successful synthesis and isolation of such a macrocycle, a post-modification should prove their potential for further reactions.

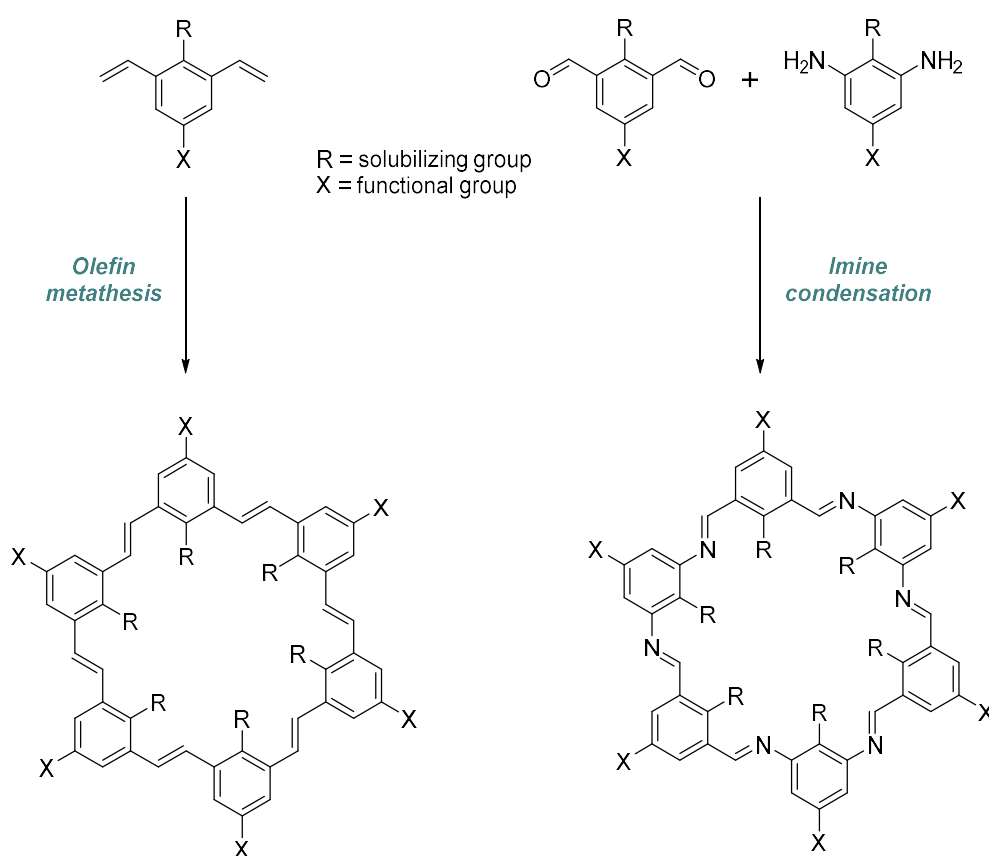


**Figure 21:** Monomer design for the cyclization by olefin metathesis (left) and imine condensation (right) and targeted hexameric macrocycles.

The aim of this thesis is to provide a basis for a future method to obtain 2D structures with functional, soluble macrocycles as building blocks. Once an efficient synthesis for these macrocycles is established, they could form a two-dimensional network. In order to minimize structural defects in the resulting sheet, the network formation could occur under thermodynamic control; *e.g.*, by olefin (Figure 22, left) or alkyne metathesis

(Figure 22, right). A vinyl or propynyl group can directly be integrated into the monomers for the imine approach. Alternatively, it could be integrated after cyclization *via* olefin approach, for example *via* cross-coupling reaction of bromine as the functional group.

Furthermore, the functional groups (*X* in Figure 21) could be used as an anchor point to add polymer chains to the cycles in order to obtain macromolecular brushes.

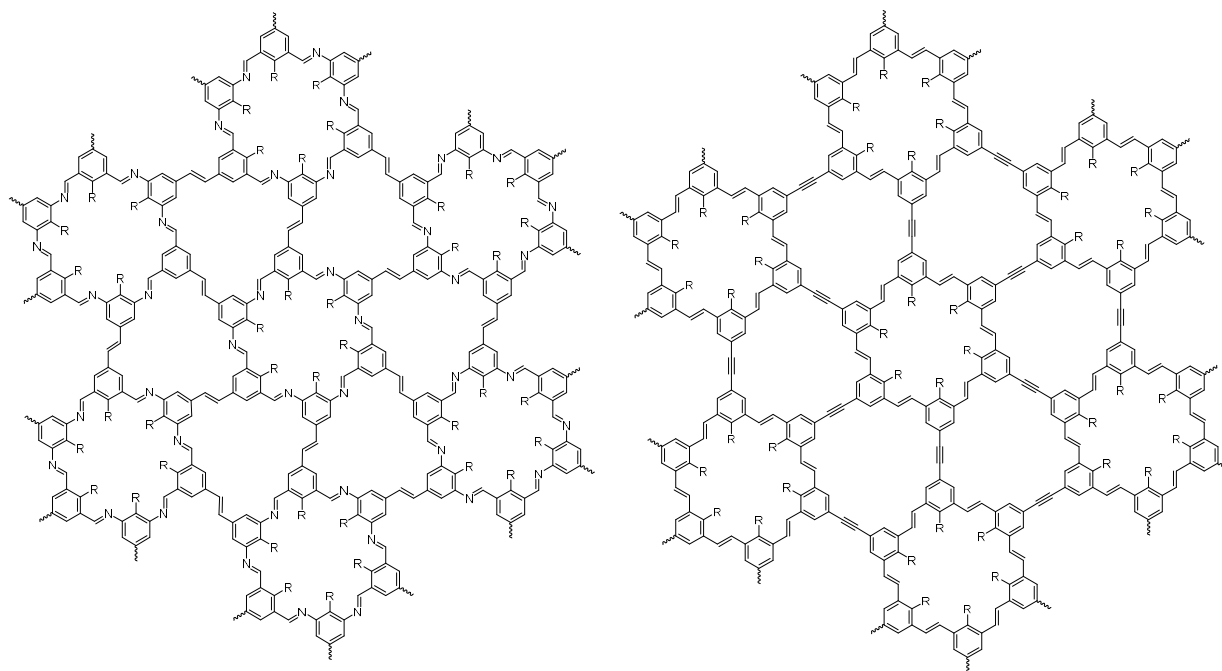


**Figure 22:** Potential 2D networks built up by olefin metathesis (left) alkyne metathesis (right) using functional, rigid but soluble macrocycles as monomers.

## IV. Results and Discussion

### IV.1. Simulations

In order to understand how solubilizing groups at the inside influence the structure and energy of a macrocycles, simulation experiments were conducted in cooperation with Dr. Julian Helfferich of the research group of Prof. Dr. Wolfgang Wenzel (Institute for Nanotechnology, KIT).

#### IV.1.1. Method

The macrocycles were calculated by density functional theory (DFT) as implemented in the nwchem [cite] code. The generalized gradient approximation (GGA) was used with the hybrid B3LYP exchange-correlation functional. The calculations were performed with the 6-31G\* basis set. In order to assess the effect of the exchange-correlation functional and the choice of the basis set, select structures were also computed with the GGA of Perdew, Burke, and Ernzerhof (PBE) with the 6-311G\*\* basis set. No effect on the resulting structure was found.

Using the DFT method, we optimized the molecular structure of each monomer. Furthermore, we added a Ca<sup>2+</sup> ion to the center of the original ring structure where it is close to all surrounding nitrogen atoms. To calculate the binding energy of the ion to the ring structure, we calculated the same structure with the ion moved 20 Angstroms away from the ring. We confirmed that both simulations used the same basis set functions.<sup>[136]</sup>

#### IV.1.2. Results

The energy of the fully optimized structure (“ground energy” in *Table 2*). was compared to the single-point energy of the structure after a couple of optimization steps when it still maintained a planar configuration (“energy of planar configuration” in *Table 2*). The energy difference  $\Delta E$  is relatively low, smaller than the typical energy gain from forming a covalent bond. Thus, the twisted ground state structure will likely contribute to an

entropic barrier but not preclude the formation of 2D networks. The calculations indicate that the twisted structure is more favorable compared to the planar one for macrocycles containing larger moieties.

**Table 2:** Comparison of the DFT energies of the ground state and a planar configuration for macrocycles with substituents of different lengths.

	Ground energy [a.u.]	Energy of planar configuration [a.u.]	$\Delta E$ [a.u.]	$\Delta E$ [kJ/mol]
<b>OH-MC-Br/Vinyl</b>	-10126.0570	-10126.0540	-0.0030	-7.75
<b>OMe-MC-Vinyl/Vinyl</b>	-2754.9575	-2754.9492	-0.0083	-21.90
<b>OPr-MC-Vinyl/Vinyl</b>	-2990.8548	-2990.8408	-0.014	-36.92

Furthermore, the energies of the macrocycles with different moieties can be compared (Table 2). Small moieties such as hydroxyl (Figure 23) or methoxy groups have enough space in the inside cavity to loom into the cycle (Figure 24). The alkyl chains of longer substituents, such as propoxyl groups, point out of the cycle (Figure 25). The energy levels of the macrocycles with different solubilizing groups are in the same range, which indicates that a macrocycle with propoxyl groups has a similar stability as the others.

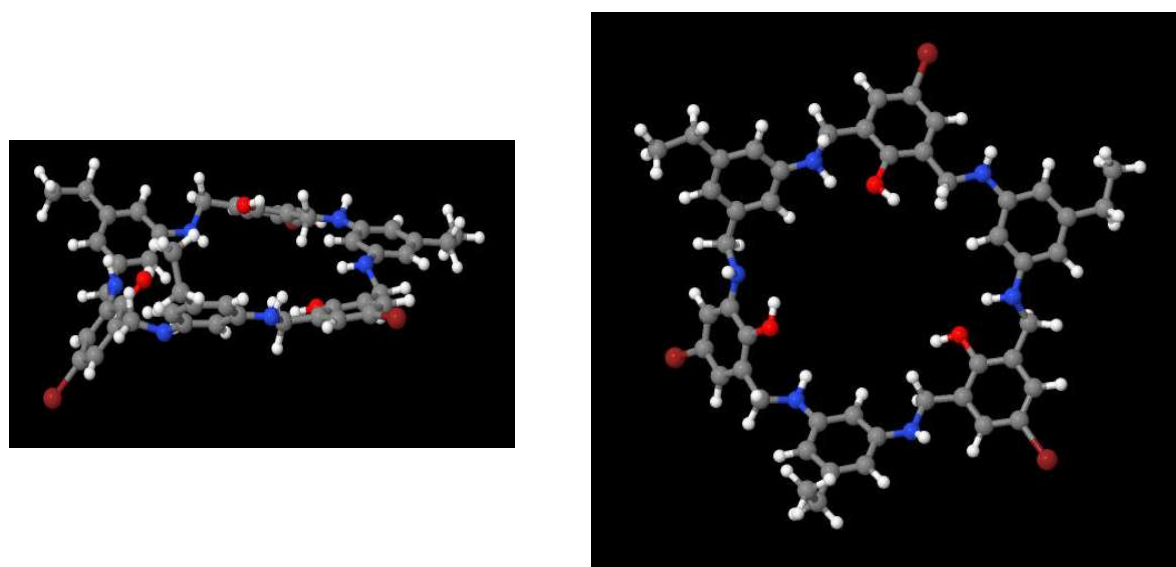


**Figure 23:** DFT simulations of a macrocycle with hydroxyl groups as solubilizing groups and bromine and vinyl groups at the outer rim (OH-MC-Br/Vinyl).

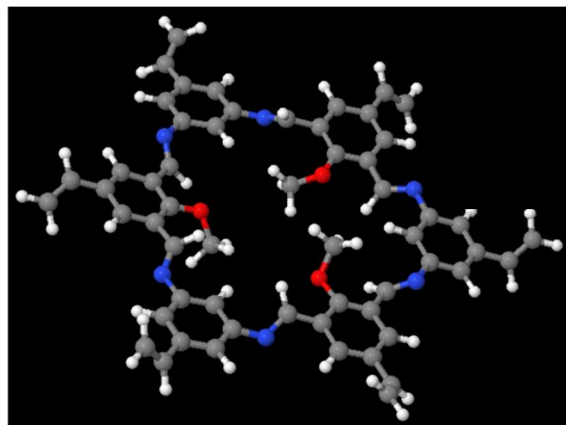
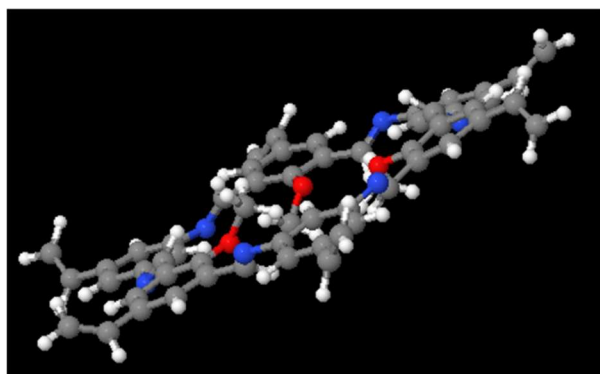


**Figure 24:** DFT simulations of a macrocycle with methoxy groups as solubilizing groups and vinyl groups at the outer rim (**OMe-MC-Vinyl/Vinyl**) in different perspectives.

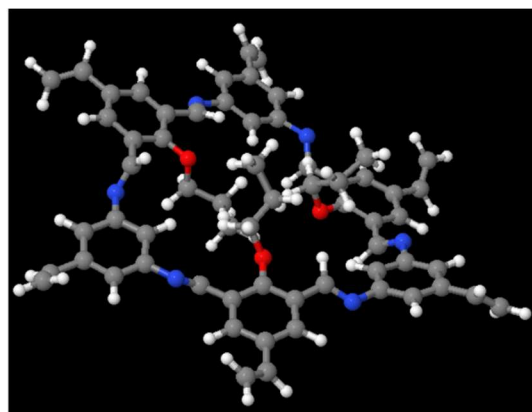
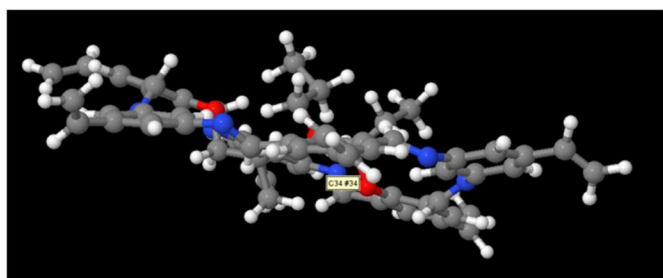


**Figure 25:** DFT simulations of a macrocycle with propoxy groups as solubilizing groups and vinyl groups at the outer rim (**OPr-MC-Vinyl/Vinyl**) in different perspectives.

By calculation of the solvent accessible surface for a range of solvent radii, the cavity of the macrocycle can be estimated. For a macrocycle with methoxy sidegroups it is 1.63 Å and for a macrocycle with propoxy groups 1.32 Å.

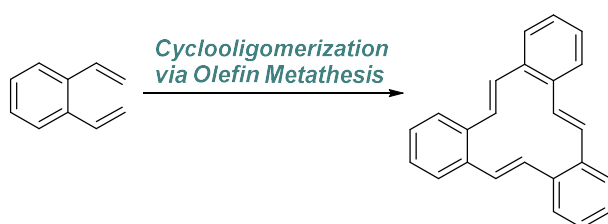
The macrocyclization by imine condensation is carried out in the presence of  $\text{CaCl}_2$ , which should act as a template and form a complex with nitrogen atoms in the cycle. Comparing the energies of a confirmation without  $\text{Ca}^{2+}$  and one with the  $\text{Ca}^{2+}$  in the center confirms that the configuration with the ion in the center is a stable confirmation; however, by addition of the ion, the structure gets deformed. By adding to two  $\text{Cl}^-$  ions, the structure becomes more planar again.

The simulations revealed two important observations: the macrocycles can have a planar structure and the moieties do not disturb the cyclization thermodynamically.

## IV.2. Olefin Metathesis

### IV.2.1. Previous Studies & Motivation

In previous studies, a 1,2-divinylbenzene monomer was synthesized and applied in a cyclooligomerization (*Scheme 68*).<sup>[137]</sup> Several reaction conditions, such as amount and nature of catalyst, solvents, concentration, reaction time and temperature, were screened. The characterization of the resulting mixture was challenging. Indeed, due to the unpolar character of the linear and cyclic oligomers resulting in a low ionization efficiency, no oligomer could be identified by ESI, neither the linear nor the cyclic ones. After purification by column chromatography, only the linear trimer could be isolated and characterized.



**Scheme 68:** Cyclooligomerization of a 1,2-divinyl monomer via olefin metathesis.<sup>[137]</sup>

In order to overcome the polarity issue, the synthesis of divinyl as well as tetravinyl monomers modified with solubilizing groups was attempted but not successful (*Figure 26*). Due to a more promising synthetic route and commercially available starting material, instead of an *ortho*-divinylbenzene, a *meta*-divinylbenzene monomer was further targeted; hence, the resulting aimed cyclic structure is not a trimeric but a hexameric macrocycle.<sup>[55]</sup>

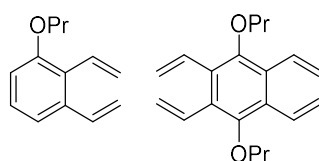


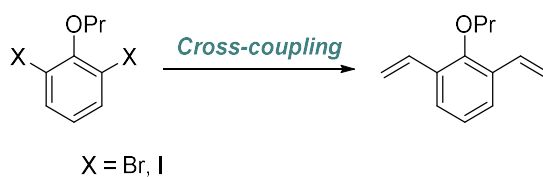
**Figure 26:** *ortho*-Divinyl- and tetravinylmonomers with incorporated solubilizing groups targeted in previous studies.<sup>[55]</sup>



## IV.2.2. Monomer Synthesis

In order to introduce a vinyl functionality, different cross-coupling reactions were tested. The reaction mixtures were characterized by GC-MS either before or after a rough purification by extraction. The formed species were assigned by mass spectrometry (GC-MS) and the amount of formed substances was estimated by GC (GC-MS). The GC-MS does not give a quantitative statement about the composition of the product mixture as no reference was used but in our case only a qualitative statement was sufficient in order to screen the applied reaction conditions. In promising cases, a further characterization by NMR spectroscopy was conducted.

Both aryl iodides and aryl bromides were tested in different cross-coupling reactions (*Scheme 69*), such as Kumada coupling (*Scheme 71*), Heck coupling (*Scheme 72*) and Suzuki coupling (*Scheme 73*); hence, a broad spectrum of different substrates can be formed during the reactions (*Figure 27*).



**Scheme 69:** General reaction equation of cross-coupling of aryl halogens to the desired product.

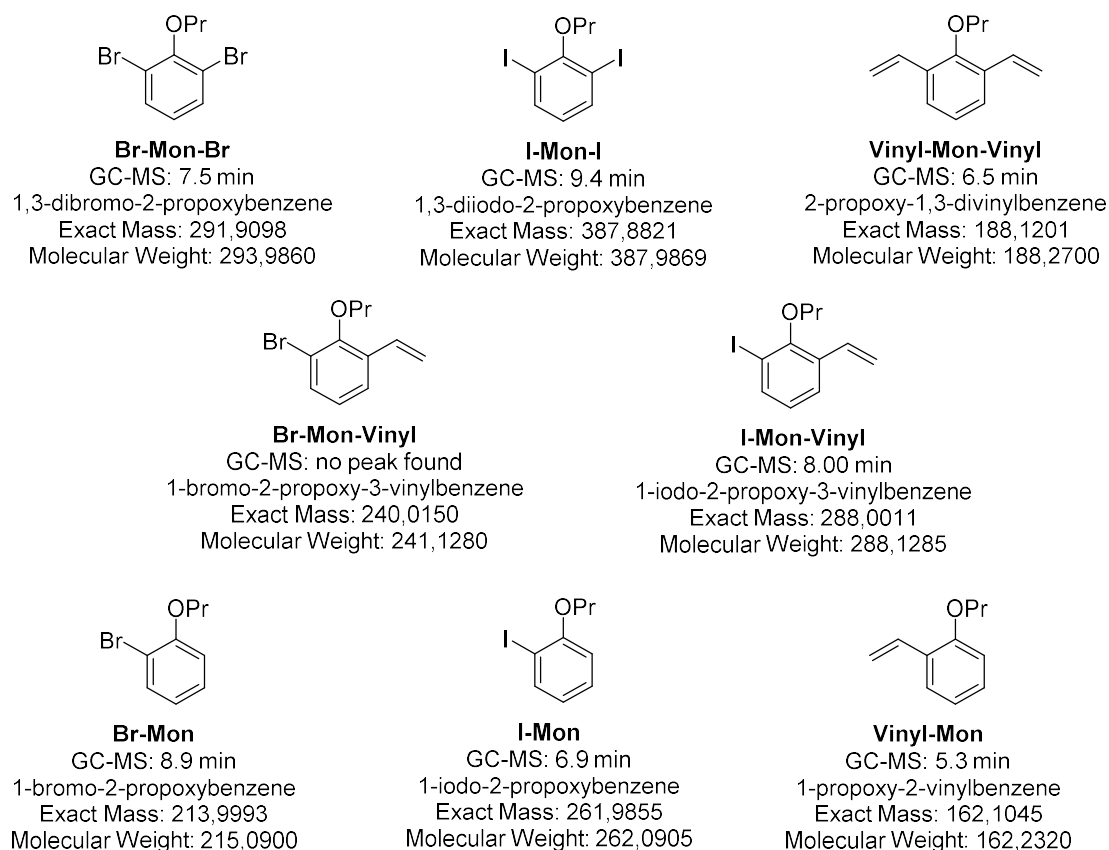
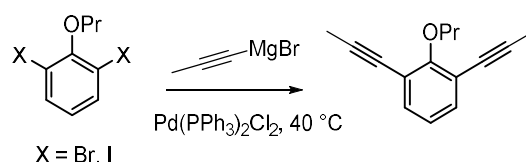


**Figure 27:** Overview of structures, exact masses and molecular weights of possible structures

The aryl iodide 1,3-diiodo-2-propoxybenzene (**I-Mon-I**) as starting material was identified as the peak at 9.4 min. ( $m/z[M]^+ = 387.6$ ;  $m/z_{\text{calc.}} = 387.9$ ). The corresponding aryl bromide 1,3-dibromo-2-propoxybenzene (**Br-Mon-Br**) was found at 7.5 min. ( $m/z[M]^+ = 291.5$ ;  $m/z_{\text{calc.}} = 291.9$ ). The peak at 6.5 min. ( $m/z[M]^+ = 188.0$ ;  $m/z_{\text{calc.}} = 188.1$ ) was identified as the desired product 2-propoxy-1,3-divinylbenzene (**Vinyl-Mon-Vinyl**) (*Scheme 69*). The mono-substituted product 1-iodo-2-propoxy-3-vinylbenzene (**I-Mon-Vinyl**) was observed at 8.00 min. ( $m/z[M]^+ = 261.8$ ;  $m/z_{\text{calc.}} = 261.9$ ); a peak for a corresponding aryl bromide could not be assigned. Furthermore, a by-product 1-propoxy-2-vinylbenzene (**Vinyl-Mon**) was identified by 5.3 min. ( $m/z[M]^+ = 161.8$ ;  $m/z_{\text{calc.}} = 162.2$ ). This structure could be generated by Palladium-catalyzed hydro-dehalogenation<sup>[138]</sup> and subsequent cross-coupling. By abstraction of one halogene, the two by-products 1-iodo-2-propoxybenzene (**I-Mon**), identified as peak at 6.9 min. ( $m/z[M]^+ = 261.8$ ;  $m/z_{\text{calc.}} = 262.0$ ) and the corresponding aryl bromide 1-bromo-2-propoxybenzene (**Br-Mon**), assigned as peak at 5.9 min. ( $m/z[M]^+ = 213.9$ ;  $m/z_{\text{calc.}} = 214.0$ ), were formed.

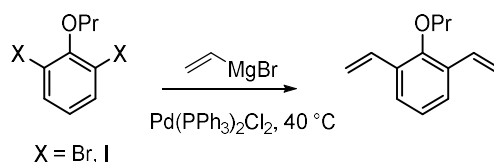
### IV.1.2.1. Kumada Coupling

First, Kumada coupling was selected to introduce the two vinyl functionalities, due to positive experience for the synthesis of alkyne monomers in previous studies (*Scheme 70*).<sup>[55]</sup>



**Scheme 70:** Synthesis of **Vinyl-Mon-Vinyl** starting either from **Br-Mon-Br** or **I-Mon-I** by Kumada coupling with prop-1-yn-1-ylmagnesium bromide.<sup>[55]</sup>

The same reaction conditions as in the previous studies were applied using a palladium catalyst and bis[2-(N,N-dimethylamino)ethyl] ether (*O*-TMEDA) to activate the Grignard reagent, in this case vinylmagnesium bromide.<sup>[55]</sup> Furthermore, the same precursors, **Br-Mon-Br** as aryl bromide and **I-Mon-I** as aryl iodide, were used (*Scheme 71*).



**Scheme 71:** Synthesis of olefin monomer by Kumada coupling with vinylmagnesium bromide.

After quenching by addition of diluted HCl and water, the reaction was roughly purified by extraction. The resulting raw product was analyzed by GC-MS. Next to the peaks described previously, further peaks appeared in the spectra which could either be assigned as ligands, activating agent or could not be assigned. Exemplarily, GC-MS spectra of both, a reaction with aryl iodide (*Figure 28*, left side) and aryl bromide (*Figure 28*, right side), are shown. The peak at 3.8 min. was identified as *O*-TMEDA.

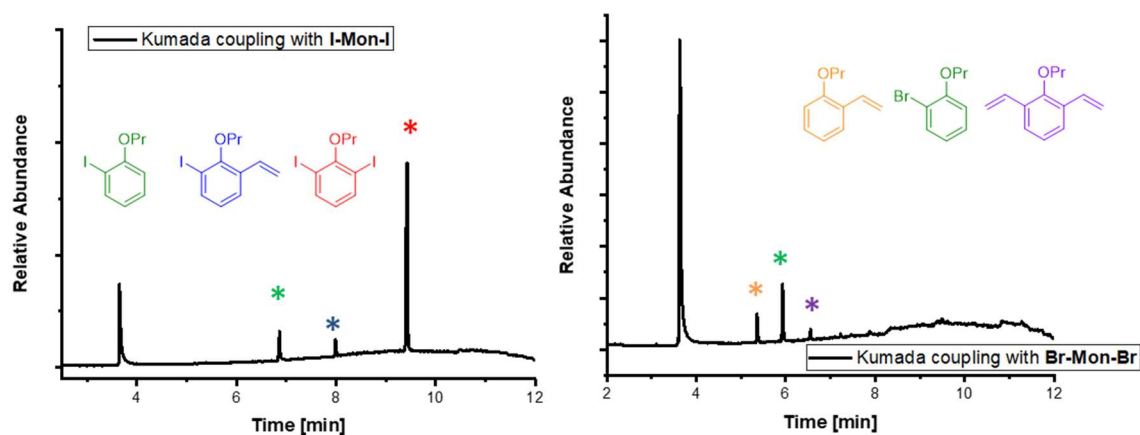


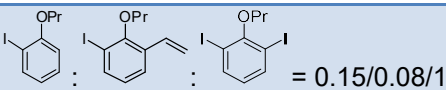
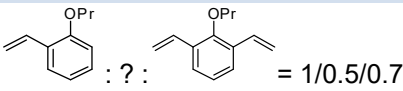
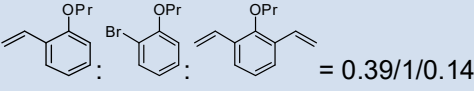
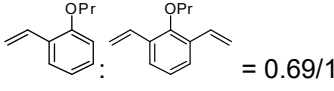
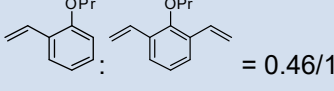
**Figure 28:** Exemplary GC-MS spectra of Kumada coupling of used aryl iodide (left side) and aryl bromide (right side).

The applied reaction conditions and resulting products are presented in *Table 3*. When **I-Mon-I** was used (*entry 1*); even after ca. 20 hours, mainly starting material and only small amounts of mono-substituted product **I-Mon-Vinyl** were present in the product mixture. Furthermore, a comparable amount of by-product **I-Mon** was formed. In the next entry, the amount of Kumada reagent was doubled and Pd(dba)<sub>3</sub> was used as catalyst (*entry 2*). As a result, the starting material was consumed completely but mainly the **Vinyl-Mon** by-product was generated. Furthermore, the desired product **Vinyl-Mon-Vinyl** and an unidentified by-product at 5.7 min. were formed in comparable amounts. This observation indicates that a cross-coupling takes place, but not as fast as the dehalogenation. No further improvements were reached by changing the aryl halogen species from iodide to bromide **Br-Mon-Br** and using Pd(PPh<sub>3</sub>)Cl<sub>2</sub> as catalyst (*entry 3*). Although, the cross-coupling took place, the dehalogenation was faster, leading mainly to the by-products **Br-Mon**. The results could be improved by changing the catalytic system to Pd(dba)<sub>3</sub> (*entry 4*) resulting in a reaction rate for the cross-coupling faster than the dehalogenization, which led to the desired divinyl product as main product. Nevertheless, the dehalogenization decreases the yield and a large amount of monovinyl by-product is still present. Test TLCs for a purification *via* column chromatography were conducted; however, no efficient separation was achieved. Therefore, the objective to reach full conversion was pursued. In order to

suppress the dehalogenization, the amount of catalyst was decreased to 0.05 eq. instead of 0.20 eq. (*entry 5*) leading indeed to a slightly smaller amount of **Vinyl-Mon**.

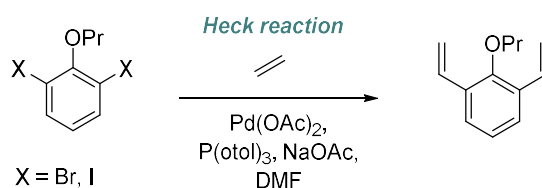
In all reactions, no adequate selectivity towards the desired product was achieved. Due to this and the fact that test TLCs show a poor separation, it was abstained from proceeding Kumada coupling, and the Heck reaction was investigated instead.

**Table 3:** Results of screening the synthesis of the divinyl monomer by Kumada coupling.

Entry	Hal	Reagent [eq.]	t [h]	Ratio of formed Substrates	Catalyst
1	I	3.00	20	 = 0.15/0.08/1	Pd(PPh <sub>3</sub> )Cl <sub>2</sub>
2	I	6.00	26	 = 1/0.5/0.7	Pd(dba) <sub>3</sub>
3	Br	6.00	21	 = 0.39/1/0.14	Pd(PPh <sub>3</sub> )Cl <sub>2</sub>
4	Br	6.00	48	 = 0.69/1	Pd(dba) <sub>3</sub>
5	Br	3.00	24	 = 0.46/1	Pd(dba) <sub>3</sub>

#### IV.1.2.2. Heck Reaction

An alternative synthetic pathway is the introduction of vinyl functionality by Heck reaction (*Scheme 72*).<sup>[139]</sup>

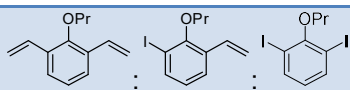
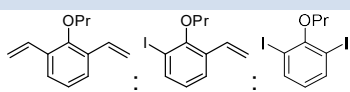
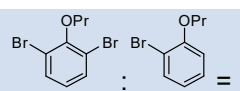


**Scheme 72:** Synthesis of olefin monomer by Heck reaction with ethylene.

Reaction conditions such as amount of catalyst and reaction time were varied. Furthermore, similar to the Kumada approach, both **Br-Mon-Br** and **I-Mon-I** were tested. For all reactions, some parameters were kept steady, such as the use of DMF as solvent, palladium(II) acetate as applied catalyst, a reaction temperature of 90 °C,

and a pressure of 10 bar ethylene. A higher pressure was not possible due to the used equipment. The screened parameters were the amount of catalyst and reaction time as well as aryl halogen species. After purification by extraction, the raw product mixture was qualitatively characterized by GC-MS analogous to the Kumada approach. The results are shown in *Table 4*.

**Table 4:** Results of screening the synthesis of the divinyl monomer by Heck reaction.

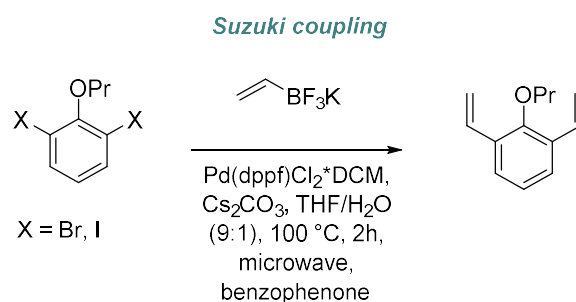
Entry	Hal	Cat. [eq]	t [h]	Ratio of formed Substrates
1	I	0.01	5.0	 = 0.14 / 0.20 / 1
2	I	0.05	24	 = 0.03 / 0.07 / 1
3	Br	0.05	24	 = 1 : 0.4

After 5 hours reaction time with 0.01 eq. of catalyst (*entry 1*), the resulting product mixture consists of mainly starting material **I-Mon-I** with small amounts of mono-substituted **I-Mon-Vinyl** and disubstituted products **Vinyl-Mon-Vinyl**. No dehalogenation was observed. In order to increase the conversion, the reaction time was extended up to 24 hours and the amount of catalyst was increased five-fold. Nevertheless, the amount of formed product was rather low. In order to achieve high or even full conversion, the corresponding aryl bromide **Br-Mon-Br** was applied to verify if another halogen would show a different reactivity. However, the conversion was even lower because neither mono- nor disubstituted product was found. Furthermore, **Br-Mon** was found as by-product, indicating that a dehalogenation took place similarly to the results of Kumada coupling. Due to these results, the Heck reaction was considered an inefficient method for the synthesis of the desired monomers.

#### IV.1.2.3. Suzuki Coupling

As a third synthetic pathway, Suzuki coupling as an efficient tool to integrate a vinyl function to aryl halogenides<sup>[140]</sup> was tested as a method to synthesize the desired monomers (*Scheme 73*). As Suzuki reagent, potassium vinyltrifluoroborate was applied.

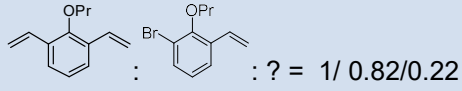
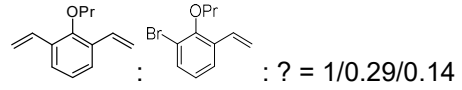
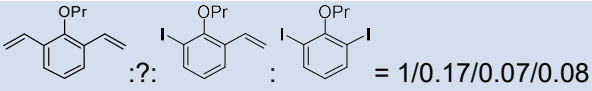
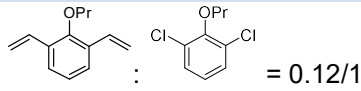
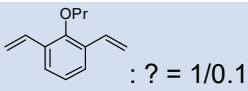
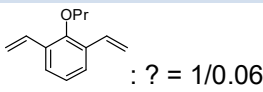
Being a solid, this reagent is practical to handle, commercially available and no degradation due to oxygen or moisture was observed, which makes storage and handling straightforward; especially in comparison to the Kumada reagent, which requires storage and reaction under inert atmosphere. Furthermore, the reaction was carried out in a microwave reactor without any inert atmosphere. After the reaction, a sample was taken from the reaction mixture and directly analyzed by GC-MS.



**Scheme 73:** Synthesis of olefin monomer by Suzuki coupling with potassium vinyltrifluoroborate.

In order to find optimal reaction conditions, different reaction conditions such as amount of Suzuki-reagent, amount of catalyst, reaction time, reaction temperature, solvent, amount of cesium carbonate as base and nature of the aryl halogen species were varied. In all reactions, the reaction concentration was 0.051 M. In literature, similar reactions are often carried out at 150 °C, but due to the formation of a too high pressure, the reactions were carried out at about 100 °C. An overview of the variations is given in *Table 5*.

**Table 5:** Results of screening the synthesis of the divinyl monomer by Suzuki coupling.

Entry	Hal	Suzuki Reagent [eq.]	Cat. [eq.]	t [h]	Ratio of formed Substrates
1	Br	5.00	0.05	1	 : ? = 1/0.82/0.22
2	Br	10.0	0.05	1	 : ? = 1/0.29/0.14
3	I	10.0	0.05	1	 = 1/0.17/0.07/0.08
4	Cl	10.0	0.05	3	 = 0.12/1
5	I	10.0	0.05	3	 : ? = 1/0.1
6	I	14.0	0.08	2	 : ? = 1/0.06
7*	I	14.0	0.08	2	Complete conversion; pure product after cc, yield: 60.2%
8*	I	14.0	0.08	2	Complete conversion; pure product after cc, yield: 66.7%

\*reaction in DMF

In the first entries of *Table 5*, **Br-Mon-Br** was used as starting material. Applying 5.00 eq. of Suzuki reagent (*entry 1*), the desired product and the mono-substituted product were formed in comparable amounts after 1 hours. Furthermore, a second unidentified species was generated in significantly smaller amounts (peak at 7.2 min.). It could not be identified by mass spectrometry; however, fragments similar to the starting material were observed, indicating that a by-product is formed. Doubling the amount of Suzuki reagent (*entry 2*), led to an increased formation of **Vinyl-Mon-Vinyl** compared to **Br-Mon-Vinyl** in a ratio of 1 to 0.3.

The reaction conditions from the 2<sup>nd</sup> entry were applied to the aryl iodide starting material (*entry 3*). Using **I-Mon-I** gave a higher conversion and a smaller amount of mono-substituted product and starting material, thus favoring the selectivity of the desired product. Furthermore, the same by-product generated in the reaction with aryl

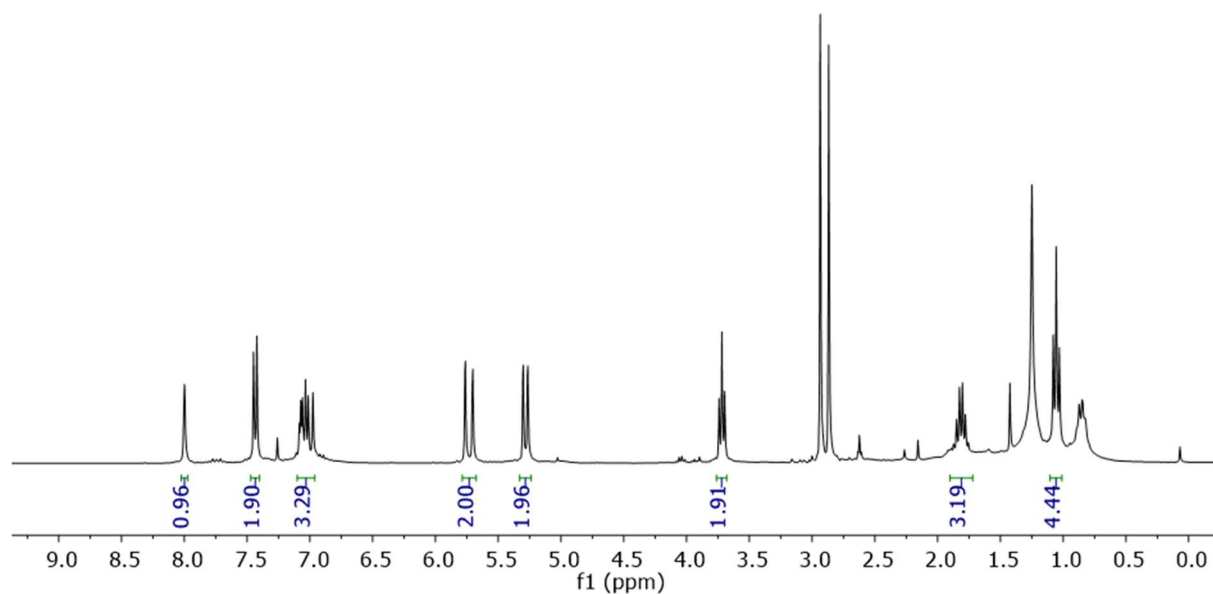


bromide appeared at 7.2 min. The aryl iodide did not give significantly better results compared to the bromide. Both product compositions showed only a low separation efficiency by column chromatography using the investigated solvent systems. Therefore, it was tried to achieve full conversion by further optimization of the reaction conditions.

The reactivity of an aryl chloride was tested (*entry 4*). 1,2-Dichloro-3-propoxybenzene, which was synthesized to obtain 1,2-divinyl-3-propoxybenzene by Heck reaction and Kumada coupling in previous studies. The same reaction parameters as for the previous entry were applied and only the reaction time was extended from 1 to 3 hours due to the predicted lower reactivity of aryl chlorides in comparison to aryl bromides and iodides.<sup>[141]</sup> Although, the desired product was formed, the reactivity was even lower than expected.

Since the precursor of the starting material, namely dibromophenol, had to be acquired commercially and was rather expensive, in all further reactions, the corresponding aryl iodide was used, which could be synthesized efficiently by phenol and iodide.

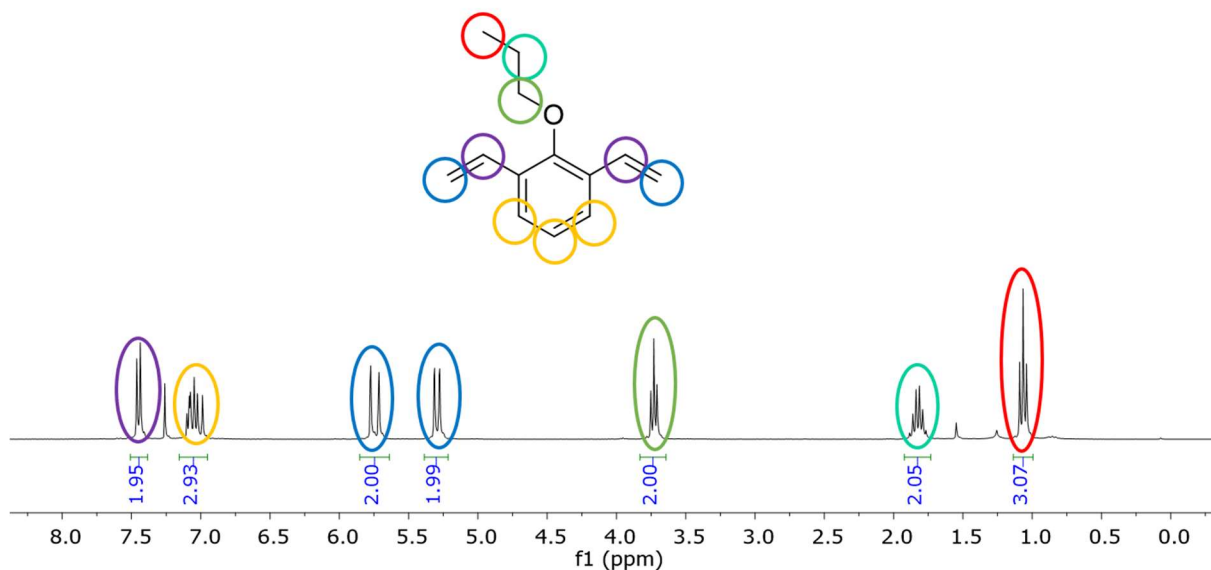
Similar to the aryl chloride, the reaction time was extended from 1 to 3 hours (*entry 5*) giving a product mixture mainly composed of the desired product with a small amount of by-product, indicating that the reaction time is not critical. Instead, the amount of Suzuki reagent was further increased up to 14.0 eq., the amount of catalyst increased, too, up to 8 mol% and the amount of cesium carbonate was changed from 3.00 to 3.50 eq. The reaction time was 2 hours (*entry 6*). In GC-MS, the by-product was almost not detectable; however, after a purification by extraction and filter column chromatography to remove the Pd catalyst and other reagents, the resulting product was characterized by <sup>1</sup>H-NMR giving a spectrum showing impurities, which could not be removed by column chromatography (*Graph 1*).



**Graph 1:**  $^1\text{H-NMR}$  spectrum of entry 6 showing the presence of impurities after column chromatography.

The solvent was changed from THF to DMF (entries 7 & 8 in *Table 5*). Although, DMF requires a more complicated extraction with additional washing steps with brine, residual traces of the solvent were removed during the column chromatography giving the desired product in pure manner (*Graph 2*). The reproducibility was proven but a further screening using DMF as solvent was not proceeded. Possibly, the reaction works with lower amounts of Suzuki reagent and catalyst, as well. In future work, these parameters could be further optimized.

In summary, Suzuki coupling under microwave conditions was a suitable tool for introducing vinyl groups and was applied in previous studies and later in further monomer syntheses for the imine approach.



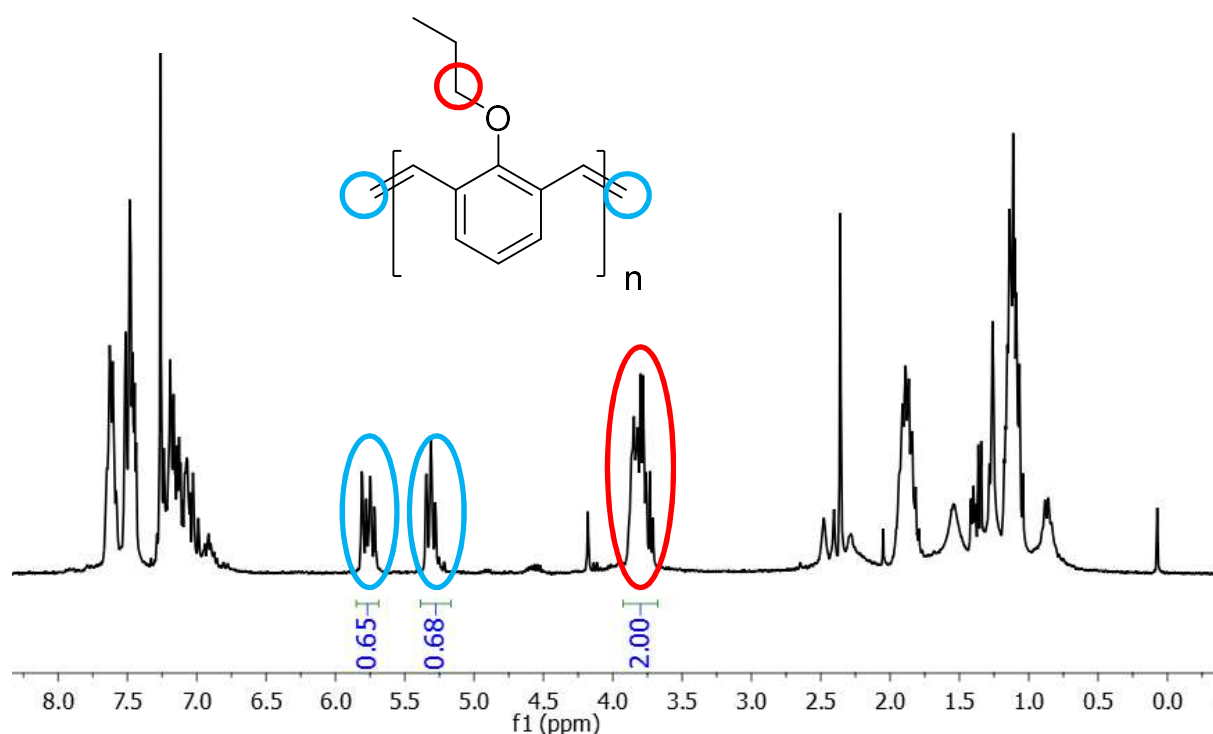
**Graph 2:** <sup>1</sup>H-NMR spectrum of **Vinyl-Mon-Vinyl** synthesized by Suzuki coupling.

### IV.2.3. Macrocyclization

After successful synthesis, 2-propoxy-1,3-divinylbenzene was applied as monomer for the synthesis of macrocycles *via* olefin metathesis. During the metathesis reaction, the progress of the reaction was observed by <sup>1</sup>H-NMR spectroscopy, especially by integration of the proton peaks for the terminal double bonds, a dd at 5.30 ppm and dt at 5.74 ppm (*Graph 3*). Cyclic compounds did not exhibit these terminal protons and in oligomers these protons were only present as end groups; therefore, the integrals of these peaks decreased with increased conversion. These integrals were compared to the integrals of the peaks corresponding to the alkyl chain, which are multiplets at 3.78 – 3.66 ppm (-OCH<sub>2</sub>) and 1.91 – 1.74 ppm (-CH<sub>2</sub>) as well as a triplet at 1.07 ppm (-CH<sub>3</sub>). The latter integrals remained equal during the metathesis reaction and were present in all monomer units in cyclic as well as linear compounds, thus they could be used as an internal reference. According to these integrals, the conversion of compound X (*Equation 2*) was calculated and are shown in *Graph 3*. The average value of the two integrals of the double bond protons was calculated and divided by the integral of the peak of the OCH<sub>2</sub>-group. At the beginning of the reactions, the integrals of the vinyl groups / have a value of 2; hence the conversion X would be 0. Cyclooligomerization is a step-growth polymerization; hence, a high conversion was necessary to reach the desired, relatively high molecular weight.

$$1 - \frac{\left(\frac{I_1+I_2}{2}\right)}{2} = X$$

**Equation 2:** Calculation of the conversion of the terminal double bonds by the average value of both integrals and the integral of the OCH<sub>2</sub>-peak as internal reference.



**Graph 3:** Exemplary <sup>1</sup>H-NMR spectrum of entry 6 to illustrate the evaluation of conversion.

The targeted hexameric macrocycle could theoretically be identified by <sup>1</sup>H-NMR, but the product was a mixture of different linear, possibly even cyclic oligomers and was thus analyzed by SEC and SEC-ESI. These methods gave an indication about the selectivity of the different products as well as their structures. Structures and calculated exact masses of possible linear and cyclic oligomers are given in *Figure 29*. Cycles smaller than the hexameric cycle were less likely obtained due to the ring strain; larger ones could be formed but are thermodynamically less favored. The six-membered macrocycle was the targeted size following the procedure known in literature.<sup>[16]</sup>

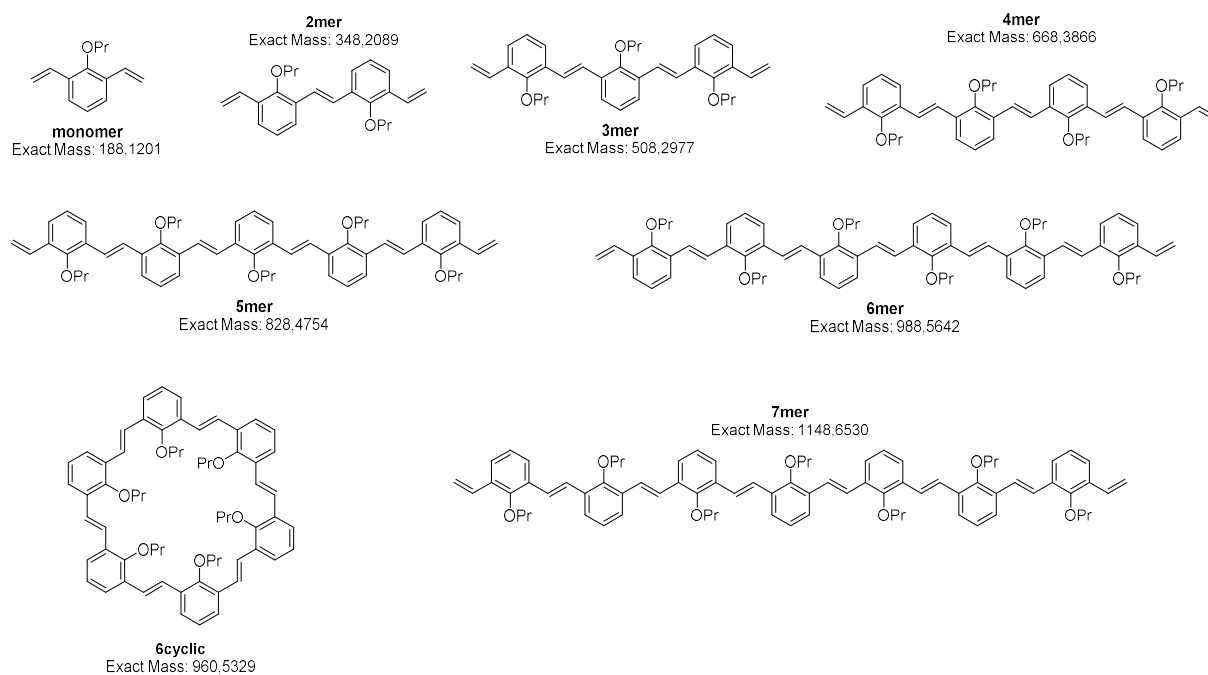


**Figure 29:** Structures and calculated exact masses of possible linear and cyclic oligomers by olefin metathesis.

In order to obtain a high selectivity towards the macrocycles, the reaction conditions were screened by varying the solvent, monomer concentration, reaction temperature, time and if the reaction system was closed or opened, as well as the catalyst. For all reactions, the initial amount of catalyst was 0.10 eq. and for some reactions, an additional amount of catalyst was added into the reaction mixture after a certain time.

**Table 6:** Overview of reaction conditions and results of cyclooligomerizations by olefin metathesis.

Entry	Catalytic species	Catalyst [eq.]	Conc. [mol/L]	T [°C]	System	t [h]	Conversion* [%]
1 <sup>1)</sup>	Grubbs 2	0.10	0.054	35	Closed	18	45
2 <sup>2)</sup>	Grubbs 2	0.10	0.054	35	Closed	18	45
3 <sup>2)</sup>	Grubbs 2	0.10	0.054	60	Closed	24	58
						44	52
4 <sup>2)</sup>	Grubbs 2	0.10	0.054	35	Open	24 <sup>3)</sup>	36
						43	32
5 <sup>2)</sup>	Grubbs 2	0.10	0.054	35	Open	47 <sup>3)</sup>	38
						60	58
6 <sup>2)</sup>	HG2	0.10	0.054	60	Open	25	67
7 <sup>2)</sup>	HG2	0.10	0.054	80	Open	16 <sup>3)</sup>	54
						40 <sup>3)</sup>	68
						64	83
8 <sup>2)</sup>	HG2	0.1	0.11	80	Open	16 <sup>3)</sup>	74
						40 <sup>3)</sup>	75
						64	97
9 <sup>2)</sup>	HG2	0.10	0.01	80	Open	16 <sup>3)</sup>	4)
						40 <sup>3)</sup>	64
						65	86
10 <sup>2)</sup>	HG2	0.10	0.005	80	Open	16 <sup>3)</sup>	37
						40 <sup>3)</sup>	53
						65 <sup>3)</sup>	64
						88	63
						110	87

\* of starting material

- 1) DCM as solvent
- 2) Toluene as solvent
- 3) Addition of 0.10 eq. catalyst in portion
- 4) Signals too low to be detected

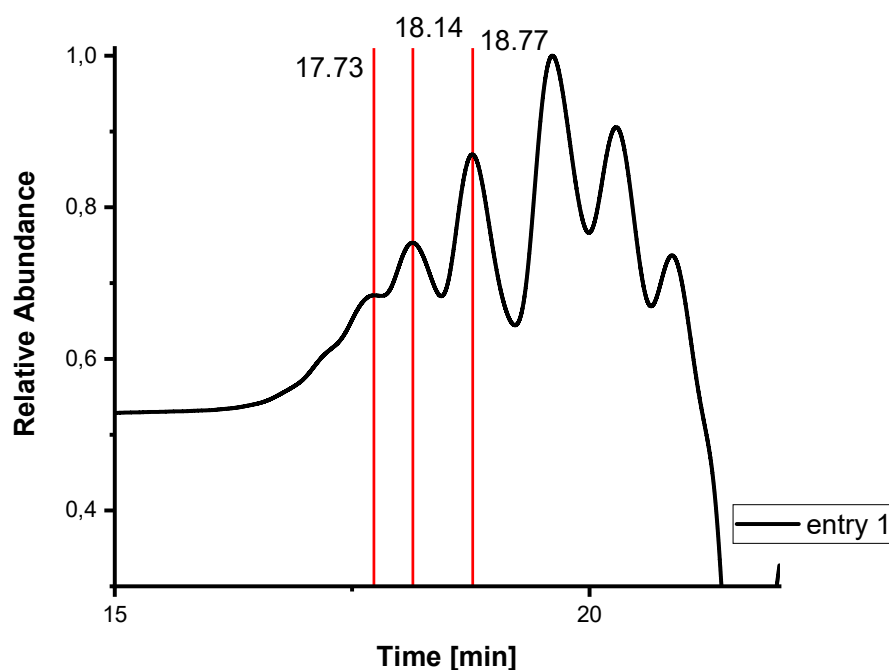
First (*Table 6, entry 1*), the olefin metathesis reaction was carried out in dry DCM as solvent and Ar-atmosphere at 35 °C and with a monomer concentration of 0.054 mol/L. In order to prevent the evaporation of the solvent, the system was closed and stirred for 18 hours. Under these conditions, about 45% of the terminal double bonds were converted. This means that more than half of the amount of terminal double bonds

were still present. To enable the formation of the desired six-membered macrocycle or any other macrocycles, higher conversions have to be achieved such that at least linear 6mers could be formed, which are necessary for subsequently forming the desired cycle. As the cyclooligomerization is a step-grow polymerization, the necessary conversion can be calculated by Carother's equation (*Equation 3*). In order to achieve the generation of 6mers (DP = 6) on the average, at least a conversion of 83% is required.

$$D = \frac{1}{1 - p}$$

**Equation 3:** Carother's equation for the calculation of the degree of polymerization (DP) with the conversion (*p*).

The <sup>1</sup>H-NMR spectroscopy results of the first reactions were confirmed by SEC-ESI (*Graph 4*). Several linear oligomers were found. At 18.77 min. retention time, the linear **3mer** ( $m/z[M+Na]^+ = 531.2867$ ;  $m/z_{calc.} = 531.2869$ ;  $\Delta m/z = 0.0002$ ) was found, at 18.14 min. a linear **4mer** ( $m/z[M+Na]^+ = 691.3758$ ;  $m/z_{calc.} = 691.3747$ ;  $\Delta m/z = 0.0011$ ) and at 17.73 min. the linear **5mer** ( $m/z[M+Na]^+ = 851.4637$ ;  $m/z_{calc.} = 851.4646$ ;  $\Delta m/z = 0.0009$ ). The SEC chromatogram showed that although these linear oligomers are formed, smaller oligomers and monomers are mainly present, which is in accordance to the low conversion of 45%. The mass for the desired hexameric macrocycle was not found.



**Graph 4:** SEC-ESI of cyclooligomerization by olefin metathesis with reaction conditions of entry 1 of Table 6.

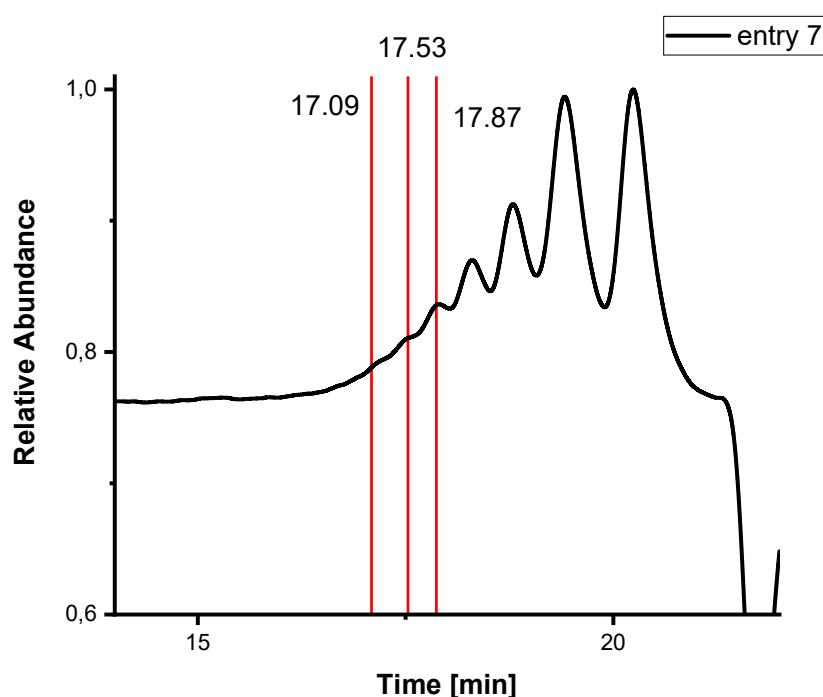
The use of dry toluene as alternative solvent (*entry 2*) did not lead to a significantly improved conversion. Furthermore, an extended reaction time did not show any influence.

The increase in reaction temperature (*entry 3*) led to a slightly higher conversion of 52-58% of terminal double bonds according to  $^1\text{H-NMR}$  spectroscopy. Expanding the reaction time to 44 hours did not lead to a higher conversion. Further reactions were carried out in an open system. Due to its lower boiling point in comparison to DCM, all further reactions were carried out in toluene making higher reaction temperatures and an open system possible.

The conversion of starting material did not increase significantly in an open system and gave a conversion between 32-36% after 43 hours (*entry 4*) the presence of oxygen and moisture in the air might deactivate the catalyst. The addition of an extra portion of catalyst (*entry 5*) could increase the conversion up to 58% and thus gave similar results as the closed system.



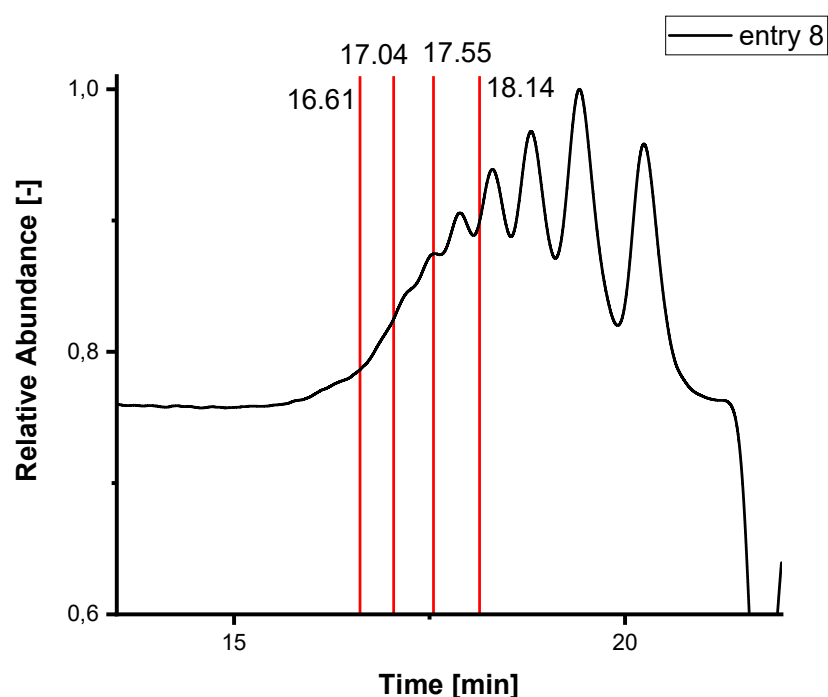
The Hoveyda-Grubbs 2<sup>nd</sup> generation catalyst, which is more stable against moisture and oxygen, was used in the next tries (*entry 6*). This catalyst gave a significantly higher conversion under the previously investigated conditions. Increasing the reaction temperature to 80 °C and adding an extra portion of catalyst (*entry 7*) resulted in a conversion of the starting material up to 83% according to NMR spectrometry. As discussed above, this is just the conversion necessary to reach hexamers. Furthermore, several species were identified by SEC-ESI (*Graph 5*). At 17.09 min, the linear **5mer** ( $m/z[M+Na]^+ = 851.4640$ ;  $m/z_{calc.} = 851.4646$ ;  $\Delta m/z = 0.0006$ ) was found and at 17.53 min. the linear **4mer** ( $m/z[M+Na]^+ = 691.3755$ ;  $m/z_{calc.} = 691.3758$ ;  $\Delta m/z = 0.0003$ ); however, these linear oligomers were only a minor fraction; mainly oligomers of smaller molecular weights were present. No adequate mass for the six-membered macrocycle was found.



**Graph 5:** SEC graph and mass spectrum of cyclooligomerization by olefin metathesis with reaction conditions entry 7 of Table 6.

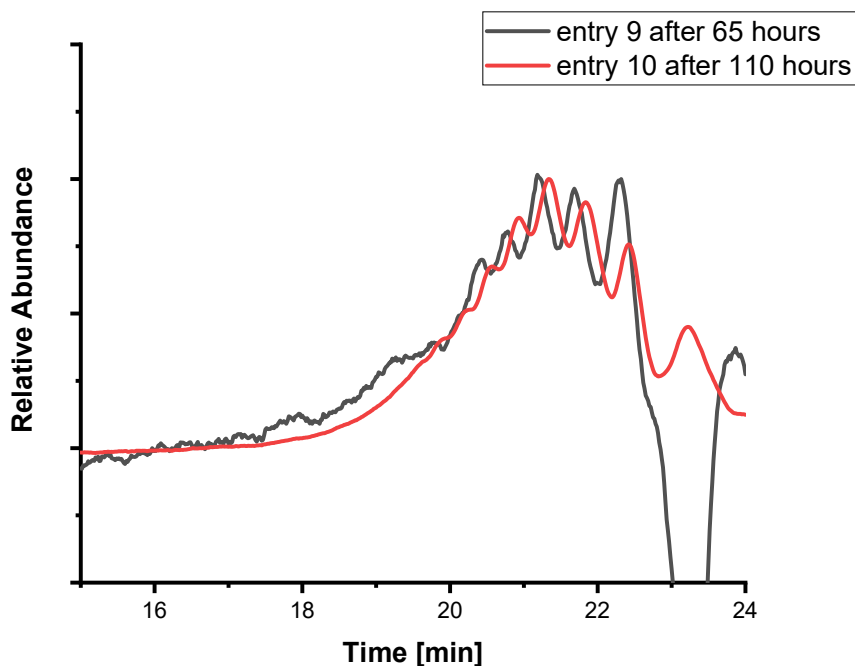
In order to further increase the conversion of the starting material, the monomer reaction mixture was concentrated (*entry 8*). As a drawback, the formation of linear oligomers with higher molecular weight is favored compared to the intramolecular

reaction leading to a cycle. As expected, a higher monomer concentration led to a higher monomer conversion of 97% after 64 hours. Although the conversion was higher, the generated oligomers are still rather short, which is indicated by SEC-ESI (*Graph 6*). At 18.14 min., the linear **3mer** ( $m/z[M+Na]^+ = 531.2870$ ;  $m/z_{\text{calc.}} = 531.2869$ ;  $\Delta m/z = 0.0001$ ) was found, at 17.55 min. the linear **4mer** ( $m/z[M+Na]^+ = 691.3752$ ;  $m/z_{\text{calc.}} = 691.3758$ ;  $\Delta m/z = 0.0006$ ) and at 17.04 min. the linear **5mer** ( $m/z[M+Na]^+ = 851.4642$ ;  $m/z_{\text{calc.}} = 851.4646$ ;  $\Delta m/z = 0.0004$ ). Furthermore, the linear **6mer** ( $m/z[M+Na]^+ = 1011.5526$ ;  $m/z_{\text{calc.}} = 1011.5534$ ;  $\Delta m/z = 0.0008$ ) was identified for the first time. However, the major fractions are still compounds of small molecular weight.



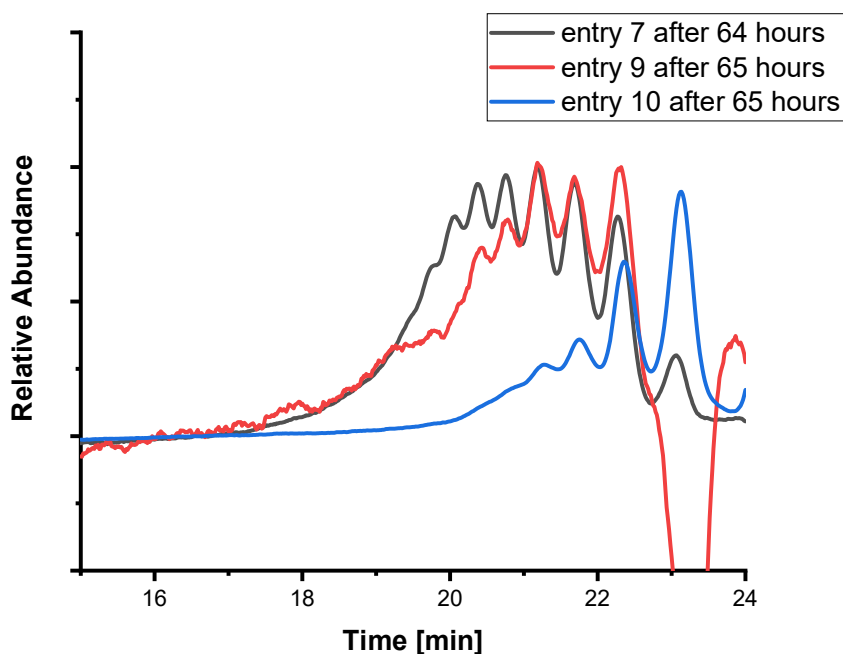
**Graph 6:** SEC graph and mass spectrum of cyclooligomerization by olefin metathesis with reaction conditions entry 8 Table 6.

In order to make an intramolecular reaction more favored, the concentration was decreased to 0.01 mol/L (*entry 9*) and 0.005 mol/L (*entry 10*) and the reaction time was extended up to 110 hours; however no effect on the selectivity was observed, but only on the conversion (*Graph 7*).



**Graph 7:** Comparison of SEC traces at different concentrations. A more diluted reaction mixture and longer reaction times led only to a lower conversion.

The desired six-membered macrocycle could not be detected by SEC-ESI, either because it was not formed at all or due to a low ionization efficiency; hence, the influence of the reaction parameters on the selectivity towards the targeted macrocycle was challenging to judge. Nevertheless, even if one of the peaks in SEC represented the macrocycle, by varying the reaction parameters no selectivity towards any oligomeric species could be achieved, but only an effect on the conversion could be observed (*Graph 8*). An extension of reaction time and a more efficient catalytic system only led to a higher conversion. Concentrating or diluting the reaction mixture had only an effect on the conversion as well. An isolation of the peaks by column chromatography was not successful; only mix fractions could be obtained.



**Graph 8:** Comparison of SEC traces of entries with decreased concentration (entry 7 to entry 10) after 65 hours. No effect on the selectivity was observed but only on the conversion.

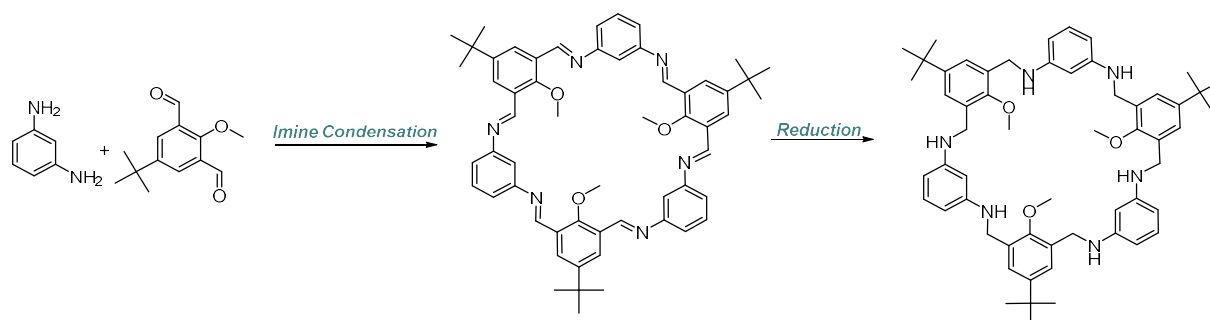
## IV.3. Imine Condensation

### IV.3.1. Previous Studies

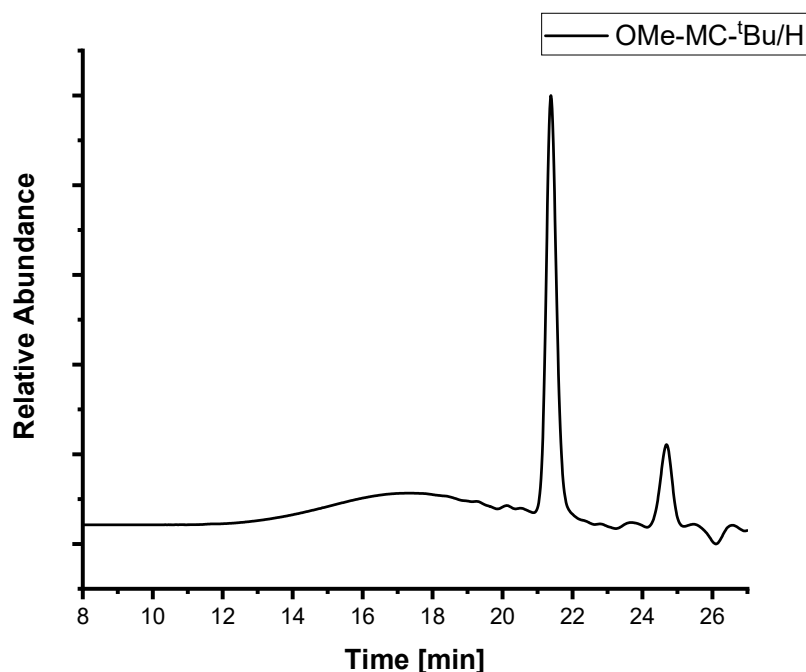
In previous studies, monomers for a test macrocycle had been synthesized, and the reaction conditions of the cyclization reaction conditions had been screened to optimize the selectivity of the macrocycle.<sup>[134,135]</sup>

As building blocks, *m*-phenylenediamine as diamine and 5-(*tert*-butyl)-2-methocisophthalaldehyde as aldehyde were investigated as model monomers to target a macrocycle with methoxy groups pointing into the cycle and *tert*-butyl groups as solubilizing alkyl group (*Scheme 74*). During the reaction carried out in methanol under reflux, a precipitate was formed, which showed a low solubility in common solvents except in benzene allowing a characterization by <sup>1</sup>H- and <sup>13</sup>C-NMR. NMR and SEC-ESI proved on one hand the formation of the desired six-membered macrocycle **OMe-MC-<sup>t</sup>Bu/H** and on the other hand the selectivity of 52% (*Graph 9*). In order to

quench the equilibrium and to facilitate a full characterization, the precipitate was suspended in a methanol/THF (1:1) mixture and reduced to the corresponding amine (**OMe-MC-<sup>t</sup>Bu/H red**) using sodium borohydride. After successful reduction, the macrocycle was soluble in common solvents and could be analyzed by SEC and SEC-ESI confirming the NMR results.<sup>[134]</sup>



**Scheme 74:** Imine condensation of 1,3-diaminebenzene and 5-(tert-butyl)-2-methoxysophthalaldehyde to a six-membered macrocycle (**OMe-MC-<sup>t</sup>Bu/H**) and the subsequent reduction to reduce the imine to the corresponding amine (**OMe-MC-<sup>t</sup>Bu/H red**).<sup>[134]</sup>

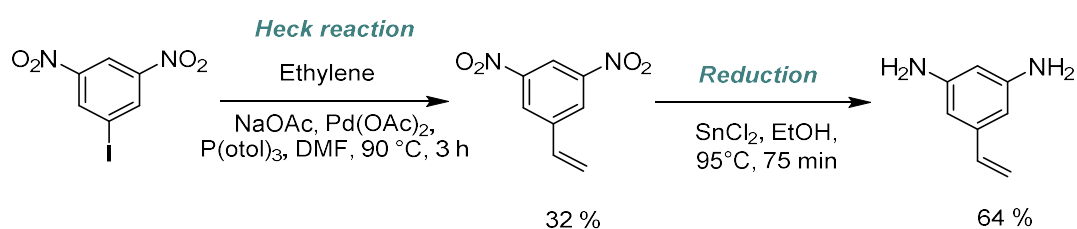


**Graph 9:** SEC graph of model amine macrocycle (**OMe-MC-<sup>t</sup>Bu/H**).

The influence of different reaction parameters such as stoichiometry and concentration were examined. Furthermore, the addition of an acid such as HBr, did not improve the reaction efficiency. In DCM, no precipitate was formed and EtOH showed a slightly

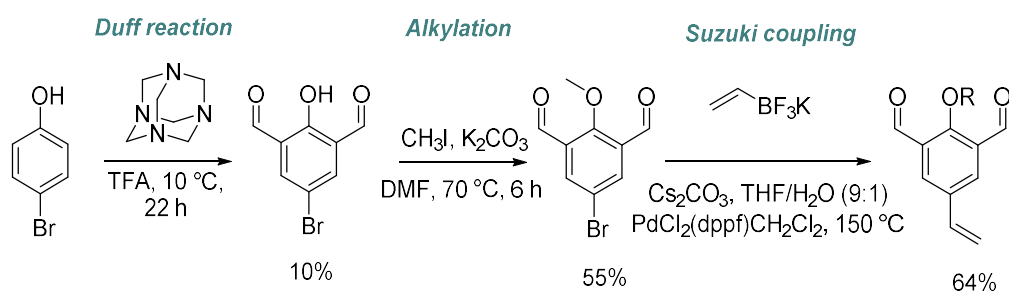
lower selectivity compared to MeOH. Besides, the influence of the template species on the reaction selectivity was investigated. The selectivity increased from Ba<sup>2+</sup> (no precipitate formed) to Zn<sup>2+</sup>, Mg<sup>2+</sup> and Ca<sup>2+</sup>; hence, for all further reactions, Ca<sup>2+</sup> was used as a template.<sup>[134]</sup>

After screening of the reaction conditions, monomers were synthesized, in which vinyl groups were incorporated as functional groups. The diamine 5-vinylbenzene-1,3-diamine (**DAm-Vinyl**) was obtained by Heck reaction of 1-Iodo-3,5-dinitrobenzene and subsequent reduction with SnCl<sub>2</sub> (*Scheme 75* *Scheme 76*).<sup>[135]</sup>



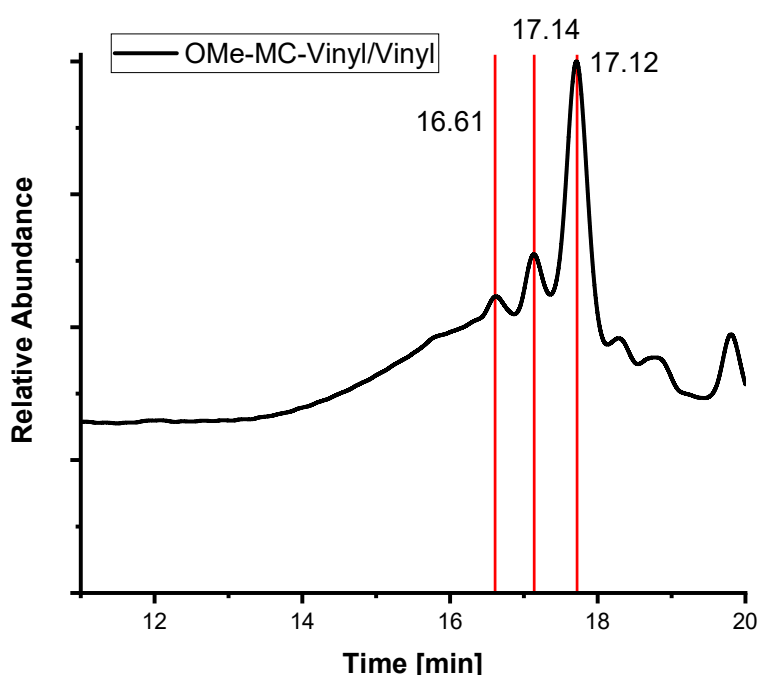
**Scheme 75:** Synthesis of 5-vinylbenzene-1,3-diamine in previous studies.<sup>[135]</sup>

The dialdehyde 5-bromo-2-hydroxyisophthalaldehyde was obtained by Duff reaction of *p*-bromophenol (*Scheme 76*), following a procedure reported in literature.<sup>[142]</sup> The alkyl chain was introduced by Williamson ether synthesis and due to the results of olefin approach, the vinyl functionality was introduced by Suzuki coupling, giving the monomers **DAI-OH**, **DAI-Br** and **DAI-Vinyl**.<sup>[135]</sup> In order to prevent an undesired polymerization, the reactions were carried out in presence of benzophenone as radical scavenger. A Suzuki coupling of 5-bromo-2-hydroxyisophthalaldehyde did not lead to the desired product. Hence, a dialdehyde carrying both a hydroxyl and a vinyl group was not obtained.



**Scheme 76:** Synthesis of 2-methoxy-5-vinylisophthalaldehyde in previous studies.<sup>[135]</sup>

The obtained monomers were applied in imine condensation and a precipitate was formed in 30% yield and 35% selectivity. In contrast to **OMe-MC-<sup>t</sup>Bu/H**, this new macrocycle **OMe-MC-Vinyl/Vinyl** showed poor solubility, both in THF and benzene, which prevented its direct characterization by NMR spectroscopy or SEC (*Graph 10*). Nevertheless, after reduction, the macrocycle became soluble and could be characterized. The obtained raw product mixture consisted of the desired macrocycle in high selectivity, observed at 17.72 min. retention time, as well as macrocycles, in different states of reduction and linear oligomers at 17.14 min. and 16.61 min.



**Graph 10:** SEC graph of *OMe-MC-Vinyl/Vinyl red*.

In previous studies, the monomers **DAm-Vinyl**, **DAI-OH**, **DAI-Br** and **DAI-Vinyl** were synthesized for the first time. Within this thesis, the monomer synthesis was optimized and further monomers were synthesized. Furthermore, previous studies showed that the cycles **OMe-MC-<sup>t</sup>Bu/H** and **OMe-MC-Vinyl/Vinyl** can be formed in high selectivity; however, it also exhibited that solubility is an issue, which has to be overcome, for example by the integration of longer alkyl chains.

## IV.3.2. Monomer Synthesis

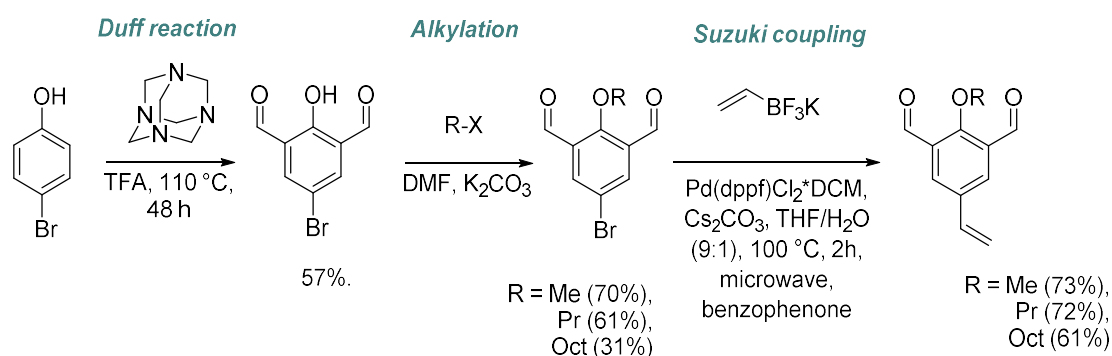
### IV.3.2.1. Synthesis of the Dialdehyde Monomers

One aim of this thesis was to optimize the monomer synthesis and introduce other solubilizing and functional groups to obtain a library of various monomers for macrocyclization. Subsequently, these monomers should be applied in an imine condensation to obtain a series of various macrocycles. The effect of moieties on the cyclization should also be investigated.

Starting from 4-bromophenol, a functional dialdehyde monomer was obtained in a three-step synthesis following the protocol of previous studies (*Scheme 77*).<sup>[135]</sup> In the first step, the aldehyde moieties were introduced *via* Duff reaction. Diverging from the protocol, the reaction time was extended from 22 to 48 hours for the reaction with hexamethylenetetramine and from 1 to 5 hours for the treatment with hydrochloric acid. Furthermore, the raw product was washed with water instead of hexane. By these actions, the yield could be quintupled up to 57%.

Following the procedure for methylation,<sup>[135]</sup> several solubilizing alkyl chains were introduced by Williamson ether synthesis using alkyl halides of different chain length. The methylation with methyl iodide gave a yield of 70%, which is similar to the one obtained in the previous studies. The same procedure was applied to integrate longer alkyl chains. The use of propyl bromide and octyl bromide resulted in alkylated products with yields of 61% and 31% respectively. Sterical hindrance could be an explanation for the decreasing yield.

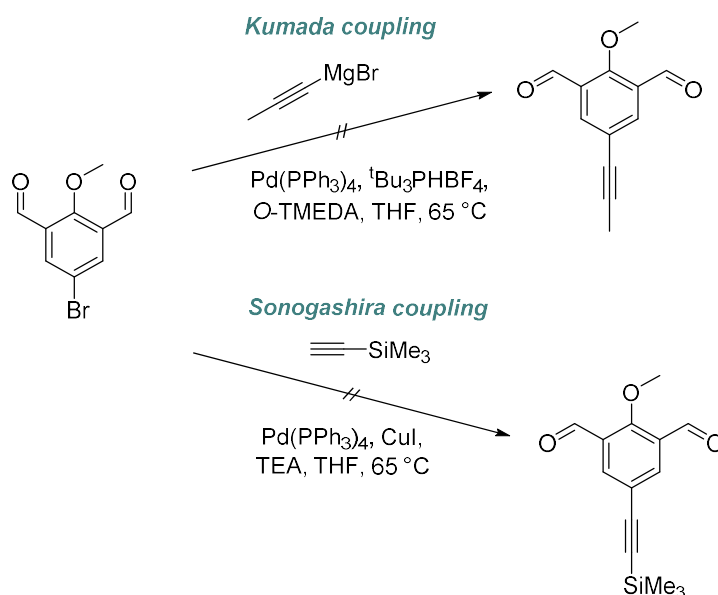
In a subsequent Suzuki coupling with potassium vinyl trifluoroborate, the vinyl functionality was introduced, providing full conversion according to GC-MS. After purification by column chromatography to remove the catalyst, the desired products were obtained in yields between 73 and 61%.



**Scheme 77:** Synthesis of a dialdehyde monomer library.



Furthermore, within the Bachelor Thesis “Synthesis of Macrocycles as Precursor for 2D Polymers” by The Anh Nguyen under supervision of Prof. Dr. Michael Meier and practical co-supervision by G. Klein in 2017, it was tried to integrate a triple bond as the functional group instead of the vinyl group in the aldehyde monomer (*Scheme 78*) by Sonogashira coupling with trimethylsilylacetylene (TMS) and Kumada coupling with 1-propynylmagnesium bromide.<sup>[143]</sup> The introduction of a triple bond as the orthogonal functional group in the macrocycle (*Figure 30*) would allow a reaction of the macrocycles with each other by alkyne metathesis, including a less flexible structure in comparison to the olefins. Due to the more rigid geometry, the procedure to form a two-dimensional network could be more straightforward. In both approaches, Sonogashira and Kumada coupling, the resulting raw product was characterized by GC-MS and <sup>1</sup>H-NMR; however, neither starting material nor product could be assigned. In Kumada coupling, the aldehyde might be reduced to the alcohol due to a nucleophilic addition of the organometallic compound. In the Sonogashira coupling approach, one compound of the raw product mixture could be assigned as the Glaser coupling product of ethynyltrimethylsilane. Further products could not be identified, suggesting that an undesired side reaction took place, and this approach was thus not further investigated



**Scheme 78:** Synthetic strategy for the integration of a triple bond to an aldehyde monomer by Kumada as well as Sonogashira coupling.

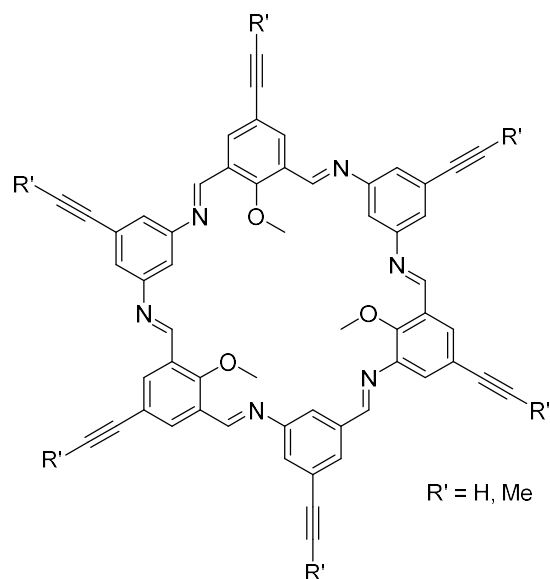


**Figure 30:** Exemplary illustration of a imine macrocycle with triple bonds as functional groups on the outer rim.

In summary, a library of seven different aldehydes could be obtained, which carry either a hydroxyl groups or alkyl chains of several length as solubilizing group and either a bromine or a vinyl group as functional group (*Figure 31*).

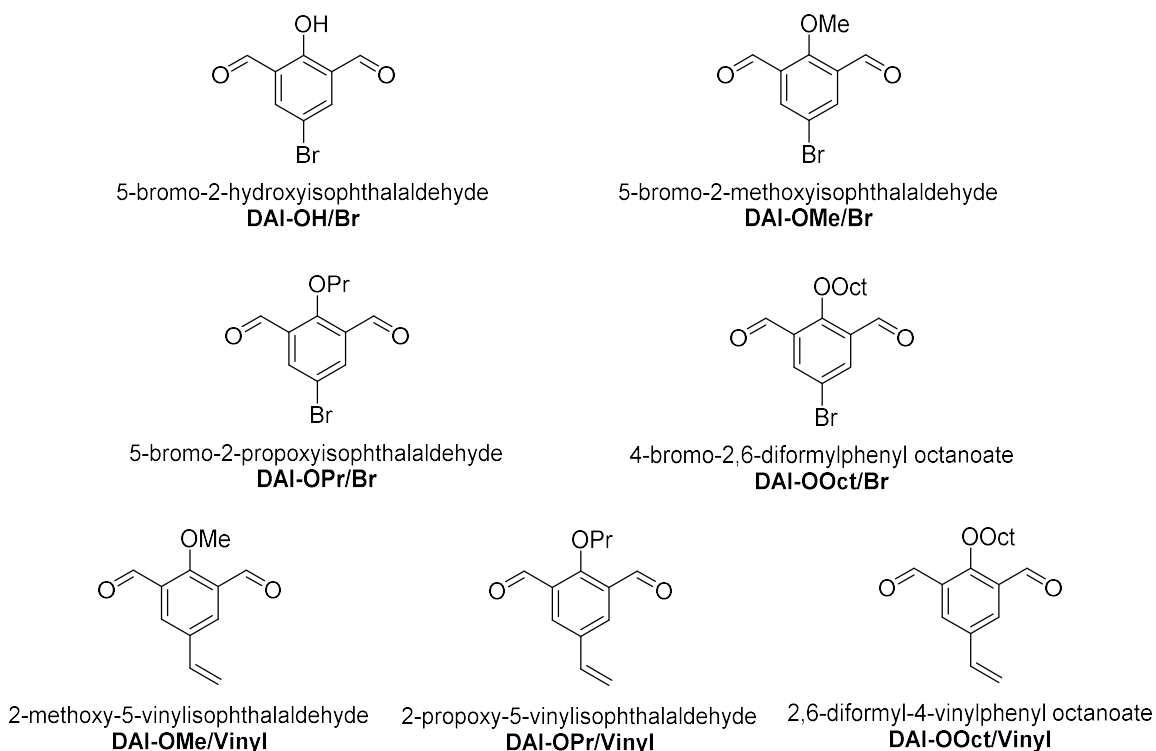
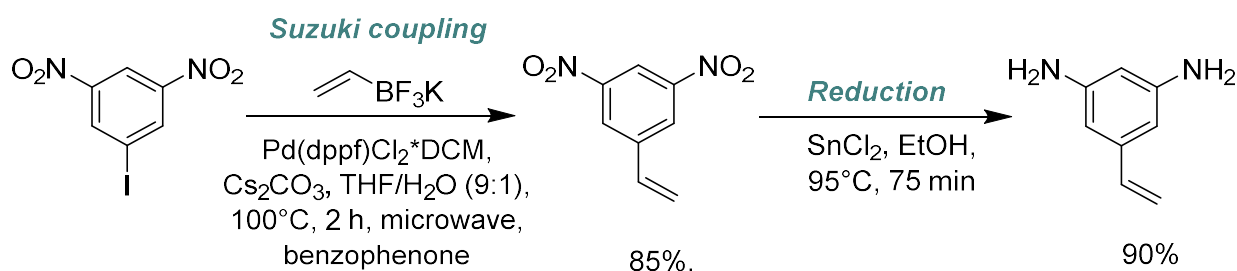


**Figure 31:** Overview of synthesized dialdehyde monomers.

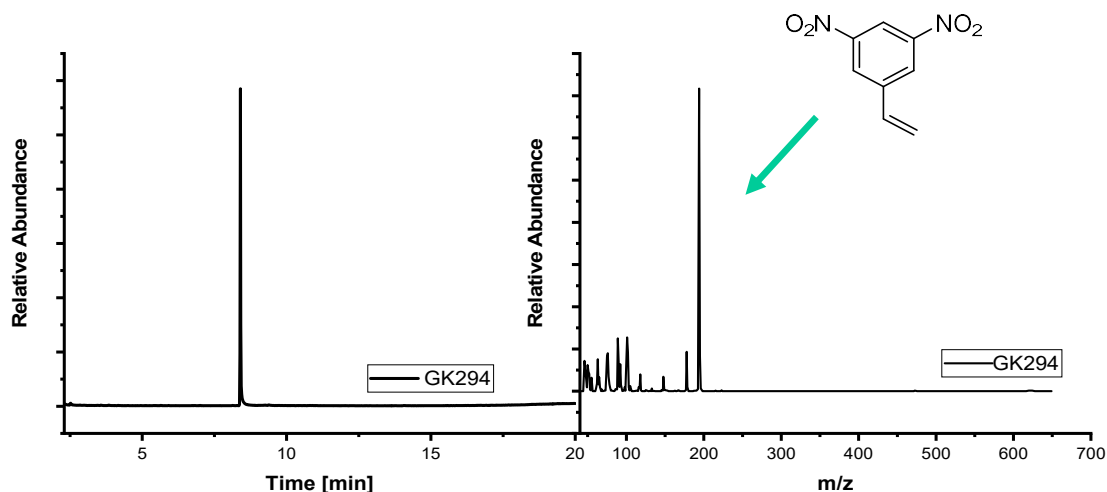
### IV.3.2.2. Synthesis of the Diamine Monomers

The synthesis of the diamine monomers previously developed in the group was optimized in this thesis. Instead of introducing the vinyl functionality by Heck reaction, here, the Suzuki was investigated. Starting from 1-iodo-3,5-dinitrobenzene, the vinyl functionality was introduced with potassium vinyltrifluoroborate in presence of benzophenone as radical scavenger to prevent an undesired polymerization (*Scheme 79*).



**Scheme 79:** Improved synthesis of 1-iodo-3,5-dinitrobenzene.

The full conversion was confirmed by GC-MS. The GC chromatogram and the mass spectrum of the Suzuki reaction depicted in *Scheme 79* are shown in *Graph 11*, exemplary for other Suzuki reactions. The peak at 8.4 min. (*Graph 11*) could be assigned as the desired 1,3-dinitro-5-vinylbenzene ( $m/z[M+H]^+ = 194.0$ ;  $m/z_{\text{calc.}} = 194.0$ ) at 8.4 min. If unreacted 1-iodo-3,5-dinitrobenzene was present, it could be identified as a peak at 9.5 min. ( $m/z[M+H]^+ = 294.0$ ;  $m/z_{\text{calc.}} = 293.9$ ). If the reaction was not complete after the respective time, the reaction time in the microwave reactor was extended until completion. In order to remove the catalyst, the product was further purified by column chromatography giving a yield of 85%, more than twice as high as in the Heck reaction.

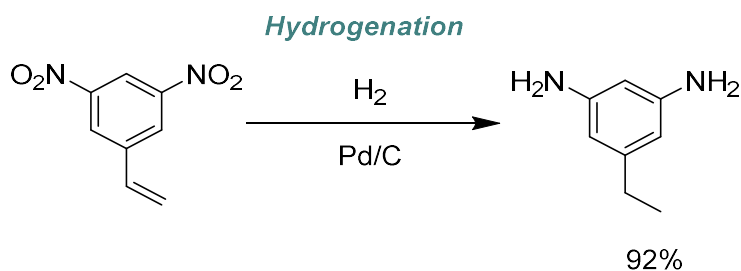


**Graph 11:** GC chromatogram (left) and mass spectrum (right) of 1,3-dinitro-5-vinylbenzene as product of the Suzuki coupling of 1-iodo-3,5-dinitrobenzene (compare Scheme 79).

Afterwards, the nitro groups were reduced by tin(II) chloride in order to get the desired diamine monomer. Previous studies showed that if the reaction was carried out in the presence of air, full conversion was not achieved even after four hours, but a reaction mixture of starting material, mono-amine and the desired diamine was obtained. To separate the product, a complicated extraction and washing procedure was necessary, including precipitation of the diamine with hydrochloride gas. Furthermore, the amine groups are sensitive to air, which means that the purification had to be carried out quickly within the a few hours, also limiting the reproducibility. Instead of air, the reaction was thus later carried out in inert atmosphere enabling full conversion after four hours. The conversion was followed by  $^1\text{H-NMR}$  and further tin(II) chloride was added or the reaction time could be extended if necessary. Once full conversion was achieved, the raw product could be obtained by a simple extraction, which was carried out quickly to prevent a degradation. Afterwards, the pure product was stored under Argon atmosphere in the fridge.

Starting from 1-iodo-3, 5-dinitrobenzene, a further diamine monomer was synthesized by hydrogenation with  $\text{H}_2$  in presence of palladium on charcoal (Scheme 80). The heterogenous catalyst could be removed by filtration, which makes the purification a handy procedure and the desired product 5-ethylbenzene-1,3-diamine was obtained

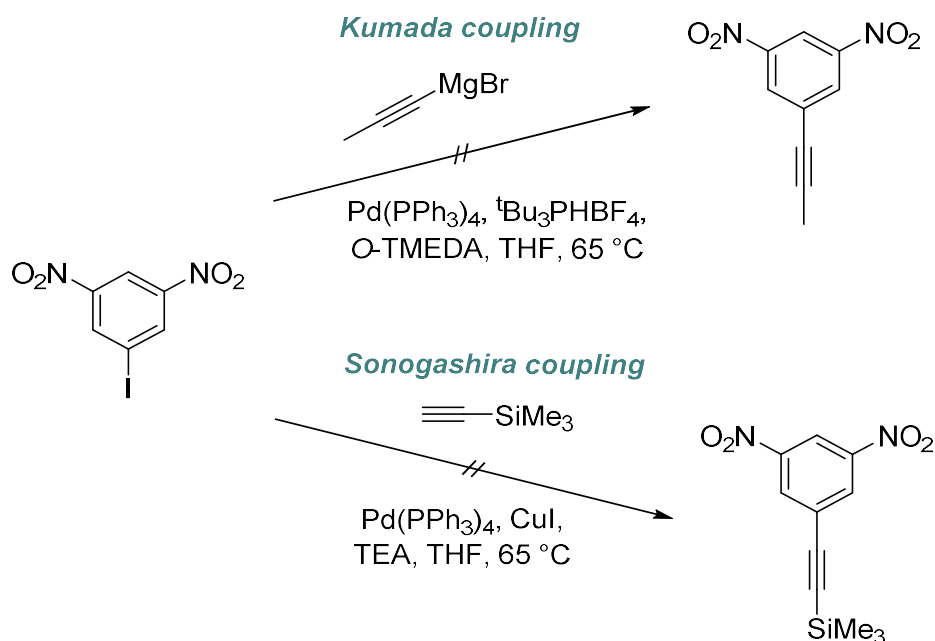
within 4 hours. Similar to 1,3-dinitro-5-vinylbenzene, the obtained product is a highly viscous liquid and has to be stored under Ar and in the fridge to prevent a degradation. In contrast to these liquid diamine monomers, which exhibited to be sensitive against degradation, the solid diamines, namely *m*-phenylenediamine and 5-(trifluoromethyl)benzene-1,3-diamine, were commercially available and stored without any cooling or inert atmosphere without showing any degradation.



**Scheme 80:** Improved synthesis of 5-ethylbenzene-1,3-diamine by hydrogenation of 1-iodo-3, 5-dinitrobenzene.

Within the Bachelor Thesis “Synthesis of Macrocycles as Precursor for 2D Polymers” (details see above), it was tried to introduce a triple bond as functional group to the amine monomer by Kumada coupling and Sonogashira coupling as well (*Scheme 81*). In Kumada coupling, the raw product mixture consists of starting material and the desired product. It was tried to optimize the reaction conditions to achieve full conversion; however, even after several optimization attempts, starting material and product were still present in ratio of about 1:1 according to GC-MS. A purification by column chromatography did not lead to the isolation of the product due to a poor separation of product and starting material.

Applying 1-iodo-3,5-dinitrobenzene in a Sonogashira coupling led to a similar result as the dialdehyde attempt.<sup>[143]</sup> Apart from the Glaser product of ethynyltrimethylsilane, no other substance of the raw product mixture could be identified, neither as starting material nor as desired product.



**Scheme 81:** Synthetic strategy for the integration of a triple bond to an diamine monomer by Kumada as well as Sonogashira coupling.

In summary of this section, a library of four different amine monomers (Figure 32) were obtained and used for the macrocyclization. One diamine did not carry any further functionality and the other three a vinyl, an ethyl or a trifluoromethyl group.

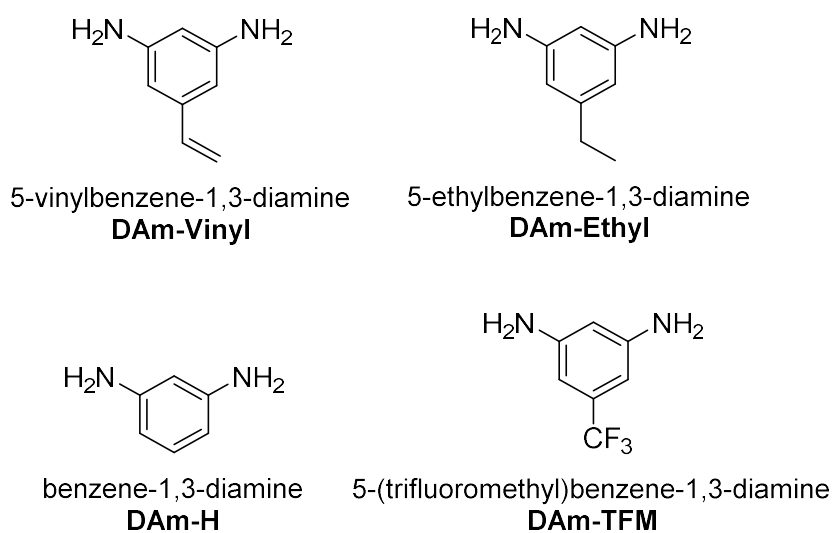
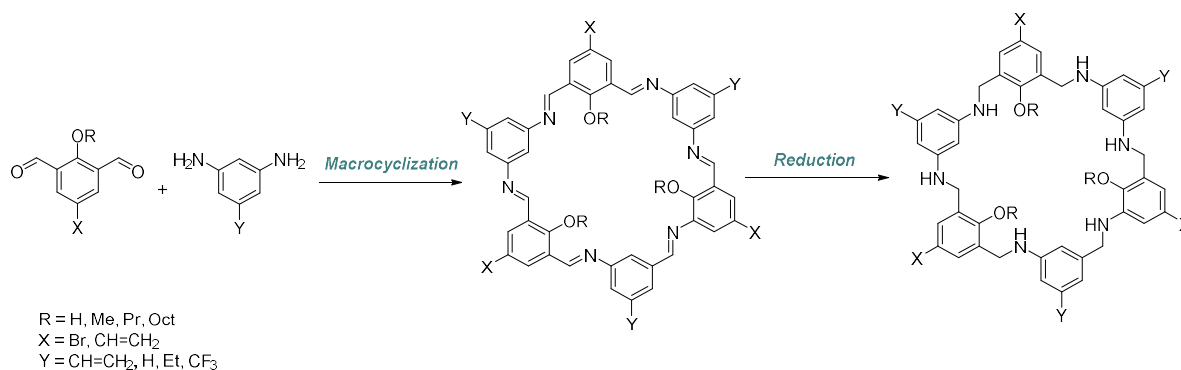


**Figure 32:** Overview of diamine monomers. Two were synthesized (top) and two were purchased from a commercial source (bottom).

### IV.3.3. Synthesis of Macrocycles

Applying the reaction conditions described in the previous studies, the monomers were combined in order to prepare a library of macrocycles with different numbers and types of functional groups at the outer rim and different alkyl chains in the inner (Scheme 82).



**Scheme 82:** Macrocyclization of a dialdehyde and diamine monomer by imine condensation and subsequent reduction to the corresponding amine.

All reactions were carried out under Argon atmosphere, with MeOH as solvent and CaCl<sub>2</sub> as template salt. During the imine condensation, the six-membered macrocycle precipitated from the reaction mixture together with other compounds, probably linear oligomers of high molecular weight or other cyclic species. Depending on the applied monomers and conditions, high selectivity (*i.e.*, a single peak observed by SEC) to a broadly distributed mixture of compounds were obtained. Nevertheless, for the calculation of the yield, the precipitation was considered macrocycles only in order to compare different batches and to evaluate the amount of formed precipitate. Additionally, the theoretical molar mass of the macrocycle was calculated considering the presence of one Ca<sup>2+</sup> ion in its structure. Due to the macrocycles' solubility after reduction, it was assumed that Ca<sup>2+</sup> was no longer present; hence, the molar mass of the reduced macrocycles was used for the calculation of the yield after reduction.

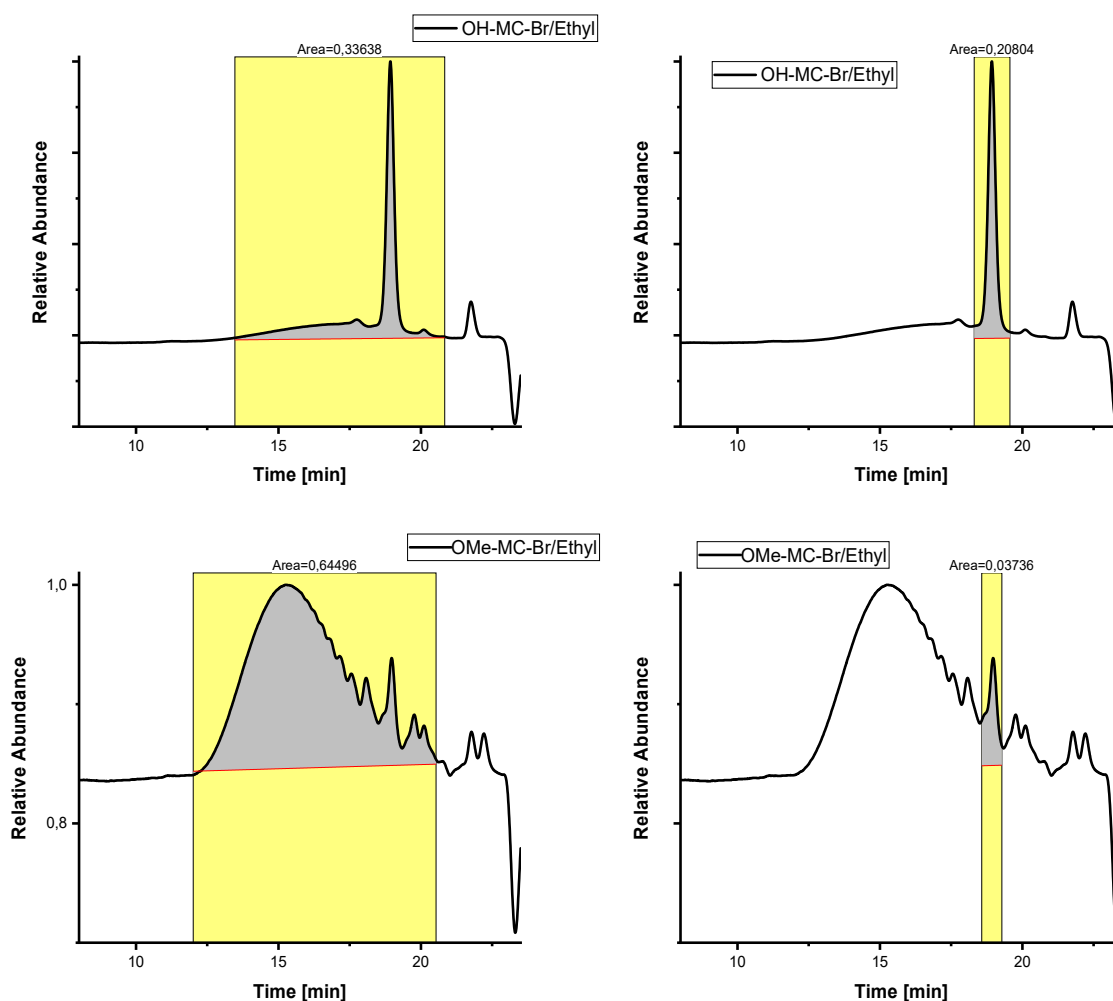
Due to their insolubility in common solvents, the precipitate was suspended in a methanol/THF mixture (1:1). Sodium borohydride was added to the reaction mixture. The better the solubility of the macrocycles, the more efficient the reduction works. Depending on the macrocyclic species, the suspension became clear during the reaction, which was a good indication for the progress of the reduction. According to

this progress, the reaction was either quenched with water or further NaBH<sub>4</sub> was added and the reaction time extended. The addition of more THF helped the reduction to proceed as well. This indicates that only a small fraction of macrocycle got solubilized and then reduced in solution. The reduced macrocycle had a better solubility and further unreduced macrocycles could go into solution.

In solution, **OMe-MC-Vinyl/Vinyl** was treated with an excess ethylenediaminetetraacetic acid (EDTA) to remove Ca<sup>2+</sup> from the macrocycle and complex it with EDTA in order to increase the solubility of the macrocycle; however, **OMe-MC-Vinyl/Vinyl** exhibited a higher affinity to complex Ca<sup>2+</sup>. However, even without a template ion, the macrocycle had a poor solubility.

The generated reduced macrocycles were characterized by SEC-ESI to confirm that the targeted compound had been formed and to attribute the corresponding SEC peak. The SEC trace gave information about the selectivity. Exemplary, the procedure to determine the selectivity by integration of **OH-MC-Ethyl red** and **OMe-MC-Ethyl red** are presented graphically in *Graph 12*. Correlating the integration area of all formed compounds to the desired macrocycle gave a good indication of the selectivity and allowed to compare different reaction parameters in an optimization process.





**Graph 12:** Procedure to determine the selectivity by integration of **OH-MC-Ethyl red** and **OMe-MC-Ethyl red** are presented graphically. Left: integration of all species; right: Integration of target macrocycle.

#### IV.2.3.1. Macrocycles with DAM-H

First, macrocycles were synthesized by combination of **DAM-H** with dialdehyde building blocks bearing Br as functional groups and different alkyl chains as solubilizing groups. The resulting macrocycles exhibited three functional groups at the outer rim and three in the inner (*Figure 33*). The results are summarized in *Table 7*.

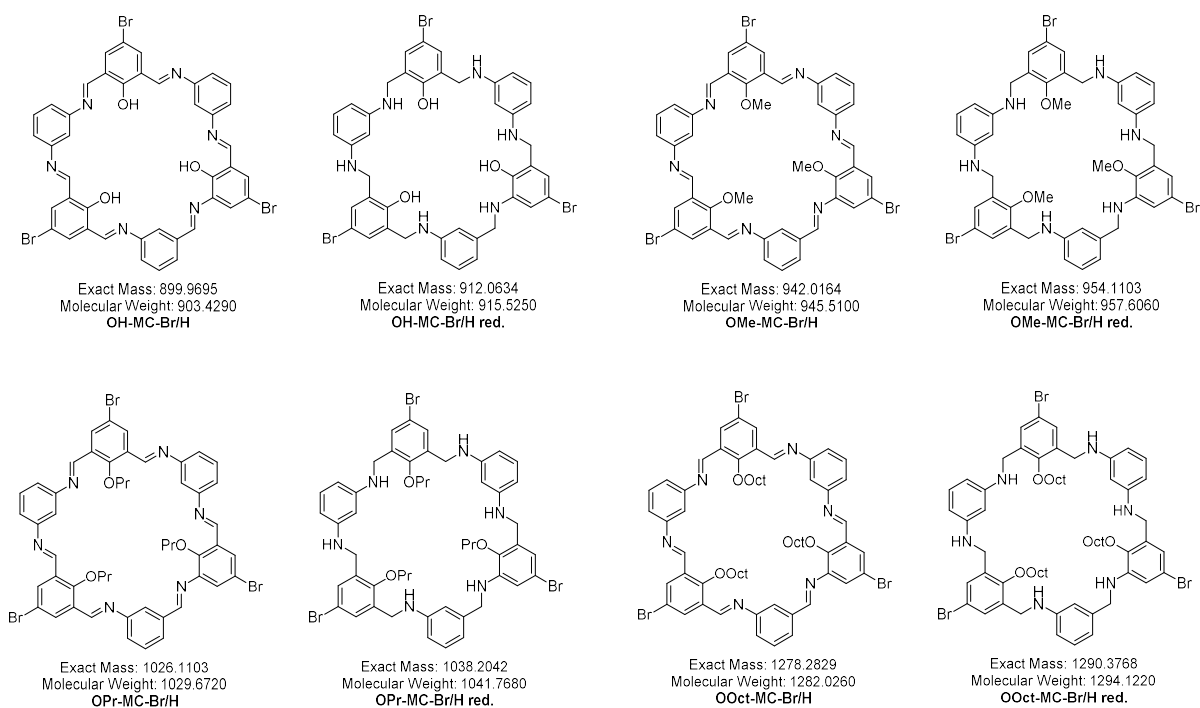


**Figure 33:** Overview of targeted macrocycles with **DAM-H** (before and after reduction).

**Table 7:** Results of macrocyclization with **DAM-H**.

Macrocycle	Diamine	Dialdehyde	Yield Precipitate [%]	Yield after Red. [%]
<b>OH-MC-Br/H</b>	<b>DAM-H</b>	<b>DAI-OH/Br</b>	79	54 <sup>1)</sup>
<b>OMe-MC-Br/H</b>	<b>DAM-H</b>	<b>DAI-OMe/Br</b>	84	98 <sup>1)</sup>
<b>OPr-MC-Br/H</b>	<b>DAM-H</b>	<b>DAI-OPr/Br</b>	87	>100 <sup>1)</sup>
<b>OOct-MC-Br/H</b>	<b>DAM-H</b>	<b>DAI-OOct/Br</b>	81	60 <sup>2)</sup>

1) Solubilized during reduction but insoluble after removal of solvent

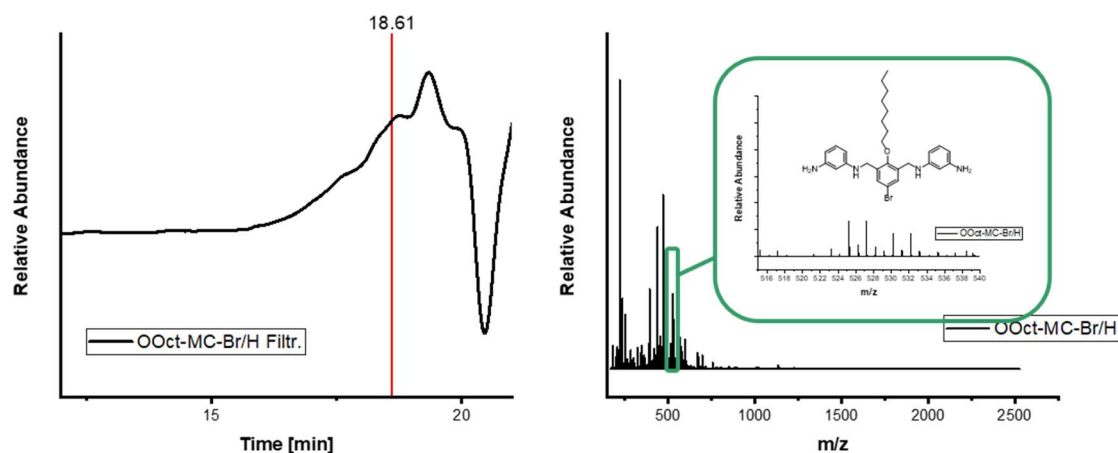
2) Not completely soluble during reduction

Applying **OH-MC-Br/H** as dialdehyde monomer, a precipitate was formed within a few minutes. In case of **OMe-MC-Br/H**, a precipitate was formed after about one hour. For **OPr-MC-Br/H**, the reaction mixture was clear after 6 hours. Applying **OOct-MC-Br/H** led to a slightly turbid reaction mixture after 6 hours. Therefore, the reaction times for the last two monomers were doubled and after 13 hours, the yield of precipitate was similar to the one of the shorter groups. Probably due to steric hindrance, the equilibrium takes longer to be established and the macrocycle was formed more slowly.

For all four macrocycles, equimolar amounts of monomer were applied. No aldehyde was present in the soluble part of the reaction mixture according to  $^1\text{H-NMR}$  spectroscopy, which indicates that all aldehyde groups were consumed. Due to the overlapping with other peaks, the consumption of the diamine monomer could not be determined. The precipitate of all macrocycles was insoluble in common solvents. In order to freeze the equilibrium and to increase the solubility, each precipitate was suspended in a methanol/THF mixture (1:1). The orange color of the suspension of **OH-MC-Br/H** disappeared within minutes, which is an indication that the conjugated system changes; hence it is an indication for a successful reduction. The other three batches did not show any change of color. Except for **OOct-MC-Br/H**, all precipitates became completely soluble during the reduction. After the reduction and work-up by extraction, the yield of **OH-MC-Br/H red** was >100%. In order to remove impurities like inorganic salts, the solid was taken up in THF to repeat the extraction an additional washing step with water. However, **OH-MC-Br/H red** was not completely soluble again, even after treatment in an ultrasonic bath. This explains the low yield of **OH-MC-Br/H red** compared to the other macrocycles. A similar problem was observed for **OPr-MC-Br/H red**. Once the solvent was removed, the residue was not soluble anymore in common solvents; hence, a washing step was not performed, which explains the yield >100%. During the reduction of **OOct-MC-Br/H**, the suspension did not become clear and the precipitate was still present even after further equivalents of  $\text{NaBH}_4$  were added. Only the soluble part of the reaction mixture was proceeded in the work-up and subsequent characterization, which explains the low yield compared to the other ones. That time, the washing step was directly integrated in the work-up procedure.

Nevertheless, once the solvent was removed, **OMe-MC-Br/H** and **OPr-MC-Br/H** also showed a low solubility in THF and other common solvents as well, which impedes a full characterization. A strong  $\pi$ - $\pi$  stacking might explain the phenomenon. The low solubility might be the reason why neither the adequate mass for **OH-MC-Br/H red**, **OMe-MC-Br/H red** nor for **OPr-MC-Br/H red** was found. Only **OOct-MC-Br/H red** was fully soluble, probably because the insoluble macrocycle was filtered off during the work-up of the reduction, which would explain why in SEC-ESI no adequate mass for **OOct-MC-Br/H red** could be assigned but only the mass for the linear trimer with

amines as end groups was found at 18.61 min. ( $m/z[M+H]^+ = 525.2218$ ;  $m/z_{\text{calc.}} = 525.2229$ ;  $m/z = 0.0011$ ) (*Graph 13*).



**Graph 13:** SEC trace and mass spectrum of the filtrate of the synthesis of **OOct-MC-Br/H**

When **DAm-H** was applied as diamine monomer, an imine condensation proceeded; however, due to a low solubility and maybe an inefficient ionization, no statements about the selectivity or presence of the targeted cycles can be issued.

#### IV.2.3.2. Macrocycles with DAm-Vinyl

Applying **DAm-Vinyl** as diamine monomer gives a macrocycle with vinyl groups, which is a potential building block for 2D structures by metathesis reaction (*Figure 34*) as discussed in chapter III. *Motivation and Aim of the Thesis*. The obtained results are summarized in *Table 8*.

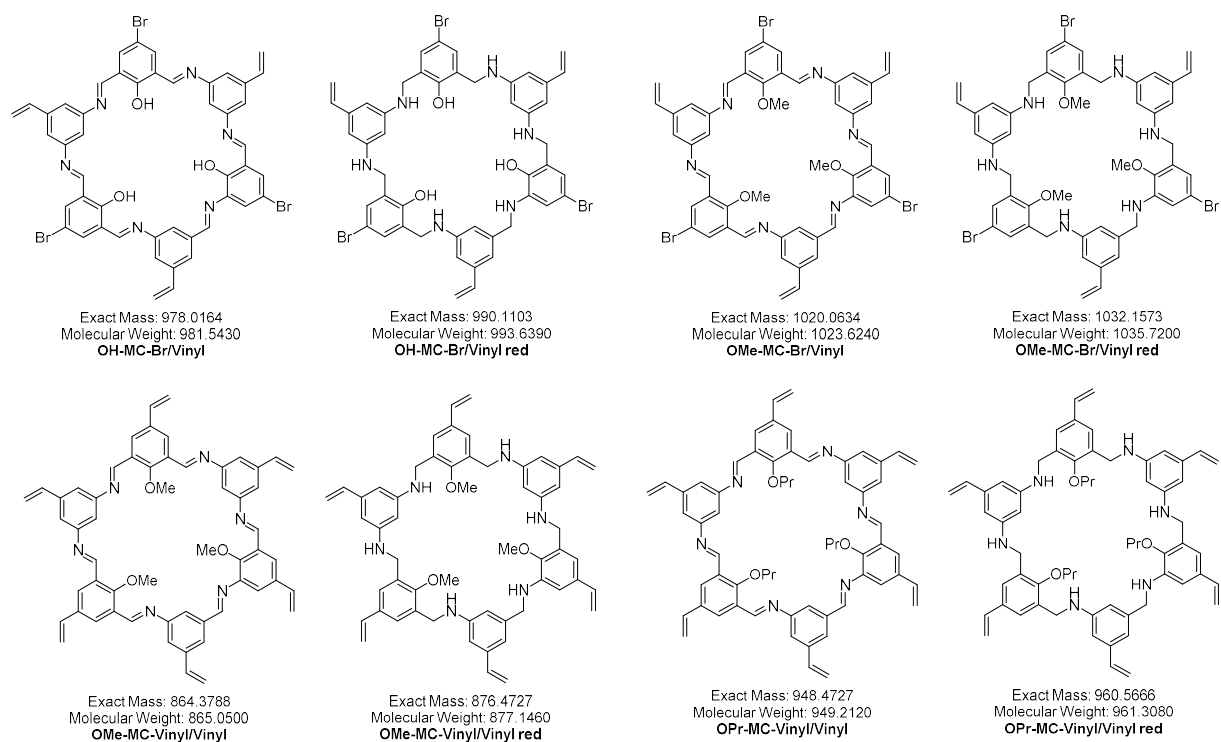
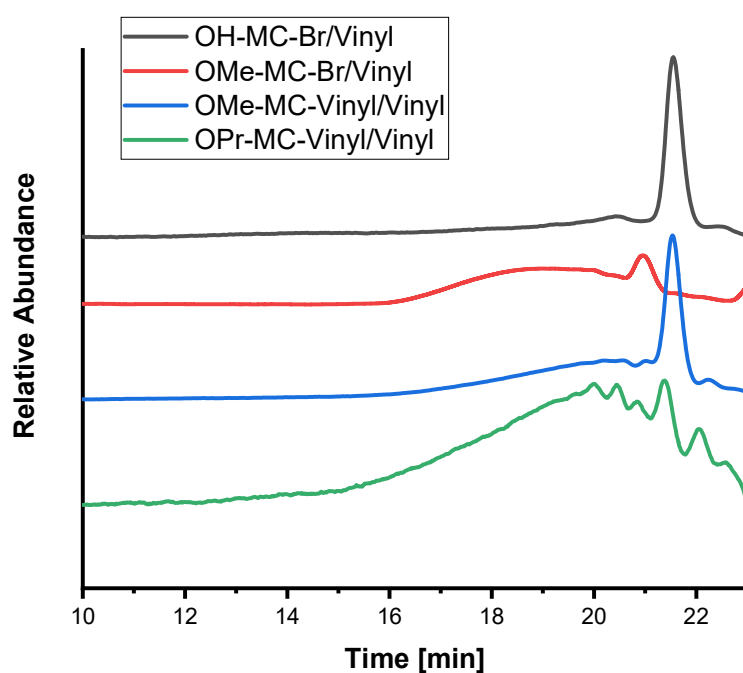


**Figure 34:** Overview of targeted macrocycles with *DAm-Vinyl* (before and after reduction).

**Table 8:** Results of the macrocyclization with **DAM-Vinyl**.

Macrocycle	Diamine	Dialdehyde	Yield Precipitate [%]	Yield after Red. [%]	Selectivity [%]
<b>OH-MC-Br/Vinyl</b>	<b>DAm-Vinyl</b>	<b>DAI-OH/Br</b>	83	87	86
<b>OH-MC-Br/Vinyl*</b>	<b>DAm-Vinyl</b>	<b>DAI-OH/Br</b>	83	86	74
<b>OMe-MC-Br/Vinyl</b>	<b>DAm-Vinyl</b>	<b>DAI-OMe/Br</b>	51	51	20
<b>OMe-MC-Vinyl/Vinyl</b>	<b>DAm-Vinyl</b>	<b>DAI-OMe/Vinyl</b>	38	40	36
<b>OPr-MC-Br/Vinyl</b>	<b>DAm-Vinyl</b>	<b>DAI-OPr/Vinyl</b>	65	64	12

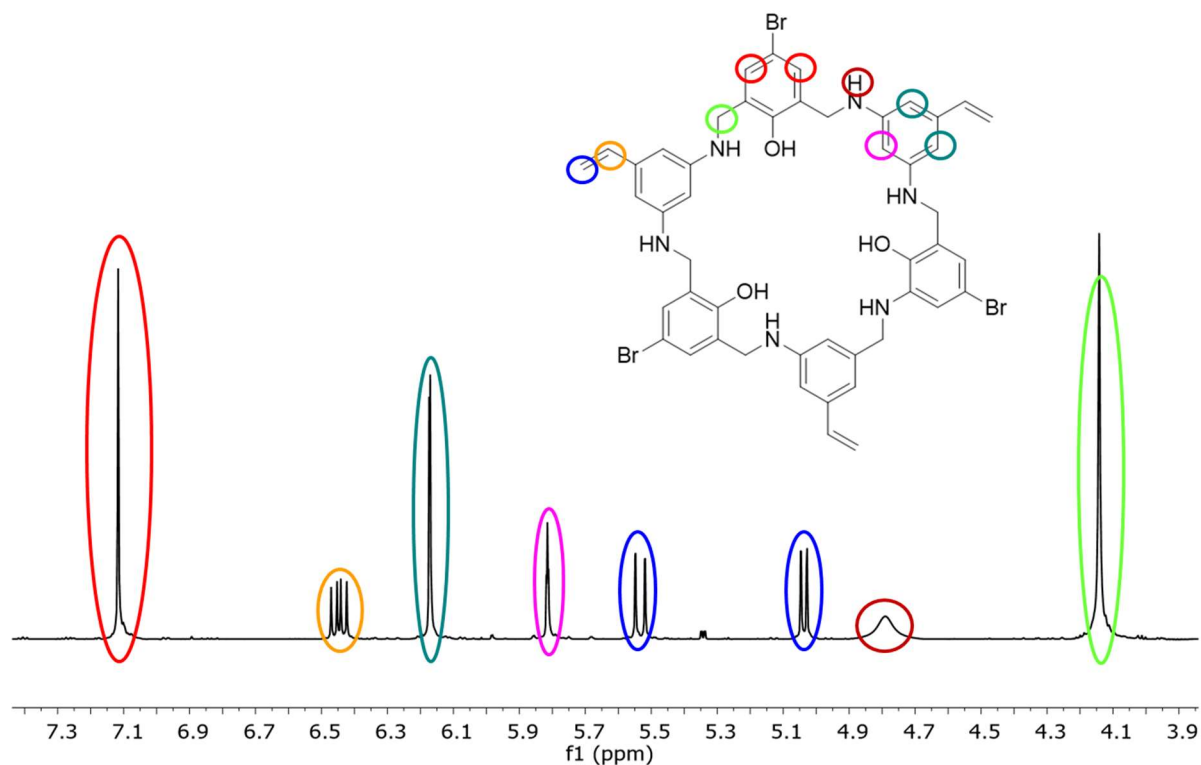
\* *DMSO as solvent*



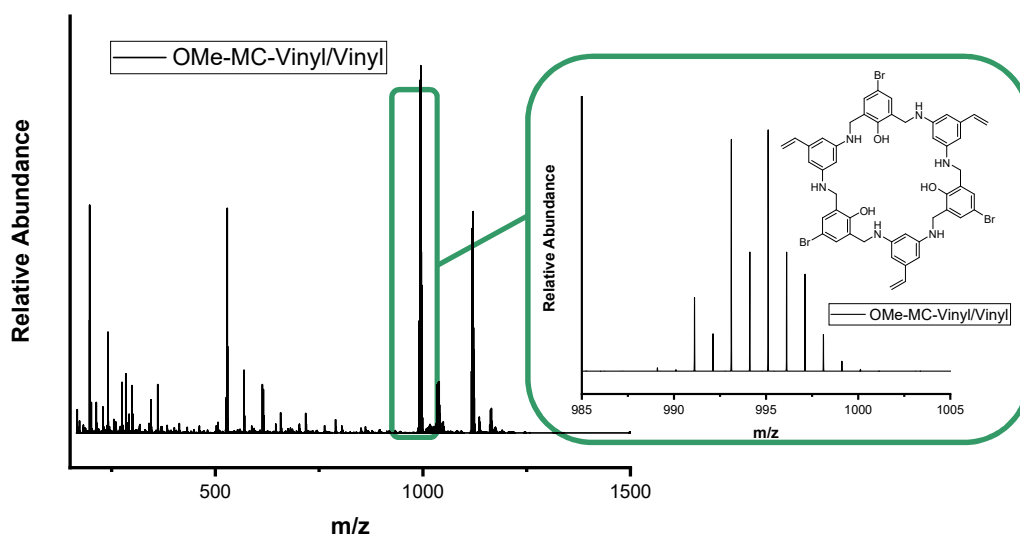
**Graph 14:** SEC traces of the cyclization by imine condensation with **DAM-Vinyl**. The **DAM-Vinyl** was combined with **DAI-OH/Br**, **DAI-OMe/Br**, **DAI-OMe/Vinyl**, **DAI-OPr/Vinyl** and **DAI-OOct/Vinyl**.

In all the cases, a precipitate was formed in yields ranging from 38% to 83%; however, in lower yields compared to cycles with **DAm-H** (Table 8) except the reaction with **DAI-**

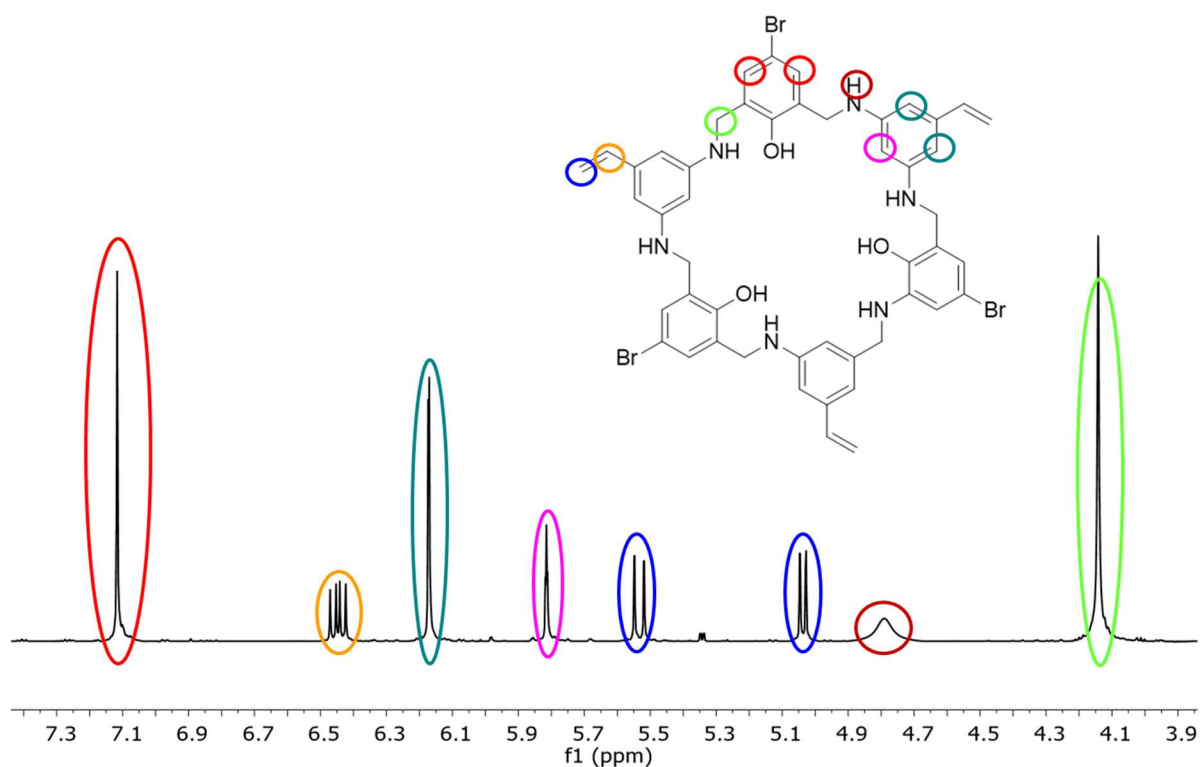
**OH/Br** which gave a yield of 82%. For all macrocycles, the precipitate went into solution during the reduction. According to SEC, the selectivity decreased with longer alkyl chains (*Graph 14*). The highest selectivity (86%) was reached for **OH-MC-Br/Vinyl**. In the SEC chromatogram, a single, intense peak at 17.70 min. with a small shoulder at 16.69 min. was observed. The peak at 17.70 min. was identified as **OH-MC-Br/Vinyl red** ( $m/z[M+H]^+ = 991.1172$ ;  $m/z_{calc.} = 991,1181$ ;  $\Delta m/z = 0.0009$ ) (*Graph 15*). The macrocycle structure was confirmed by  $^1H$ -NMR (



*Graph 16*). Due to contamination, unidentified peaks appeared at 0.81, 1.20 and 2.20 pm.



**Graph 15:** Mass spectrum of *OH-MC-Br/Vinyl red*.



**Graph 16:**  $^1\text{H-NMR}$  spectrum of crude *OH-MC-Br/Vinyl red*.

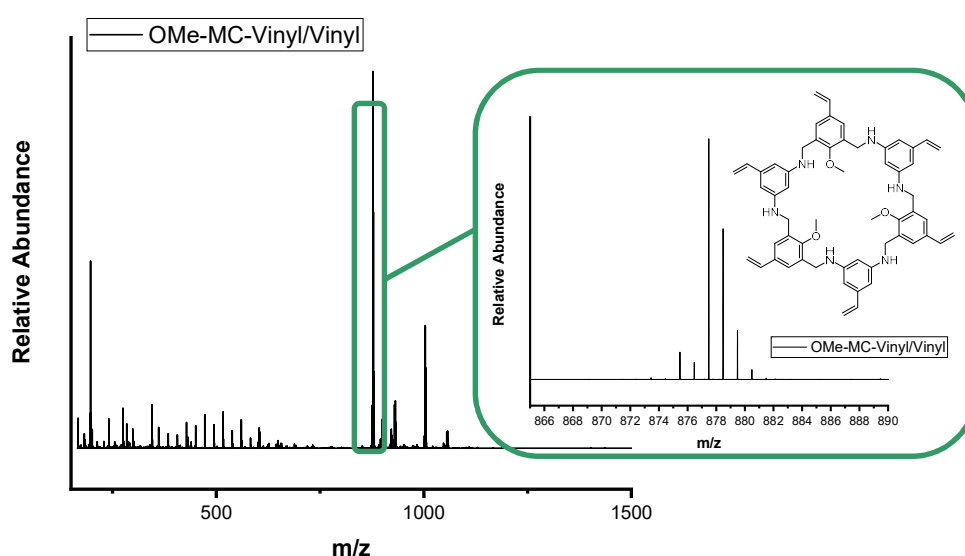
The synthesis of **OH-MC-Br/Vinyl** can be carried out in DMSO as well, giving similar results as in MeOH. In methanol, the aldehyde monomer underwent an acetal



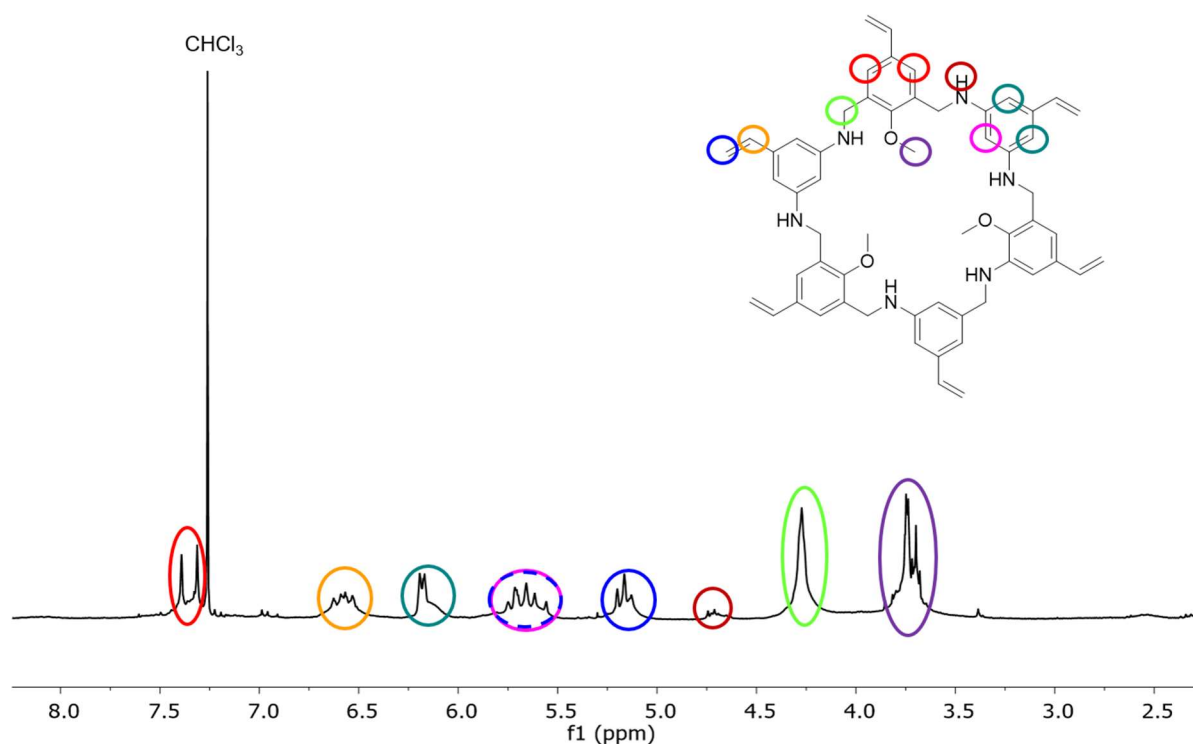
formation according to  $^1\text{H-NMR}$  spectroscopy. In DMSO, this reaction did not occur. Due to the similar results, the acetal formation did obviously not impair the macrocyclization. Acetal formation is a reversible reaction. Once the remaining aldehyde was consumed, the equilibrium was shifted and the imine condensation proceeded. When DMSO was used as solvent in the synthesis of **OMe-MC-Br/Vinyl** and **OMe-MC-Vinyl/Vinyl**, even after days of the precipitate appeared, the aldehyde groups were not converted completely according to  $^1\text{H-NMR}$  spectroscopy.

**OH-MC-Br/Vinyl** can be converted back to its monomers by hydrolysis with TFA in a water/THF mixture, confirming the expected reversibility of the macrocyclization.

**OMe-MC-Vinyl/Vinyl** showed an intense peak at 17.53 min. According to SEC-ESI, it corresponds to the targeted macrocycle **OMe-MC-Vinyl/Vinyl red** ( $m/z[M+H]^+ = 877.4770$ ;  $m/z_{\text{calc.}} = 877.4805$ ;  $\Delta m/z = 0.0035$ ) (*Graph 17*). Impurities can be detected by a broad distribution between 13 and 17 min. (*Graph 14*) as well as in  $^1\text{H-NMR}$ . The integrals are broad and integration does not fit completely, probably due to the presence of linear oligomers. Similar to **OH-MC-Br/Vinyl red**, unidentified contaminations appeared at 0.85, 1.25 and 1.69 ppm (*Graph 18*).



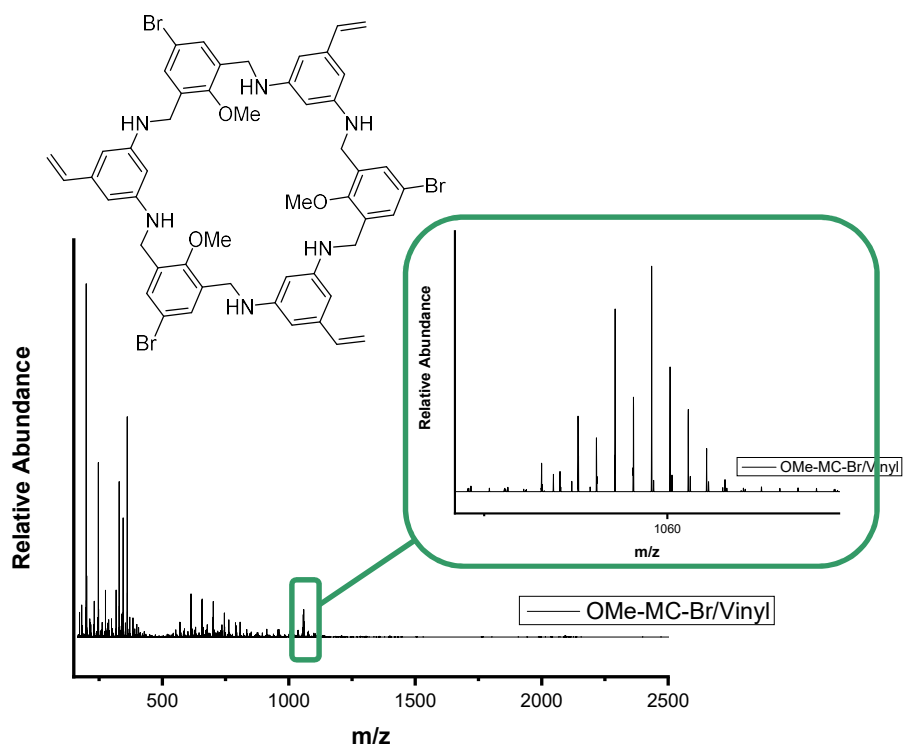
**Graph 17:** Mass spectrum of **OMe-MC-Vinyl/Vinyl red**.



**Graph 18:**  $^1\text{H-NMR}$  spectrum of crude **OMe-MC-Vinyl/Vinyl red**.

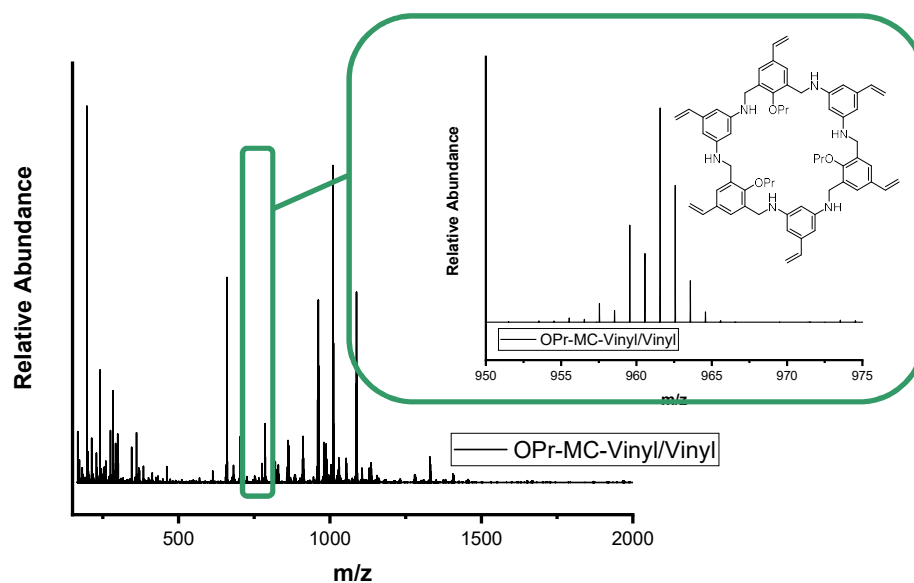
If **OH-MC-Br/Vinyl red** and **OMe-MC-Vinyl/Vinyl red** were stored in  $\text{CHCl}_3$  or THF, a precipitate was formed after several days, though they were soluble directly after reduction; however, after several steps of solubilizing and removing the solvent, the macrocycle did not go fully into solution anymore. An explanation for that could be radical polymerization initiated by light of the vinyl groups with each other forming an insoluble network, the temperature of the water bath or the removal of the solvent. Due to the insolubility, the network could not be further characterized.

Within the Bachelor Thesis “Synthesis of Macrocycles as Precursor for 2D Polymers” (for details see above), **OMe-MC-Br/Vinyl** was synthesized and characterized.<sup>[143]</sup> According to the SEC, the selectivity was rather low compared **OH-MC-Br/Vinyl** or **OMe-MC-Vinyl/Vinyl**. The peak at 21.0 min. was identified as **OMe-MC-Br/Vinyl red** by SEC-ESI ( $m/z[\text{M}+\text{H}]^+ = 1055.1249$ ;  $m/z_{\text{calc.}} = 1055.1471$ ;  $\Delta m/z = 0.0222$ ).



**Graph 19:** Mass spectrum of **OMe-MC-Br/Vinyl red**.

Applying **OPr-DAI-Vinyl/Vinyl** as monomer led to the formation of a broad distribution according to the SEC. The peak at 17.57 min. could be identified by SEC-ESI as **OPr-MC-Vinyl/Vinyl red** ( $m/z[M+H]^+ = 961.5719$ ;  $m/z_{\text{calc.}} = 961.5744$ ;  $\Delta m/z = 0.0025$ ) (Graph 20).



**Graph 20:** Mass spectrum of **OPr-MC-Vinyl/Vinyl red**.

Further linear oligomers were detected: the linear 4mer at 17.80 min. ( $m/z[M+H]^+ = 657.3790$ ;  $m/z_{\text{calc.}} = 657.3804$ ;  $\Delta m/z = 0.0014$ ), the linear 5mer with the aldehyde end groups at 17.30 min. ( $m/z[M+H]^+ = 859.4774$ ;  $m/z_{\text{calc.}} = 859.4798$ ;  $\Delta m/z = 0.0024$ ), the linear 6mer at 17.05 min. ( $m/z[M+H]^+ = 977.5679$ ;  $m/z_{\text{calc.}} = 977.5693$ ;  $\Delta m/z = 0.0014$ ), the linear 7mer with the aldehyde end groups at 16.71 min. ( $m/z[M+H]^+ = 1179.6670$ ;  $m/z_{\text{calc.}} = 1179.6687$ ;  $\Delta m/z = 0.0017$ ) and the linear 8mer at 16.54 min. ( $m/z[M+H]^+ = 1297.7556$ ;  $m/z_{\text{calc.}} = 1297.7582$ ;  $\Delta m/z = 0.0026$ ) (*Figure 35*). The lower selectivity could be explained by the steric hindrance due to the longer alkyl chains impeding a templation and the ring-closing.

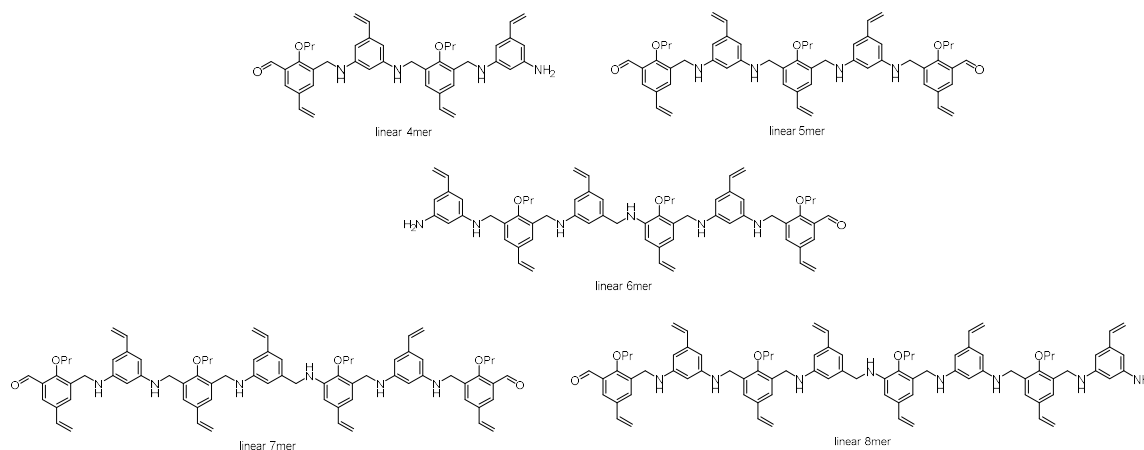


**Figure 35:** Overview of linear oligomers obtained during the macrocyclization of **OPr-MC-Vinyl/Vinyl**.

### IV.2.3.3. Macrocycles with DAM-Ethyl

In order to overcome the solubility issues due to polymerization of the vinyl moieties, a further diamine monomer was synthesized. By hydrogenation, the vinyl group was transformed into an ethyl group, which should increase the solubility of the resulting cycles and does of course not allow polymerization (*Figure 36*). The obtained results are summarized in *Table 9*.

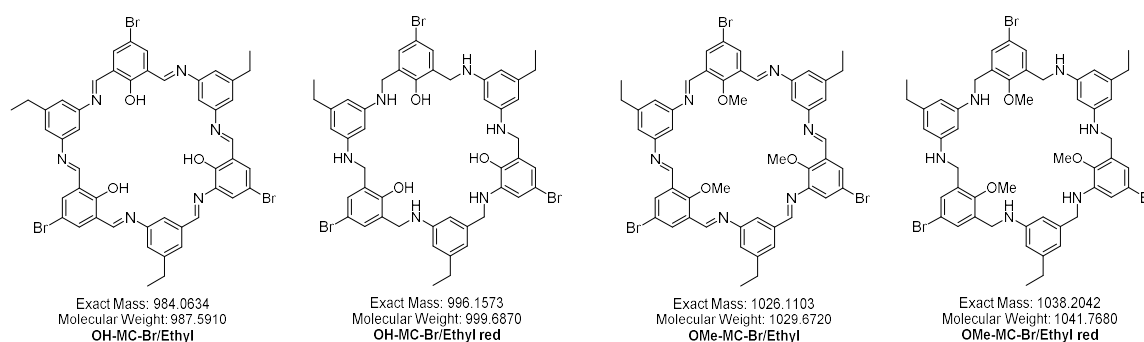
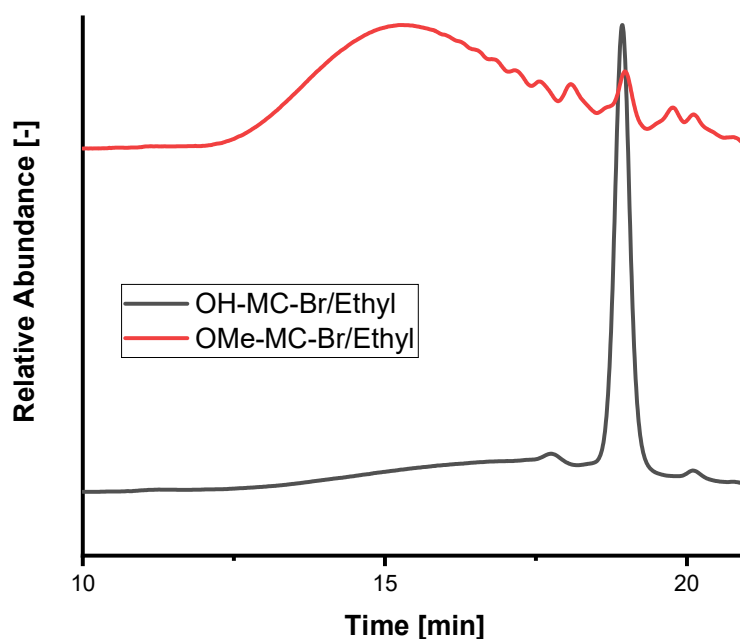


**Figure 36:** Overview of targeted macrocycles with **DAM-Ethyl** (before and after reduction).

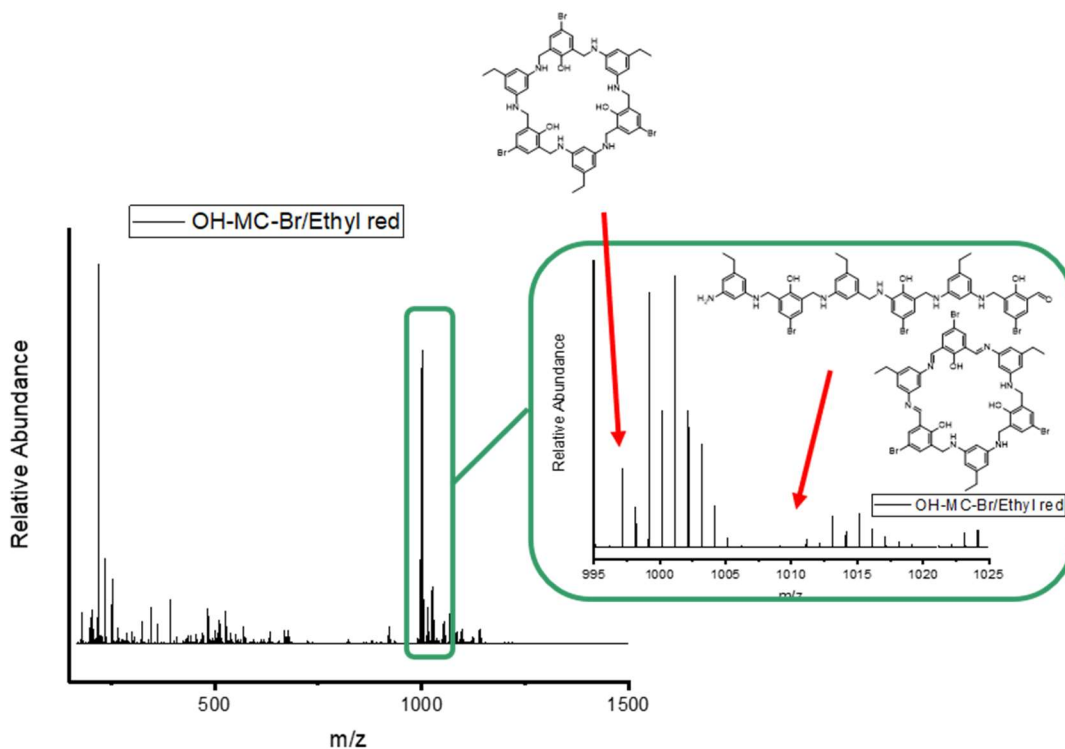
**Table 9:** Results of the macrocyclization with **DAM-Ethyl**.

Macrocycle	Diamine	Dialdehyde	Yield Precipitate [%]	Yield nach Red. [%]	Selectivity [%]
<b>OH-MC-Br/Ethyl</b>	<b>DAm- Ethyl</b>	<b>DAI-OH/Br</b>	82	88	62
<b>OMe-MC- Br/Ethyl</b>	<b>DAm- Ethyl</b>	<b>DAI- OMe/Br</b>	87	81	6



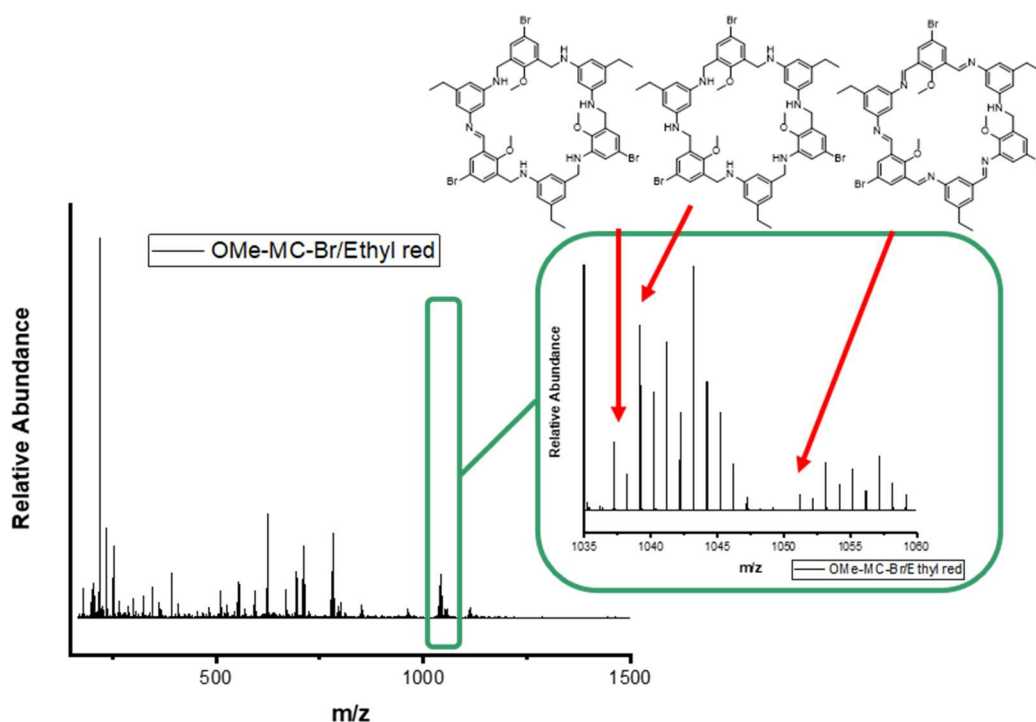
**Graph 21:** SEC trace of **OH-MC-Br/Ethyl** (black) and **OMe-MC-Br/Ethyl** (red).

According to the SEC analysis, **OH-MC-Br/Ethyl red** was obtained with a high selectivity indicated by the intense peak at 18.20 min. (*Graph 21*). In SEC-ESI, this peak with the highest intensity could be assigned to **OH-MC-Br/Ethyl red** ( $m/z[M+H]^+ = 997.1640$ ;  $m/z_{\text{calc.}} = 997.1651$ ;  $m/z = 0.0011$ ) (*Graph 22*). Furthermore, a peak of weaker intensity could be assigned either to the linear 6mer ( $m/z[M+H]^+ = 1013.1600$ ;  $m/z_{\text{calc.}} = 1013.1412$ ;  $m/z = 0.0188$ ) or the cycle with 3 imine bonds present ( $m/z[M+H]^+ = 1013.1600$ ;  $m/z_{\text{calc.}} = 1013,1001$ ;  $m/z = 0.0599$ ). The small shoulder at 17.05. min can be seen, which could not be assigned to any linear or cyclic compound.



**Graph 22:** Mass spectrum of **OH-MC-Br/Ethyl red**.

Compared to **OH-MC-Br/Ethyl**, the selectivity of **OMe-MC-Br/Ethyl** was significantly lower. Instead of one main peak, a broad distribution was obtained. The peak at 18.15 min. was identified as **OMe-MC-Br/Ethyl red** ( $m/z[M+H]^+ = 1039.1920$ ;  $m/z_{\text{calc.}} = 1039.212$ ;  $m/z = 0.02$ ) by SEC-ESI (*Graph 23*). Furthermore, masses of the cycle with one remaining imine bond ( $m/z[M+H]^+ = 1037.1970$ ;  $m/z_{\text{calc.}} = 1037.1964$ ;  $m/z = 0.0006$ ) as well as the cycle with five imine bonds ( $m/z[M+Na]^+ = 1051.1757$ ;  $m/z_{\text{calc.}} = 1051.1158$ ;  $m/z = 0.0599$ ) were present. The other peaks might consist of linear oligomers of high molecular mass; however, no appropriate mass could be assigned. An explanation for this, could be a low ionization efficiency due to a high molecular weight. Interestingly, **OMe-MC-Br/Ethyl** is already soluble before the reduction.



**Graph 23:** Mass spectrum of **OMe-MC-Br/Ethyl red**.

#### IV.2.3.4. Macrocycles with DAM-CF<sub>3</sub>

Applying 5-(trifluoromethyl)benzene-1,3-diamine as diamine led to macrocycles carrying a trifluoromethyl group (Figure 37). Similar to the ones with **DAM-Ethyl**, this monomer was chosen to increase the solubility of the resulting macrocycles. Furthermore, the trifluoromethyl groups allow a post-functionalization, e.g., the fluorides can be exchanged to carbons with organoaluminium reagents.<sup>[144]</sup> By sulphuric acid, the benzoic acid can be obtained *via* hydrolysis<sup>[145]</sup> and in presence of an alcohol the corresponding ester *via* alcoholysis<sup>[146]</sup>, which could be a method to integrate polyethylene glycol as molecular branches to the macrocycle. The trifluoromethyl group can undergo a catalytic benzylation and alkylation as well.<sup>[147]</sup> The obtained results were summarized in *Table 10*.



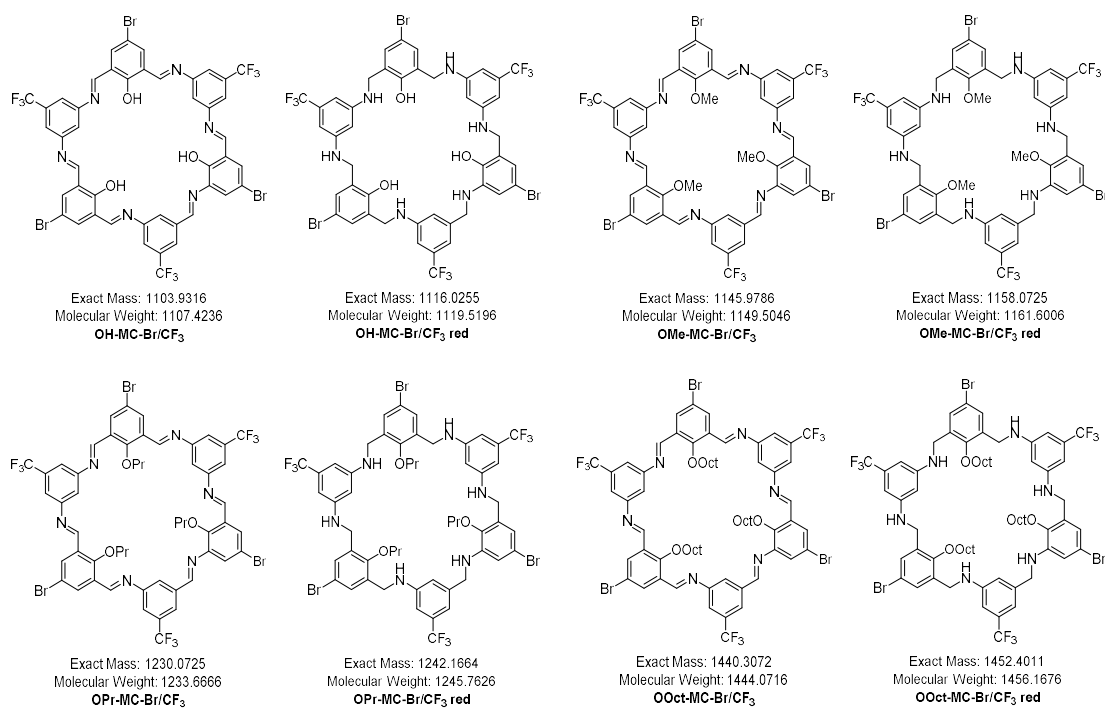


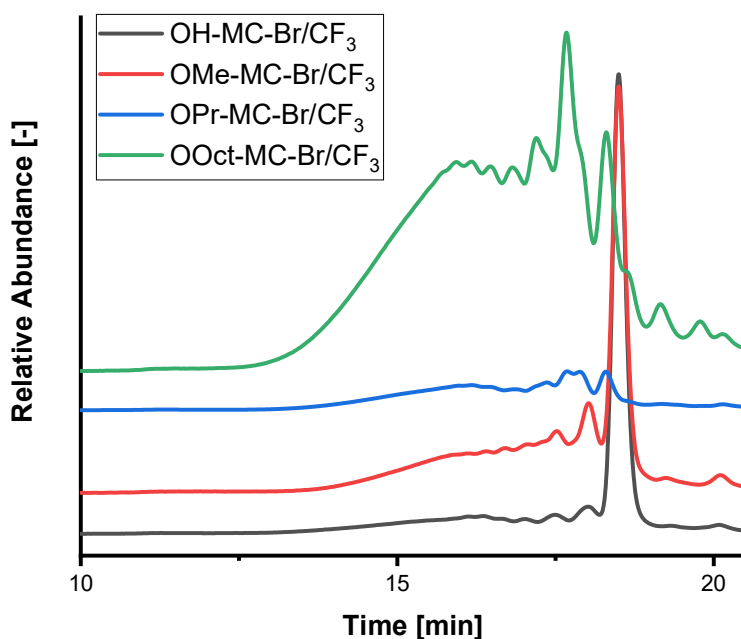
**Figure 37:** Overview of targeted macrocycles with DAM-CF<sub>3</sub> (before and after reduction).

**Table 10:** Results of the macrocyclization with DAM- CF<sub>3</sub>.

Macrocycle	Diamine	Dialdehyde	Yield Precipitate [%]	Yield after Red. [%]	Selectivity
OH-MC-Br/CF <sub>3</sub>	DAm-CF <sub>3</sub>	DAI-OH/Br	81	93	93
OH-MC-Br/CF <sub>3</sub> <sup>1)</sup>	DAI-OH/Br	DAI-OH/Br	78	73	49
OMe-MC- Br/CF <sub>3</sub> <sup>2)</sup>	DAm-CF <sub>3</sub>	DAI-OMe/Br	47	quant.	43
OPr-MC-Br/CF <sub>3</sub>	DAm-CF <sub>3</sub>	DAI-OPr/Br	21	87	-
OOct-MC-Br/CF <sub>3</sub>	DAm-CF <sub>3</sub>	DAI-OOct/Br	62	93	-

1) Without CaCl<sub>2</sub>

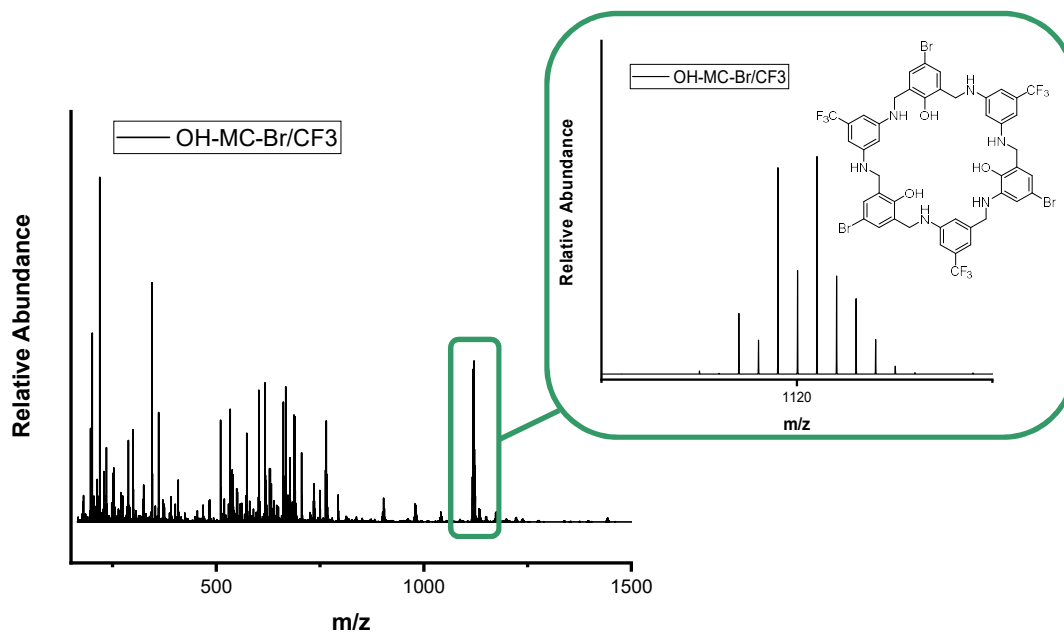
2) Extra portion of CaCl<sub>2</sub>



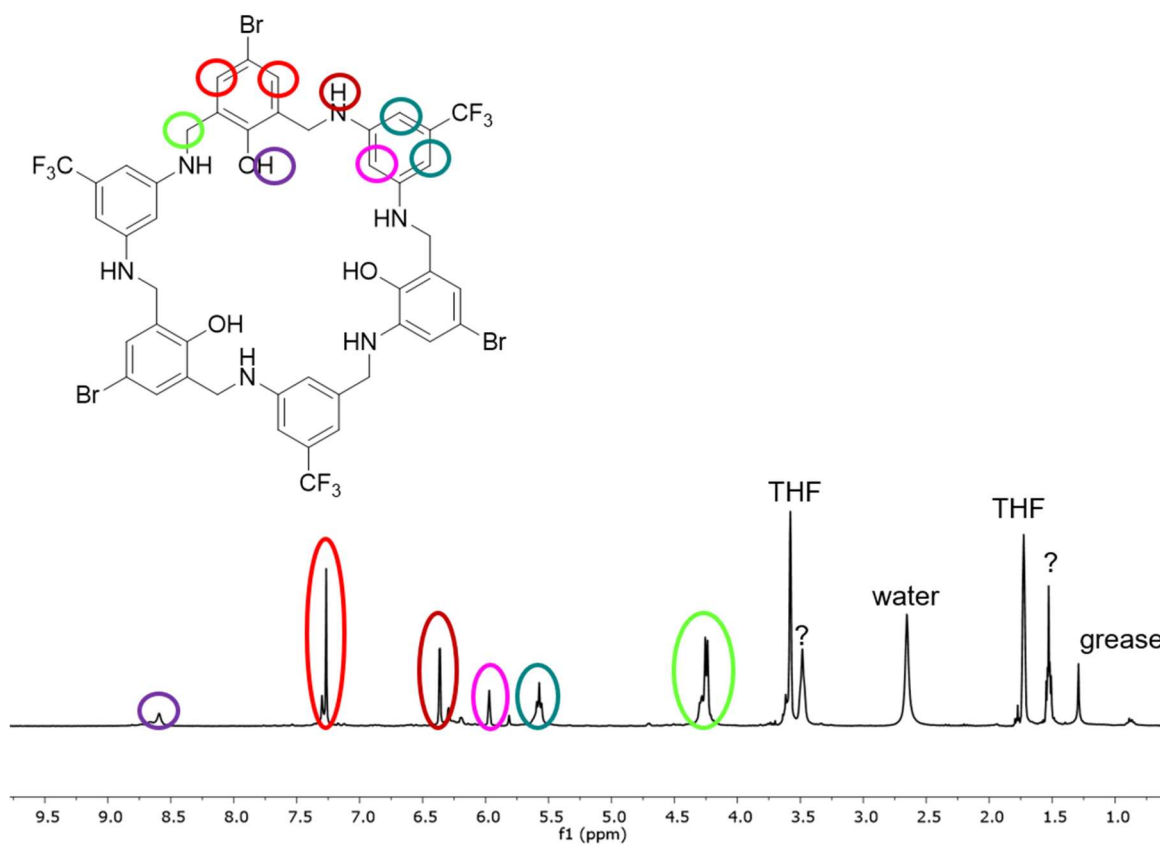
**Graph 24:** SEC traces *OH-MC-Br/CF<sub>3</sub>*, *OMe-MC-Br/CF<sub>3</sub>*, *OPr-MC-Br/CF<sub>3</sub>* and *OOct-MC-Br/CF<sub>3</sub>*.

Similar to the macrocycles with **DAm-Vinyl**, the selectivity decreases with longer alkyl chains. Nevertheless, in all cases, the reduction works efficiently and the resulting reduced macrocycles are soluble in THF and toluene.

**OH-MC-Br/CF<sub>3</sub>** was obtained in high selectivity according to the SEC chromatogram (*Graph 24*). A peak was detected at 17.88 min., which was identified by SEC-ESI as **OH-MC-Br/CF<sub>3</sub> red** ( $m/z[M+H]^+ = 1117.0319$ ;  $m/z_{calc.} = 1117.0333$ ;  $m/z = 0.0014$ ) (*Graph 25*). However, the desired cycle was not synthesized in pure manner. A small shoulder at 15.96 min. was detected; however, no adequate mass could be assigned. The selectivity is the highest compared to all other macrocycles (including the ones synthesized in the preliminary studies). Nevertheless, in <sup>1</sup>H-NMR spectroscopy impurities were present, which could not be identified (*Graph 26*). The small peaks between 6.00 and 6.50 ppm could be due to macrocycles of different reduction states; however peak at 1.53 and 3.48 ppm were not identified.



**Graph 25:** Mass spectrum of *OH-MC-Br/CF<sub>3</sub>* red.

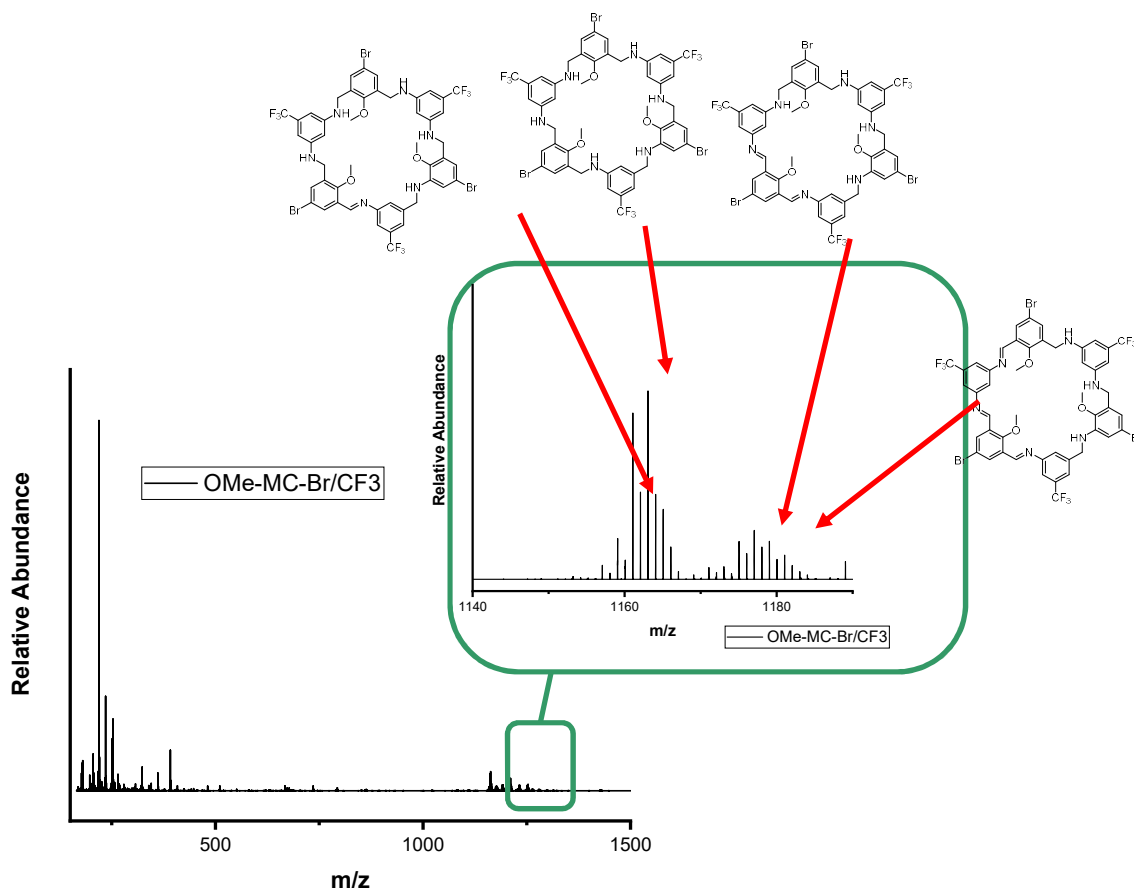


**Graph 26:** <sup>1</sup>H-NMR spectrum of crude *OH-MC-Br/CF<sub>3</sub>*.

**OMe-MC-Br/CF<sub>3</sub>** showed a significantly lower selectivity. The peak at 17.82 min. was identified as **OMe-MC-Br/CF<sub>3</sub> red** ( $m/z[M+H]^+ = 1159.0790$ ;  $m/z_{\text{calc.}} = 1159.0803$ ;  $\Delta m/z = 0.0013$ ) (*Graph 27*). Furthermore, the macrocycle with one remaining imine bond was found ( $m/z[M+H]^+ = 1157.0657$ ;  $m/z_{\text{calc.}} = 1157.0646$ ;  $\Delta m/z = 0.0011$ ) as well as with two ( $m/z[M+Na]^+ = 1177.0535$ ;  $m/z_{\text{calc.}} = 1177.031$ ;  $\Delta m/z = 0.0225$ ) and three imine bonds ( $m/z[M+Na]^+ = 1175.0577$ ;  $m/z_{\text{calc.}} = 1175.0153$ ;  $\Delta m/z = 0.0424$ ). The shoulder could consist of oligomers of larger molecular weight; however, no adequate mass could be assigned.

Although a precipitate was formed and according to SEC some selective peaks had a similar retention time as **OH-MC-Br/CF<sub>3</sub>** and **OMe-MC-Br/CF<sub>3</sub>**, no selectivity value for **OPr-MC-Br/CF<sub>3</sub>** and **OOct-MC-Br/CF<sub>3</sub>** could be given, due to the fact that no adequate mass for the macrocycle could be found in SEC-ESI.

Generally, macrocycles with hydroxyl groups showed significantly higher selectivity compared to the others. As the selectivity of hydroxyl-macrocycles is in some cases twice as high than their methoxy-counterparts, the steric effect might not be the only relevant factor. To prove this, the cyclization of **OH-MC-Br/CF<sub>3</sub>** was proceeded without the presence of CaCl<sub>2</sub> and interestingly, a cyclization occurred in high yield and selectivity compared to other macrocycles. Similar to the macrocycles described in chapter *II.2.2.3. Shape-persistent Macrocycles via Imine Condensation*, hydrogen bonds might be formed and were responsible for the increase of selectivity additionally to the template effect. In comparison, targeting **OMe-MC-Br/CF<sub>3</sub>** or **OMe-MC-Vinyl/Vinyl**, no precipitate was formed in absence of CaCl<sub>2</sub>.



**Graph 27:** Mass spectrum of **OH-MC-Br/CF<sub>3</sub>** red.

#### IV.3.4. Purification of Macrocycle

Some of the macrocycles, such as **OH-MC-Br/CF<sub>3</sub>** and **OH-MC-Br/Vinyl**, were obtained in high selectivity but impurities were present. In order to remove those, several purification methods were investigated.

TLC tests were conducted for the purification by column chromatography on normal phase silica gel, for the macrocycles **OMe-MC-Vinyl/Vinyl**, **OH-MC-Br/Vinyl** and **OH-MC-Br/CF<sub>3</sub>**. Using cyclohexane/ethyl acetate or cyclohexane/dichloromethane as eluent systems, the compounds were not eluted on the TLC, neither when 1-5% Et<sub>3</sub>N was added. Further solvent systems were investigated: cyclohexane/MeOH, cyclohexane/THF, THF/water, THF/methanol for several stationary phases, namely normal phase silica gel, reverse phase C<sub>18</sub>-silica gel and aluminium oxide. The crude product exhibited a similar behavior on all stationary phases. Depending on the amount of methanol or THF, one or two spots (depending on the batch) were eluted on the

TLC and could be isolated by flash chromatography. A third spot stayed on the baseline, even when Et<sub>3</sub>N or NH<sub>3</sub> in MeOH as modifier were applied. However, the isolated spots were not identified as the desired compounds according to <sup>1</sup>H-NMR, the macrocycle could not be recovered.

Preparative TLC was used to try to recover the compound on the baseline. The stationary phase was scratched off the TLC plate and washed with THF; however, the macrocycle could not be reobtained from the stationary phase, neither normal phase silica gel nor reverse phase C<sub>18</sub>-silica gel.

The synthesized macrocycles exhibit a similar structure including secondary amines and the presence of hydroxyl groups to the macrocycles mentioned in chapter II.2.2.3. *Shape-persistent Macrocycles via Imine Condensation*. MacLachlan and co-workers reported a degradation during flash chromatography as well, which is why the macrocycles were purified by recrystallization instead.<sup>[18]</sup> The authors also postulated that branched alkyl chains can prevent a crystallization and thus facilitate a purification. Nevertheless, recrystallization was not successful for the macrocycles described in this thesis, due to the fact that they are either well soluble in THF, CHCl<sub>3</sub> or toluene (depending on the cyclic species) or did not show any solubility in common solvents. Additionally, no precipitate was formed by precipitation in another solvent, e.g., cold methanol or diethylether.

Thus, alternative solid phases were investigated. In the next step, the purification of **OH-MC-Br/Vinyl**, **OH-MC-Br/Ethyl** and **OH-MC-Br/CF<sub>3</sub>** by flash chromatography using either a styrol-divinylbenzol-copolymer or a polyamide as stationary phase was attempted. The observations for the polymer stationary phases were similar to previous stationary phases: one large peak was observed at the beginning and broad smaller peaks in the end, when the column was purged with pure THF, which is exemplary for all conducted flash chromatography runs shown in *Figure 38*. None of the peaks was identified as the desired macrocycle by <sup>1</sup>H-NMR spectroscopy.

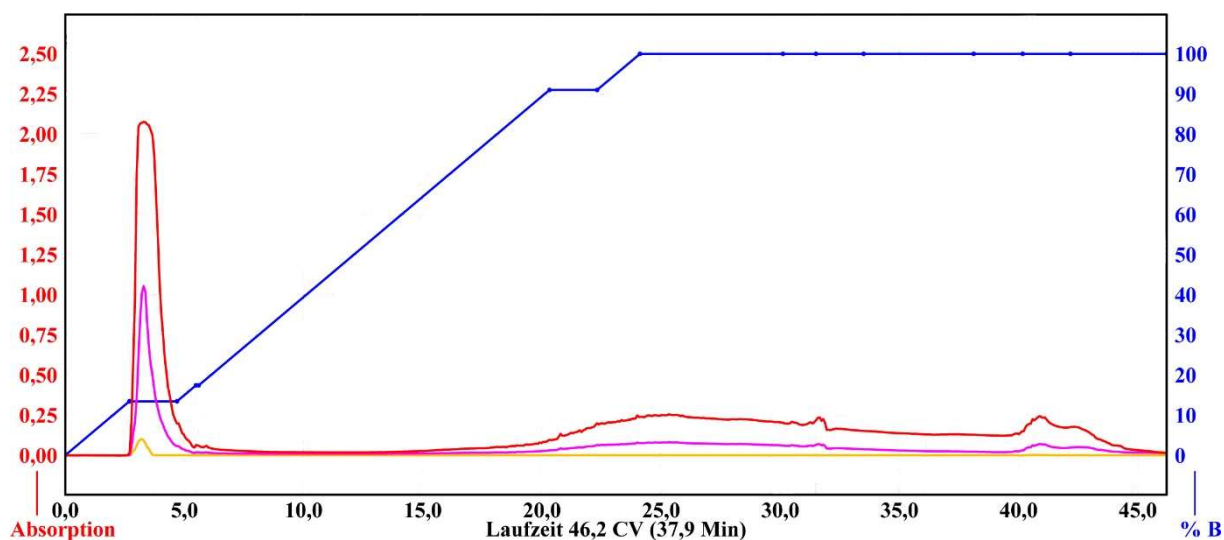


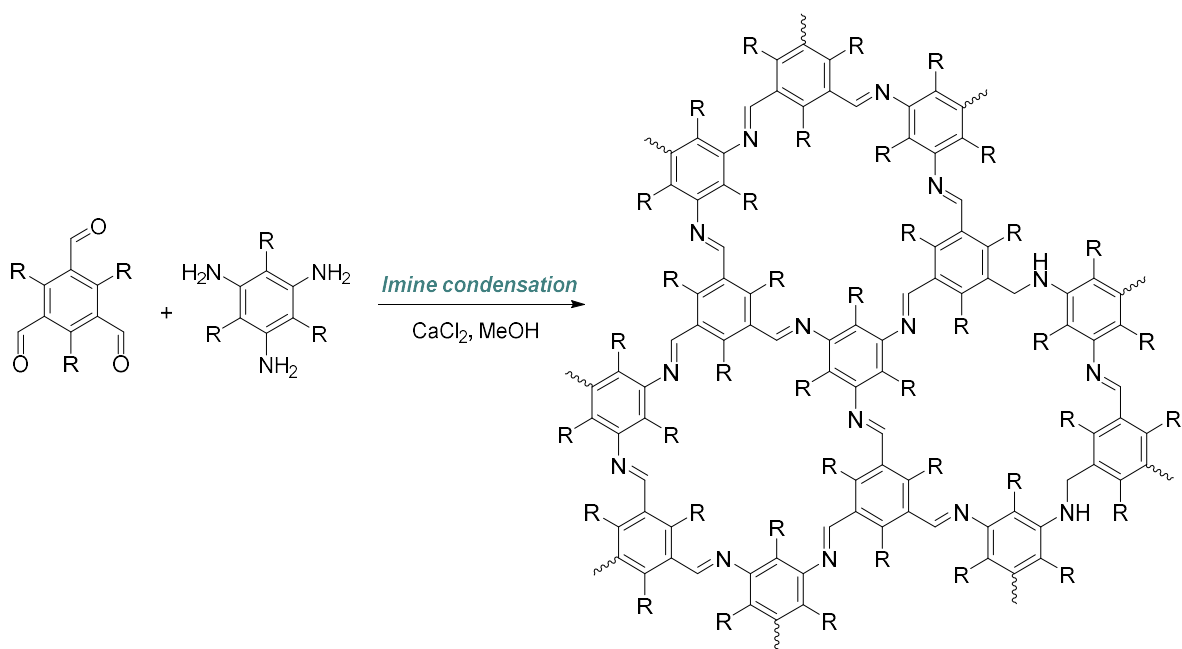
**Figure 38:** Exemplary UV spectrum of the flash-chromatography using styrol-divinylbenzol-copolymer for the purification of **OH-MC-Br/CF<sub>3</sub>**. With increasing time (black x-axes, bottom), the ratio of solvent THF (blue y-axes) was increased and the collected fractions (black numbers top) analyzed by UV absorption (red y-axes).

As the compounds either did not move at all or a degradation took place on the stationary phases during column chromatography separation, they were able to pass through the SEC instrument without degradation, we assume that a purification *via* preparative SEC should be a suitable purification method.

Höger and co-workers reported the purification of oligomers by recycling-SEC. In that system, the sample passed the same separation column several times in a row. In that way, the effective column length was extended and hence, the resolution of the SEC system was increased.<sup>[148]</sup>

#### IV.3.5. Network Formation

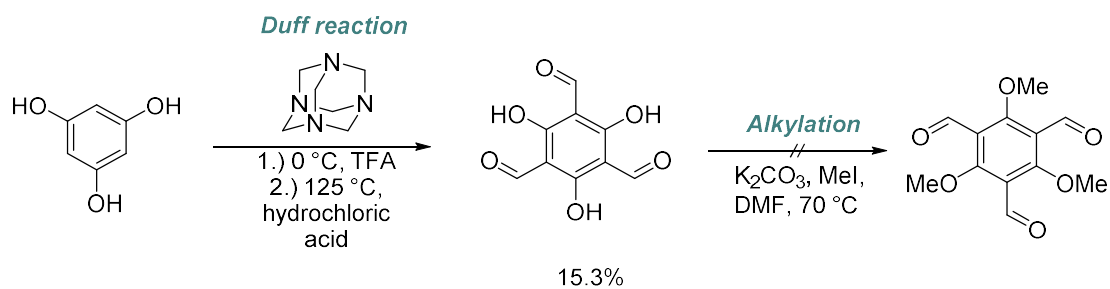
As discussed in chapter III. *Motivation and Aim of the Thesis*, the rigid macrocycles could be used as building blocks for the synthesis of 2D polymers. Alternatively to the use of macrocycles as building blocks in a two-step procedure, a direct method to obtain 2D polymers by imine condensation was investigated. By application of the template salts, trialdehydes and triamines should form macrocycles *in situ* and subsequently a 2D network (Scheme 83).



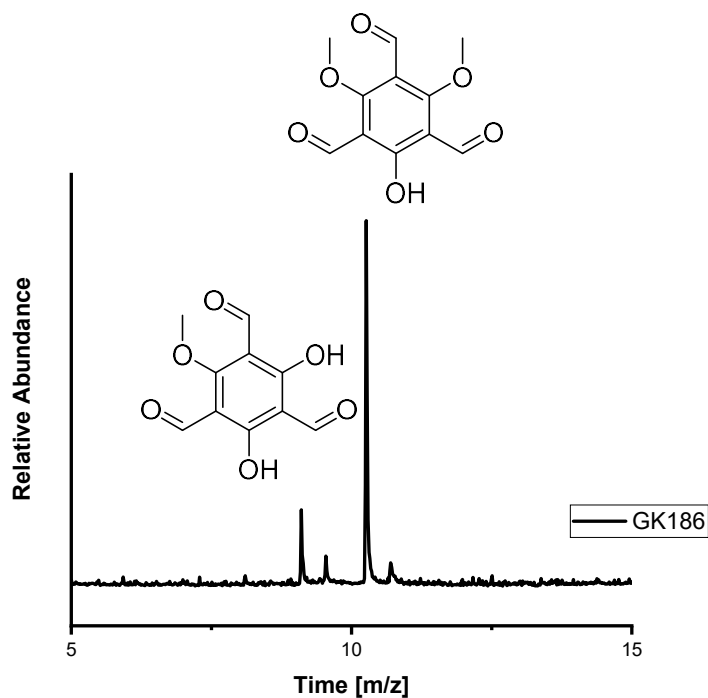
**Scheme 83:** Formation of a 2D polymer by imine condensation of a trialdehyde and a triamine.

Thus, trialdehydes and triamines were synthesized. Starting from phloroglucinol, a trifunctional aldehyde, namely of 2,4,6-trihydroxy-1,3,5-tricarbaldehyde, was obtained in low yield of 15.3% by Duff reaction (*Scheme 84*). For a subsequent alkylation, in order to improve the solubility, the same reaction conditions as for the alkylation of the dialdehyde were applied but with the triple amount of base and methyl iodide. According to GC-MS (*Graph 28*), mainly the disubstituted product was formed, which was indicated by the peak at 10.6 min. A further peak at 9.1 min., was identified as the monosubstituted product, which represents approximately 15% of the reaction mixture according to integration of GC-MS. The presence of peaks at 9.5 and 10.7 min. revealed the formation of further products which were not identified clearly; however, the fragments hinted to derivatives of 2,4,6-trihydroxy-1,3,5-tricarbaldehyde. Even the sextuple amount of base and methyl iodide did not change the ratio of the reaction mixture significantly. Neither did the application of a stronger base, namely KOH. Due to an insufficient separation of the generated products by column chromatography and due to the higher selectivity of aldehyde monomers with hydroxyl groups towards cyclization, the alkylation of the trialdehyde was not further followed, instead 2,4,6-trihydroxy-1,3,5-tricarbaldehyde was directly utilized as monomer.



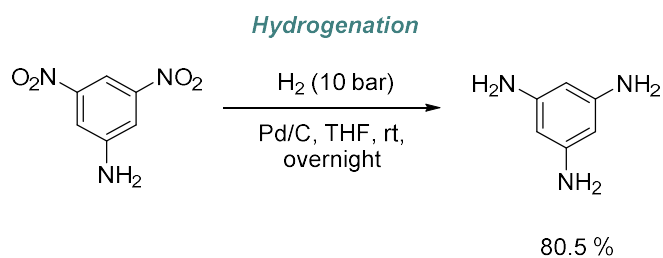


**Scheme 84:** Synthesis of a trialdehyde by Duff reaction.



**Graph 28:** GC trace measured by GC-MS of the methylation of 2,4,6-trihydroxy-1,3,5-tricarbaldehyde.

The trifunctional amine monomer was synthesized by hydrogenation of 3,5-dinitroaniline in presence of a palladium catalyst on charcoal. After a handy purification, the desired triamine was obtained giving a yield of 80.5% (*Scheme 85*).



**Scheme 85:** Synthesis of a triamine by hydrogenation.

Subsequently, those monomers were applied under the same reaction conditions as for the cyclization reactions, including the reaction of  $\text{CaCl}_2$ . The formation of a precipitate that was not even soluble after reduction was observed. It was attributed to the production of a network.

In order to increase the solubility and limit the size of the resulting network, poly(ethylene glycol) methyl ether amine ( $M_n = 500$ ) was added as chain stopper in the ratios 3, 6 and 12 eq in order to obtain “2D oligomers”, consisting in condensed macrocycle units modified with methoxyPEG chains (*Figure 39*).

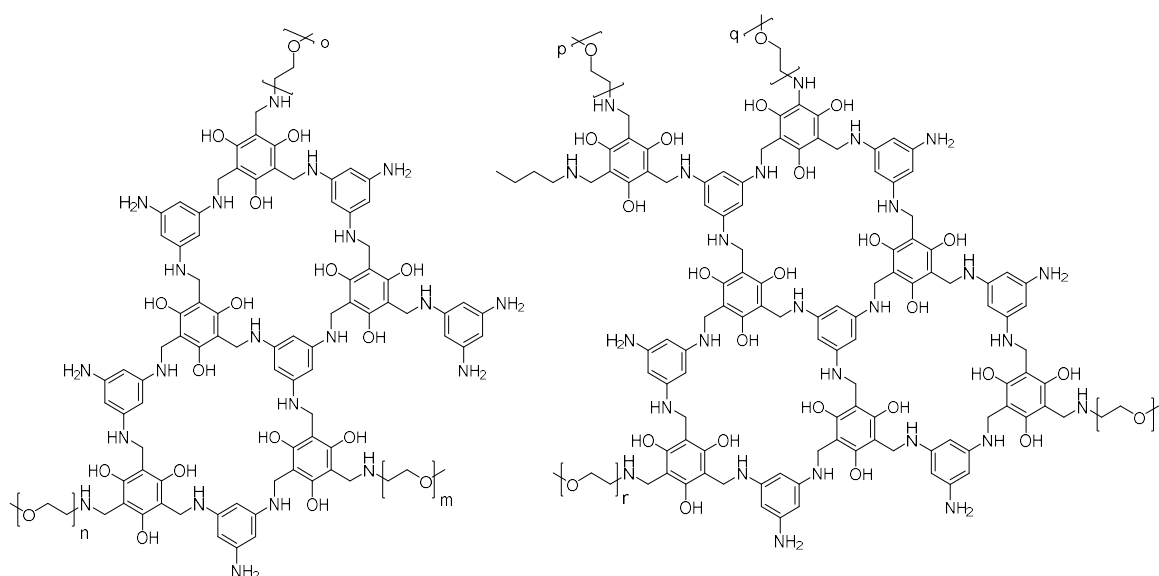
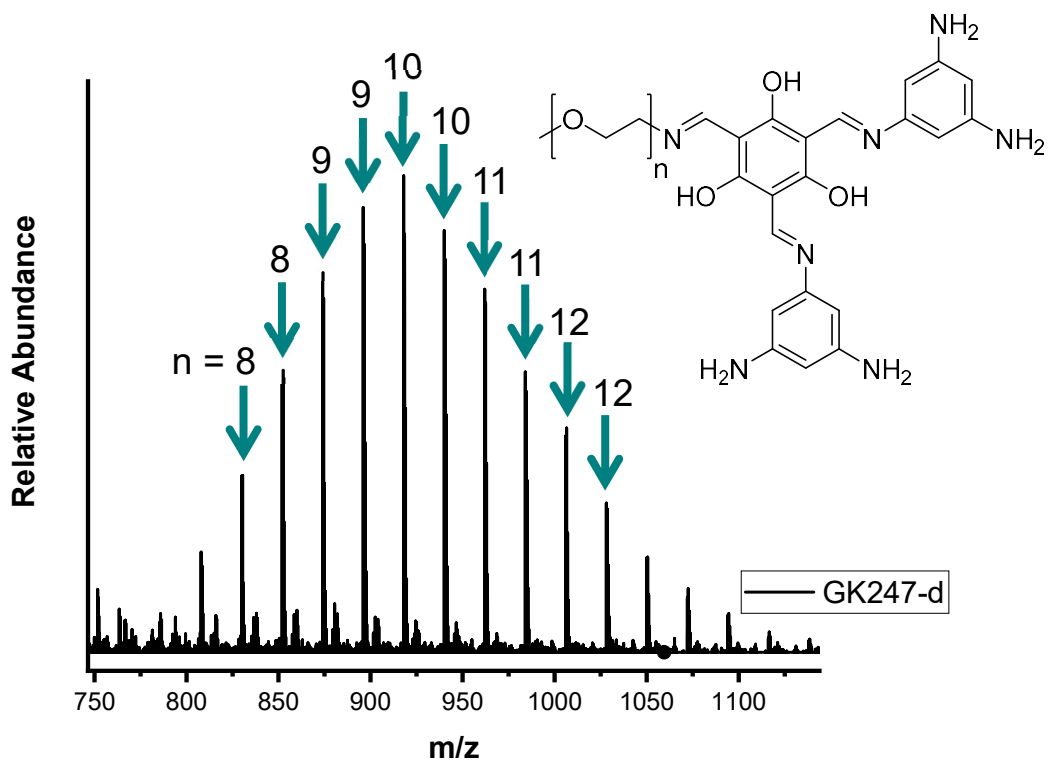


**Figure 39:** Exemplary structures of 2D oligomers consisting of condensed macrocycle units modified with methoxyPEG.

For all ratios, from the reaction mixture a powder precipitated, which was insoluble in common solvents and remained insoluble during reduction. The amount of insoluble precipitate increases with decreasing amount of poly(ethylene glycol) methyl ether amine. The filtrate of the imine condensation was characterized by SEC-ESI to determine if any 2D oligomers were generated; however, only trialdehyde substituted with the triamine and mPEG chains of different lengths were identified (*Graph 29*). The presence of any macrocyclic species could not be confirmed.



**Graph 29:** Mass spectrum of a trialdehyde monomer substituted with two triamine monomer and mPEG-amine of different length.

Although the selectivity of the cyclization of dialdehydes and diamines were carried out in high selectivity, it is likely that a random-network was formed. Due to the low solubility, the random-network would not re-arrange itself to an ordered sheet. Furthermore, due to the lack of solubility of the precipitate, no clear statement can be given about the ratio of ordered domains in the network. For future investigations, new characterization methods have to be found to analyze the planarity and the order of the resulting networks.

At this state of research, imine condensation of trialdehydes and triamine in the presence of a template salt is no adequate method to obtain two-dimensional ordered structures.

## V. Conclusion & Outlook

After successful divinyl monomer synthesis by Suzuki coupling, the formation of a six-membered rigid macrocycle by olefin metathesis was investigated. In order to increase the selectivity, the reaction parameters, such as amount and nature of the catalyst, the reaction time, the reaction temperature, the reaction concentration and the nature of the system were varied. The screening showed that a variation of the reaction parameters did only affect the conversion, but not the selectivity towards specific compounds. Although linear oligomers of different length were identified within the product mixture, the presence of the desired macrocycle could not be confirmed.

After optimization of the monomer synthesis and synthesis of new diamine and dialdehyde monomers, the formation of six-membered, rigid macrocycles by imine condensation was investigated. According to a recent literature research, these functional, six-membered macrocycles consisting of monomers with amines and aldehyde in *meta*-position have not been reported before. By integration of additional functional groups in the monomers and combination of different monomers, the synthesis of rigid and functional macrocycles was successfully optimized. The lengths of the solubilizing groups, integrated in the monomers, significantly influenced the selectivity of the macrocycles. While macrocycles with small moieties, such as hydroxyl or methoxy groups, could be obtained in moderate and high selectivity, the selectivity dropped once monomers with longer alkyl chains, such as propoxyl and octoxyl groups, were utilized. The negative effect of the long alkyl chains on the cyclization might also explain the low selectivity in the olefin metathesis approach. The effect of the application of monomers with shorter solubilizing groups on the selectivity in olefin metathesis could be investigated in future research.

While  $\text{CaCl}_2$  as template ion is necessary to form macrocycles with alkyl chains, macrocycles with hydroxyl groups can be formed in absence of a template, which could be explained by the formation of hydrogen bonds.

The synthesized macrocycles showed a low solubility in common organic solvents. The solubility could be increased by reduction to the corresponding secondary amines,

which made a characterization by  $^1\text{H-NMR}$ , SEC and SEC-ESI possible. When **DAm-H** and **DAm-Vinyl** were used as monomers, the low solubility remained an issue even after the reduction, which impeded a full characterization and a purification. The poor solubility of the imine macrocycles prevented their application as building blocks for 2D networks, in a two step procedure (first synthesis of the macrocycles, subsequently formation of 2D sheets) or in a direct approach applying trialdehydes and triamines and forming the macrocycle *in situ*. Only **OMe-MC-Br/CF<sub>3</sub>** was soluble in THF before reduction; however, the selectivity was rather low to play a role as monomers for an efficient synthesis of 2D networks.

Due to immobility or even degradation of the macrocycles on the applied stationary phases, no macrocycle could be obtained in pure manner. New purification methods, e.g., by recycling GPC have to be investigated.

## VI. Experimental Part

### VI.1 Analytics and Equipment

#### VI.1.1 Nuclear Magnetic Resonance (NMR) Spectroscopy

$^1\text{H}$ - and  $^{13}\text{C}$ -NMR spectra were recorded on Bruker AVANCE DPK spectrometers operating at 300 MHz for  $^1\text{H}$ -NMR and 75 MHz for  $^{13}\text{C}$ -NMR and on Bruker AVANCE DRX with 400 MHz for  $^1\text{H}$ -NMR and 100 MHz for  $^{13}\text{C}$ -NMR.  $^1\text{H}$ -NMR spectra were reported in parts per million (ppm) relative to the solvent signal (a quintet at 2.05 ppm for acetone, a singlet at 7.16 ppm for *d*-benzene, a quintet at 2.50 ppm for DMSO, a singlet at 7.26 ppm for  $\text{CHCl}_3$ , and a quintet at 3.31 ppm for methanol and for tetrahydrofuran singlet at 1.72 ppm and 3.58 ppm).  $^{13}\text{C}$ -NMR spectra were reported in ppm relative to the central line of the singlet for acetone at 205.87 ppm, triplet for *d*-benzene at 128.06 ppm, triplet for  $\text{CDCl}_3$  at 77.00 ppm, septet for methanol at 49.86 ppm and for tetrahydrofuran a quintet at 67.57 ppm and a quintet 25.37 ppm. All measurements were performed at room temperature. The signal patterns were abbreviated in the following way: s = singlet, d = doublet, t = triplet, q = quartet, dd = doublet of doublets, dt = doublet of triplets, ddt = doublet of doublet of triplets, dtd = doublet of triplet of doublets, m = multiplet, br = broad.

#### VI.1.2 Mass Spectrometry (MS)

The samples were measured by fast atom bombardment mass spectrometry (FAB-MS) on a FINNIGAN MAT 95 instrument. Molecular fragments were specified as mass/charge ratio ( $m/z$ ). The protonated molecular ion was abbreviated as  $[\text{M}+\text{H}]^+$ .

Gas chromatography-mass spectrometry (GC-MS) (Electron ionization) chromatograms were recorded using a Varian 431 GC instrument with a capillary column FactorFour™ VF-5 ms (30 m × 0.25 mm × 0.25 μm) and a Varian 210 ion trap mass detector. Scans were performed from 40 to 650  $m/z$  at rate of 1.0 scan  $\text{s}^{-1}$ . The oven temperature program was: initial temperature 95 °C, held for 1 min., heated up at 15 °C per min. to 200 °C, the temperature was held for 2 min., heated up at 15 °C per min. to 325 °C, the temperature was held for 5 min. The temperature of the

injector transfer line temperature was set to 250 °C. Measurements were performed in split-split mode (split ratio 50:1) using helium as the carrier gas (flow rate 1.0 mL per min.).

### **VI.1.3 Size exclusion chromatography (SEC)**

The linear and cyclic oligomers were characterized on two systems:

The first system was a Shimadzu LC-20AD system equipped with a DGU-20A3R degassing unit, SIL-20A autosampler, RID-20A refractive index detector (24 °C), CBM-20A communications bus module and a Varian Pro Star column oven Model 510, operating at 40 °C. For separation, two SDV 3 µm linear S columns (8 × 300 mm) and a guard column (8 × 50 mm) were used. Detection was done by a differential refractive index detector operating in THF (flow rate 1.0 mL per min.). For calibration linear poly(methylmethacrylate) standards (Agilent) ranging from 875 Da to 1677 kDa were used.

All runs were characterized on a Varian-SEC-LC gel permeation chromatography (SEC) system equipped with a LC-290 pump (Varian), refractive index detector (24 °C), PL AS RT SEC-autosampler (Polymer laboratories) and a Varian Pro Star column oven Model 510, operating at 40 °C. For separation, two PLgel 5 µm Mixed-d columns (8 x 300mm) and a guard column (8 x 50 mm) were used. Detection was done by a refractive index detector operating in THF (flow rate 1.0 mL per min.).

### **VI.1.4 Size Exclusion Chromatography- Electrospray Ionization (SEC-ESI)**

Spectra were recorded on a Q Exactive (Orbitrap) mass spectrometer (Thermo Fisher Scientific, San Jose, CA, USA) equipped with an HESI II probe. The instrument was calibrated in the  $m/z$  range 74-1822 using premixed calibration solutions (Thermo Scientific). A constant spray voltage of 4.6 kV, a dimensionless sheath gas of 8, and a dimensionless auxiliary gas flow rate of 2 were applied. The capillary temperature and the S-lens RF level were set to 320 °C and 62.0, respectively. The Q Exactive was coupled to a UltiMate 3000 UHPLC System (Dionex, Sunnyvale, CA, USA) consisting

of a pump (LPG 3400SD), an autosampler (WPS 3000TSL), and a thermostated column department (TCC 3000SD). Separation was performed on two mixed bed size exclusion chromatography columns (Polymer Laboratories, Mesopore 250 × 4.6 mm, particle diameter 3 μm) with precolumn (Mesopore 50 × 4.6 mm) operating at 30 °C using THF at a flow rate of 0.30 mL per min. was used as eluent. The mass spectrometer was coupled to the column in parallel to (an UV-Detector (VWD 3400 RS), and) a RI-detector (RefractoMax520, ERC, Japan) in a setup described earlier.<sup>[55]</sup> 0.27 mL per min. of the eluent were directed through the RI-detector and 30 μL per min. infused into the electrospray source after postcolumn addition of a 100 μM solution of sodium iodide in methanol at 20 μL per min. by a micro-flow HPLC syringe pump (Teledyne ISCO, Model 100DM). A 20 μL aliquot of a polymer solution with a concentration of 2 mg mL<sup>-1</sup> was injected into the HPLC system.

### VI.1.5 Solvents and Reagents

Technical grade solvents of ethyl acetate (EA), dichloromethane (DCM). EA and DCM were distilled prior to use. Anhydrous *N,N*-dimethylformamide (DMF) (Sigma Aldrich) was used as received. HPLC grade solvents of chloroform (Fisher Chemicals), DCM (Fisher Chemicals), ethanol (EtOH) (Fisher Chemicals), methanol (MeOH) (VWR), triethylamine (NEt<sub>3</sub>), THF (VWR) and toluene (99.7%, Bernd Kraft) were used. Furthermore, NEt<sub>3</sub> and THF was dried with calcium hydride (CaH<sub>2</sub>) and distilled prior to use. Water was deionized by passing through columns packed with ion exchange resins. As solvents for NMR spectroscopy following deuterated solvents were used acetone-d<sub>6</sub> (99.8%, EuroIsotop), chloroform-d (99.8%, EuroIsotop), methanol-d<sub>4</sub> (99.8%, EuroIsotop) and THF-d<sub>8</sub> (99.8%, EuroIsotop).

The following chemicals were used as received:

*p*-Benzoquinone (98%, Merck), *bis*[2-(*N,N*-dimethylamino)ethyl] ether (*O*-TMEDA) (97%, Sigma Aldrich), [1,1'-bis(diphenylphosphino) ferrocene] dichloropalladium(II) complex with dichloromethane (PdCl<sub>2</sub>(dppf)CH<sub>2</sub>Cl<sub>2</sub>) (ChemPur Feinchemikalien), (1,3-*bis*-(2,4,6-trimethylphenyl)-2-imidazolidinylidene)dichloro(*o*-isopropoxyphenylmethylene)ruthenium (Hoveyda-Grubbs catalyst of the 2<sup>nd</sup> generation, Sigma Aldrich), *bis*(triphenylphosphine) palladium(II) dichloride (PdCl<sub>2</sub>(PPh<sub>3</sub>)<sub>2</sub>) (≥99 % trace metals basis, Sigma Aldrich), *p*-bromophenol (99%,



Sigma Aldrich), 1-bromopropane (99.0%, Acros), calcium chloride (Roth, 94%), celite (pore volume 0.02-0.1 mm, Merck) cesium carbonate ( $\text{Cs}_2\text{CO}_3$ ) (fluorochem), copper(I) iodide (98%, Sigma Aldrich), 2,6-di-*tert*-butyl-4-methoxyphenol (99.8%, Acros), 3,5-dinitroaniline (97%, Sigma Aldrich), ethylene (99.95% air liquid), 1-iodo-3,5-dinitrobenzene (99%, abcr), hexamethylenetetramine (Merck), 37% hydrochloride acid (analytic grade, Fisher Chemicals), methyl iodide (VWR), octyl bromide (99%, Sigma Aldrich), palladium acetate ( $\text{Pd}(\text{OAc})_2$ ) (ChemPur), palladium on activated charcoal (Pd/C) (10% Pd base, Aldrich), Phloroglucinol (99% Sigma-Aldrich), potassium carbonate (Sigma Aldrich), potassium hydroxide (85%, Riedel de Haën), potassium vinyltrifluoroboraten (95%, Ark Pharm. Inc.), prop-1-ynylmagnesium bromide solution (0.5 M in THF, Sigma Aldrich), sodium acetate ( $\text{NaOAc}$ ) (98%, anhydrous, Riedel de Haën), sodium borohydride ( $\text{NaBH}_4$ ) (98%, abcr), sodium hydroxide ( $\text{NaOH}$ ) (98%, Bernd Kraft), sodium sulfate ( $\text{Na}_2\text{SO}_4$ ) (pure, Bernd Kraft), tetrakis (triphenylphosphine) palladium(0) ( $\text{Pd}(\text{PPh}_3)_4$ , 99%, Sigma Aldrich, tin(II)chloride ( $\text{SnCl}_2$ ) (Acros, anhydrous, 98%), trifluoroacetic acid (TFA) (Acros 99%), 1,3,5-Trimethoxybenzene (99% Acros), trimethylsilylacetylene (98%, abcr GmbH), tri(*o*-tolyl)phosphine (95%, TCI), tri-*tert*-butylphosphonium tetrafluoroborate ( $\text{tBu}_3\text{PHBF}_4$ , 99%, abcr GmbH), vinylmagnesium bromide solution (1 M in THF, Sigma Aldrich). 1,3-diiodo-2-propoxybenzene. 1,3-bromo-2-propoxybenzene by M.Sc. Gregor Klein in previous research at the groups of Prof. Dr. Barner-Kowollik and Prof. Dr. Meier).

### **VI.1.6 High-Pressure Laboratory Reactor**

Reactions with ethylene and hydrogen were carried out in a high-pressure laboratory reactor (highpreactor<sup>TM</sup>) BR-100 of the company Berghof equipped with grease-free valves and connections.

### **VI.1.7 Microwave Reactor**

Microwave assisted syntheses were performed in a CEM EXPLORER 12 HYBRID microwave reactor using dynamic program at 150 W, 100 °C for one or two hours. The reaction mixture was stirred with a magnetic stir bar at high speed in a 35 mL glass vessel sealed with a PTFE rubber band.

### **VI.1.8. Thin-layer chromatography**

All thin layer chromatography experiments were performed on silica gel coated aluminium foil (silica gel 60 F254, Merck), reverse phase silica gel coated on aluminium foil (silica gel 60 RP-18) and on neutral aluminium oxide coated aluminium foil (aluminium oxide 60 F254, neutral, Merck) and on polyamide coated aluminium foil (Polygram Polyamid-6 UV<sub>254</sub>, Macherey-Nagel). Compounds were visualized by irradiation with a UV-lamp.

### **VI.1.9. Flash Chromatography**

Flash chromatography was performed on a CombiFlash Rf+ (Teledyne ISCO). The fractions were collected via a UV detector (254 and 280 nm). Custom-filled cartridges (Puriflash, empty, interchim) of 4 and 12 g were employed for the purification in direct mode and a 4 g puriflash Atoll X (Interchim) and a 12 g puriflash C18-HP (Interchim) cartridge for the reverse mode. The analyte was dried on Celite and was transferred into an adapted pre-column prior to purification

Furthermore, flash chromatography was performed on a Interchim XS420+ flash chromatography system consisting of a SP-in-line filter 20- $\mu$ m, an UV-VIS detector (200-800 nm) and a SofTA Model 400 ELSD (55 °C drift tube temperature, 25 °C spray chamber temperature, filter 5, EDR gain mode) connected *via* a flow splitter (Interchim Split ELSD F04590). The separations were performed using a Interchim dry load column (liquid injection) and a Interchim Puriflash Silica HP 30  $\mu$ m column and Interchim Puriflash Silica HP 15  $\mu$ m column).

Besides, flash chromatography was performed on a Revelris PREP purification system equipped with a 4 g Flash Pure EcoFlex Amino 50  $\mu$ m spherical column was used. Elution solvents were cyclohexane and tetrahydrofuran with a gradient such as: 2<sup>nd</sup> solvent percentage starts at 0% and directly goes to 7% for 0.8 min. then 7 % for 5.1 min., 15% for 1.6 min. and finally 100% for 5.4 min.

## VI.2. Reaction Procedures

### VI.2.1. Reaction Procedures for the Olefin Metathesis Approach

#### VI.2.1.1. Monomer Synthesis for the Olefin Metathesis Approach

*a) General Procedure for Kumada coupling of Diiodo- as well as Dibromopropoxybenzene with vinylmagnesium bromide*

A two-neck round-bottom flask equipped with a reflux condenser was dried in an oven or heated by a heat gun and flushed with argon three times. In the reverse flow of argon, the aryl halide (1.00 eq.) and the respective amount of catalyst were added. As catalyst either Pd(PPh<sub>3</sub>Cl<sub>2</sub>) or a complex made of Pd<sub>2</sub>(dba)<sub>3</sub> tBu<sub>3</sub>PHBF<sub>4</sub> (4.00 eq. per equivalent catalyst) were used. O-TMEDA (same equivalent as Grignard reagent) and the respective amount of vinylmagnesium bromide (1 M solution in THF) were with a syringe through the septum. The reaction mixture was refluxed for the respectively time period. The reaction was observed by GC-MS.

The reaction was quenched by adding 1 M HCl. THF was removed from the reaction mixture *in vacuo*. The residue was mixed with water. The aqueous phase was extracted with DCM several times until the aqueous phase did not change its color anymore. The combined organic phase was dried over MgSO<sub>4</sub> and the solvent was removed *in vacuo* giving a crude product, which was further analyzed.

*b) General Procedure for Heck reaction of Diiodo- as well as Dibromopropoxybenzene with ethylene*

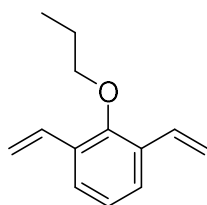
The aryl halide (1.00 eq.) was given into an autoclave together with the respective amount of Pd(OAc)<sub>2</sub> and P(otol)<sub>3</sub> (4.00 eq. per equivalent catalyst) and 1.10 eq. NaOAc in DMF (c = 0.1 mol L<sup>-1</sup>). The reactor was closed and flushed with ethylene to remove any air. Afterwards, an ethylene atmosphere of 10 bar was established. The reaction was heated up to 90 °C and stirred for the respective time.

*c) General Procedure for Suzuki coupling of Diiodo- as well as Dibromopropoxybenzene with potassium vinyltrifluoride*

To a microwave vessel equipped with a magnetic stirrer the desired halogen aryl (1.00 eq.), the respective amount of potassium vinyltrifluoride, [1,1'-

Bis(diphenylphosphino)ferrocene]dichloropalladium(II) complex with dichloromethane (0.08 eq.), cesium carbonate (3.50 eq.) as well as a mixture of the organic solvent (THF or DMF) and water (9:1) were added. The reaction was carried out in a microwave at 100 °C for the respective time in order to achieve complete conversion (controlled by GC-MS). To the reaction mixture water and hydrochloride acid were added and extracted three times with ethyl acetate. The combined organic phase was dried over sodium sulfate and the solvent removed *in vacuo*. The raw product was purified by cc with cyclohexane and ethyl acetate (20:1) as eluent in order to obtain the desired product.

### 2-propoxy-1,3-divinylbenzene



**<sup>1</sup>H-NMR (CDCl<sub>3</sub>, 300 MHz):**  $\delta$  = 1.07 (t,  $J$  = 7.40 Hz, 3H, -CH<sub>3</sub>), 1.75 – 1.90 (m, 2H, -CH<sub>2</sub>-, 2), 3.73 (t,  $J$  = 6.7 Hz, 2H, -OCH<sub>2</sub>-, 3), 5.30 (dd,  $J$  = 11.1, 1.3 Hz; 2H, HC=CHC<sub>Ar</sub>), 5.74 (dt,  $J$  = 16.6, 4.2 Hz; 2H, HC=CHC<sub>Ar</sub>), 6.95-7.12 (m, 3H, HC=CHC<sub>Ar</sub> & HC<sub>Ar</sub>), 7.44 (t,  $J$  = 8.1 Hz, 2H HC<sub>A</sub>) ppm; **<sup>13</sup>C-NMR (CDCl<sub>3</sub>, 75 MHz):**  $\delta$  = 10.71 (-CH<sub>3</sub>), 23.54 (-CH<sub>2</sub>-), 76.32 (-OCH<sub>2</sub>-), 115.01 (HC=CHC<sub>Ar</sub>), 124.20 (C<sub>Ar</sub>H-), 125.82 (C<sub>Ar</sub>H), 131.77 (=HC-), 154.50 (-C<sub>Ar</sub>O-) ppm; **HRMS (FAB):** C<sub>13</sub>H<sub>16</sub>O [M]<sup>+</sup>  $m/z$ : calcd. 188.1197 found 188.1196.

**Yield:** 67%. The product was obtained as a **yellow liquid**.

#### VI.2.1.2. Cyclization by Olefin Metathesis

##### a) Closed System

A three-neck round-bottom flask was equipped with a magnetic stirrer and closed with septa and *via* a needle a balloon was attached. The glassware was dried with a heat-gun and purged with argon three times. Through the septum, the respective volume of dry toluene was added and the solvent degassed with Ar. In argon reverse flow, 2-propoxy-1,3-divinylbenzene (1.00 eq) and the respective catalytic species in the adequate amount was added. The reaction was stirred at the respective temperature

for the respective time. The conversion was observed by proton NMR spectroscopy, SEC and SEC-ESI.

### b) Open System

To a round-bottom flask, equipped with a magnetic stirrer and a condenser, 2-propoxy-1,3-divinylbenzene (1.00 eq), the respective volume of toluene and the respective catalytic species in the adequate amount were added. The reaction was stirred at the respective temperature for the respective time. The conversion was observed by proton NMR spectroscopy, SEC and SEC-ESI.

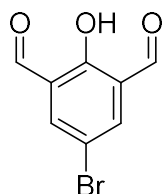
## VI.2.2. Reaction Procedures for the Imine Condensation Approach

### VI.2.2.1. Monomer Synthesis for the Imine Condensation Approach

#### a) Synthesis of 5-bromo-2-hydroxyisophthalaldehyde by Duff reaction

Bromophenol (1.00 eq.) was given into a round-bottom flask equipped with condenser and stirring bar together with hexamethylenetetramine (8.00 eq.) and in a solution with trifluoroacetic acid ( $C_{\text{Bromophenol}} = 0.34 \text{ mol L}^{-1}$ ). Under continuous stirring, the reaction mixture was heated up to 110 °C. After 48 hours the reaction mixture was cooled down to room temperature. The same volume of 4 M hydrochloric acid compared to the volume of trifluoroacetic acid (TFA) was added to the reaction mixture which was stirred for further 5 hours. The resulting solid was filtered off, washed six times with water and dissolved in DCM. The solvent was removed *in vacuo* and the desired product was obtained.

#### 5-bromo-2-hydroxyisophthalaldehyde



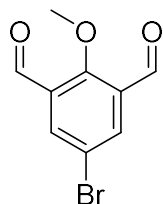
**$^1\text{H-NMR}$  ( $\text{CDCl}_3$ , 300 MHz):**  $\delta = 8.06$  (s, 2H,  $\text{HC}_{\text{Ar}}$ ), 10.19 (s, 2H,  $-(\text{CO})\text{H}$ ), 11.54 (s, 1H,  $-\text{OH}$ ) ppm;  **$^{13}\text{C-NMR}$  ( $\text{CDCl}_3$ , 75 MHz):**  $\delta = 112.28$  ( $-\text{C}_{\text{Ar}}\text{Br}$ ), 124.72 ( $-\text{C}_{\text{Ar}}-$ ), 139.90 ( $-\text{C}_{\text{Ar}}\text{H}-$ ), 162.39 ( $-\text{C}_{\text{Ar}}\text{O}-$ ), 190.97 ( $\text{C}=\text{O}$ ) ppm; **HRMS (FAB):**  $\text{C}_8\text{H}_5\text{BrO}_3$   $[\text{M}]^+$  m/z: calcd. 228.9495 found 228.9493.

**Yield:** 57% The product was obtained as a **yellow crystals**.

b) *General Procedure for the Alkylation of 5-bromo-2-hydroxyisophthalaldehyde via Williamson Ether Synthesis*

5-bromo-2-hydroxyisophthalaldehyde (1.00 eq.) was given into a round-bottom flask equipped with condenser and stirring bar and suspended with potassium carbonate (1.25 eq.) in DMF ( $c = 0.098 \text{ mol L}^{-1}$ ). After that, the corresponding halogene alky (1.25 eq.) was added and heated up to  $70 \text{ }^\circ\text{C}$  for 6 hours. For introduction of a methyl group, methyl iodide was used; for a propyl group, propyl bromide and for an octyl group, octyl bromide was added. After cooling down to room temperature, the reaction mixture was taken in brine and extracted with ethyl acetate for three times. The combined organic phases were washed with brine three times and dried over sodium sulfate. The solvent was removed *in vacuo* and the desired product was obtained.

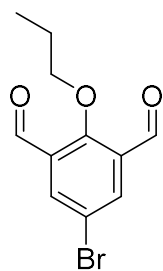
**5-bromo-2-methoxyisophthalaldehyde**



**$^1\text{H-NMR}$  ( $\text{CDCl}_3$ , 300 MHz):**  $\delta = 10.35$  (s, 2H,  $-(\text{CO})\text{H}$ ), 8.20 (s, 2H,  $\text{CH}_{\text{Ar}}$ ), 4.09 (s, 1H,  $-\text{OCH}_3$ ) ppm;  **$^{13}\text{C-NMR}$  ( $\text{CDCl}_3$ , 75 MHz):**  $\delta = 67.12$  ( $-\text{OCH}_2$ ), 118.73 ( $-\text{C}_{\text{Ar}}\text{Br}$ ), 131.71 ( $-\text{C}_{\text{Ar}}$ ), 137.69 ( $-\text{C}_{\text{Ar}}\text{H}$ ), 164.22 ( $-\text{C}_{\text{Ar}}\text{O}$ ), 187.17 ( $\text{C}=\text{O}$ ) ppm; **HRMS (FAB):**  $\text{C}_9\text{H}_7\text{BrO}_3$   $[\text{M}]^+$   $m/z$ : calcd. 241.9573 found 241.9572.

**Yield:** 70%. The product was obtained as **yellow crystals**.

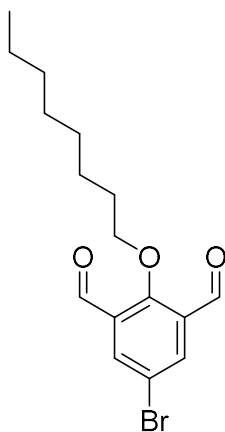
**5-bromo-2-propoxyisophthalaldehyde**



**$^1\text{H-NMR}$  ( $\text{CDCl}_3$ , 300 MHz):**  $\delta = 10.34$  (s, 2H,  $-(\text{CO})\text{H}$ ), 8.19 (s, 2H,  $\text{CH}_{\text{Ar}}$ ), 4.08 (td,  $J = 6.6, 2.5 \text{ Hz}$ , 2H,  $-\text{OCH}_2-$ ), 1.82 – 2.02 (m, 2H,  $-\text{CH}_2-$ ), 1.04 – 1.15 (m, 3H,  $-\text{CH}_3$ ) ppm;  **$^{13}\text{C-NMR}$  ( $\text{CDCl}_3$ , 75 MHz):**  $\delta = 10.29$  ( $-\text{CH}_3$ ), 23.21 ( $-\text{CH}_2-$ ), 82.38 ( $-\text{OCH}_2-$ ), 118.33 ( $-\text{C}_{\text{Ar}}\text{Br}$ ), 131.74 ( $-\text{C}_{\text{Ar}}$ ), 137.26 ( $-\text{C}_{\text{Ar}}\text{H}$ ), 163.37 ( $-\text{C}_{\text{Ar}}\text{O}$ ), 187.15 ( $\text{C}=\text{O}$ ) ppm; **HRMS (FAB):**  $\text{C}_{11}\text{H}_{11}\text{BrO}_3$   $[\text{M}]^+$   $m/z$ : calcd. 269.9886 found 269.9888.

**Yield:** 61%. The product was obtained as **slightly yellow crystals**.

## 5-bromo-2-(octyloxy)isophthalaldehyde



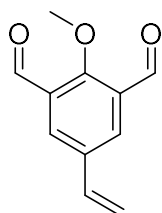
**<sup>1</sup>H-NMR (CDCl<sub>3</sub>, 300 MHz):**  $\delta$  = 10.28 (s, 2H, -(CO)H), 8.11 (s, 2H, CH<sub>Ar</sub>), 4.02 – 4.16 (m, 2H, -OCH<sub>2</sub>-), 1.78 – 1.94 (m, 2H, -OCH<sub>2</sub>CH<sub>2</sub>-), 1.13 – 1.53 (m, 10H, -(CH<sub>2</sub>)<sub>5</sub>-), 0.78 – 0.92 (m, 3H, -CH<sub>3</sub>) ppm; **<sup>13</sup>C-NMR (CDCl<sub>3</sub>, 75 MHz):**  $\delta$  = 14.16 (-CH<sub>3</sub>), 22.70 (-CH<sub>2</sub>-), 25.89 (-CH<sub>2</sub>-), 29.23 (-CH<sub>2</sub>-), 29.38 (-CH<sub>2</sub>-), 29.98 (-CH<sub>2</sub>-), 31.81 (-OCH<sub>2</sub>CH<sub>2</sub>-), 81.18 (-OCH<sub>2</sub>-), 118.38 (-C<sub>Ar</sub>Br), 131.82 (-C<sub>Ar</sub>-), 137.28 (-C<sub>Ar</sub>H-), 163.51 (-C<sub>Ar</sub>O-), 187.25 (C=O) ppm; **HRMS (FAB):** C<sub>16</sub>H<sub>21</sub>BrO<sub>3</sub> [M+H]<sup>+</sup> *m/z*: calcd. 341.0747 found 341.0748.

**Yield:** 31%. The product was obtained as **beige solid**.

### c) General Procedure for the Integration of Double Bond via Suzuki coupling

The adequate compound (1.00 eq.) was given into a microwave vial together with a stirring bar and potassium vinyltrifluoroborate (5.00 eq.), cesium carbonate (3.00 eq.), [1,1'-Bis(diphenylphosphino)ferrocene]dichloropalladium(II) complex with dichloromethane (0.05 eq.) and *p*-benzoquinone (0.05 eq.). As solvent, a mixture of THF/water (9:1) was added with a concentration of 0.048 mmol mL<sup>-1</sup>. After 1 hours for the dialdehydes and after 2 hours for the iodonitrobenzol at 100 °C, the reaction mixture was taken in water and extracted with diethyl ether for five times. The combined organic phases were washed with diluted hydrochloric acid, brine and dried over sodium sulfate. The solvent was removed *in vacuo*. The raw material was purified by column chromatography (cyclohexane:ethyl acetate = 4:1) in order to obtain the desired product.

## 2-methoxy-5-vinylisophthalaldehyde

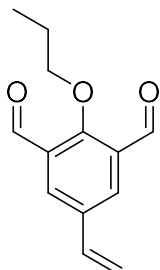


**<sup>1</sup>H-NMR (CDCl<sub>3</sub>, 300 MHz):**  $\delta$  = 10.40 (t, J = 10.7 Hz, 2H, -(CO)H), 8.16 (d, J = 20.5, 2H, CH<sub>Ar</sub>), 6.79 (dd, J = 17.6, 10.9 Hz, 1H, C<sub>Ar</sub>CHCH<sub>2</sub>), 5.86 (d, J = 17.6, 1H, C<sub>Ar</sub>CHCH<sub>2</sub>), 5.41 (d, J = 10.8, 1H, C<sub>Ar</sub>CHCH<sub>2</sub>), 4.09 (s, 3H, -OCH<sub>3</sub>) ppm; **<sup>13</sup>C-NMR (CDCl<sub>3</sub>, 75 MHz):**  $\delta$  = 66.63 (-OCH<sub>3</sub>), 116.79 (-CH=CH<sub>2</sub>), 130.13 (-C(=O)C<sub>Ar</sub>), 132.35 (-C<sub>Ar</sub>H-), 134.23 (-CH=CH<sub>2</sub>), 134.78 (C<sub>Ar</sub>),

164.81 (-C<sub>Ar</sub>O-) 188.51 (C=O), ppm; **HRMS (FAB):** C<sub>11</sub>H<sub>10</sub>O<sub>3</sub> [M]<sup>+</sup>  
*m/z*: calcd. 190.0624 found 190.0624.

**Yield:** 73%. The product was obtained as **white solid**.

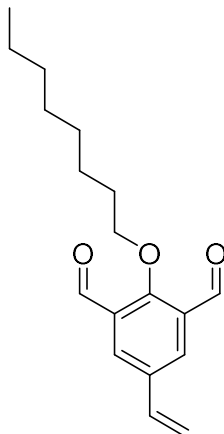
### 2-propoxy-5-vinylisophthalaldehyde



**<sup>1</sup>H-NMR (CDCl<sub>3</sub>, 300 MHz):** δ = 10.42 (s, 2H, -(CO)H), 8.12 (s, 2H, CH<sub>Ar</sub>), 6.73 (dd, J = 17.6, 10.9 Hz, 1H, C<sub>Ar</sub>CHCH<sub>2</sub>), 5.85 (d, J = 17.6, 1H, C<sub>Ar</sub>CHCH<sub>2</sub>), 5.46-5.31 (m, 1H, C<sub>Ar</sub>CHCH<sub>2</sub>), 4.09 (t, J = 6.6 Hz, 2H, -OCH<sub>2</sub>-), 2.03-1.85 (m, 2H, -CH<sub>2</sub>-), 1.10 (t, J = 7.4 Hz, 3H, -CH<sub>3</sub>) ppm; **<sup>13</sup>C-NMR (CDCl<sub>3</sub>, 75 MHz):** δ = 10.43 (-CH<sub>3</sub>), 23.33 (-CH<sub>2</sub>-), 82.19 (-OCH<sub>2</sub>-), 116.59 (-CH=CH<sub>2</sub>), 130.26 (C(=O)C<sub>Ar</sub>), 132.03 (-C<sub>Ar</sub>H-), 134.26 (CH=CH<sub>2</sub>), 134.47 (C<sub>Ar</sub>), 164.12 (-C<sub>Ar</sub>O-), 188.64 (C=O) ppm; **HRMS (FAB):** C<sub>13</sub>H<sub>14</sub>O<sub>3</sub> [M]<sup>+</sup>  
*m/z*: calcd. 218.0937 found 218.0939.

**Yield:** 72%. The product was obtained as **yellow solid**.

### 2-(octyloxy)-5-vinylisophthalaldehyde

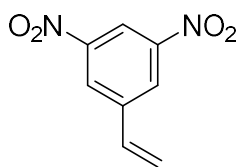


**<sup>1</sup>H-NMR (CDCl<sub>3</sub>, 300 MHz):** δ = 10.39 (s, 2H, -(CO)H), 8.10 (s, 2H, CH<sub>Ar</sub>), 6.71 (ddd, J = 15.9, 10.9, 5.0 Hz, 1H, C<sub>Ar</sub>CHCH<sub>2</sub>), 5.83 (dd, J = 17.6, 5.0 Hz, 1H, C<sub>Ar</sub>CHCH<sub>2</sub>), 5.38 (dd, J = 10.9, 5.0 Hz, 1H, C<sub>Ar</sub>CHCH<sub>2</sub>), 4.14 – 4.06 (m, 2H, -OCH<sub>2</sub>-), 1.95 – 1.81 (m, 2H, -OCH<sub>2</sub>CH<sub>2</sub>-), 1.36 (dt, J = 20.5, 9.2 Hz, 10H, -CH<sub>2</sub>-), 0.90 (t, J = 12.9 Hz, 3H, -CH<sub>3</sub>) ppm; **<sup>13</sup>C-NMR (CDCl<sub>3</sub>, 75 MHz):** δ = 14.18 (-CH<sub>3</sub>), 22.73 (-CH<sub>2</sub>-), 25.97 (-CH<sub>2</sub>-), 29.27 (-CH<sub>2</sub>-), 29.44 (-CH<sub>2</sub>-), 30.05 (-OCH<sub>2</sub>CH<sub>2</sub>-), 31.85 (-CH<sub>2</sub>-), 80.90 (-OCH<sub>2</sub>-), 116.60 (-CH=CH<sub>2</sub>), 130.31 (C(=O)C<sub>Ar</sub>), 132.07 (-C<sub>Ar</sub>H-), 134.31 (CH=CH<sub>2</sub>), 134.50 (C<sub>Ar</sub>), 164.20 (-C<sub>Ar</sub>O-), 188.67 (C=O) ppm; **HRMS (FAB):** C<sub>18</sub>H<sub>24</sub>O<sub>3</sub> [M]<sup>+</sup>  
*m/z*: calcd. 288.1725 found 288.1719.

**Yield:** 61%. The product was obtained as **yellow solid**.



### 1,3-dinitro-5-vinylbenzene



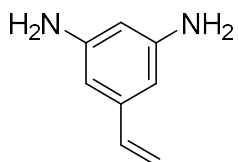
**<sup>1</sup>H-NMR (CDCl<sub>3</sub>, 300 MHz):** δ = 5.67 (d, J = 10.9 Hz, 1H, -CH=CH<sub>2</sub>), 6.08 (d, J = 17.5, 1H, -CH=CH<sub>2</sub>), 6.85 (dd, J = 17.5; 10.9 Hz, 1H, -CH=CH<sub>2</sub>), 8.56 (d, J = 2.0 Hz, 1H), 8.93 (t, J = 2.0 Hz, 1H, CH<sub>Ar</sub>) ppm; **<sup>13</sup>C-NMR (CDCl<sub>3</sub>, 75 MHz):** δ = 117.58 (-C<sub>Ar</sub>H), 120.51 (-CH=CH<sub>2</sub>), 126.03 (-C<sub>Ar</sub>H), 133.15 (CH=CH<sub>2</sub>), 141.37 (C<sub>Ar</sub>CH=), 149.00 (C<sub>Ar</sub>NO<sub>2</sub>) ppm; **HRMS (GC-MS)** C<sub>8</sub>H<sub>6</sub>N<sub>2</sub>O<sub>4</sub> [-H]<sup>+</sup> m/z: calcd. 194.0328 found 193.6653.

**Yield:** 85%. The product was obtained as **beige solid**.

#### d) Synthesis of 1,3-dinitro-5-vinylbenzene by Reduction

Ethanol (c = 0.092 mol L<sup>-1</sup>) was given into a round-bottom flask equipped with a stirring bar and a condenser closed with septum. The solvent was degassed with Argon for 10 min. In Ar counter-stream, 1,3-dinitro-5-vinylbenzene and SnCl<sub>2</sub> were given in. The reaction mixture was stirred at 95 °C for 4 hours. Afterwards, the full conversion was checked by <sup>1</sup>H-NMR spectroscopy, and if necessary, further SnCl<sub>2</sub> was added and the reaction time expanded. Once full conversion was reached, the reaction mixture was concentrated by removing the solvent *in vacuo*. The residue was taken up in water. KOH was added to make the aqueous phase basic. Subsequently, the aqueous phase was extracted with diethyl ether for three times and the combined organic phases were washed once with water. After drying the organic phase over sodium sulphate and removing the solvent *in vacuo* the desired compound was obtained. The product was stored under Ar and in the fridge.

### 1,3-dinitro-5-vinylbenzene



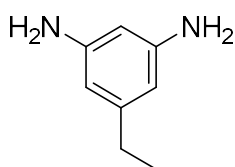
**<sup>1</sup>H-NMR (MeOD, 300 MHz):** δ = 4.69 (s, 4H, -NH<sub>2</sub>), 5.03 (dd, J = 10.8, 1H, 1.2 Hz, -CH=CH<sub>2</sub>), 5.49 (dd, J = 17.6, 1H, -CH=CH<sub>2</sub>), 5.77 (t, J = 1.9 Hz, 1H, -CH<sub>Ar</sub>), 5.91 (t, J = 4.9 Hz, 2H, -CH<sub>Ar</sub>), 6.40 (dd, J = 17.6, 10.8 Hz, 1H, -CH=CH<sub>2</sub>) ppm; **<sup>13</sup>C-NMR (MeOD, 75 MHz):** δ = 100.20 (-C<sub>Ar</sub>H), 101.59 (-C<sub>Ar</sub>H), 111.60 (-CH=CH<sub>2</sub>), 137.76 (CH=CH<sub>2</sub>), 137.90 (C<sub>Ar</sub>CH=CH<sub>2</sub>), 148.73 (C<sub>Ar</sub>NH<sub>2</sub>) ppm; **HRMS (GC-MS):** C<sub>8</sub>H<sub>10</sub>N<sub>2</sub> [-H]<sup>+</sup> m/z: calcd. 134.1 found 134.1.

**Yield:** 90%. The product was obtained as **red highly viscous liquid**.

*d) Synthesis of 5-ethylbenzene-1,3-diamine by Hydrogenation*

Iodonitrobenzol (1.00 eq) was given into a vessel, equipped with a stirring bar, together with 10 mg palladium on activated charcoal (10% Pd basis) per 0.1 mmol starting material and toluene ( $c = 0.05 \text{ mol L}^{-1}$ ). The vessel was given into a high-pressure laboratory reactor and an ethylene pressure of 45 bar was applied. The reaction was stirred for 4 hour at room temperature. The progress of the conversion was checked by GC-MS. The color of the reaction mixture also gave a hint on the conversion. When the starting material was still present, the reaction mixture had a green color. A colorless reaction mixture indicated a full conversion. Afterwards, the turbid reaction mixture was filtered-off and washed with toluene for several times. The solvent was removed *in vacuo* and the desired product was obtained, which had to be stored under Argon in the fridge to prevent a degradation.

**5-ethylbenzene-1,3-diamine**



**<sup>1</sup>H-NMR (d-Benzene, 300 MHz)**  $\delta = 1.18$  (t,  $J = 7.6$  Hz, 3H, -CH<sub>3</sub>), 2.44 (q,  $J = 7.6$  Hz, 2H, -CH<sub>2</sub>-), 2.94 (s, 4H, -NH<sub>2</sub>), 5.48 (s, 1H, -C<sub>Ar</sub>H), 5.81 (s, 2H, -C<sub>Ar</sub>H) ppm; **<sup>13</sup>C-NMR (d-Benzene, 75 MHz)**  $\delta = 15.94$  (-CH<sub>3</sub>), 29.48 (-CH<sub>2</sub>-), 99.81 (-C<sub>Ar</sub>H), 105.61 (-C<sub>Ar</sub>H), 146.23 (-C<sub>Ar</sub>Ethyl), 148.21 (C<sub>Ar</sub>NO<sub>2</sub>) ppm; **HRMS (GC-MS)** C<sub>8</sub>H<sub>12</sub>N<sub>2</sub> [-H]<sup>+</sup>  $m/z$ : calcd. 135.1 found 135.2.

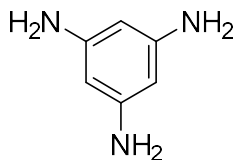
**Yield:** 92%. The product was obtained as **red highly-viscous liquid**.

*e) Synthesis of Benzene-1,3,5-triamine by Hydrogenation*

3,5-Dinitroaniline was given into a vessel, equipped with a stirring bar, together with THF ( $c_{\text{starting material}} = 0.27 \text{ mol L}^{-1}$ ) and presence of Pd/C (0.015 g per 2.7 mmol starting material). The vessel was given into high-pressure laboratory reactor and a hydrogen pressure of 10 bar was applied. The reaction mixture was stirred over night at room temperature. Subsequently, the reaction mixture was filtered in order to remove the

catalyst. The filtrate was concentrated to dryness by evaporation under reduced pressure giving the desired product as black powder.

### benzene-1,3,5-triamine



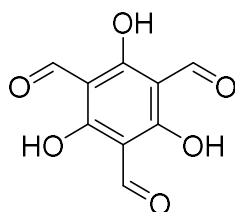
**<sup>1</sup>H-NMR (DMSO, 300 MHz):**  $\delta$  = 4.32 (s, 6H, -NH<sub>2</sub>), 5.14 (s, 3H, CH<sub>Ar</sub>) ppm; **<sup>13</sup>C-NMR (DMSO, 75 MHz):**  $\delta$  = 90.81 (C<sub>Ar</sub>H), 149.34 (C<sub>Ar</sub>NH<sub>2</sub>) ppm; **HRMS (FAB) C<sub>5</sub>H<sub>9</sub>N<sub>3</sub> [M<sup>+</sup>]** m/z: calcd. 123.0796 found 123.0790.

**Yield:** 81%. The product was obtained as **black solid**.

### f) Synthesis of 2,4,6-Trihydroxy-1,3,5-tricarbaldehyde by Duff reaction

A three-neck round-bottom flask was equipped with a magnetic stirrer, a condenser and a dropping funnel. The system was closed with three septa and *via* a needle a balloon was attached. The glassware was dried out with a heat-gun and purged with Ar three times. In Ar counter-flow, Phloroglucinol (1.00 eq.) and hexamethylenetetramine (3.00 eq.) were added. The reaction mixture was cooled down to 0 °C with an ice bath and TFA (C<sub>phloroglucinol</sub> = 0.55 mol L<sup>-1</sup>) was added dropwise over a time period of 30 min. Subsequently, the reaction mixture was heated up to 125 °C and stirred for 4 hours. After the reaction mixture was cooled down to room temperature, 3M hydrochloric acid (3.1 mL per 1 mmol phloroglucinol) was added and the reaction mixture was stirred at 100 °C for one hour. After cooling down to room temperature, the generated precipitate was filtered-off and the filtrate was extracted with DCM five times. The combined organic phases were washed with water two times, dried over sodium sulphate. After removal of the solvent *in vacuo*, the desired product was obtained.

### 2,4,6-Trihydroxybenzene-1,3,5-tricarbaldehyde



**<sup>1</sup>H-NMR (CDCl<sub>3</sub>, 300 MHz):**  $\delta$  = 10.13 (s, 3H, C(O)H), 14.12 (s, 3H, OH) ppm; **<sup>13</sup>C-NMR (CDCl<sub>3</sub>, 75 MHz):**  $\delta$  = 103.04 (-C<sub>Ar</sub>-), 173.74 (C<sub>Ar</sub>OH), 192.22 (C=O) ppm; **HRMS (FAB): C<sub>6</sub>H<sub>6</sub>O<sub>6</sub> [M<sup>+</sup>]** m/z: calcd. 210.1410 found 210.0158.

**Yield:** 15%. The product was obtained as **orange solid**.

### VI.2.2.2. Synthesis of Macrocycles

#### a) Macrocyclization by Imine Condensation

A three-neck round-bottom flask was equipped with a stirring bar and a condenser. The system was closed with three septa and *via* a needle a balloon was attached. Methanol ( $C_{\text{Dialdehyde}} = 0.006 \text{ mol/L}$ ) was added to the flask and the system closed. The solvent was degassed with Argon for 10 min. In Ar reverse flow, the dialdehyde (1.00 eq.), the diamine (1.00 eq.) and  $\text{CaCl}_2$  (1.00 eq.) were added. The reaction was heated up to  $80 \text{ }^\circ\text{C}$  and stirred continuously for the respective time. The formed precipitate was filtered off by centrifugation and decanting off the overlaying solution. By this procedure, the precipitate was washed with methanol until the wash solution was colorless, but at least three times, and dried at high vacuum.

#### b) Reduction

The precipitate was suspended in a mixture of methanol/THF (1:1) ( $C_{\text{precipitate}} = 0.079 \text{ mol L}^{-1}$ ) and  $\text{NaBH}_4$  (20.0 eq.) was added. The reaction mixture was stirred at room temperature for at least 4 hours at which further  $\text{NaBH}_4$  was added after 2 hours. If all precipitate became soluble and the reaction suspension turned into a clear solution, the reaction was quenched by the addition of water. Otherwise, the reaction time was expended and further  $\text{NaBH}_4$  was added. If the reaction mixture did not change its appearance overnight, the reaction was quenched anyway. Subsequently, the reaction mixture was extracted with chloroform three times. The combined organic phases were washed with water one time, dried over sodium sulphate and the solvent was removed *in vacuo*. The residue was characterized by  $^1\text{H-NMR}$  spectroscopy, SEC and SEC-ESI.

## VII. Appendix

### VII.1. List of Abbreviations

ADMAC	acyclic diene metathesis macrocyclization
ADMET	acyclic diene metathesis polymerization
AFM	atomic force microscopy
AEM	arylene-ethynylene macrocycles
ATRP	atom transfer radical polymerization
AVM	arylenevinylene macrocycles
Boc	<i>tert</i> -butyloxycarbonyl
BET	Brunauer-Emmett-Teller
BHT	3,5-di- <i>tert</i> -butyl-4-hydroxytoluene
DCM	dichloromethane
DMF	<i>N,N</i> -dimethylformamide
CCP	conjugated porous polymers
CM	cross metathesis
COF	covalent organic framework
CP	conjugated polymers
CPDMS	(3-cyanopropyl)dimethylsilyl
CVD	chemical vapor deposition
DAA	1,8-diazaanthracene
DCC	dynamic combinatorial chemistry
DCvC	dynamic covalent chemistry

DFT	density functional theory
DIBAL	diisobutylaluminium hydride
DIC	diisopropylcarboimide
DNT	2,4-dinitrotoluene
DPTS	<i>p</i> -toluenesulfonate
EDTA	ethylenediaminetetraacetic acid
FAB	fast atom bombardment
FT-IR	Fourier-transform infrared spectroscopy
GC-MS	GC-MS
GNR	graphene nanoribbons
HHTP	2,3,6,7,10,11-hexahydrotriphenylene
LDA	Lithium diisopropylamide
MALDI	matrix-assisted laser desorption/ionization
MIMs	mechanically interlocked molecules
MS	mass spectrometry
NMR	nuclear magnetic resonance
O-TMEDA	bis[2-( <i>N,N</i> -dimethylamino)ethyl] ether
ODOC	orthogonal dynamic covalent chemistry
PBBA	1,4-phenylenebis(boronic acid)
PCP	porous coordination polymer
PDA	terephthalaldehyde
RCM	ring-closing metathesis
RDX	1,3,5-trinitroperhydro-1,3,5-triazine

RMOP	ring-opening metathesis polymerization
ROCM	ring-opening cross-metathesis
TAPB	1,3,5-tris(4-aminophenyl)benzene
TBAF	<i>tetra-n</i> -butylammonium fluoride
TCB	trichlorobenzene
TEM	transmission electron microscopy
TERS	tip-enhanced raman spectroscopy
TFA	trifluoroacetic acid
TGA	thermogravimetric analysis
THF	tetrahydrofuran
TIPS	triisopropylsilyl ether
TMEDA	N,N,N',N'-tetramethylethylenediamine
TMS	trimethylsilylacetylene
TNT	1,3,5-trinitrotoluene
TOF	time of flight
SEC	size exclusion chromatography
SEC-ESI	size exclusion chromatography-electrospray ionization
SEM	scanning electron microscopy
SHOP	shell higher olefins process
UV/Vis	ultraviolet-visible spectroscopy
XRD	x-ray diffraction

## VII.2. List of References

- [1] S. Hger, *J. Polym. Sci. A Polym. Chem.* **1999**, *37*, 2685.
- [2] S. Höger, *Chemistry (Weinheim an der Bergstrasse, Germany)* **2004**, *10*, 1320.
- [3] M. Iyoda, J. Yamakawa, M. J. Rahman, *Angewandte Chemie (International ed. in English)* **2011**, *50*, 10522.
- [4] T. Naddo, Y. Che, W. Zhang, K. Balakrishnan, X. Yang, M. Yen, J. Zhao, J. S. Moore, L. Zang, *J. Am. Chem. Soc.* **2007**, *129*, 6978.
- [5] D. Venkataraman, S. Lee, J. Zhang, J. S. Moore, *Nature* **1994**, *371*, 591.
- [6] R. May, S.-S. Jester, S. Höger, *J. Am. Chem. Soc.* **2014**, *136*, 16732.
- [7] C. Schweez, P. Shushkov, S. Grimme, S. Höger, *Angew. Chem.* **2016**, *128*, 3389.
- [8] Y. Du, H. Yang, S. Wan, Y. Jin, W. Zhang, *J. Mater. Chem. A* **2017**, *5*, 9163.
- [9] X. Hu, C. Yu, K. D Okochi, Y. Jin, Z. Liu, W. Zhang, *Chem. Commun.* **2016**, *52*, 5848.
- [10] W. Zhang, Y. Jin (Eds.) *Dynamic covalent chemistry. Principles, reactions, and applications*, John Wiley & Sons, Inc, Hoboken, NJ, **2018**.
- [11] O. Š. Miljanić, K. P. Vollhardt, G. D. Whitener, *Synlett* **2003**, 29.
- [12] W. Zhang, S. M. Brombosz, J. L. Mendoza, J. S. Moore, *J. Org. Chem.* **2005**, *70*, 10198.
- [13] J. Heppekausen, R. Stade, R. Goddard, A. Fürstner, *J. Am. Chem. Soc.* **2010**, *132*, 11045.
- [14] H. Yang, Z. Liu, W. Zhang, *Adv. Synth. Catal.* **2013**, *355*, 885.
- [15] D. E. Gross, J. S. Moore, *Macromolecules* **2011**, *44*, 3685.
- [16] Y. Jin, A. Zhang, Y. Huang, W. Zhang, *Chemical communications (Cambridge, England)* **2010**, *46*, 8258.
- [17] S. Akine, T. Taniguchi, T. Nabeshima, *Tetrahedron Letters* **2001**, *42*, 8861.
- [18] A. J. Gallant, J. K.-H. Hui, F. E. Zahariev, Y. A. Wang, M. J. MacLachlan, *J. Org. Chem.* **2005**, *70*, 7936.
- [19] K. D. Okochi, Y. Jin, W. Zhang, *Chemical communications (Cambridge, England)* **2013**, *49*, 4418.
- [20] J. Gregoliński, K. Ślepokura, T. Paćkowski, J. Panek, P. Stefanowicz, J. Lisowski, *The Journal of organic chemistry* **2016**, *81*, 5285.
- [21] Y. Jin, C. Yu, R. J. Denman, W. Zhang, *Chemical Society reviews* **2013**, *42*, 6634.
- [22] S. J. Rowan, S. J. Cantrill, G. R. L. Cousins, J. K. M. Sanders, J. F. Stoddart, *Angewandte Chemie (International ed. in English)* **2002**, *41*, 898.
- [23] P. T. Corbett, J. Leclaire, L. Vial, K. R. West, J.-L. Wietor, J. K. M. Sanders, S. Otto, *Chemical reviews* **2006**, *106*, 3652.
- [24] M. E. Belowich, J. F. Stoddart, *Chemical Society reviews* **2012**, *41*, 2003.
- [25] Y. Jin, Q. Wang, P. Taynton, W. Zhang, *Accounts of chemical research* **2014**, *47*, 1575.
- [26] P. Vongvilai, M. Angelin, R. Larsson, O. Ramström, *Angewandte Chemie (International ed. in English)* **2007**, *46*, 948.
- [27] Á. Martínez-Castañeda, H. Rodríguez-Solla, C. Concellón, V. del Amo, *J. Org. Chem.* **2012**, *77*, 10375.



- [28] a) P. Reutenauer, P. J. Boul, J.-M. Lehn, *Eur. J. Org. Chem.* **2009**, 2009, 1691; b) B. Masci, S. Pasquale, P. Thuéry, *Organic letters* **2008**, 10, 4835.
- [29] C. D. Gutsche, D. E. Johnston, D. R. Stewart, *J. Org. Chem.* **1999**, 64, 3747.
- [30] M. Holler, N. Allenbach, J. Sonet, J.-F. Nierengarten, *Chem. Commun.* **2012**, 48, 2576.
- [31] P. Vongvilai, O. Ramström, *J. Am. Chem. Soc.* **2009**, 131, 14419.
- [32] N. Wilhelms, S. Kulchat, J.-M. Lehn, *Helv. Chim. Acta* **2012**, 95, 2635.
- [33] G. C. Vougioukalakis, R. H. Grubbs, *Chem. Rev.* **2010**, 110, 1746.
- [34] J. W. Kamplain, C. W. Bielawski, *Chem. Commun.* **2006**, 1727.
- [35] B. Buchs née Levrard, G. Godin, A. Trachsel, J.-Y. de Saint Laumer, J.-M. Lehn, A. Herrmann, *Eur. J. Org. Chem.* **2011**, 2011, 681.
- [36] J. M. Hoerter, K. M. Otte, S. H. Gellman, Q. Cui, S. S. Stahl, *J. Am. Chem. Soc.* **2008**, 130, 647.
- [37] J. A. Berrocal, R. Cacciapaglia, S. Di Stefano, *Organic & biomolecular chemistry* **2011**, 9, 8190.
- [38] N. Kihara, K. Kidoba, *Organic letters* **2009**, 11, 1313.
- [39] L. You, J. S. Berman, E. V. Anslyn, *Nature Chem* **2011**, 3, 943.
- [40] H. Otsuka, K. Aotani, Y. Higaki, Y. Amamoto, A. Takahara, *Macromolecules* **2007**, 40, 1429.
- [41] M. Sakulsombat, Y. Zhang, O. Ramström, *Chemistry (Weinheim an der Bergstrasse, Germany)* **2012**, 18, 6129.
- [42] L. R. Sutton, W. A. Donaubauer, F. Hampel, A. Hirsch, *Chem. Commun.* **2004**, 1758.
- [43] G. Joshi, E. V. Anslyn, *Organic letters* **2012**, 14, 4714.
- [44] R. Nishiyabu, Y. Kubo, T. D. James, J. S. Fossey, *Chem. Commun.* **2011**, 47, 1124.
- [45] N. Ponnuswamy, F. B. L. Cougnon, J. M. Clough, G. D. Pantoş, J. K. M. Sanders, *Science* **2012**, 338, 783.
- [46] B. Rasmussen, A. Sørensen, H. Gotfredsen, M. Pittelkow, *Chem. Commun.* **2014**, 50, 3716.
- [47] C. Janiak, *Moderne anorganische Chemie*, De Gruyter, Berlin, **2012**.
- [48] A. Fürstner, *Angewandte Chemie (International ed. in English)* **2013**, 52, 2794.
- [49] W. Zhang, S. Kraft, J. S. Moore, *J. Am. Chem. Soc.* **2004**, 126, 329.
- [50] A. Mortreux, O. Coutelier, *Journal of Molecular Catalysis A: Chemical* **2006**, 254, 96.
- [51] A. Fürstner, P. W. Davies, *Chemical communications (Cambridge, England)* **2005**, 2307.
- [52] R. H. Grubbs (Ed.) *Handbook of metathesis. Volume 3: Polymer Synthesis*, Wiley-VCH, Weinheim, **2015**.
- [53] D. Astruc, *ChemInform* **2005**, 36, 42.
- [54] G. C. Vougioukalakis, R. H. Grubbs, *Chem. Rev.* **2010**, 110, 1746.
- [55] K. Gregor, Karlsruhe Institut für Technologie, Karlsruhe, **2015**.
- [56] R. H. Grubbs, A. G. Wenzel, D. J. O'Leary, E. Khosravi (Eds.) *Handbook of metathesis. Volume 1: Catalyst Development and Mechanism*, Wiley-VCH, Weinheim, Germany, **2015**.
- [57] J. A. Love, J. P. Morgan, T. M. Trnka, R. H. Grubbs, *Angew. Chem. Int. Ed. Engl.* **2002**, 41, 4035.
- [58] J. S. Kingsbury, J. P. A. Harrity, P. J. Bonitatebus, A. H. Hoveyda, *J. Am. Chem. Soc.* **1999**, 121, 791.
- [59] W. Liu, P. J. Nichols, N. Smith, *Tetrahedron Letters* **2009**, 50, 6103.
- [60] Y. Chauvin, *Angew. Chem. Int. Ed. Engl.* **2006**, 45, 3740.

- [61] H.-J. Arpe, K. Weissermel (Eds.) *Industrielle organische Chemie. Bedeutende Vor- und Zwischenprodukte*, Wiley-VCH, Weinheim, **2007**.
- [62] K. P. C. Vollhardt, H. Butenschön, B. Elvers, N. E. Schore (Eds.) *Organische Chemie*, Wiley-VCH, Weinheim, **2009**.
- [63] N. Giuseppone, J.-L. Schmitt, E. Schwartz, J.-M. Lehn, *J. Am. Chem. Soc.* **2005**, *127*, 5528.
- [64] P. Taynton, C. Zhu, S. Loob, R. Shoemaker, J. Pritchard, Y. Jin, W. Zhang, *Polym. Chem.* **2016**, *7*, 7052.
- [65] J. F. Stoddart, *Angew. Chem. Int. Ed. Engl.* **2017**, *56*, 11094.
- [66] P. T. Glink, A. I. Oliva, J. F. Stoddart, A. J. P. White, D. J. Williams, *Angew. Chem. Int. Ed. Engl.* **2001**, *40*, 1870.
- [67] P. C. Haussmann, J. F. Stoddart, *Chemical record (New York, N.Y.)* **2009**, *9*, 136.
- [68] A. D. Finke, D. E. Gross, A. Han, J. S. Moore, *J. Am. Chem. Soc.* **2011**, *133*, 14063.
- [69] W. Zhang, J. S. Moore, *Angewandte Chemie (International ed. in English)* **2006**, *45*, 4416.
- [70] H. A. Staab, F. Binnig, *Chem. Ber.* **1967**, *100*, 293.
- [71] T. Nishinaga, Y. Miyata, N. Nodera, K. Komatsu, *Tetrahedron* **2004**, *60*, 3375.
- [72] H. A. Staab, K. NEUNHOEFFER, *Synthesis* **1974**, *1974*, 424.
- [73] M. J. MacLachlan, *Pure and Applied Chemistry* **2006**, *78*, 873.
- [74] J. S. Moore, J. Zhang, *Angew. Chem. Int. Ed. Engl.* **1992**, *31*, 922.
- [75] S. Höger, V. Enkelmann, *Angew. Chem. Int. Ed. Engl.* **1996**, *34*, 2713.
- [76] S. Höger, *Macromol. Symp.* **1999**, *142*, 185.
- [77] S. K. Yang, H. C. Ahn, S.-J. Jeon, I. Asselberghs, K. Clays, A. Persoons, B. R. Cho, *Chemical Physics Letters* **2005**, *403*, 68.
- [78] H. L. Anderson, J. K. M. Sanders, *Angew. Chem. Int. Ed. Engl.* **1990**, *29*, 1400.
- [79] J. Zhang, D. J. Pesak, J. L. Ludwick, J. S. Moore, *J. Am. Chem. Soc.* **1994**, *116*, 4227.
- [80] W. Zhang, J. S. Moore, *Adv. Synth. Catal.* **2007**, *349*, 93.
- [81] S. Otto, R. L. E. Furlan, J. K. M. Sanders, *J. Am. Chem. Soc.* **2000**, *122*, 12063.
- [82] D. Zhao, J. S. Moore, *J. Org. Chem.* **2002**, *67*, 3548.
- [83] W. Zhang, J. S. Moore, *J. Am. Chem. Soc.* **2004**, *126*, 12796.
- [84] P.-H. Ge, W. Fu, W. A. Herrmann, E. Herdtweck, C. Campana, R. D. Adams, U. H. F. Bunz, *Angew. Chem. Int. Ed. Engl.* **2000**, *39*, 3607.
- [85] F. Xu, L. Peng, K. Shinohara, T. Morita, S. Yoshida, T. Hosoya, A. Orita, J. Otera, *J. Org. Chem.* **2014**, *79*, 11592.
- [86] T. Balandina, K. Tahara, N. Sändig, M. O. Blunt, J. Adisojoso, S. Lei, F. Zerbetto, Y. Tobe, S. de Feyter, *ACS nano* **2012**, *6*, 8381.
- [87] *Org. Synth.* **2007**, *84*, 177.
- [88] S. W. Sisco, J. S. Moore, *J. Am. Chem. Soc.* **2012**, *134*, 9114.
- [89] A. K. Chatterjee, T.-L. Choi, D. P. Sanders, R. H. Grubbs, *J. Am. Chem. Soc.* **2003**, *125*, 11360.
- [90] C. Zhang, C. Yu, H. Long, R. J. Denman, Y. Jin, W. Zhang, *Chemistry (Weinheim an der Bergstrasse, Germany)* **2015**, *21*, 16935.
- [91] S. E. Wheeler, *J. Am. Chem. Soc.* **2011**, *133*, 10262.
- [92] D. Gopalakrishnan, W. R. Dichtel, *J. Am. Chem. Soc.* **2013**, *135*, 8357.

- [93] B. J. Smith, A. C. Overholts, N. Hwang, W. R. Dichtel, *Chem. Commun.*, **52**, 3690.
- [94] K. E. Shopsowitz, D. Edwards, A. J. Gallant, M. J. MacLachlan, *Tetrahedron* **2009**, *65*, 8113.
- [95] M. K. Smith, N. E. Powers-Riggs, B. H. Northrop, *Chem. Commun.* **2013**, *49*, 6167.
- [96] C. S. Hartley, J. S. Moore, *Journal of the American Chemical Society* **2007**, *129*, 11682.
- [97] S. Akine, Z. Varadi, T. Nabeshima, *Eur. J. Inorg. Chem.* **2013**, *2013*, 5987.
- [98] A. González-Alvarez, I. Alfonso, V. Gotor, *Chem. Commun.* **2006**, 2224.
- [99] J. Lisowski, *Inorganic chemistry* **2011**, *50*, 5567.
- [100] C. J. Walter, H. L. Anderson, J. K. M. Sanders, *J. Chem. Soc., Chem. Commun.* **1993**, *27*, 458.
- [101] L. G. Mackay, R. S. Wylie, J. K. M. Sanders, *J. Am. Chem. Soc.* **1994**, *116*, 3141.
- [102] H. G. Börner, S. Höger, S. Rosselli, S. S. Sheiko, *Polymer* **2015**, *72*, 422.
- [103] S. A. Pendergraph, G. Klein, M. K. G. Johansson, A. Carlmark, *RSC Adv.* **2014**, *4*, 20737.
- [104] J. Sakamoto, J. van Heijst, O. Lukin, A. D. Schlüter, *Angew. Chem. Int. Ed. Engl.* **2009**, *48*, 1030.
- [105] M. Sano, D. Y. Sasaki, T. Kunitake, *Science* **1992**, *258*, 441.
- [106] a) J. F. Dienstmaier, A. M. Gigler, A. J. Goetz, P. Knochel, T. Bein, A. Lyapin, S. Reichlmaier, W. M. Heckl, M. Lackinger, *ACS nano* **2011**, *5*, 9737; b) L. Grill, M. Dyer, L. Lafferentz, M. Persson, M. V. Peters, S. Hecht, *Nature Nanotech* **2007**, *2*, 687; c) S. I. Stupp, S. Son, H. C. Lin, L. S. Li, *Science* **1993**, *259*, 59; d) N. A. A. Zwaneveld, R. Pawlak, M. Abel, D. Catalin, D. Gimes, D. Bertin, L. Porte, *J. Am. Chem. Soc.* **2008**, *130*, 6678.
- [107] J. C. Meyer, A. K. Geim, M. I. Katsnelson, K. S. Novoselov, T. J. Booth, S. Roth, *Nature* **2007**, *446*, 60.
- [108] J. W. Colson, W. R. Dichtel, *Nature Chem* **2013**, *5*, 453.
- [109] A. D. Schlüter, P. Payamyar, H. C. Öttinger, *Macromol. Rapid Commun.* **2016**, *37*, 1638.
- [110] P. Payamyar, B. T. King, H. C. Öttinger, A. D. Schlüter, *Chem. Commun.* **2016**, *52*, 18.
- [111] K. S. Novoselov, A. K. Geim, S. V. Morozov, D. Jiang, Y. Zhang, S. V. Dubonos, I. V. Grigorieva, A. A. Firsov, *Science* **2004**, *306*, 666.
- [112] C. Berger, *Science* **2006**, *312*, 1191.
- [113] X. Li, W. Cai, J. An, S. Kim, J. Nah, D. Yang, R. Piner, A. Velamakanni, I. Jung, E. Tutuc et al., *Nature Nanotech* **2009**, *324*, 1312.
- [114] M. Binnewies, *Allgemeine und anorganische Chemie*, Spektrum Akademischer Verlag, Heidelberg, **2011**.
- [115] C. D. Simpson, J. D. Brand, A. J. Berresheim, L. Przybilla, H. J. Räder, K. Müllen, *Chemistry (Weinheim an der Bergstrasse, Germany)* **2002**, *8*, 1424.
- [116] Q. Xiang, J. Yu, M. Jaroniec, *Chemical Society reviews* **2012**, *41*, 782.
- [117] C. Lee, X. Wei, J. W. Kysar, J. Hone, *Science* **2008**, *321*, 385.
- [118] Q. Peng, A. K. Dearden, J. Crean, L. Han, S. Liu, X. Wen, S. De, *Nanotechnology, science and applications* **2014**, *7*, 1.
- [119] G. Li, Y. Li, H. Liu, Y. Guo, Y. Li, D. Zhu, *Chem. Commun.* **2010**, *46*, 3256.
- [120] Y. Zhao, J. Wan, H. Yao, L. Zhang, K. Lin, L. Wang, N. Yang, D. Liu, L. Song, J. Zhu et al., *Nature Chem* **2018**.

- [121] J. A. Marsden, M. M. Haley, *J. Org. Chem.* **2005**, *70*, 10213.
- [122] D. Mössinger, J. Hornung, S. Lei, S. De Feyter, S. Höger, *Angew. Chem.* **2007**, *119*, 6926.
- [123] C. S. Hartley, E. L. Elliott, J. S. Moore, *J. Am. Chem. Soc.* **2007**, *129*, 4512.
- [124] X. Yang, X. Dou, A. Rouhanipour, L. Zhi, H. J. Räder, K. Müllen, *J. Am. Chem. Soc.* **2008**, *130*, 4216.
- [125] J. Wu, L. Gherghel, M. D. Watson, J. Li, Z. Wang, C. D. Simpson, U. Kolb, K. Müllen, *Macromolecules* **2003**, *36*, 7082.
- [126] R. Wakabayashi, Y. Kubo, K. Kaneko, M. Takeuchi, S. Shinkai, *J. Am. Chem. Soc.* **2006**, *128*, 8744.
- [127] W. Dai, F. Shao, J. Szczerbiński, R. McCaffrey, R. Zenobi, Y. Jin, A. D. Schlüter, W. Zhang, *Angewandte Chemie (International ed. in English)* **2016**, *55*, 213.
- [128] B. J. Smith, A. C. Overholts, N. Hwang, W. R. Dichtel, *Chemical communications (Cambridge, England)* **2016**, *52*, 3690.
- [129] J. W. Colson, A. R. Woll, A. Mukherjee, M. P. Levendorf, E. L. Spitler, V. B. Shields, M. G. Spencer, J. Park, W. R. Dichtel, *J. Am. Chem. Soc.* **2011**, *332*, 228.
- [130] T. Kaercher, *Vision Research* **1995**, *35*, S97.
- [131] L. Chen, Y. Hernandez, X. Feng, K. Müllen, *Angew. Chem. Int. Ed. Engl.* **2012**, *51*, 7640.
- [132] M. Treier, C. A. Pignedoli, T. Laino, R. Rieger, K. Müllen, D. Passerone, R. Fasel, *Nature Chem* **2011**, *3*, 61.
- [133] Y. Chen, M. Li, P. Payamyar, Z. Zheng, J. Sakamoto, A. D. Schlüter, *ACS Macro Lett.* **2014**, *3*, 153.
- [134] B. Bitterer, *Vertieferarbeit*, Karlsruher Institut für Technologie, Karlsruhe, **2016**.
- [135] P. Löser, *Vertieferarbeit*, Karlsruher Institut für Technologie, Karlsruhe, **2016**.
- [136] a) Perdew, Burke, Ernzerhof, *Physical review letters* **1996**, *77*, 3865; b) A. D. Becke, *Phys. Rev. A* **1988**, *38*, 3098; c) C. Lee, W. Yang, R. G. Parr, *Phys. Rev. B* **1988**, *37*, 785; d) A. D. Becke, *The Journal of Chemical Physics* **1993**, *98*, 1372; e) M. Valiev, E. J. Bylaska, N. Govind, K. Kowalski, T. P. Straatsma, H.J.J. van Dam, D. Wang, J. Nieplocha, E. Apra, T. L. Windus et al., *Computer Physics Communications* **2010**, *181*, 1477.
- [137] P.-K. Dannecker, *Masterarbeit*, Karlsruher Institut für Technologie, Karlsruhe, **2014**.
- [138] a) V. V. Grushin, H. Alper, *Chem. Rev.* **1994**, *94*, 1047; b) T. You, Z. Wang, J. Chen, Y. Xia, *J. Org. Chem.* **2017**, *82*, 1340.
- [139] H. Detert, E. Sugiono, *J. prakt. Chem.* **1999**, *341*, 358.
- [140] M. D. Brooker, S. M. Cooper, D. R. Hodges, R. R. Carter, J. K. Wyatt, *Tetrahedron Letters* **2010**, *51*, 6748.
- [141] A. F. Littke, G. C. Fu, *J. Am. Chem. Soc.* **2001**, *123*, 6989.
- [142] D. Reinhard, L. Schöttner, V. Brosius, F. Rominger, M. Mastalerz, *Eur. J. Org. Chem.* **2015**, *2015*, 3274.
- [143] T. A. Nguyen, *Batchelorarbeit*, Karlsruher Institut für Technologie, Karlsruhe, **2017**.
- [144] J. Terao, M. Nakamura, N. Kambe, *Chem. Commun.* **2009**, 6011.
- [145] G. M. L. Fave, *J. Am. Chem. Soc.* **1949**, *71*, 4148.
- [146] G. M. Le Fave, P. G. Scheurer, *J. Am. Chem. Soc.* **1950**, *72*, 2464.

- [147] J. Zhu, M. Pérez, C. B. Caputo, D. W. Stephan, *Angew. Chem.* **2016**, *128*, 1439.
- [148] a) S. Höger, *Nachr. Chem.* **2011**, *59*, 453; b) S.-S. Jester, E. Sigmund, S. Höger, *J. Am. Chem. Soc.* **2011**, *133*, 11062.